University of Antwerp

Faculty of Applied Engineering

Research Group Bio-Chemical Green Engineering & Materials (BioGEM)

Catalytic detoxification of lignocellulose hydrolyzate

Thesis submitted for the degree of doctor in applied engineering at the University of Antwerp to be defended by

Valentin SÓTI

Promotors:

Prof. dr. ir. Iris Cornet

Prof. dr. Silvia Lenaerts

Antwerp, 2019

Faculty of Applied Engineering

Research Group Bio-Chemical Green Engineering & Materials (BioGEM)

Catalytic detoxification of lignocellulose hydrolyzate

Thesis submitted for the degree of doctor in applied engineering at the University of Antwerp to be defended by

Valentin SÓTI

Promotors:

Prof. dr. ir. Iris Cornet

Prof. dr. Silvia Lenaerts

Antwerp, 2019

Faculty of Applied Engineering

Research Group Bio-Chemical Green Engineering & Materials (BioGEM)

Catalytic detoxification of lignocellulose hydrolyzate

Thesis submitted for the degree of doctor in applied engineering at the University of Antwerp to be defended by

Valentin SÓTI

Members of the jury:

Prof. dr. ir. Iris Cornet	**Promotor, University of Antwerp**
Prof. dr. Silvia Lenaerts	**Promotor, University of Antwerp**
Prof. dr. ir. Jan Dries	**President, University of Antwerp**
Prof. dr. ir. Pieter Billen	**University of Antwerp**
Prof. dr. Aurore Richel	**University of Liège**
dr. ir. Frederik Vaningelgem	**DuPont Industrial Biosciences**

Acknowledgements

After several years of research and a few years of writing, today is the day that I'm typing this final but important note as the last part of my dissertation. I would have never imagined that this will be the most difficult from all the subparts.

I would first like to thank my promoter, professor Iris Cornet, for the invested time, guidance and suggestions throughout the PhD research, the thesis would not have reached this stage without her. I would like to thank professor Silvia Lenaerts, my IDC and jury members for investing their time and taking part in the PhD pipeline. My colleagues at both University Antwerp and Karel de Grote College, my fellow PhD students for accompanying me in the turmoil of scientific research. For all of my thesis students, who have supported the research with results, many thanks. I would like to thank University Antwerp and Karel de Grote College as institutions for making this thesis happen by providing the tools that I needed, Google Scholar and StackOverflow for unlimited, immediate and straight-to-the-point suggestions. You can see further if you are standing on the shoulders of giants.

In addition, I would like to thank my travel mates, roommates and friends for showing me what life should be about. Especially Julie, for reminding me to get stuff done and Monika for providing me with the productive environment that I needed to finalize the thesis in Budapest and, last but not least, my familiy to stand behind me regardless of my decisions made. Love you all.

Abstract

The present PhD research investigated the possibility of catalytic detoxification of poplar wood based and steam exploded lignocellulosic hydrolyzate with different types of laccase enzymes, with special focus on ethanol and lactic acid products at industrially relevant parameters: high final product concentration, high initial substrate loading and integrated processes.

The simultaneous saccharification and fermentation (SSF) process was taken as a base case and five types of laccases were thoroughly investigated on their utilization potential. Phenolic removal from the liquid xylose rich fraction (XRF) was higher with fungal laccases (65-90 %) compared to approximately 30 % removal with bacterial laccase. Moreover, the optimal pH of fungal laccases was close to pH 4.5, the optimum for cellulase, while the bacterial laccase worked at basic pH.

Integrating laccase treatment and hydrolysis together showed that fungal laccases have negative impact on final sugar concentration, while bacterial laccase had a strong positive effect. Although bacterial laccase removed less phenol and although its optimal conditions are difficult to integrate with hydrolysis, its enhancing effect on cellulase activity makes it a better candidate for application. The presence of the solid fraction (SF) alters the phenolic concentration evolution significantly, thus screening experiments with the liquid fraction alone do not provide sufficient information for the combined process.

Magnetic Cross-Linked Enzyme Aggregates (m-CLEAs) immobilization was assessed for bacterial laccase. m-CLEAs decreased phenolic concentration faster at every pH compared to free bacterial laccase; however, the removal was caused by adsorption rather than by enzyme activity. Although the size of m-CLEAs particles are in the μm range, around 90 % of the initial catalyst mass was recycled from a dense (15 % substrate loading) mixture via magnetic separation. The high recycling rate is promising; m-CLEAs immobilization method can have industrial utilization potential.

Minimum sugar revenue (MSR) estimations show that currently hardwood based MSR is 70 % more expensive than corn grain based MSR. About 7-10 fold cellulase activity increase will be needed until MSR will be competitive with corn grain MSR. However, m-CLEAs cellulase can already be competitive if the corn prices are in the higher regime of last year's prices.

Katalytische detoxificatie van lignocellulose hydrolysaat

Het huidige doctoraatsonderzoek onderzocht de mogelijkheid tot katalytische detoxificatie van populierenhout gebaseerd en stoom geëxplodeerd lignocellulosehydrolysaat met verschillende soorten laccase-enzymen, met speciale aandacht voor ethanol en melkzuurproducten op industrieel relevante parameters: hoge eindproductconcentratie, hoge initiële substraatbelading en geïntegreerde processen.

Het simultane saccharificatie- en fermentatieproces (SSF) werd als een basisscenario genomen en vijf types laccasen werden grondig onderzocht op hun gebruikspotentieel in dit proces. De fenolische verwijdering uit de vloeibare xylose-rijke fractie (XRF) was hoger voor fungale laccasen (65-90 %) dan voor bacterieel laccase (ongeveer 30 % verwijdering). Bovendien was de optimale pH van fungale laccasen dicht bij pH 4,5, het optimum voor cellulase activiteit, terwijl het bacteriële laccase werkte bij een basische pH.

Integratie van laccase-behandeling en hydrolyse samen toonden aan dat fungale laccases een negatieve invloed hebben op de uiteindelijke suikeropbrengst, terwijl bacterieel laccase een sterk positief effect had. Hoewel bacterieel laccase minder fenol verwijderde en hoewel de optimale condities moeilijk te combineren zijn met die voor hydrolyse, maakt zijn positief invloed op de cellulaseactiviteit hem een betere kandidaat voor toepassing in simultane detoxificatie en saccharificatie. De aanwezigheid van de vaste fractie (SF) tijdens het proces wijzigt de evolutie van de fenolconcentratie aanzienlijk, dus screening-experimenten met de vloeibare fractie alleen verschaffen niet voldoende informatie voor het gecombineerde proces.

Magnetic Cross-Linked Enzyme Aggregates (m-CLEAs) immobilisatie werd beoordeeld voor bacterieel laccase. m-CLEAs verminderden de fenolconcentratie bij om het even welke pH sneller dan bij vrij bacterieel laccase; de verwijdering werd echter voornamelijk veroorzaakt door adsorptie in plaats van door enzymactiviteit. Hoewel de grootte van de deeltjes van m-CLEAs in het µm-gebied ligt, werd ongeveer 90% van de oorspronkelijke katalysatormassa gerecirculeerd uit een dens (15% substraatbelading) mengsel via magnetische scheiding. Het hoge recyclagepercentage is veelbelovend; m-CLEAs immobilisatiemethode heeft mogelijk industrieel toepassingspotentieel.

Minimale verkoopprijzen van suikers (MSR) tonen aan dat MSR op basis van hardhout momenteel 70 % duurder is dan de MSR op basis van maïsgranen. Ongeveer 7-10-voudige cellulase-activiteitstoename zal nodig zijn vooraleer MSR concurrerend zal zijn met maïsgraan MSR. Echter, m-CLEAs cellulase kan al concurrerend zijn als de maisprijzen in het hogere regime van de prijzen van het afgelopen jaar liggen.

Contents

List of figures and tables

Abbreviations

ABTS	2,2'-azinobis-(3-ethylbenzothiazoline-6-sulfonate)
ADP	adenosine diphosphate
AFEX	ammonia fiber explosion
ATP	adenosine triphosphate
CAPEX	capital expenses
CBP	consolidated bioprocessing
CLEAs	cross-linked enzyme aggregates
CLECs	cross-linked enzyme crystals
GC	gas chromatography
GRF	glucose rich fraction
HBA	hydroxybenzaldehyde
HMF	hydroxymethylfurfural
HPLC	high performance liquid chromatography
m-CLEAs	magnetic cross-linked enzyme aggregates
MESP	minimum ethanol selling price
MS	mass spectrometry
MSR	minimum sugar revenue
MSW	municipal solid waste
NAD	nicotinamide adenine dinucleotide
RI	refractive index
SE	steam explosion
SF	solid fraction
SFD	simultaneous fermentation and detoxification
SHF	separate hydrolysis and fermentation
SSCF	simultaneous saccharification and co-fermentation
SSD	simultaneous saccharification and detoxification
SSF	simultaneous saccharification and fermentation
SSFD	simultaneous saccharification, fermentation and detoxification
SYR	syringaldehyde
UV	ultra violet light
VIS	visible light
XRF	xylose rich fraction

Chapter 1 **INTRODUCTION AND OUTLINE**

1.1 Motivation

Lignocellulosic biomass is the most abundant biomass on Earth and it is considered to have the highest potential to become the substitute for our decreasing fossil resources. Lignocellulosic biomass, such as agricultural waste, wood residues and energy crops, contains cellulose, hemicellulose and lignin. The fermentative lignocellulose-to-chemicals conversion has four mandatory steps: pretreatment, hydrolysis, fermentation and downstream processing. Different kinds of pretreatments (physical, chemical and physico-chemical) are required to degrade the rigid structure and to allow efficient saccharification of the polysaccharides (hydrolysis) afterwards. Steam explosion is considered as one of the simplest, yet most effective pretreatment method, already commercialized.

During any kind of thermal pretreatment step, toxic compounds such as weak acids, furan derivatives and phenolic compounds are formed which can inhibit the enzymatic hydrolysis as well as the growth of the fermenting microorganisms. This leads to reduced yields and volumetric productivities; therefore, detoxification is often desired however not mandatory. Laccase enzymes from various sources are known to remove/transform phenolics in lignocellulosic hydrolyzates, thus increasing fermentation efficiency. However, amongst other open questions, no previous study has addressed the cost of laccase enzyme treatment yet. Other questions also investigated in the research are the possible use of enzyme immobilization and recycling from the fermentation broth, process integration by overlapping process steps and investigating their interactions.

The production of second-generation bio-ethanol is currently more expensive than that of first-generation bio-ethanol, but techno-economic analyses point out that the turnover is within reach. It is a widely accepted opinion that enzymes should be utilized for the hydrolysis of the saccharide polymers in lignocellulose, including different types of cellulases, possibly laccases. Enzyme cost is considered one of the most significant factors defining the final product price in lignocellulose hydrolysis and fermentation, but the exact estimated prices vary greatly in literature, thus currently enzyme price uncertainty is responsible for the most variability in the overall process cost. Enzyme immobilization and recycling can be a tool to decrease these costs, but techno-

economic investigations for immobilized enzyme utilization are non-existent. Cellulases are known to suffer from inhibition from their product, glucose, as well as from other inhibitors in the hydrolyzate. Overlapping hydrolysis and fermentation in a so-called simultaneous saccharification and fermentation process (SSF) is a known way to overcome end-product inhibition, thus possibly lowering needed enzyme amounts for reaching industrially relevant final concentrations and corresponding costs. Removing other inhibitors from the broth – detoxification – can also be beneficial for hydrolysis. High solid substrate loading is a key factor towards high product titers in SSF, and recovery of immobilized enzymes from this thick liquid is often overlooked and rarely investigated. Process integration and simplification (such as SSF) is a method to decrease CAPEX through simplified equipment design and shortened processing times, and can lead to other beneficial properties too (e.g., overcoming product inhibition).

1.2 Aim

The aim of this research is to use lignocellulose to produce chemicals in an efficient way with special attention to steam-exploded poplar wood and laccase detoxification, considering the economic viability of the process.

1.3 Chapter by chapter overview

The PhD manuscript is organized in seven chapters, among which five are experimental. In Chapter 1, a general introduction, the research questions and the objectives of the doctoral research are presented. Chapter 2-6 are experimental chapters, while Chapter 7 is the general conclusion summarizing the findings of the whole thesis, the last part is the Appendix.

All experimental chapters follow the same structure: (i) an introduction containing a literature study about the subtopic, with detailed experimental conditions and reported parameters (exact values), (ii) a method part describing the exact experiments conducted, (iii) a results part where the findings are discussed and, (iv) a conclusion part summarizing a (sub)chapter, with comparison to literature.

Each chapter is summarized below.

1.3.1 Chapter 2: Literature overview

The objective of this chapter is to introduce basic concepts without exact numbers, such as lignocellulose, lignocellulose-to-chemicals process and its subprocesses, inhibitors, detoxification and laccase enzyme.

A detailed overview of fermentative lignocellulose-to-chemicals production processes is given, with special interest on ethanol and lactic acid production. A comparison between starch-based glucose and lignocellulosic sugar as starting substrate is given, i.e., the production steps, the advantages and drawbacks. The four steps of fermentative lignocellulose-based production are discussed: pretreatment (with special interest on **steam explosion**), hydrolysis (with focus on the **enzymatic process**), fermentation (with special interest on **simultaneous saccharification and fermentation**) and the subsequent downstream process (distillation and crystallization for ethanol and lactic acid production respectively).

The different types of formed **inhibitors**, their removal possibilities, and inhibition effects on microorganisms are discussed. **Laccase** enzyme and its application possibilities for phenolic removal/transformation, in general, are introduced. Thereafter, an overview on laccase utilization specific for hydrolyzate detoxification is given. Current **enzyme immobilization** methods in general as well as in case of laccases are shown.

1.3.2 Chapter 3: Laccase detoxification

The objective of this chapter is to determine the basic aspects of the research in general: define the analytical techniques, characterize the materials (SF, XRF) that are used throughout the research, investigate laccase reaction on a model substrate, and screen the laccases based on literature methods.

After an overview of the relevant **measurement techniques** for inhibitors (with focus on phenolics), carbohydrates (structural and free) and fermentation products has been given, the techniques and methods selected for application in the PhD are described. Poplar wood was pretreated with **autocatalyzed steam explosion** and a partial optimization of pretreatment parameters was performed. Starting and final lignocellulosic substrate was characterized via structural carbohydrate measurements, and initial enzymatic hydrolysis experiments were done to investigate the sugar yield for different pretreatment parameters and enzyme loading. **Five laccases from different sources and with different purity were characterized**. Hereto, the standard

enzyme activity was determined with ABTS substrate, at different pH and temperature values. The laccase reaction mechanism was investigated on vanillin as a standard substrate and XRF as an industrially relevant substrate. A method for robust reaction monitoring is shown.

Part of the results is published in:

Sóti, V. , Jacquet, N. , Apers, S. , Richel, A. , Lenaerts, S. and Cornet, I. (2016), Monitoring the laccase reaction of vanillin and poplar hydrolysate. *J. Chem. Technol. Biotechnol.*, 91: 1914-1922. doi:10.1002/jctb.4789

1.3.3 Chapter 4: Magnetic Cross-Linked Enzyme Aggregates

The objective of this chapter is to investigate the properties of bacterial m-CLEAs laccase: physical properties and handling routines, detoxification effect on liquid XRF and adsorption capacity.

Procedures to determine organic loading and precise mass addition of m-CLEAs are developed. **Detoxification** of the XRF liquid with both free and immobilized enzyme is performed and compared, both with and without pH control during the reaction. Phenolic **adsorption** on the immobilized catalyst is investigated and quantified. A **mathematical model** was constructed to estimate the adsorption effect during the recycling cycles, for different activity m-CLEAs laccases.

1.3.4 Chapter 5: Process integration

The objective of this chapter is to assess different process integration possibilities between hydrolysis, fermentation and detoxification at industrially relevant high substrate loading.

Experiments were performed for four specific **process integration cases**, i.e., **SSF** (simultaneous saccharification and fermentation), **SSD** (simultaneous saccharification and detoxification), **SFD** (simultaneous fermentation and detoxification) and **SSFD** (simultaneous saccharification, fermentation and detoxification), using the economically relevant windows (starting substrate concentration, industrial grade enzyme activities, realistic catalyst organic loading). General conclusions are drawn and best practices determined. A lab-scale reactor setup is shown for **high viscosity fermentations**. A lab-scale **inoculum adaptation** setup is introduced and documented.

Part of the results of Chapter 4 and 5 are combined in a published paper:

Sóti, V., Lenaerts, S. and Cornet, I. (2018), Of enzyme use in cost-effective high solid simultaneous saccharification and fermentation processes. *J. Biotechnol.*, 270:70-76, https://doi.org/10.1016/j.jbiotec.2018.01.020

1.3.5 Chapter 6: Techno-economic analysis

The objective of this chapter is to give a better insight of the economics of the process, determine the required initial substrate concentration, enzyme cost and expected future improvements, investigate the potential of m-CLEAs immobilization, and expected unit price of cellulase enzyme.

The minimum **initial substrate concentration** of SSF was determined from the required **final product titers**, calculated from economic and energetic requirements. Experiments were conducted to quantify the m-CLEAs catalyst **recovery**. Estimations of the hardwood based **minimum sugar revenue (MSR)** were performed by using a published model for both free and immobilized cellulase. Results were compared to MSR values for corn grain-derived sugar. Relevance windows (parameter ranges where the application is feasible on theoretical level) were identified in function of enzyme unit price and enzyme activity improvement. The **uncertainty and parameter sensitivity** of the model was assessed with Monte Carlo simulations. **Enzyme price estimations** were investigated thoroughly and a published model was modified to show, how decreased fermentation times and inoculum recycling would modify the production costs.

1.3.6 Chapter 7: General discussion and conclusion

This chapter combines the findings of the whole PhD research and indicates possible future research directions.

The global situation is discussed, the findings of the current research summarized and the research is positioned in the state of the art. Possible future research directions are proposed and considerations for initial SSFD parameter estimation are presented.

1.3.7 Appendix

The Appendix contains code snippets, drawings and documentation about the utilized equipment.

The setup for inoculum adaptation (including code), for lime-based pH control and laccase fast screening SSD/SSFD equipment are documented.

Chapter 2 DETOXIFICATION OF LIGNOCELLULOSE, A SUBSTRATE FOR FERMENTATION

2.1 Introduction to renewable-to-chemicals process

In general, renewable materials incorporate every material from the flora and fauna alike [1], but generally it will mean plant derived materials or algae. Plant derived sources can be further divided into sucrose/starch type and lignocellulose type. The latter can play the utmost role in future as a renewable resource for bioethanol production. The actual conversion from renewables to chemicals can use different techniques and follow different routes, i.e., (thermo)chemical or biochemical, wherefrom the latter can be subdivided into fermentative and enzymatic methods [2].

2.2 Lignocellulose

The utilization of lignocellulosic raw materials for chemical production has several advantages compared to the other feedstocks [3], i.e., lower cost, it cannot be used as nourishment and it is present in significant quantities as waste from food industry, agricultural waste, paper industry or forestry residues. More specifically, important types of lignocellulosic materials are hardwood from trees such as birch, maple, poplar, sycamore etc., and softwood from trees such as pine, Douglas and spruce, but also agricultural and agro-industrial wastes such as wheat straw, corn cobs, corn stover, sugar cane bagasse, switchgrass etc., and finally municipal solid waste (e.g., paper based, processed, newspaper) [4]–[6]. On the other hand, grasses or fast-growing trees, such as poplar, can be cultivated for their conversion to bioenergy and are commonly called as energy crops.

2.2.1 Structure and composition

Lignocellulose contains two main carbohydrate polymer components (cellulose and hemicellulose) and a complex aromatic polymer (lignin). Lignin is the main component of the cell wall and is an, approximately, 10-15 % w/w part of the structure (see Figure 2-1) and more than 20 % of the dry content. The ratio of the components varies according to the biomass, species type and cultivation conditions (see Table 2-1).

Cellulose is a linear syndiotactic homopolymer. D-glucose molecules that are linked to each other by β-(1,4)-glycosidic bonds result in a massive, compact crystalline

structure. The cellulose chains are assembled into long microfibrils, stabilized by hydrogen bonds that make the polymer rigid and difficult to break. The microfibrils are embedded in a matrix of hemicelluloses, lignin and, eventually, other amorphous sugar polymers such as pectin. The individual microfibrils in crystalline cellulose are packed so tightly that not only enzymes but also even water molecules cannot enter the complex framework. Therefore, the crystalline regions are resistant to biodegradation. Non-crystalline parts of microfibrils with a less ordered structure are referred to as amorphous regions that are easier to hydrolyze. The highly ordered tertiary structure and high molecular weight make natural cellulose insoluble in water [5], [7].

Hemicellulose is a highly branched and amorphous variable structure, formed out of heteropolymers consisting of pentose sugars (xylose and arabinose), hexose sugars (galactose, glucose, and mannose) and uronic acids that may carry acetyl groups. There are four general groups of structurally different hemicellulose types: xyloglycans (xylans), mannoglycans (mannans), xyloglucans and mixed-linkage β-glycans. They all occur in many structural variations with different types of side chains and distribution of glycoside linkages in the main macromolecular chain [5], [7].

The composition of hemicellulose types varies between different lignocellulosic feedstocks. The hemicelluloses of softwood are typically glucomannans, a subtype of mannans. Therefore, hemicellulose of softwoods consists mostly of mannose as sugar monomer, followed by xylose, glucose, galactose and arabinose, whereas hemicellulose of hardwood and agricultural plants is mainly composed of xylans with a linear backbone of β-(1 → 4) linked xylopyranose. Therefore, xylose is the most important hemicellulose monomer in hardwood and agricultural plants. Its branched and amorphous structure makes hemicellulose easier to hydrolyze compared to cellulose [5], [7].

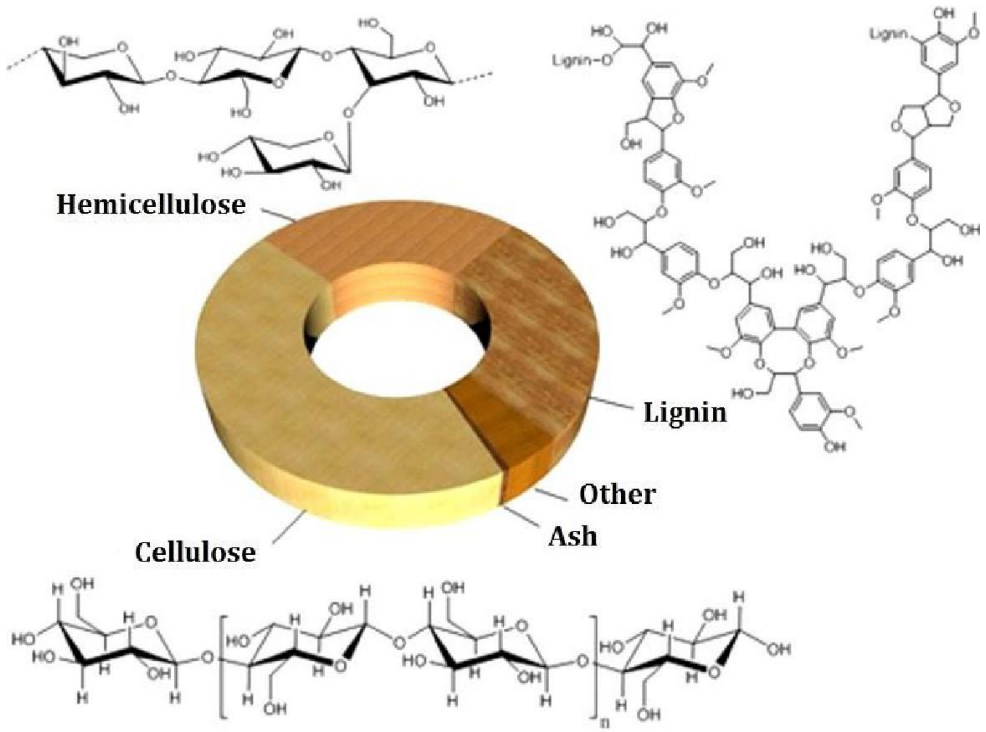

Figure 2-1: Composition of lignocellulose [8].

Lignin connects to hemicellulose and cellulose with covalent and hydrogen bonds, i.e. substituting a carboxymethyl group in the lignin matrix [9]; therefore it helps to form a rigid and recalcitrant structure in plant cell walls. This explains the defying nature of lignocellulose degradation. Lignin is an aromatic polymer derived from three different phenolic precursors. These monomers of lignin are the monolignols; coniferyl alcohol, sinapyl alcohol, and minor amounts of p-coumaryl alcohol, they differ in the number of methoxyl units (see Figure 2-2A). The monolignols in lignin are linked via oxidative coupling (5-5, β-β, 5-O-4, β-5, β-O-4 linkages) to a very complex matrix, probably catalyzed by both peroxidases and laccases as shown in Figure 2-2B [5]–[7]. The units resulting from the monolignols, when incorporated into the lignin polymer, are called guaiacyl (G), syringyl (S), and p-hydroxyphenyl (H) units. This complex matrix consists of a variety of hydroxyl, methoxyl and carbonyl groups, which results in a low polarity of the lignin macromolecule. Lignin makes the biomass resistant to chemical and biological degradation.

Table 2-1: Composition of different lignocellulosic sources expressed in % dry weight [5], [10].

Feedstock	Cellulose [%]	Hemicellulose [%]	Lignin [%]
Agricultural waste [5]	37 – 50	25 – 50	5 – 15
Wheat straw [10]	35 – 39	22 – 30	12 – 16
Corn stover [10]	35 - 39	20 – 25	11 – 19
Sugarcane bagasse [10]	25 – 45	28 – 32	15 – 25
Hardwood [5]	45 – 47	25 – 40	20 – 25
Poplar [10]	45 – 51	25 – 28	20 – 23
Softwood [5]	40 – 45	25 – 29	30 – 60
Pine [10]	42 – 49	13 – 25	23 – 29
Grasses [5]	25 – 40	35 – 50	10 – 30
Switchgrass [5]	40 – 45	30 – 35	12
Newspaper [5]	40 – 55	25 – 40	18 – 30

2.2.2 Poplar

Among lignocellulose feedstocks the following are considered as front-runners: hybrid poplar, switchgrass, *Miscanthus*, southern pine, willow, and corn stover [11]. Each has its specific advantages, but poplar is among the fastest growing trees, the nominal yield (including moisture) is around the same as switchgrass and considerably higher than corn stover. Yields may vary depending on the plantation type: full-grown trees can be harvested or bush type in two or five years cycles (Lochristi, Belgium). Poplar has the highest energy density from the above-mentioned examples; its dry heating value (0 % water content) is around 19 MJ/kg, which is 5 % lower than softwoods, 5 % higher than switchgrass, and 10 % higher than corn stover and wheat straw. Besides that, it is able to grow on contaminated soils, and there are significant reserves in the Northern hemisphere (America and Eurasia). Typical lignin content of poplar wood is 21-23 % (up to 25 %), 40-48 % for cellulose, 20-23 % for hemicellulose. From sugar compounds glucan is the main component with 40-45 %, galactan around and less than 1 %, mannan 2-4 %, xylan 13-18 %, arabinan less than 1 %.

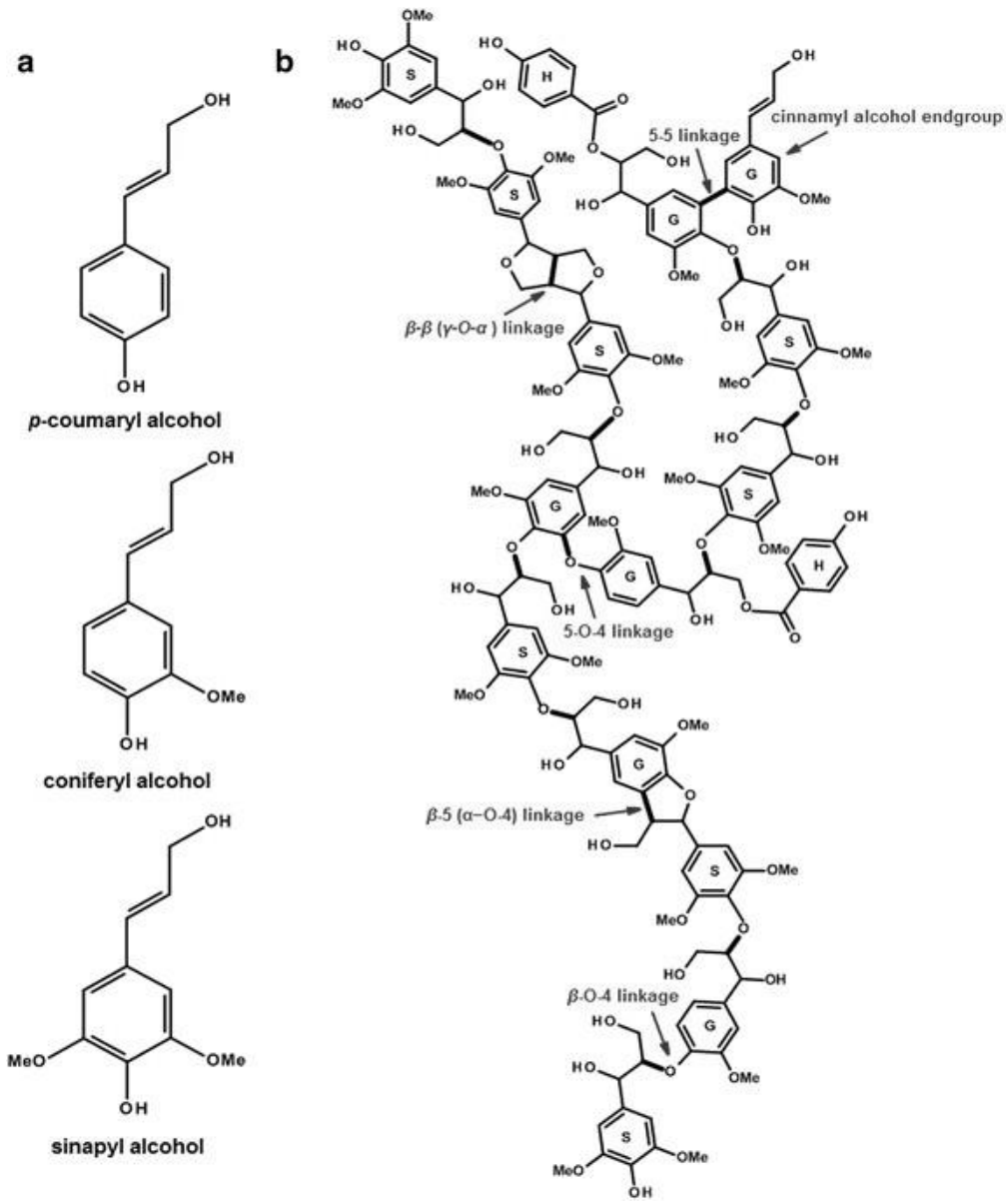

Figure 2-2: Monolignols and an example polymer lignin structure [12].

Additionally, its genome has been sequenced, and thus opened the way to gene modifications. Most appealing is a modification to reduce the lignin content [13], which could also result in a higher cellulose content. The resulting decrease in chemical/mechanical resistance can also be interesting, as it can cause easier pretreatment and more effective hydrolysis [14]. A study showed that downregulating the caffeoyl shikimate esterase gene expression in hybrid poplar leads to reduced

lignin (by 19-25 % in lignin content, i.e. from 22 % to 17 % lignin in poplar) and increased cellulose content (8-13 % increase, i.e. from 38 % to 43 %), and 62-91 % increased glucose recovery during saccharification depending on the applied parameters [15]. Another study found that downregulating the gene encoding cinnamyl alcohol dehydrogenase (CAD) caused 10 % decrease in lignin, resulting in up to 81 % and 153 % increase in glucose and xylose recovery respectively [16].

2.3 Process overview: Fermentative lignocellulose to chemicals conversion

The conventional lignocellulosic biomass based fermentative chemical production consists of the following four main steps [17]:

(1) Pretreatment: Making hemi(cellulose) available for subsequent steps, conditioning/detoxifying the liquid matrix.

(2) Enzymatic hydrolysis: Depolymerizing lignocellulose to fermentable sugars, such as glucose and xylose, by means of hydrolytic enzymes.

(3) Fermentation: Metabolizing the sugars to products, generally by bacteria or yeast.

(4) Purification: Separation and purification of products to meet the standards of commercial applications.

Detoxification/conditioning step, included in pretreatment, is not a mandatory step theoretically, but it is often needed depending on the source of lignocellulose, the pretreatment and its conditions, and the resistance and specifications of the fermenting microorganism.

Although the actual order of the process steps is pretreatment, hydrolysis, fermentation and purification, intuitively one can say that the fermentation is the main process where the substrate is converted to the product. Purification only transforms the fermentation product to market grade product. Hydrolysis transforms the bounded substrate to a form that is digestible for the fermenting microorganism.

Pretreatment helps the hydrolysis by opening up the rigid lignocellulosic structure, thus increasing hydrolysis yield.

Yield, titer and volumetric productivity are the three main parameters used to describe a process. Yield describes the ratio of substrate converted to product compared to theoretical, the stoichiometric maximum. Titer is the final concentration of the product, thus the multiplication of yield and initial substrate concentration. Volumetric productivity is the titer divided by the time necessary to reach it, thus the parameter that incorporates time.

2.3.1 Pretreatment

The main goals of pretreatment techniques are to alter the lignocellulosic structure by breaking the lignin matrix to increase the accessibility of the cellulose fibers and breaking the crystalline construction of cellulose to obtain amorphous phases that are more sensitive to enzymatic attack (Figure 2-3). Moreover, the process costs can increase substantially if not the adequate pretreatment technique is applied. Without pretreatment the hydrolysis percentage of the fermentable sugars reaches only <20 %, or an extremely long time is needed [4], [18], [19].

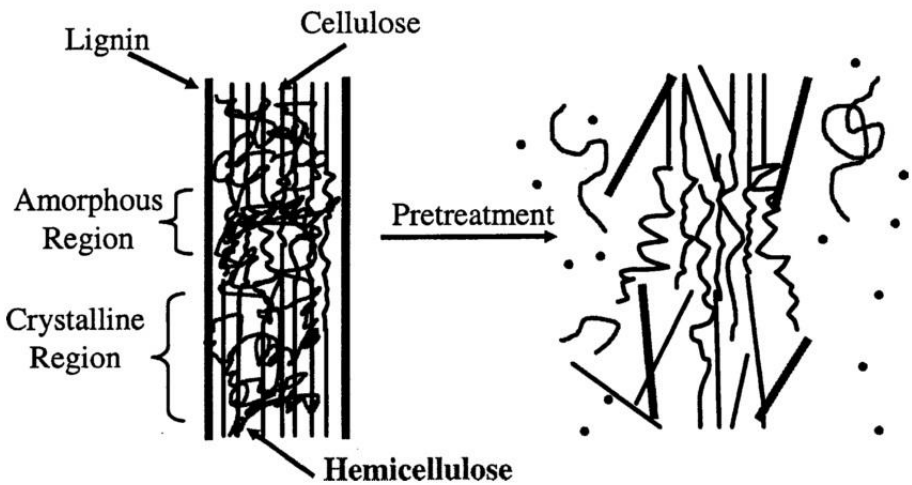

Figure 2-3: Breakdown of the lignocellulosic matrix during pretreatment [19].

There are several points that should be considered before choosing a proper and efficient pretreatment method, such as, obtaining highly digestible cellulose and hemicellulose; minimizing the quantity of formed toxic compounds (carboxylic acids, furan derivatives and phenolic matters), minimizing residue and sugar loss.

Additionally, maximizing the recovery of other useful by-products is also important (e.g., lignin). A minimal size reduction will be certainly needed (chipping, grinding, or milling), except maybe grass types of lignocellulose. Furthermore the pretreatment process needs to be available at industrial scale, and heat, power and chemical demand should be as low as possible [4], [20], [21].

Pretreatment methods are either physical, physicochemical, chemical, biological or a combination of these, although the categories can be overlapping in some cases [22]. Physical pretreatments of lignocellulosic materials include chipping, grinding, and milling to cause a reduction of the cellulose crystallinity. The energy needed for mechanical treatment varies with the original and required terminal particle sizes; the type and the moistness of the resource. The size of the particles is fluctuating typically between 10-30 mm after chipping and 0.2-2 mm after milling or grinding. Another (thermo)physical method is pyrolysis which needs less energy input but part of the carbon will be converted to less valuable char and it is difficult to control the product formation, typically wide range of chemicals are formed. During the promising technique of thermo-physical extrusion, a combination of shearing, heating and mixing takes part in the size reduction. Microwaving is also a feasible, fast and selective method that requires less energy than regular heating. Freeze pretreatment is a newly researched but promising and more environmentally friendly pathway; it is highly efficient with rice straw [4], [7], [19], [22].

Physicochemical methods include steam explosion, ammonia fiber explosion, carbon dioxide explosion, wet oxidation, and liquid hot water treatment, among others. Currently the most applied physico-chemical pretreatment is steam-explosion. In this complex thermo-mechano-chemical procedure the lignocellulosic biomass is maintained in a reactor with saturated high pressurized steam which is abruptly expanded after a certain time which provokes a decompressive explosion [10], [21]. AFEX (Ammonia Fiber Explosion) and CO_2 explosion pretreatment are similar to the process of steam explosion; the differences are the utilization of ammonia (recyclable) or CO_2 instead of water. The latter has advantages such as the need for a lower temperature; no waste products are forming and, no need of recovery techniques. Furthermore, it is cheaper compared to AFEX, but its efficiency is lower.

Chemical methods include acid pre-hydrolysis, alkaline hydrolysis, organosolv treatment and ozonolysis. Acid pretreatment is the most well spread chemical

pretreatment method due to the effectiveness on a wide scale of lignocellulose resources, even though it is expensive. Generally sulfuric, nitric or hydrochloric acid is utilized in various conditions such as high temperature and low acid concentration followed by a subsequent step at low temperature with high concentration [4], [21]. Alkaline pretreatments are generally operating on lower temperature ranges with the use of sodium hydroxide, potassium hydroxide or calcium hydroxide (lime). These chemicals are responsible for dissociating the cross-linking ester bonds between lignin and xylan [21]. In the procedure of organosolv pretreatment, organic solvents are used such as methanol, ethanol, acetone, ethylene glycol etc. Ionic liquid pretreatment technique requires a combination of organic salts, usually large cations and small anions [21].

Biological pretreatment has several advantages, for instance, it is an environmentally friendly (green) pathway with significantly lower capital investment required and the demand for chemicals is negligible compared to all other pretreatment types. Furthermore, its energy consumption is low. White-, brown- and soft-rot fungi are the types of microbes that are mainly used for hemicellulose and lignin degradation during a biological pretreatment. Considerable drawbacks can be listed as low efficiency, the long processing time and, in addition, the demand for large space and constant supervising of the microbial growth [7], [21].

2.3.1.1 Diluted Acid pretreatment

Acid pretreatment with diluted sulfuric acid is probably the most common method of chemical pretreatment methods. The concentration of sulfuric acid is 2 to 5 %, while the mixture of biomass and diluted sulfuric acid is constantly mixed at temperatures between 130 and 210 °C [23]. The process will be typically performed at a low temperature (120 °C) during 30 - 90 min [21]. In general, diluted acid pretreatment results in a high sugar yield during the subsequent enzymatic hydrolysis. Hemicellulose is solubilized and hydrolyzed completely to fermentable sugars. Therefore, cellulose is more exposed and available for hydrolysis in a subsequent enzymatic hydrolysis [21]. The major drawback is the formation of toxic compounds (see Figure 2-4). High temperatures cause dehydration of sugar monomers into furfural and 5-hydroxymethyl furfural (HMF). Further degradation of these compounds can lead to formation of formic acid and levulinic acid. Partial breakdown of lignin generates phenolic compounds [23].

Diluted acid pretreatment is effective for a wide variety of lignocellulosic feedstocks. It has the potential to be one of the most cost-effective chemical pretreatment methods. However, costs are usually still higher than some physicochemical pretreatments such as steam explosion or ammonia fiber explosion (AFEX), mainly due to relatively longer treatment times and the cost of utilization/recuperation of chemicals [23].

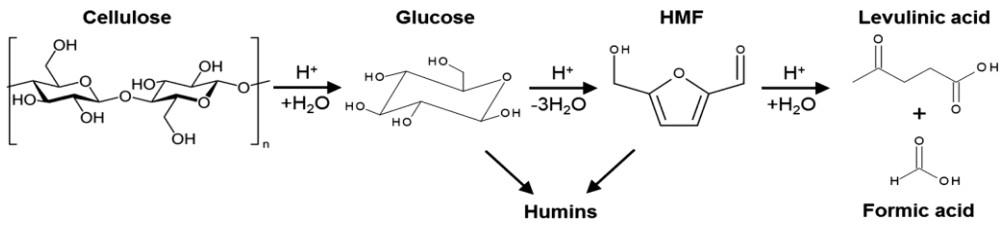

Figure 2-4: Possible reactions during cellulose acid hydrolysis [24].

2.3.1.2 Steam explosion

This physicochemical process exposes the lignocellulosic biomass to high-pressure saturated steam. When the pressure is suddenly reduced, the material undergoes an explosive decompression. Steam explosion is typically initiated at a temperature of 160 to 260 °C and a corresponding pressure of 0.69 to 4.83 MPa. These conditions are held for several seconds to a few minutes – hence it is much faster than dilute acid treatment - before the material is exposed to atmospheric pressure [22].

The high temperature, and the acids formed during the process (acetic acid from deacetylation and formic, levulinic and uronic acids formed by sugar degradation) cause hemicellulose hydrolysis during the process, called auto-hydrolysis. Part of the lignin will be solubilized (acid soluble lignin) and part deformed. Removal of lignin is limited because of its low solubility in the aqueous matrix, however it can melt and later solidify on the surface of the lignocellulose particle, although this effect is reduced by sudden decompression at the end, compared to heat treatments without explosion [25]. In a recent publication, significant depolymerization/repolymerization was reported during steam explosion, but only in the case of softwood, which explains why softwood behaves very differently compared to other biomass types. The depolymerization was tracked back to guaiacyl units, which are present in softwood in much higher ratio than in other lignocellulose sources [26]. The elimination of the hemicellulose and part of the lignin from the cellulose microfibrils exposes the

cellulose surface and will increase enzyme accessibility later, during enzymatic hydrolysis. Partial hydrolysis of cellulose can occur even during the pretreatment, depending on the severity of the process. The explosive decompression causes water in the material to expand rapidly, resulting in fragmentation of the lignocellulosic biomass with increased accessible surface area [22].

Steam explosion is considered as one of the most cost-effective pretreatment processes for hardwoods and agricultural residues [25]. The process results in high sugar yields during enzymatic hydrolysis. Larger initial particle size can be used as the explosive decompression fragments the particles further, which reduces energy requirement for mechanical preprocessing, the process itself is energy efficient and relatively easily scaled-up [22]. Some researchers state that avoiding sugar degradation is more important than better digestibility, therefore lower temperatures and longer treatment times are preferred [27]. The environmental impact is considered lower than most other pretreatment techniques as no additional chemicals are utilized or in catalytic concentration [21]. In the meantime, steam explosion with relatively short treatment times and smaller volumes are closest to continuous processes (compared to dilute acid treatment). Extrusion type modification can lead to a fully continuous design. In this case, the material is fed at one side of the extruder and compressed/heated up through friction as it is transported by the Archimedes screw. The severity can be set by outer heating and the design of the screw (similar to polymer extrusion techniques). The main drawbacks of steam explosion is the generation of toxic compounds, including phenolic compounds from lignin degradation, furan derivatives from sugar degradation and weak acids formation [21].

Another very interesting pretreatment technique, which could be also considered as steam explosion, is dry dilute acid pretreatment [28]. This technique results in extreme high solid content mixture, as the initial acid solution/solid ratio is ½, thereafter the steam is used to heat the mixture to defined temperature (185 °C, typically under 200) for few minutes (under 10 minutes, typically 3-5 minutes), under intensive stirring via helical stirrer. The valves were suddenly released after treatment time (this makes it steam explosion). The substrate was corn stover at extremely high dry content (50 m/m%).

Addition of an acid catalyst improves hemicellulose hydrolysis and sugar yield during enzymatic hydrolysis. Therefore, less severe conditions are required, resulting in reduction of toxic compound formation when lower temperature is used, also xylose

degradation is less. When the same process severity is used, additional acids cause the formation of higher amounts of toxic compounds [21]. For effective pretreatment of softwood, addition of an acid catalyst is a prerequisite due the absence of sugar acids in its hemicellulose structure [22]. Steam explosion with addition of H_2SO_4 or SO_2 is considered as one of the most effective pretreatment methods for softwoods. Autocatalyzed steam explosion seems sufficient for hardwood [21].

A two stage steam explosion was suggested for both high hemicellulose and cellulose recovery [29]. The first step is performed under mild conditions, where hydrolysis of hemicellulose takes place. The solid is separated by centrifugal air classifiers and a second steam explosion with more severe conditions at high temperature follows, resulting in 12.82 % improved sugar yield during enzymatic hydrolysis [30].

2.3.1.3 Summary of promising cost-effective pretreatment methods

The choice of pretreatment technology depends on the composition of the lignocellulosic feedstock and has a large impact on the applied enzymes and microorganisms in the subsequent process steps. Some methods are highly effective for specific feedstocks while others are applied in a wide range of feedstocks but less effective. An overview of different pretreatment methods and their advantages, disadvantages and inhibitor formation is given in the Table 2-2 below.

Table 2-2: Overview of the advantages and disadvantages of different pretreatment methods prior hydrolysis [4], [5].

Pretreatment method	Inhibitor formation	Advantages	Disadvantages
Milling	None	- Reduction cellulose crystallinity - Increases accessible surface area - Prerequisite for each pretreatment method	- High power and energy consumption - No chemical changes in composition - Always required
Dilute acid	High	- Effective hydrolysis and high sugar yield	- Generation of toxic compounds

		- Applicable for different feedstocks - Easy scale up	- Hazardous, corrosive and toxic
Lime (Alkaline)	Medium	- High sugar yield - Effective against hardwood and agricultural residues - Reduces inhibitor quantity - Lower temperature	- Long treatment time - Sugar loss due to high pH - Commercially difficult
Ozonolysis	Low	- Reduces lignin content - No toxic residues	- Expensive amount of ozone required - Not commercially viable
Organosolv	High	- Causes lignin and hemicellulose hydrolysis - Less inhibitor	- Solvents need to be drained and recycled - High cost of regeneration - Without value added aromatic products it is not feasible commercially
Wet Oxidation	Low	- Removal of lignin, dissolves hemicellulose and causes cellulose decrystallization	- High cost of oxygen and alkaline catalyst
Steam explosion	High	- Causes lignin transformation and hemicellulose solubilization - Cost-effective	- Partial hemicellulose degradation - Generation of toxic compounds
CO_2-explosion	Low	- Hemicellulose removal - Cellulose recrystallization - Cost-effective	- No effect to lignin - Very high-pressure requirements

AFEX	Low	- Removal of lignin and hemicellulose - Effective for agricultural residues without the formation of toxic compounds	- Not suitable for material with high lignin content - High-cost due ammonia and recovery
Liquid hot water	High	- Removal of hemicellulose - Making enzymes accessible to cellulose	- Long residence time - Less lignin removal
Biological	Low	- Degrades lignin and hemicellulose through enzymes released by fungi - Low energy consumption - Low cost	- Slow bioconversion

2.3.2 Hydrolysis

Hydrolysis is the cleavage of the polysaccharides, cellulose and hemicellulose, into their monomeric sugar building blocks by binding H_2O (see Figure 2-5). Depending on the kind of pretreatment used, the more fragile hemicellulose structure is already partially hydrolyzed, removed or degraded into furfural. For example SO_2 catalyzed steam explosion of softwood chips released 80-90 % of the original hemicellulose content [31]. Polysaccharide hydrolysis can be realized by acid catalyzed hydrolysis or enzymatic hydrolysis. Acid catalyzed hydrolysis can be divided into diluted acid and concentrated acid processes. Hydrolysis with diluted acid (0.7-3.0 % HCl or sulfuric acid) requires high operating temperatures (200-240 °C) and therefore inhibitor compounds are formed, such as sugar degradation products and phenolics, the same as during steam explosion. Concentrated acid hydrolysis results in higher yields of glucose, less inhibitors, but requires high amounts of acids and becomes uneconomical when acid recycling is taken into account [32]. Another downside is the lack of reaction specificity and the formation of byproducts [19]. While the reagents are cheap, corrosive conditions require investment in specific reactors.

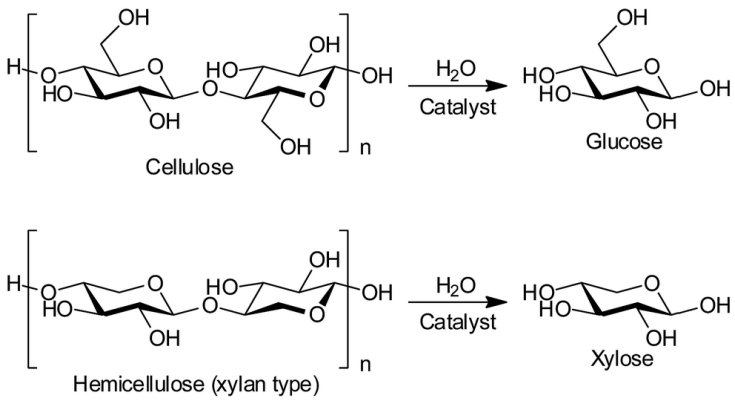

Figure 2-5: Reactions schemes during catalytic (hemi)cellulose hydrolysis [33].

Enzymatic hydrolysis demands less energy and milder reaction circumstances; furthermore, there is no formation of inhibitors throughout this method. The reaction rate is generally lower than that of acid hydrolysis, and enzymes are strongly inhibited by free sugars. Cellulolytic enzymes are being produced most commonly by fungi (e.g. *Trichoderma reesei*), but also by other microorganisms and they are performing synergistic degradation of celluloses and hemicelluloses [4], [5]. The cellulose hydrolyzing enzymes (cellulases) include endo-β-glucanases (endoglucanases), cellobiohydrolases (exoglucanases) and β-glucosidases (see Figure 2-6). The endoglucanases catalyze random cleavage of the internal glycosidic bonds, reducing the degree of polymerization. The cellobiohydrolases only catalyze cleavage at the reducing or non-reducing ends of the cellulose chain, releasing cellobiose (glucose β(1→4) glucose). The β-glucosidases are specifically active on cello-oligosaccharides and cellobiose, and catalyse hydrolysis of non-reducing chain ends with release of glucose [34]. Hydrolysis enzymes are inhibited by inhibitors formed during pretreatment, as also fermentation is.

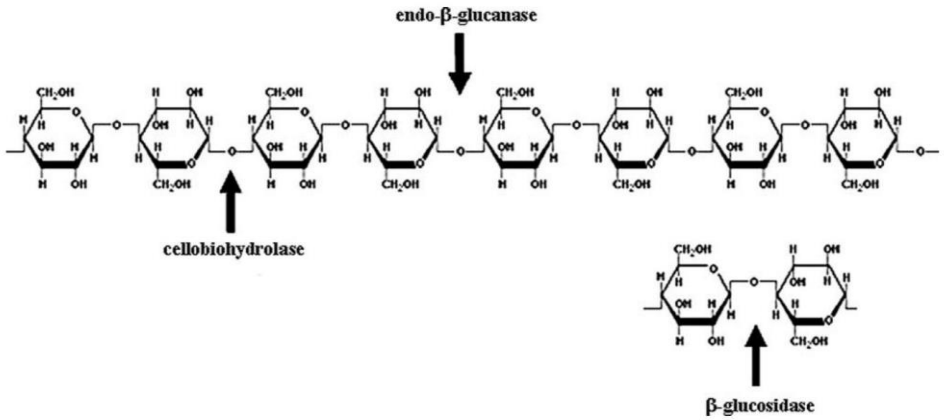

Figure 2-6: Different enzymatic reactions during cellulose hydrolysis by cellulase enzyme mixture [34].

Effective enzymatic hydrolysis of hemicellulose requires a larger number of enzymes because hemicellulose has a more complex composition compared to cellulose, including endo-1,4-β-xylanase, β-xylosidase, α-glucuronidase, α-L-arabinofuranosidase and acetylxylan esterase [35]. There are also some enzymes capable to react with the lignin structure; these will be discussed more in detail later. A summary of the different enzymes that can play a role in hydrolysis is given in Table 2-3.

Table 2-3: Some of the main enzymes required to degrade lignocellulose [35].

Lignin	Laccase, Manganese peroxidase, Lignin peroxidase
Pectin	Pectin methyl esterase, pectate lyase, polygalacturonase, rhamnogalacturonan lyase
Hemicellulose	Endo-xylanase, acetyl xylan esterase, β-xylosidase, endo-mannanase, β-mannosidase, α-L-arabinofuranosidase, α-glucuronidase, ferulic acid esterase, α-galactosidase, *p*-coumaric acid esterase
Cellulose	Cellobiohydrolase, endoglucanase, β-glucosidase

2.3.3 Fermentation

During the fermentation step, the simple sugars are converted to the desired products, i.e., ethanol or lactic acid, by using microorganisms, mainly bacteria or yeasts. The three most important parameters defining the fermentation economy are the final titer, the carbon yield and the volumetric productivity. The titer, the final product

concentration, strongly affects the purification costs of the products; this is often considered the most important parameter of the three. The carbon yield defines the ratio of the substrate carbon that is converted to valuable product. Both incomplete fermentation and side product formation will decrease this number, thus increase the substrate costs for a given mass of final product. The volumetric productivity will define the fermenter volume needed for a certain product mass flow, thus influencing CAPEX. In case of lignocellulosic hydrolyzate, fermentation resistance to inhibitors is also an important microbial parameter, which will influence the productivity and/or titer. Choosing the right pH in lignocellulosic fermentation processes is highly determinative for the growth. The explanation is that weak acids in the non-dissociated form, i.e., at low pH, can hinder cell growth (see Section 2.4.1.1) [4], [36].

For enhancing the product yield and improving the efficacy of the fermentation procedure, diverse feeding patterns are employed. The methods are usually classified into three main groups, i.e., batch, fed-batch and continuous operation, that are presented in the following subsections. The proper adaptation of a convenient strategy depends on several different matters, for example, the maximum specific growth rate of microbes, the lignocellulosic feedstock type and financial aspects are important to take into consideration when a suitable fermentation strategy is being designed. Selecting the correspondent technique is crucial for reaching high productivity [36].

Fermentation strategies can also be divided based on the simultaneous operation of the different process steps. Separate hydrolysis and fermentation (SHF) is the conventional and the most widely spread way. If hydrolysis and fermentation are accomplished in the same vessel in a combined step, it is called simultaneous saccharification and fermentation (SSF) (See Figure 2-7). There are several advantages of this overlap, such as the organism applied for the fermentation immediately consumes the formed sugars, while reducing end-product enzyme inhibition and CAPEX. The fermenting microorganism (or another microorganism next to the fermenting microorganism) can also produce cellulolytic enzymes simultaneously; this is perhaps the newest technology. The setup is called consolidated bioprocessing (CBP), and furthermore it reduces enzyme costs by avoiding enzyme product purification/concentration and transporting costs [37].

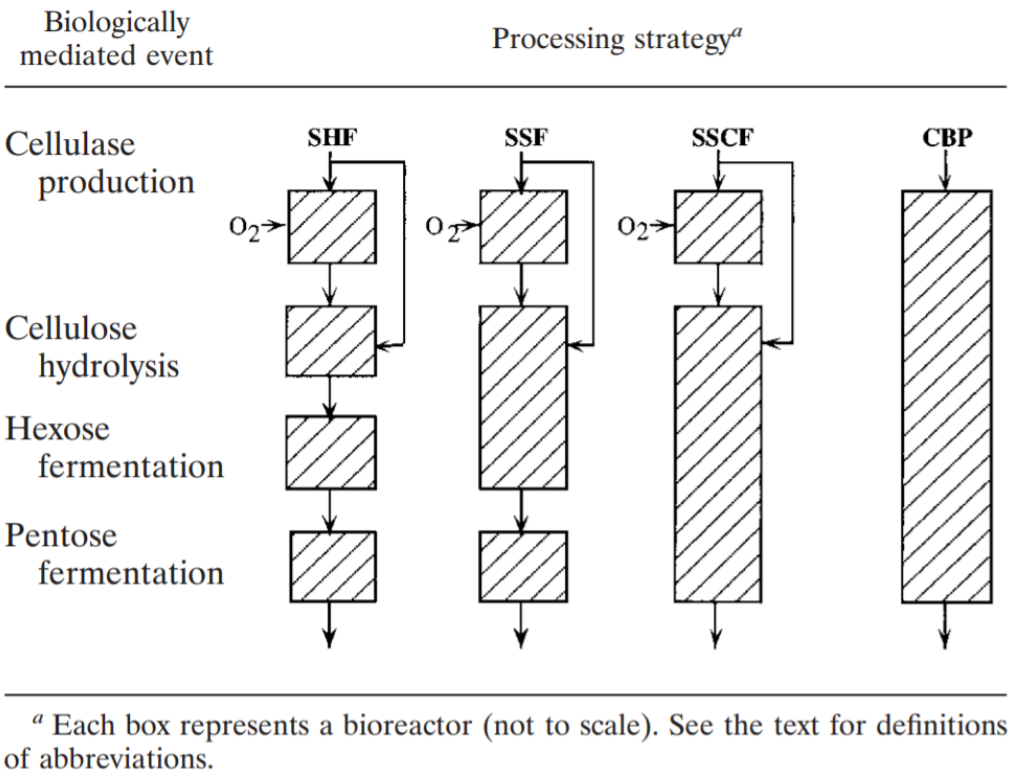

Figure 2-7: The route from raw material to bioethanol product [38]. SHF is the abbreviation for separate hydrolysis and fermentation, SSF for simultaneous saccharification and fermentation, SSCF for simultaneous saccharification and co-fermentation, CBP for consolidated bioprocessing.

2.3.3.1 Microorganisms

As the doctoral research will focus on fermentations to produce ethanol and lactic acid, an overview will be given about the possible microorganisms for this specific purpose.

Ethanol

For the fermentation of hexose sugars from lignocellulosic derived hydrolyzates, ***Saccharomyces cerevisiae*** (also known as baker's yeast or brewer's yeast) appears to be the most preferable, applicable and widely used yeast. It seems to be the least sensitive among other evaluated microorganisms (also compared to bacteria), due to its great tolerance to toxic compounds, high osmotic pressure and high end-product concentrations (which are diverse in different strains). In addition, it shows high carbon yield (close to the theoretical maximum) and one of the highest titers applied

for fermentation to bioethanol. Generally, *S. cerevisiae* is applied in industrial fermentations including sucrose, starch and cellulose based fermentations, it converts pyruvate yielding from the glycolysis cycle to ethanol through acetaldehyde (See Figure 2-8, the pathway starting from glucose). The main disadvantage of *S. cerevisiae* is the fact that it is incapable of converting pentose sugars (e.g. D-xylose, L-arabinose) [36], [39], [40]. However genetically engineered species can be capable to ferment pentoses too, more concretely *S. cerevisiae* TMB3400 strain was modified by introducing xylose reductase, xylitol dehydrogenase and xylulokinase from *P. stipitis* (See Figure 2-8, pathways starting from xylose) [41]. As a result it could ferment xylose, however it is known that high glucose amounts inhibit xylose uptake due to shared transport systems [42]. Best xylose utilization rates were achieved by fed-batch fermentation, constantly feeding glucose rich hydrolyzate to the fermentation, keeping glucose at low concentration [43]. Another option for xylose conversion is to co-culture *S. cerevisiae* with a xylose utilizing yeast like *Candida shehata* [44].

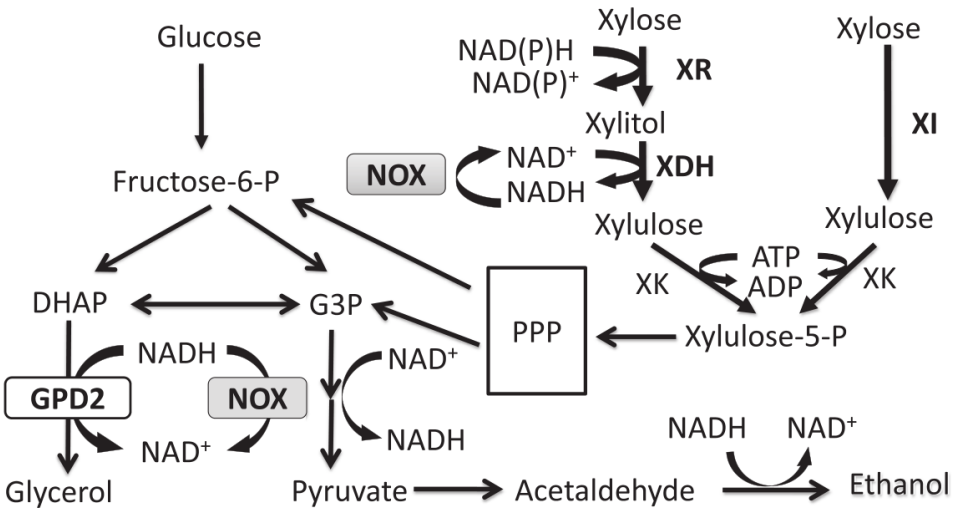

Figure 2-8: Glucose and xylose metabolic pathways in recombinant S. cerevisiae [45]. PPP=pentose phosphate pathway, XR=xylose reductase, XDH=xylitol dehydrogenase, XK=xylulose kinase, XI=xylose isomerase, NOX=NADH oxidase, DHAP=dihydroxyacetone phosphate, GPD2=glycerol-3-phosphate dehydrogenase 2, G3P=glycerol-3-phosphate.

After 2-3 days at 25 °C incubation in agar free medium containing malt extract, the cells are generally globose (3-8 × 5-10 µm), round shaped or ovoid, appearing in single or in small clusters, sedimenting. On agar plates the surface is usually flat, cream-colored, opaque and smooth [46].

Scheffersomyces stipitis is an ascomycetous yeast that was isolated from wood infesting insect larvae and their frass, from the guts of beetles and rotten wood. A symbiotic relationship can be considered between *S. stipitis* and beetles at their habitat, probably insects have benefits by metabolizing D-xylose. The yeasts' natural habitat is mostly located in Europe, North and Central America. In literature it is common to use the name *Pichia stipitis*, although lately the genetic analysis of the sequence showed that *Scheffersomyces stipitis* strain is only distantly related to the genus *Pichia* [47].

Cells usually appear as ovoid or spherical form, sometimes in pairs but generally single and they are reaching an average size around 2-6 μm. The colonies form cream-colored, round shaped humpy units. Commonly the surface of the colonies is smooth, although it can be matt or glazing. *S. stipitis* is able to ferment glucose, maltose and trehalose but primarily it is applied and known for fermenting D-xylose efficiently and relatively rapidly to ethanol. The metabolic application consists of two oxido-reductive steps for the utilization of xylose such as degradation with xylose reductase and xylitol dehydrogenase enzymes [46], [47]. *Scheffersomyces stipitis* is capable of fermenting both xylose and glucose to ethanol (through the pathways shown in Figure 2-8) with high ethanol yield achievement by converting xylose. It is acknowledged that ethanol yields can reach ~0.41 $g/g_{substrate}$, although it varies according to reaction circumstances [46], [48].

Other strains, investigated before for ethanol fermentation, are pentose fermenters, like *Scheffersomyces stipitis* or capable to grow at higher temperatures compared to *Saccharomyces cerevisiae*. Pentose fermenting microorganisms include *Candida guilliermondii*, *Candida shehatae*, and *Pachysolen tannophilus* [47]. Heat tolerant microorganisms include *Trichoderma viride*, *Clostridium thermocellum*, *Bacillus sp.* [47] and *Kluyveromyces marxianus* [49].

Lactic acid

Bioconversion of hemicellulosic sugars to lactic acid requires a strain that is capable of fermenting sugar mixtures of hexoses and pentoses to maximize the product yield. Genetically engineered strains can efficiently utilize both five-carbon and six-carbon sugars. However the recombinant cells involved have a tendency to become genetically unstable on repeated application [50]. Out of a screening of 296 tested

Lactobacillus and *Pediococcus* strains three isolates were found to be resistant to the inhibitory compounds, and able to metabolize xylose and arabinose [51]. These strains are *L. pentosus, Pediococcus acidilactici* and *Pediococcus pentosaceus*. Since these strains are not genetically engineered, they are also more favorable in the public opinion. Lactic acid bacteria (LAB) are found in various environments ranging from the human intestinal tract to decaying plant material in the soil. Especially the latter makes them interesting as efficient utilizers of lignocellulosic biomass. Their ability to grow anaerobically at relatively low pH values makes them even more attractive. Within the *Lactobacillales*, as the lactic acid producing bacteria are formally called, *lactobacillus* is a very diverse genus with over 150 species displaying a wide range of catabolic activities [51]. The versatility of *Lactobacillus pentosus* makes it a potential alternative to genetically modified strains.

Lactic acid bacteria ferment sugars via different pathways resulting in homo-, hetero- or mixed acid fermentation. Homofermentation results in only lactic acid as the product of glucose metabolism and the Embden-Meyerhof-Parnas (EMP) pathway is used (see Figure 2-9). In heterofermentation, equimolar amounts of lactic acid, carbon dioxide and ethanol or acetate are formed from glucose via the phosphoketolase pathway (see Figure 2-10). The ratio of ethanol and acetate formed is dependent on the redox potential of the system. This pathway is used by facultative heterofermenters, for the fermentation of pentoses, and for the fermentation of hexoses and pentoses by obligate heterofermenters [52]. *Lactobacillus pentosus* ferments hexoses using the Embden-Meyerhof-Parnas (EMP) pathway to lactic acid, the so-called homolactic fermentation. Pentoses are fermented to lactic acid and acetic acid using the phosphoketolase (PK) pathway, the so-called heterolactic fermentation [53]. Heterolactic fermentation, which is used by most LAB, extends the range of usable sugars, but results in the production of acetic acid alongside other by-products such as ethanol and formate. This will result in a lower overall lactic acid yield. With appropriate actions such as buffering or simultaneous detoxification, the yield can be somewhat increased. Some LAB and other bacteria such as *Bacillus coagulans* use the pentose phosphate pathway to convert pentoses to lactic acid homofermentatively, resulting in over 90 % conversion of xylose to lactate with a theoretical yield of 3 mol xylose to 5 mol of lactate without carbon loss [17], [54], [55]. The EMP pathway is therefore the better choice for increasing lactate yield [56]. In the presence of oxygen, *Lactobacilli* also ferment glucose to lactate. Upon depletion of glucose, previously produced lactate is further metabolized to acetic acid. During this

process hydrogen peroxide, carbon dioxide and ATP are produced. This is unfavorable and would result in a higher lactic acid purification cost [55].

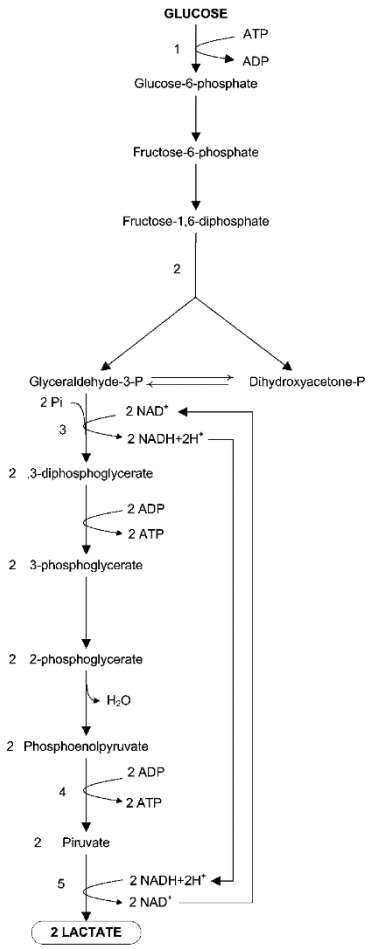

Figure 2-9: Bioconversion of glucose to lactic acid via Embden-Meyerhof-Parnas pathway [57].

Most lactic acid bacteria produce only one isomeric form of lactic acid, but sometimes there is a slight production of the other isomer. The lactate dehydrogenase (LDH) enzyme is stereospecific, giving either D- or L- lactic acid. The product specificity of the enzyme present in the applied lactic acid strain determines the isomerism of the produced lactic acid [52].

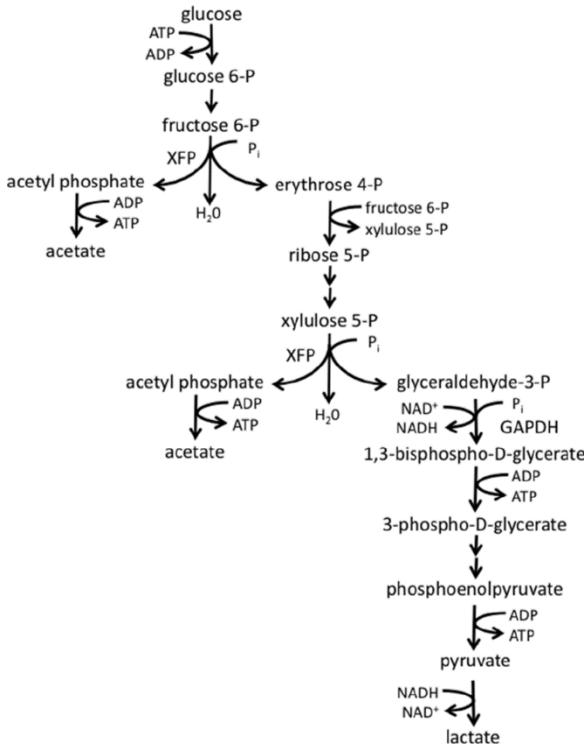

Figure 2-10: Bioconversion of pentoses to lactic acid via phosphoketolase pathway [58]. XFP=xylulose 5-phosphate phosphoketolase, GAPDH=Glyceraldehyde 3-phosphate dehydrogenase.

The produced lactic acid acts as a product inhibitor, mainly because of the pH decrease. In general, the optimal fermentation pH is between 4.5 and 7 [59]. Trapping the lactic acid produced during fermentation as calcium lactate by the addition of $Ca(OH)_2$ or $CaCO_3$ to the fermentation results in higher yields. The addition of $CaCO_3$ can also be used for passive pH control as carbonate can work as a buffer [52]. The use of $Ca(OH)_2$ can be more difficult as it is actively reducing the pH, but by constant pH monitoring and addition, the pH can be kept precisely.

Lactic acid bacteria have complex nutrient requirements, due to their limited ability to synthesize B-vitamins and amino acids. Addition of these nutrients to the lignocellulose hydrolyzates provides a higher product yield. These nutrients can be found in peptone, meat extract and yeast extract that are present in synthetic MRS growth media. Corn steep liquor or wheat bran extract can be a cheap alternative for these nutrients [52], [59]. Additional minerals as $MgSO_4 \cdot 7H_2O$, KH_2PO_4, sodium citrate,

NaCl, and sodium succinate, sodium sulfate, sodium acetate, K_2HPO_4, $MnSO_4 \cdot 4H_2O$ and $FeSO_4 \cdot 7H_2O$ can also have significant effect.

2.3.3.2 Simultaneous saccharification and fermentation (SSF)

There are some good reasons to combine the above-mentioned steps into one unit operation. From a kinetic point of view, the SSF is interesting. It has the advantage of sugar consumption during cellulose hydrolysis that results in less product inhibition for cellulase. Since the availability of sugars for microbial conversion is a rate determining step [60], repressing the feedback inhibition on hydrolysis can increase the hydrolysis rate, the reactor's yield and the productivity. Because there is less inhibition, lower enzyme loadings can be used as well. The equipment costs are lowered because of the simpler process design.

Besides these positive effects, the process has some known drawbacks as well. The major disadvantage of the SSF lies in the different optimal temperature and pH of saccharification and fermentation [61]. In general, the optimal temperature for hydrolyzing enzymes lies at 50 °C and below pH 5. Lactic acid fermentation however is generally efficient around 40 (37-43) °C and at a pH range around 5-7 [52]. For example, Novozymes Cellic CTec3 cellulase cocktail has highest activity at 53-55 °C, at 45 °C it is only 78 % of the maximal value, 65 % at 40 °C, 57 % at 37 °C, 50 % at 35 °C, 40 % at 30 °C [62]. Temperature is crucial.

Thermotolerant LAB are currently being studied. Their utilization could potentially increase the fermentation temperature to the enzymatic optimum. Successful fermentations by *Bacillus coagulans* have already been reported [63], [64]. Inhibitory effects of lactic acid upon cellulase have been reported. These effects are much lower than feedback inhibition caused by glucose [65]. In case of ethanol fermentation the temperature difference is even bigger as *Saccharomyces cerevisiae* goes through cell deactivation above 35-37 °C [66]. *Saccharomyces cerevisiae* SSF experiments are conducted at 35 °C for both wild types [49], [67] and genetically engineered, xylose fermenting types [68], [69]. *Kluyveromyces marxianus* was successfully utilized for lignocellulose based SSF at 42 °C [49].

SSF is typically performed in the range of 10-15 m/m% dry solid substrate loading [27], [70] with a few examples going up to 30 m/m% [28], [71]. This high solid loading mixture requires special mixing in most of the cases. Here it should be noted that in

case of extreme high solid content experiments even some traditional calculations, like ethanol/lactate content should be reconsidered [72].

2.3.3.3 Consolidated bioprocessing (CBP)

Consolidated bioprocessing (CBP), compared to SSF, also incorporates cellulase enzyme production by the microbial culture in the fermenter (See Figure 2-7) [73]. The CBP technology has all the benefits of on-site enzyme production, no purification, stabilization, bottling or transportation costs, and further lowers costs by avoiding CAPEX related to enzyme production infrastructure. Although it is very appealing in theory, the implementation is questionable, as it would require integrating aerobic and aerobic processes together and complex gene engineering [74]. Microorganisms suitable for CBP are not known currently, two paths are investigated: either introducing cellulolytic microbes with genes related to valuable product formation, or introducing cellulolytic genes to microbes producing the desired product [73].

2.3.4 Downstream processing

Ethanol

After fermentation, a separation from water and purification of the main product is necessary and indispensable. The implemented method is a two-step fractional distillation. The concept of the separation is based on the volatility of azeotropic mixtures. Boiling of the mixture makes ethanol evaporate at 78.3 °C, and it can be converted to vapor in a rectification column and condensed to 95 % alcohol. The water remains with the solid parts in the residue. In large industrial utilization, further purification by continuous distillation is employed by using at least two columns, first to separate all the ethanol from the crude broth (here the most important is to remove all ethanol), the further columns are used to purify and separate the ethanol from the relatively clean water-ethanol mixture (here purity and recovery are both important). Lignin can be found in the residue and consumed as an energy source for the whole procedure by burning it. At the end of the distillation process the expected result is near to the azeotropic point of the water-ethanol mixture (95.5 m/m%), which can be further purified by adsorption on zeolite or ternary distillation and used afterwards as fuel either pure or mixed with gasoline [4], [5], [75].

Lactic acid

As lactic acid is non-volatile (boiling point at 122 °C), distillation could not be used as purification process. In the first step, a filtration is needed to remove all insoluble compounds. If this is done after a short treatment at pH 10 and elevated temperature, most of the protein content is precipitated, cells killed, while the sugar residues and part of the inhibitors are degraded, leading to a simpler post processing [59]. Further steps usually require evaporation of the solvent and volatile compounds. An active carbon treatment is often needed at the end to achieve a transparent product [76]. The traditional method then converts the salt to free acid by the addition of sulfuric acid, and parallel gypsum formation. This corresponds to a big portion of the costs, so alternative methods are also developed, like electrodialysis, extraction [77], adsorption, or industrial scale ion exchange chromatography. The final step is crystallization in most of the cases [78]–[80].

2.4 Detoxification

2.4.1 Inhibitor formation

During the pretreatment of lignocellulosic materials, which is explained in Section 2.3.1, various inhibitory substances are formed (see

Figure 2-11). These by-products can be grouped, based on their structure in weak acids, furan derivatives, phenolic compounds and heavy metal ions, and based on their origin in sugar/lignin degradation products and fermentation products. The inhibitors are negatively affecting the subsequent hydrolysis and fermentation step by inactivating enzymatic and microbial bioconversion processes, thus limiting substrate consumption and attenuating conversion kinetics.

The amount and type of formed inhibitors are dependent on the source's cell wall composition, on pentose, hexose and lignin degradation and on thermo-chemical circumstances [81]–[83]. Furthermore, the toxic effect of the inhibitors can increase or decrease depending on the fermentation conditions such as pH and oxygen concentration of the medium, cell physiological attitude and the synergies between inhibitors [84]. Reported inhibition examples are visible in

Table 2-4. The inhibition mechanism can be very different; it mainly depends on the type of the inhibitor (see Figure 2-12).

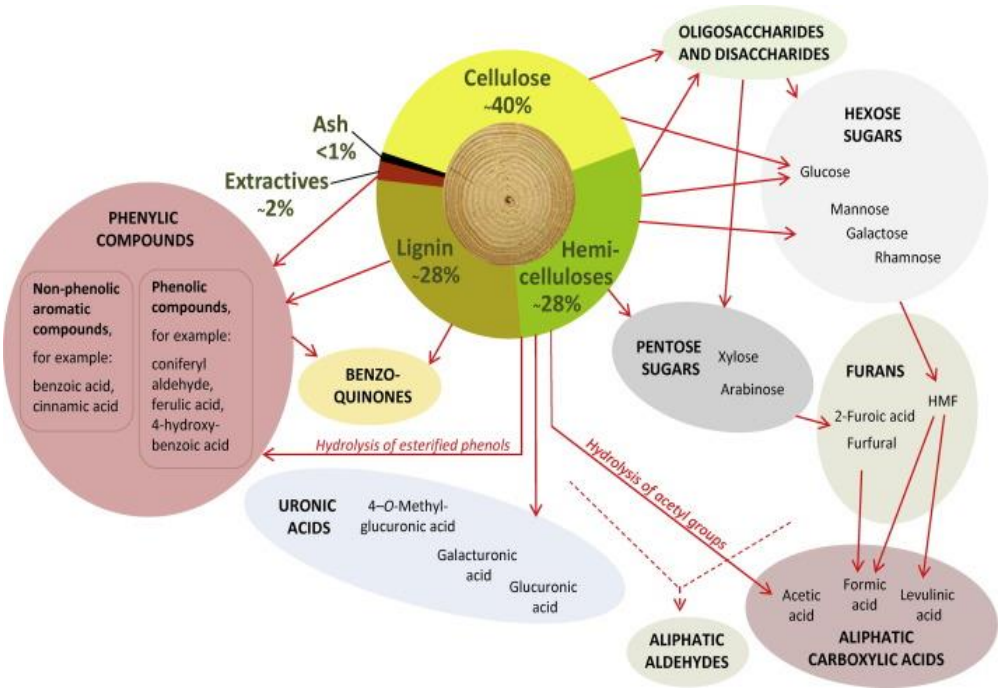

Figure 2-11: Inhibitor formation pathways during pretreatment [85].

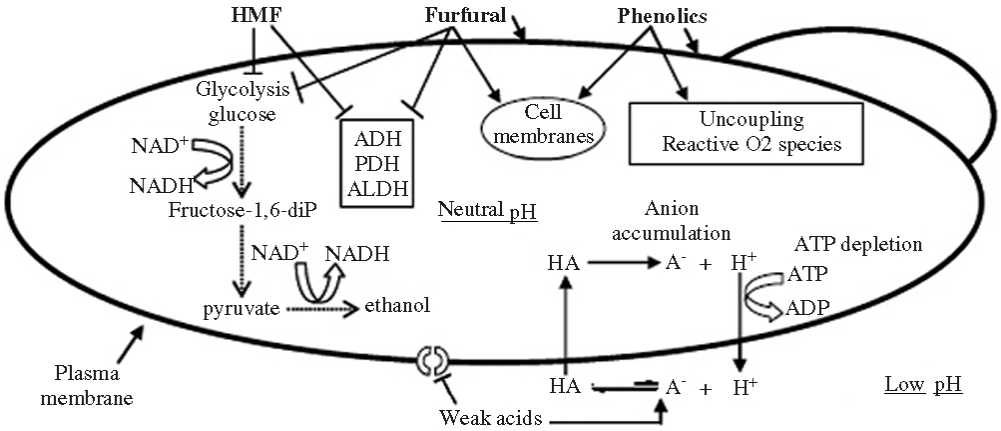

Figure 2-12: Inhibition mechanisms of formed toxic compounds on cell level [86]. ADH=alcohol dehydrogenase, PDH=pyruvate dehydrogenase, ALDH=aldehyde dehydrogenase.

Table 2-4: Influence of inhibiting compounds on the fermentation with different microorganisms [6].

Group of inhibitors	Inhibitor	Conc. (g/l)	Microorg.	Percent of growth (g) or fermentation (f) inhibition*
Deacetylation	Acetic acid	1.4	*S. cerevisiae*	50 (f)
		4.3	*S. cerevisiae*	50 (f)
		8.0	*S. stipitis*	98 (f)
		8.0	*S. stipitis*	25 (f)
Sugar degradation products	Furfural	1.0	*S. stipitis*	47 (g)
	HMF	3.0	*S. stipitis*	69 (g)
Lignin degradation products	Cinnamaldehyde	1.0	*S. cerevisiae*	100 (f)
	Hydroxybenzaldehyde	0.4	*K. pneumoniae*	68 (g)
	Hydroxybenzaldehyde	1.0	*S. cerevisiae*	48 (f)
	Syringaldehyde	0.5	*K. pneumoniae*	40 (g)
	Syringaldehyde	0.22	*S. stipitis*	72 (f)
Fermentation products	Acetaldehyde	5.0	*S. cerevisiae*	80 (g)
	Ethanol	120	*S. cerevisiae*	100 (g)
	Formic acid	2.7	*S. cerevisiae*	80 (g)
	Lactic acid	38	*S. cerevisiae*	80 (g)
Heavy metal ions	Chromium	0.1	*P. tannophilus*	95 (f)
	Copper	0.04	*P. tannophilus*	29 (f)
	Iron	0.5	*P. tannophilus*	45 (f)
	Nickel	0.05	*P. tannophilus*	92 (f)

***Growth inhibition means decrease in cell concentration; fermentation inhibition means decrease in product concentration.**

2.4.1.1 Weak acids

Levulinic acid, acetic acid and formic acid are weak organic acids which are forming during the degradation of carbohydrates, while acetic acid can also be formed by detachment of acetyl groups from hemicellulose and lignin structure. The alluded acids are not that severely toxic compared to furan derivatives or phenolic compounds, but can be present in high concentrations [83], [87]. Since acetic acid is mostly formed during hemicellulose hydrolysis, its presence is unavoidable and strongly dependent on the biomass source, while the degraded acids concentration depends on the severity of the pretreatment. Softwoods have typically low acetyl content, while in hardwood and agricultural residues the content is higher. This can be especially

hindering at high solid content, because in that case, up to 10-15 g/l acetic acid can be present [85].

Weak acids inhibit the growth of the microorganisms; this is why they are used as food preservatives. There are two main mechanisms interfering on the metabolic level of the microorganism (see Figure 2-12). One is the depletion of ATP by plasma membrane proton pumps [88], [89], while another is the acidification of the medium. Both effects are connected and will be explained here. A weak acid in a relatively acidic environment exists in its protonated form. Since it has no charge, it can diffuse through the microorganism's outer membrane. The rate at which this happens is related to the lipophilicity of the acid. The molecule deprotonates while it enters the cytosol, as the cytosol has a higher pH. The internal pH is buffered to some extent, but acidification of the cytosol occurs at higher proton concentrations. To restore the internal pH, trans-membrane pumps will cause a net efflux of protons consuming ATP in the process. In the meantime ATP supply is limited by acid inhibition of the glycolysis [90]. A third suggested mechanism of inhibition is the intracellular accumulation of anions. Depending on the type of anion, accumulation can result in either inhibition of ATP generating processes or a lower proton efflux due to electrostatic effects in the cell. The type of action depends on the combination of inhibitors and the intensity of energy consumption, trans-membrane activity and metabolic inhibition [91]. In low concentrations, however, it can be beneficial by increasing ATP generation at the expense of biomass formation [85].

Model experiments performed by several research groups, demonstrated that the toxicity varies with the concentration and the composition of inhibitors as there are synergistic effects between them. At low concentrations, the presence of the inhibitors can be even beneficial to the fermentation, e.g., xylose-xylitol bioconversion can be improved in the presence of up to 1 g/l acetic acid, while, on the contrary, 3 g/l denotes high inhibitory effect for bioethanol production. The conclusion of the project was that at pH 5.5 the ethanol yield can be increased with low acid concentrations (<100 mmol/l), whereas higher concentrations (>200 mmol/l) clearly show an inhibitory effect [83], [84].

2.4.1.2 Furan derivatives

Furfural (2-furaldehyde) and HMF (5-hydroxymethyl-2-furaldehyde) are the main representatives of furan derivatives, formed by the dehydration of pentoses and hexoses respectively. The ratio of the inhibitors varies in accordance to the

pretreatment process type/conditions and the initial raw material type. HMF usually appears in higher concentrations and has less inhibitory effect in comparison with furfural. They are decreasing the ethanol production by blocking ADH (alcohol dehydrogenase), PDH (pyruvate dehydrogenase) and ALDH (aldehyde dehydrogenase) or by inhibiting the growth of the microorganisms, or they can cause a longer lag phase (see Figure 2-12). Furans, in synergism with acetic acid, can strongly inhibit the growth of *Scheffersomyces stipitis* [81], [86]. Although in pursuance with another experiment, furfural and HMF were less toxic to *Scheffersomyces stipitis* than lignin degradation products (aromatics) [92].

The fermentation of furfural generates high yields of furfuryl alcohol that causes inhibition on the aerobic growth of *S. stipitis,* but shows only a slightly detectable influence on the growth of *S. cerevisiae*. *S. cerevisiae* can metabolize furfural in both aerobic and anaerobic conditions and it is reported to be adaptive to furfural in batch, fed-batch and continuous cultures as it showed increased growth and ethanol yields [83]. Typical concentrations of furan degradation products are under 1.5 g/l, usually around 0.5-0.05 g/l [27]. At higher severity, temperature and treatment time, furans degrade further towards levulinic and formic acid [85].

2.4.1.3 Phenolic compounds

A wide range of toxic chemical products is released during the degradation of lignin, such as aromatics, polyaromatics and phenolics. These lignin derived toxic compounds have considerable effects on biological membranes, which main function is that of a selective diaphragm, including the increase of the fluidity, which goes hand in hand with the loss of the membrane structure's integrity [49]. Phenolic compounds with low molecular weight are reckoned the most toxic compounds on the fermentation of steam exploded lignocellulosic hydrolyzates. The total phenolic content showed to have a high inhibitory effect on the cell growth, sugar assimilation and, as a result, the product yield. Their inhibition effect is much higher than the inhibitors discussed in the previous sections, but their concentration is significantly lower [85]. Table 2-5 shows measured phenolic inhibitor concentrations in autocatalyzed steam exploded (205 °C and 10 min) hydrolyzate at 50 % dry content [93]. Calculating to 10 % dry content, assuming that everything else remains the same, the sum concentration would be 1.35 g/l. A connection between functional groups and toxicity is most probable, but synergistic effects also appear [94].

Table 2-5: Example phenolic inhibitor concentrations in autocatalyzed steam exploded poplar wood [93].

	Weight/dry poplar weight [%]	Percent [%]
p-Hydroxybenzoic acid	0.55	40.7
Syringic acid	0.37	27.4
p-Hydroxybenzaldehyde	0.29	21.5
Vanillin	0.05	3.7
m-Hydroxybenzoic acid	0.04	3.0
Cinnamic acid	0.03	2.2
Vanillic acid	0.02	1.5
Sum	1.35	100.0

Phenolic compounds can appear in three basic variations: acidic, ketone and aldehyde forms (e.g. vanillic acid, syringic acid, vanillin and syringaldehyde) [87], [92]. Several articles proclaim that hydrolyzates from softwood (e.g., spruce, red oak and pine) contains higher amount of vanillin and vanillic acid generated from the decomposition of guaiacylpropane units of lignin. Generally hardwood hydrolyzates consist mainly of syringaldehyde and syringic acid, which are forming through the degradation of syringyl propane units [83]. The biomass source specifies the type of phenolic compounds formed, since lignin has diverse degrees of methoxylation, internal bonding and conjunction with hemicellulose and cellulose in the cell wall of plants. Based on the position of the substituents the degree of the compound's inhibition can vary. Substituents in ortho position are increasing the inhibitory effect, while methoxyl and hydroxyl in meta- and para-position do not seem to have any effect on the toxicity levels of the compounds. The mechanism of the inhibition on *Saccharomyces cerevisiae* and other eukaryotic microorganisms has not been properly clarified because of the heterogeneity of the compounds and the lack of adequate and dependable analytical methods. Although, in general, ketones and aldehydes have a higher inhibitory effect for *S. cerevisiae* and *E. coli* than acids [95].

According to the investigation of Klinke et al., the presence of phenolics, even in small concentrations such as 0.1 g/l is lethal to microorganisms [96]. The effect of model inhibitors on sugar consumption was measured for different types of ethanol producing microbes. Vanillin is deemed the strongest inhibitor (1 g/l) in both xylose and hexose fermenting yeasts, inhibiting cell growth and final ethanol titer. Villa et al. demonstrated that 0.1 g/l phenolic inhibitors may withdraw the intake of xylose that inflicts *C. guillermondii* to produce xylitol [97]. Tran and Chambers proved that the model and inhibitory molecules for *Scheffersomyces stipitis* can be arrayed in a queue

as the following: pelargonic acid (C9) > caprylic acid (C8) > caproic acid (C6) > vanillin > syringaldehyde > vanillinic acid > syringic acid [98].

2.4.1.4 Heavy metal irons

The applied microorganisms can be slightly inhibited by heavy metal ions such as chromium, iron, nickel and copper. These ions are originating from the corrosion of the hydrolysis equipment vessels. Watson et al. demonstrated that 60 % reduction of cell growth took place when 100 mg/l concentration of nickel ions were added into the model medium for *P. tannophilus* [99], but these high concentrations cannot realistically appear in the actual process [84]. Overall, it can be said that heavy metal inhibition is negligible.

2.4.1.5 Inhibition of hydrolysis

Besides inhibition on cell growth, fermentation yield, and product concentration, inhibitors can have a significant inhibition on hydrolysis. Unproductive binding to solid parts (lignin, unhydrolyzed hemicellulose) is a common inhibition pathway, which could be decreased with addition of other protein, e.g. serum albumin [85]. Soluble compounds can also cause inhibition; best known is the product inhibition by glucose and its dimer. Research showed that other sugars, such as xylose and mannose can also have inhibitory effect [100].

Phenolics are also known to alter enzyme activity, as it depends strongly on their macromolecular conformation. Since hydrophobicity is the main driving force behind enzyme folding and function, it is logical that hydrophobic lignin derivatives (compared to water) have a disturbing influence on their functionality [101]. Ximenes et al. studied the decreased cellulase activity in the presence of phenols when liquid hot water treated maple solid concentrations were higher than 10 g/L [102], [103]. They concluded that the strength of inhibition or deactivation is dependent on the type of enzyme, the microorganism where the enzyme comes from and the type of phenolic compounds present. They examined the inhibition effect of vanillin, syringaldehyde, trans-cinnamic acid and 4-hydroxybenzoic acid on cellulase (Spezyme CP) + β-glucosidase (Novozyme 188), β-glucosidase (Spezyme CP) and β-glucosidase (Novozyme 188) (see Table 2-6) [103]. Cavka and Jonsson concluded that reducing the phenolic inhibitors in spruce hydrolyzate with sodium dithionate or sodium sulfite improved hydrolysis yield, while reduction with sodium borohydride did not, indicating that the enzyme inhibition is mainly from hydrophobicity rather than reactivity [104].

Table 2-6: Ranking of the inhibitory effect of phenolic compounds on the hydrolysis of cellulose and cellobiose [103].

Phenolic compound	Vanillin	Syringaldehyde	Trans-cinnamic acid	4-hydroxybenzoic acid
Inhibition of cellulase (Spezyme CP) + β-glucosidase (Novozyme 188)	4	3	2	1
β-glucosidase (Spezyme CP)	3	2	1	4
β-glucosidase (Novozyme 188)	1	3	1	4

Inhibition follows the designation of 4>3>2>1, with 4 being the most severe inhibition and 1 being the least. β-glucosidase from Novozyme 188 is not significantly inhibited and it has the ranking of "1" for two of the phenolic compounds shown.

2.4.2 Detoxification techniques

Simplifying and commercializing the conversion of lignocellulosic biomass occurs to be the major challenge [95], [105]. Due to the raw materials used and the conditions employed for the hydrolyzation process, the hydrolyzate composition differs, which plays a significant role in choosing a correspondent and efficient detoxification method. Fermentation from non-detoxified hydrolyzates of hemicellulose can be characterized by slow kinetics with limited carbon yield, final titer and/or volumetric productivity. According to Taherzadeh et al. there are four main different pathways for detoxifying of hydrolyzates [106]. One is to try to eliminate the formation of toxic compounds during the pretreatment. The second is seeking for a convenient strategy to remove or convert the inhibitors to inert compounds in the hydrolyzate before the next step, i.e., the fermentation. The third possibility is to find microorganism species that are resistant to the typical toxic components in the applied hydrolyzate by either adaptation or metabolic engineering. Currently several approaches are presented for detoxification that can be classified into three general groups such as biological, physical and chemical methods [87]. The employed detoxification processes are required to be susceptible to remove the inhibitors selectively, to be affordable and to be easily utilizable in the whole process [36].

2.4.2.1 Physical detoxification

Detoxification by physical routes is rather simple and easy to scale. Evaporation, rota-evaporation, vacuum evaporation and membrane-based separations are the typical

physical detoxification methods mentioned in literature. **Evaporation** techniques can be used to decrease the amount of volatile toxic components of the hydrolyzate (e.g., vanillin, furfural, acetic acid). Diminishing the volume of wood hydrolyzate with 90 % by the usage of vacuum evaporation, a complete detoxification of furfural was presented by Larsson et al [107]. Meanwhile this method is proven to increase the concentration of non-volatile inhibitors such as extractives and lignin derivatives which are toxic to microorganisms and interfere with fermentation as alluded beforehand [84], [87]. Membrane techniques (pervaporation) require additional filtration steps and the membrane material itself is usually expensive.

2.4.2.2 Chemical detoxification

The application of chemical methods for improving the bioethanol production process gives several advantages in yield and financial aspects. The group of chemical methods includes alkali treatment (NaOH, Na_2SO_3, NH_3), over-liming with $Ca(OH)_2$, activated charcoal treatment and ion exchangers (anionic, cationic). The alluded routes are based on precipitation of the inhibitors and the ionization of toxic compounds by adjusting to certain pH values. Adsorption of toxic compounds can take place by activated charcoal (cost-effective), diatomaceous earth and ion exchange resins (the most effective but expensive). The effect of detoxification by **over-liming** has already been introduced in 1945 by Leonard and Hajny by increasing the pH with $Ca(OH)_2$ to 9-10 and resetting it to 5.5 with H_2SO_4 [108]. The detoxification occurs due to the instability of toxic components in the hydrolyzate at high pH level, moreover many decomposition products precipitate, decreasing the osmotic stress. According to the review of Palmqvist et al., applying **sodium sulfite** or higher amounts of cell inoculum shows decreasing values of HMF and furfural concentrations, although acetic acid concentration stagnates. Combining sulfite treatment with over-liming resulted the highest yields in case of willow hydrolyzate fermentation with recombinant *Escherichia coli* [36].

Charcoal treatment is a very effective method, removing a wide variety of inhibitors from the liquid fraction (XRF) by adsorption on activated carbon (=charcoal). The effectiveness of the charcoal treatment depends on the pH, contact time, temperature and amount of used charcoal [84]. Compounds are strongly adsorbed to the surface when they are in non-ionized form: weak acids and phenolics at low pH [109].

Mussatto et al. detoxified rice straw hydrolyzate with charcoal treatment at different pH values [110]. At low pH, lignin degradation products (=phenolics) were partly removed without sugar degradation. When the pH is high, the sugar concentration decreased by 30 %. A certain contact time is necessary to reach equilibrium between the adsorbent and adsorbate. During this period, the surface of the activated adsorbent should be completely surrounded by the hydrolyzate containing the adsorbate. When the equilibrium is reached, charcoal cannot adsorb extra toxic compounds anymore. Parajó et al. investigated the effect of contact time between activated charcoal and wood hydrolyzate. At industrially relevant amounts, the maximum amount of phenolics adsorbed was reached after only 20 minutes [111]. Higher temperatures cause a faster adsorption of compounds on activated charcoal, because the rate of diffusion of toxic compounds in the hydrolyzate to the surface of the charcoal is faster compared to lower temperatures. Mussatto studied the effect of temperature on adsorption of rice straw hydrolyzate on activated charcoal. Lignin degradation compounds were adsorbed at 25 °C and 45 °C, and removal was six times faster at 45 °C [110].

When increasing the charcoal to hydrolyzate ratio, the inhibitor removal will reach equilibrium, but it was reported that increasing it further can lead to sugar adsorption/removal also: Parojó et al. [111], [112], Silva et al. [113], Lee et al. [114] and Mussatto and Roberto [115]. Silva et al. studied charcoal amounts from 1 % to 30 % on treated sugarcane bagasse: 94 % of the phenolics were removed with only 0.47 % loss of sugar concentration by 1 % charcoal [113].

2.4.2.3 Biological detoxification

Biological routes for detoxification, i.e. biodetoxification, mean the use of microorganisms or specific enzymes that are able to interact with toxic compounds and change their composition (see Table 2-7 for examples) [87]. Treating lignocellulosic hydrolyzate with laccase and peroxidase retrieved from the lignolytic white-rot fungus *Trametes versicolor* indicates higher ethanol yields and increases sugar consumption due to the enzymes impact on phenolic compounds. According to Palmqvist et al. the treatment of the hydrolyzate with laccase enzyme left no phenolic monomers or phenolic acids in the solution, therefore it presented a complete detoxification. The mechanism of detoxifying low molecular weight phenolic compounds with enzymes is likely based on oxidative polymerization and the following precipitation [36], [87].

Table 2-7: Removal rate of inhibitors with different biotechnological methods [87].

Lignocellulosic hydrolyzate type	Applied microorganisms or enzymes	Effect of the method	Ethanol yield
Sugarcane bagasse	Laccase	80 % removal of phenolics	0,18 g/g dry bagasse
	Issatchenkia occidentalis	Reduction of 5-HMF (85 %), furfural (62 %), ferulic acid (73.33 %), syringaldehyde (66.67 %)	-
Spruce	Residue lignin		0.44 g/g
	Continuous fermentation	Continuous flocculating yeast was grown which withstood to inhibitors	0.42-0.46 g/g
Willow	*T. reesei*	Removal of furans, phenols and weak acids	0.44 g/g
	High cell density fermentation	High ethanol productivity was shown likewise in undetoxified hydrolyzate	0.44 g/g
Lignocellulosic hydrolyzate	Peroxidase from *C. cinereus*	100 % removal of p-coumaric acid, ferulic acid, vanillinic acid and vanillin	Butanol: 8.9±0.43 g/l
Corn stover	*Coniochaeta ligniaria*	80 % removal of furfural and 5-HMF	-

Comparing laccase detoxification with anion-exchange treatment, they result in the same decrease in phenolics concentration, i.e., 80 %. However, since a remarkable loss of fermentable sugar has been observed during the latter method, this is not considered a viable route [36], [84], [87], [116].

Biotechnological methods for detoxifying lignocellulosic hydrolyzates have several advantages, though also disadvantage, which can put these techniques in an undesirable position for biorefineries. Comparing to the other detoxification methods, the application of biological routes is beneficial in lower energy requirements and in avoiding the use of chemicals (so achieving milder conditions), which also lowers the abundance of side reactions. Although on the other hand the reaction time is usually long, there is a noticeable sugar loss if a microorganism is used, and the used enzyme is usually inhibitor specific [87].

2.4.2.4 Adaptation

Although, strictly saying, inoculum adaptation is not a detoxification technique, it is somewhat similar to biological detoxification. In general, the microorganism will be more resistant to inhibitors or they will convert them to other, less harmful products. This effect is the same as in case of biological detoxification, just in this case the detoxifying and the producing microbe is the same. Adaptation has been shown to increase *S. cerevisiae* tolerance towards inhibitors during SSF, especially at high solid loadings [117].

2.4.3 Laccase

Laccase is a multi-copper protein, a dioxygen oxidoreductase type of enzyme appearing in a benzenediol form and it can be found in eukaryotes (fungi, higher plants and insects) and lately in prokaryotes too. Fungal laccases are the most common used in literature. Wood-rotting fungi such as *Trametes versicolor, Trametes hirsute, Trametes ochracea, Trametes villosa, Trametes gallica, Cerrana maxima, Coriolopsis polyzona, Lentinus tigrinus* and *Pleurotus eryngii* are typical producers of laccase [118].

Laccases are multicopper oxidases containing four copper atoms, which are classified into three groups: type 1 (blue copper), type 2 (normal copper) and type 3 (antiferromagnetically coupled binuclear copper pair). Type 2 and type 3 copper centers are grouped to form a trinuclear copper cluster [119], [120]. Laccase derived from fungi presents a complex structure formed by oligomerized isoenzymes. The range of the monomer molecule mass is from 50-100 kDa. The stability of the enzyme mainly originates from the covalently linked carbohydrates. The catalytic activity only occurs if four or more copper atoms are present in one protein.

Laccase in its original state contains monovalent Cu^{+}. The catalytic cycle of the enzyme, starting from the depleted enzyme, can be described as follows: the four copper atoms in the trinuclear copper cluster oxidize to Cu^{2+} in the presence of oxygen. Thereby oxygen is first reduced to divalent oxygen and then to water. Electrons are abstracted from the T1 copper site to the substrate by a His-Cys-His tripeptide. When the electrons are captured by the substrate(s), laccase will return to its original state and the substrate undergoes a one-electron oxidation forming a radical (see Figure 2-13) [121], [122]. The radicals can couple with each other by polymerization. The catalytic capacity of the enzyme is affected by the redox potential of the T1 copper site. The redox potentials of different laccases are situated between 0.340 and 0.790 V versus the NHE (normal hydrogen electrode). *Trametes versicolor* laccase has the

highest redox potential which is beneficial because it can oxidize various substrates [119]. Monophenols are typical substrates of laccase. The substituents of the phenolic ring can occur on the ortho or the para position that will influence the oxidation process. Electrophiles in ortho position have a negative effect on the substrate affinity for laccase whereas nucleophiles have a positive effect. Substrates with larger substituents and high redox potential causes steric overcrowding and low oxidation rates [119], [122]. Laccase utilizes molecular oxygen as an electron acceptor, this way it can oxidize a wide variety of aromatic amines and phenolic compounds through a radical catalyzed reaction mechanism. The mechanism of detoxification of lignocellulosic materials is based on oxidative polymerization of low-molecular phenolic compounds that are formed during steam explosion pretreatment [87].

During steam explosion, the C-C bond opens between aromatic rings in the lignin macromolecule, while the rings themselves remain unchanged. The formed small molecules, called phenolic inhibitors, are water-soluble. Laccase decreases the soluble phenolic content with more than 90 % in some cases [101]; meanwhile it has only a minor effect on other components of the hydrolyzate. The actual reaction is a radical formation followed by a repolymerization of radicals, and the resulting product will in most cases precipitate [84], [123]. Phenolic monomers can be variously affected by laccase: 4-hydroxybenzaldehyde is only removable by the highest redox potential laccase, vanillin typically requires 24 hours to be removed (depends on the amounts), but on the other hand ferulic acid, syringaldehyde and p-coumaric acid compounds show to be removed immediately [49].

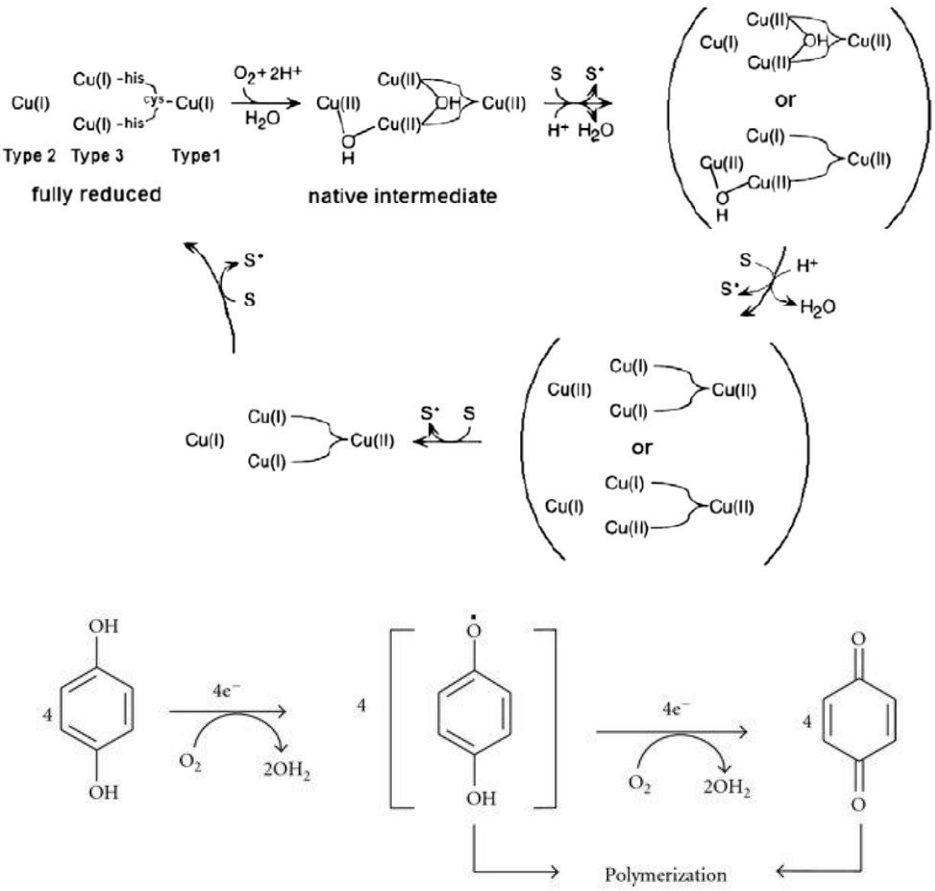

Figure 2-13: Catalytic cycle of laccase and an example reaction [124]. Cu=copper, O2=oxygen, S=substrate.

Laccase already has a wide range of possible substrates, but to enhance the range to oxidation of substrates with a high redox potential, a **mediator** can be added. A mediator is a small molecular weight compound that first is oxidized by laccase using oxygen, and then oxidizes other substrates (see Figure 2-14). The latter substrates are mostly large molecules and non-phenolic units. A mediator should have a stable oxidized and reduced form and may not inhibit the enzymatic reaction [125]. The used mediators can be natural or synthetic. Natural mediators are lignin degradation products such as phenolics present in biomass, e.g., 4-hydroxybenzylic alcohol, p-cinnamic acid and sinapic acid. Natural mediator systems always have to be taken into account when investigating the action of laccase. Synthetic mediators are 2,2'-azinobis(3-ethylbenzthiazoline-6-sulphonate) (ABTS), hydroxybenzotriazole (HBT), 2,2,6,6-tetramethylpiperidine 1-oxyl (TEMPO) and violuric acid [120]. The redox

potential of the mediator plays an important role in the catalytic efficiency of the oxidation process. The effect of the mediator will depend on the chemical reactivity of the formed radicals after the first oxidation step [120].

Figure 2-14: Laccase mediator system [125] and the scheme how a substrate is indirectly oxidized by laccase through a mediator.

Laccases have a wide application potential as a green biocatalyst for various biotechnological methods such as in demethylation reactions and as a detoxifying agent, but current commercial utilization is limited, i.e. textile dying [126]. Regularly utilized sources for laccase production are fungal microorganisms such as *Trametes versicolor* (a white-rot fungi from the basidiomycetes group), *Phlebia radia* and recently *Panus conchatus*. Alongside laccase *Trametes versicolor* produces lignin peroxidase (LiP) and manganese dependent peroxidase (MnP), which are enzymes that also have delignifying activity [84], [123], [127]. Comparing the enzymes to each other, LiP acts slower than laccase, MnP and peroxidase need extra chemicals (Manganese and/or peroxide) to function, while laccase only requires oxygen.

2.4.3.1 Immobilization of laccase

Because of their high activity, selectivity and specificity laccases are perfect biocatalysts for biotechnological and environmental applications. But the use of these enzymes in industrial processes is limited because of their instability and high production costs [118]. To overcome these limitations, a stable and recoverable enzyme should be created. Immobilization of the enzyme is a possible strategy. Immobilization has major advantages because it can increase the enzyme activity, increase thermostability and makes enzymes more resistant to extreme conditions and chemicals [118], [121]. Moreover, it makes biocatalyst recycling possible, i.e., enzymes can be separated by filtration or centrifugation. There are several immobilization techniques (see Figure 2-15) which will be described hereafter [128], [129].

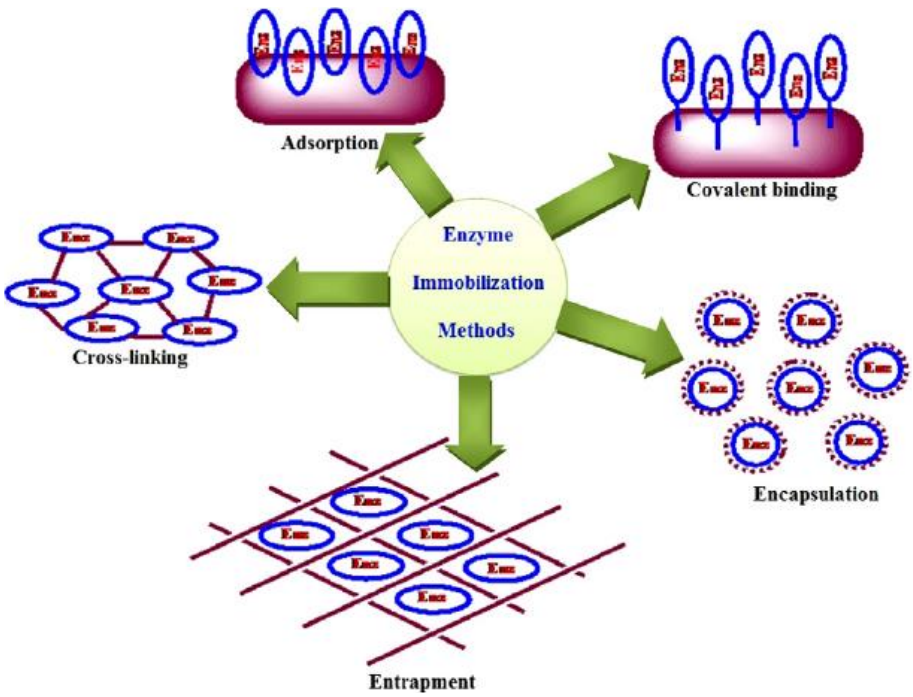

Figure 2-15: Different enzyme immobilization techniques [129].

The enzymes can be attached to a support by **adsorption**: hydrophobic, van der Waals or ionic interactions. These interactions take place on the surface of the carrier. This adsorption process is physical and is frequently used because of the low cost and easy procedure. The support is simply added to an enzyme solution and mixed for several hours, and an enzyme-support complex is formed. It is a reversible process that makes it possible to reuse the support. Most of the time hydrophobic and van der Waals interactions are too weak and the complex bond will not stay intact under industrial conditions. Leakage will cause loss of enzyme, which is why not all can be reused. Ionic interactions are strong, so the complex bond will not break. But the enzyme can be deactivated by changes in conformation which makes enzyme and support unusable [128], [129].

The enzyme can be linked to a support by **covalent binding**. This chemical reaction connects the enzyme directly to the solid support or a cross linking reagent is used which attaches to the enzyme on one side and to the support on the other sideThe latter is favored as a spacer molecule, such as poly(ethylene glycol), will reduce steric hindrance of the substrate. Spacer molecules can provide many different reactive groups, such as epoxy rings and activated carbonyl groups, to enable multipoint

covalent attachment. This is favorable because the activity, stability and reusability of the enzyme will increase[128], [129].

By **entrapment,** the enzyme is introduced into a porous solid matrix such as an organic polymer or sol-gel. First, the enzyme is solubilized in the monomer followed by polymerization that retains the enzyme in the matrix. This hinders direct contact with the environment but there is still a small chance of leakage. In contrast to adsorption, entrapment ensures no changes in enzyme conformation. Drawbacks are mass transfer limitations and lower enzyme loading than cross-linking [128], [129].

The enzyme can be **encapsulated**, i.e., immobilized by surrounding it with a semipermeable membrane, polymer or inorganic material. Encapsulation has the same characteristics as entrapment. Direct contact with the environment is avoided and there are also mass transfer limitations, although lower [118], [128], [129].

Cross-linked enzyme aggregates (CLEAs) and cross-linked enzyme crystals (CLECs) are methods for immobilization without the use of a support, which can cause structural alterations of the enzyme that in turn decreases the specific and volumetric activity. Bifunctional cross-linkers are used such as dialdehydes, diamines. diisocyanates and diiminoesters. Two systems are distinguished, i.e., CLECs and CLEAs. The formation of CLECs involves cross-linking crystallized enzymes. Crystallization has one major drawback: a purification process is needed which is very expensive. CLEAs are produced (see Figure 2-16:) by first precipitating the enzyme through addition of salts, organic solvents or non-ionic polymers. After precipitation is completed enzyme aggregates are formed which are kept together by non-covalent bonds. These aggregates can redissolve in water. The second step is cross-linking the aggregates for creating insoluble CLEAs [128], [129].

Magnetic-CLEAs (m-CLEAs) are CLEAs incorporating a specific kind of support material (see Figure 2-16). Production of m-CLEAs is based on aggregation of enzymes in the presence of the support material such as magnetite nanoparticles [130]. The material can act as a core for precipitation, or attach to the precipitated enzyme later on. It has to be noted that the support material should be ferromagnetic and not permanent magnetic, as the particles should only aggregate in presence of a magnetic field.

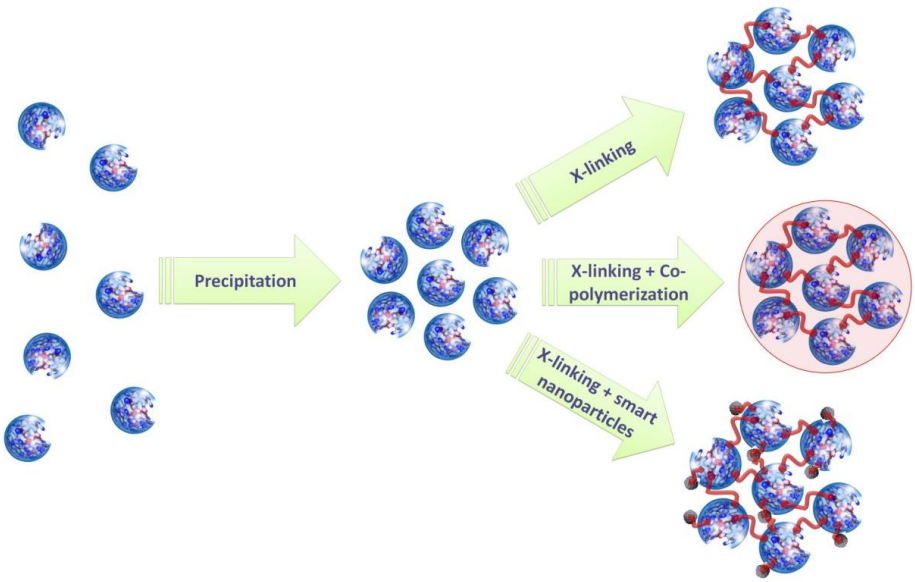

Figure 2-16: Immobilization of enzymes as CLEAs. Left: free enzymes. Middle: precipitated enzymes. Right above: CLEAs; middle: combi-CLEAs; under: magnetic-CLEAs [131]**.**

2.5 Cost estimation

There are numerous techno-economic cost estimations published about lignocellulose-based bio-ethanol production, and a few about lignocellulose based lactic acid production. Seven of them are summarized in Table 2-8.

Kazi et al. calculated, after a detailed cost estimation, including pioneer-nth plant and uncertainty analysis, a minimum ethanol selling price (MESP) of 0.37-0.50 $/kg [132]. When they compared the price to literature, it was visibly higher than nearly all other cases even, after adjustment by the consumer price index (see Figure 2-17). There are two significant factors behind this. The first one is that enzyme prices are lower in literature, i.e. 10-30 % of the value used in the analysis by Kazi et al. [132]. The second factor is the capital cost, as a rather conservative/old technology was studied by Kazi et al., while, in literature, generally advanced technologies were investigated (SSF, SSCF, CBP) that are expected to have lower CAPEX due to process integration. This example shows the major problems in cost estimation comparison, as the concrete process design and the price of the starting materials, especially the enzymes, vary greatly.

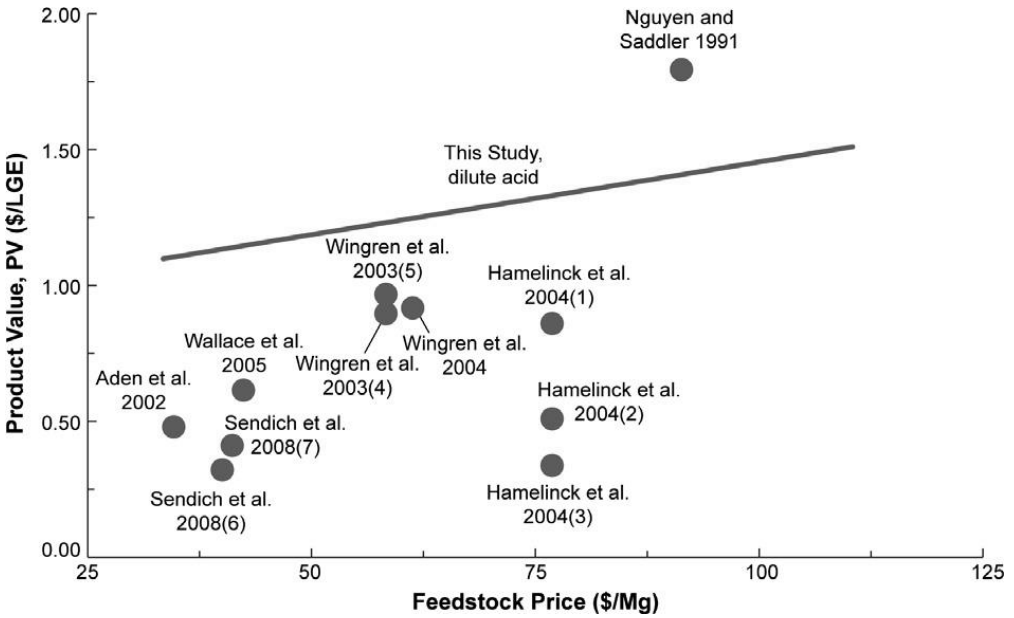

Figure 2-17: Example of calculated ethanol prices from Kazi et al. [132].

Liu et al. published a techno-economic assessment for lignocellulose based lactic acid production [71]. Several interesting and novel steps were incorporated, most notably SSF with high solid loading, biodetoxification [133] and extreme high solid loading pretreatment The overall yield was 71 m/m% lactic acid from the starting carbon, which is considered realistic. A selling price of 0.62-1.17 $/kg lactic acid was calculated. To counter the controversies with the actual enzyme prices, the selling price was calculated with a range of cellulase prices. Modifying the cellulase price to the one estimated by Klein-Marcuschamer (10.14 $/kg$_{protein}$), the production cost of lactic acid is still as low as 0.8 $/kg, with the cellulase contributing to 0.355 $/kg lactic acid (44 %) and the feedstock 0.237 $/kg lactic acid (30 %).

Table 2-8: Summary of seven techno-economic cost estimation articles.

REF	Product	Raw material	Pretreatment	MPSP [$/kg]	Enzyme unit price [$/kg$_{protein}$]	Enzyme activity [FPU/g$_{product}$]	Enzyme conc [prot m/m%]	DM [%]	Enzyme conc in broth [m/v%]	Cost breakdown [%]	
										Feedstock	Enzyme
[132]	Ethanol	Corn stover	Dilute acid at high solids	0.74	5.00	60	10	20	5.04	35	21
[134]	Ethanol	Grain and straw	Steam explosion	0.69-0.77	2.05, 3.42 $/MFPU**	60 assumed	10 assumed	12*	2.4, 1.2kFPU/l		
[135]	Ethanol	Softwood	Two stage acid steam explosion	0.70	1.52, 2.53 $/MFPU**	60 assumed	10 assumed	8.4*	2.4, 1.2kFPU/l	33	15
[136]	Ethanol	Corn stover	Dilute acid pretreatment	0.72	4.24		5	20	4.8	34	16
[137]	Ethanol	Corn stover, hardwood, softwood	Sulfur dioxide steam explosion	0.59-0.71	1.52, 2.53 $/MFPU**	60 assumed	10 assumed	9*	2.44, 1.35 kFPU/l	38-46	12
[138]	Ethanol	Sugarcane bagasse	Phosphoric acid steam explosion	0.80	5.00		20	15*	3	33	24
[71]	Lactic acid	Corn stover	Steam explosion at high solid loading	0.62	5.07	135	9	30	4.08	38	29
				0.80	10.14					30	45
				1.17	23.30					20	62

*Original values in water insoluble solid (WIS), DM usually higher, **Original prices were given in $/MFPU, thus $/kg prices were calculated assuming FPU values.
MPSP=minimum product selling price, **Enzyme activity** is the activity of the liquid enzyme product, **Enzyme conc** is the protein concentration of the liquid enzyme product, **DM** is the dry matter in the fermentation broth, **Enzyme conc in broth** is the concentration of liquid enzyme product in the fermentation broth.

2.5.1 Substrate

The price of the substrate used in lignocellulose-based refineries is expected to be volatile: agricultural products (stover, bagasse) are seasonal as they are "produced" strictly during harvest, thus seasonal cycles will appear from the supply side. However, wood bioresources are used significantly for heating during winter, thus cycles in availability can originate from the demand side.

Raw material prices, as estimated by Kazi et al., correspond to 35 % of total production costs of ethanol [132]. Chandel et al., estimated the biomass costs to be 34 % of overall costs of ethanol production [139]**.** It can be concluded that generally estimations state that feedstock is responsible for about one third of the production price (see Table 2-8). Ethanol FOB (free on board) selling price was 0.424 $/l± 5 % in 2018 [140]. Calculating with a density of 0.8 kg/l and theoretical yield of 51 % $kg_{ethanol}/kg_{glucose}$, this gives 0.27 $/$kg_{glucose}$ revenue from selling ethanol.

As for ethanol production, estimations showed that the carbon source represents around 34 % of the final production price of lactic acid, assuming wheat flour based fermentation where the wheat's own hydrolyzing enzymes (amylase, amyloglucosidase and a protease) were necessary [59]. Other authors estimated this number much higher, i.e. 70 % of production costs in a corn based lactic acid production comes from substrate cost [71]. The lactic acid market price is about 1.5 $/kg [141]. Calculating with a theoretical yield of 100 % $kg_{lactic\ acid}/kg_{glucose}$, this gives 1.5 $/$kg_{glucose}$ revenue from selling lactic acid.

Theoretically, lignocellulose-based ethanol and lactic acid production will only be economically viable if the production price will be lower or equal to the current selling price of the same products based on simple sugar (starch or sucrose). Practically, governmental interaction, such as tax reduction can also play a role, but the best scenario would be if the process is viable on its own, without external support.

As expected, most published techno-economic analyses estimate the selling price of the product, incorporating fermentation also. It is also fairly easy to investigate how much an actual substrate does cost, i.e. as of September 2018 on, the current price for white sugar in the EU is 400 $/ton (between 380 and 480 $/ton in the past year [142]). In September 2018, the corn maize price was 213 $/ton (170-228 $/ton) [143] and poplar wood about 80 $/dry ton (50 % glucan, 20 % xylan). However, the optimal steps to arrive to fermentable sugars from different substrates can be very different. A

recent study investigated the costs of sugars in case of different biological substrates [144]. The market price of raw carbohydrates, thus calculating with the price of the raw biomass and taking the sugar concentration in the material itself into account, increases from sugar cane ≈ eucalyptus < softwood ≈ hardwood < switchgrass < pulps. Different pretreatments are optimal for different materials. Hardwood, like poplar, obtains best results with autocatalyzed steam explosion. Several scenarios were investigated: different pretreatment techniques with power generation or pelletization from the residues, collocation with craft pulp mill or green field investment. The best outcomes are summarized in Table 2-9. The cheapest option is sugar cane, but only in Latin America. In the northern hemisphere, corn grain is the most cost-effective carbohydrate source, while Eucalyptus, hardwood and softwood is currently more expensive with 13, 19 and 25 % respectively in case of co-location.

Table 2-9: Minimum sugar revenue for different sources and scenarios [144]**.**

Feedstock	Pretreatment	Residue	Location	Minimum sugar revenue [$/$t_{carbohydrate}$]
Sugar cane (Latin America)	Hot water extraction	Power generation	Co-location	**153**
Corn grain	Hot water extraction	Pellets	Co-location	**229**
Eucalyptus	Steam explosion	Pellets	Co-location	**258**
Hardwood	Steam explosion	Pellets	Co-location	**272**
Loblolly pine	Steam explosion with acid catalysis	Pellets	Co-location	**287**

2.5.2 Pretreatment

As was discussed in Section 2.3.1, there are numerous possible **pretreatment** techniques, but from an economic point of view, very few are interesting. Basic physical (chopping) pretreatment is always needed until chip sizes of a few cm, but not

further, as costs rise sharply with further size reduction and further non-physical pretreatment often decrease the size too [145].

Almost all published techno economic analyses use aqueous, thermal pretreatment with/without diluted mineral catalysis (see Table 2-8), because of three reasons, i.e., the relatively simple process configuration (stirred tank), the cheap chemical catalysts (water, acid or base) and since there is no catalyst recovery setup as diluted chemicals cannot be recycled efficiently. The choice of catalysts is limited by their utilized amounts and costs; usually the most common chemicals are used in low as possible concentrations. The acid catalyst is usually sulfuric acid (0.2-0.3 $/kg [141]), or sometimes hydrochloric acid (0.2-0.25, 30 % [141]), but halides should be avoided to allow simpler waste treatment. For example, using 1 m/v% sulfuric acid during steam explosion would cost 0.25/1000= 0.025¢/l, which could fit in the process. From the possible alkali, lime is favored for its low cost (0.15 $/kg [141]), and because it can be precipitated with sulfuric acid. Sodium and potassium hydroxide are more expensive (0.3 and 0.4 $/kg [141]) and they remain solubilized in the liquid phase after neutralization increasing osmotic pressure and possibly hindering fermentation. Ammonia can also be an interesting alkali, although it is often less efficient than lime and more expensive (0.55 $/kg [141]), but it can be directly utilized as nitrogen source for the fermentation in the later process, thus decreasing nutrition costs.

If the pretreatment temperature is significantly above 100 °C, the equipment has to be pressurized, as an aqueous environment cannot be heated over the boiling point at atmospheric pressure. Pressurized treatments are appealing in general; although the equipment is more expensive, the treatment time decreases sharply with temperature and part of the utilized heat energy can be recycled. Reducing the pressure suddenly after pretreatment (e.g. explosion), instead of slow decompression, causes increase in sugar yield during the subsequent hydrolysis step [25].

Steam explosion (SE) and its varieties are the combination of the mentioned parameters: low-cost catalyst, high temperature/pressure and sudden decompression. Most published cost estimations use a kind of SE (see Table 2-8), although naming can be different, the process description resembles steam explosion. It is already commercialized, and most authors refer to it as currently the best pretreatment method for straw, hardwood and softwood [144]. The equipment has a simple design in the base case: it is a pressurized tank without stirring, combined with

a high-pressure valve for sudden decompression (see later Figure 3-2). The CAPEX connected to it are significant because of the resistant design (high temperature/pressure, possibly acidic pH) and the steam needed for heating.

Industrial experts say that the typical dry concentration of the lignocellulose material after steam explosion is around 20 %, without stirring in the equipment. However, some cost estimations start from over 30 % of solid loading for SSF [138], which means that the steam explosion has to be performed at 30 % solid loading, or an extra centrifugation step is needed after pretreatment. Research on steam explosion was done at higher dry mass concentrations also (50 %) with a pretreatment technique called dry dilute acid pretreatment (steam explosion equipped with a helical stirrer) [28], [71], but it is not yet industrially utilized. It was found that in case of dry dilute acid pretreatment, active mixing is necessary for efficiency; furthermore, higher (70 %) dry content damaged the bearings around the axis due to the extreme high viscosity.

A more detailed explanation about the dry dilute acid process is necessary to understand the influence of stirring on the practical feasibility. In an industrial setting, steam explosion equipment is already at (or close to) the working temperature from the previous batch. The input stream of wood is heated up until about 100 °C, and not higher, as above this, the water will boil and it will dry the material rather than heat it up. Further heating in the reactor is done by introducing higher temperature saturated steam; the vapor will condense and heat up the system with its latent heat. This is the reason why the energy demand of steam explosion is greatly affected by the dry matter content of the input substrate [137]. The freshly cut poplar will already have a moisture content of 50 % but can go down to 10 % if it is air dried for a year, of course this would increase storage costs. To keep the water content low, the amount of steam that can be introduced to the system is low, the resulting mixture will be rather a solid than a liquid, active stirring is needed for homogenization. Active stirring means that a rotating agitator has to be in the reactor. The motor itself can be placed outside of the reactor; however, the point where the axis enters the reactor will be subjected to a pressure difference (value between atmospheric pressure and the treatment pressure) and it will be prone to extreme pressure changes during explosive decompression. The motor can be placed also inside of the reactor, this way the pressure difference will be approximately zero, but it will be at 100-200 °C, possibly in an acidic environment. Both solutions could be costly, and would most probably need intensive maintenance.

Wingren et al. estimated the cost of the steam explosion, excluding steam generators, to be around 15 % of the total capital cost of the softwood-to-ethanol refinery [146]. Chandel estimated the pretreatment to be responsible for 17.5 % of the overall costs of bioethanol production [139].

2.5.3 Hydrolysis

In general it can be said that for hydrolysis the enzymatic route is preferred over acid catalysis in the long term [135]. In this scenario, the enzyme is responsible for the major part of the costs, as no high temperature/pressure or extra chemicals are needed. However, enzyme price determination/estimation alone can be a very difficult task. Typical hydrolysis final sugar concentrations (titers) are 40-50 g/l glucose when starting from steam pretreated biomass [27] and dependent on the solid and enzyme loading. An option to increase the fermentable sugar titers is to utilize the crops (corn, grain) as whole, as after lignocellulose hydrolysis is inhibited, starch can be further hydrolyzed to sugars [134]. The equipment used for hydrolysis is rather standard except for the stirring of viscous mixtures at the high solid loadings. As recent publications deal with solely SSF instead of SHF [71], [134], [136], [138], exact machinery will be discussed in Section 2.5.4.1.

2.5.4 Fermentation

Fermentation itself is a relatively simple process as it is performed at ambient conditions (temperature, pressure); however, there are a number of parameters that increase its costs. Most of the chemicals used in the overall lignocellulose-to-chemicals process will be used here: nutrients for the microorganism, conditioning of the broth (pH, antifoam), carbohydrates during inoculum preparation. In case of lactic acid fermentation there is an extra consumption of lime for the neutralization of the formed acidic product. The reactor itself is also a simple stirred tank, however since the fermentation is relatively long, it has to be much bigger in dimension than the pretreatment reactor. There are also significant auxiliary systems needed for fermentation: pH/temperature control (sensors and piping), train of seed tanks for inoculum preparation.

2.5.4.1 SSF

As SSF is the combination of hydrolysis and fermentation, considerations about the cost for both processes apply also for SSF. The CAPEX is decreased, as only one reactor

is needed instead of two in the case of separate processes. The main difference compared to separate fermentation is the required viscous stirring, as the mixture will contain 15 % dry content or more. Possible setups are screw mixers, helical mixers, or mixers with extended rotational arms. During hydrolysis the fibers break down, leading to a less viscous material, hence the mixing is crucial at the start of the SSF [147]. Optionally a prehydrolysis can be applied, where the slurry will be partially hydrolyzed which will decrease viscosity to the extent that the material can be handled as a classical liquid [138]. The CAPEX for fermentations were estimated 30 % more than steam explosion by Gubicza et al. [138], 10 % more by Wingren et al. [146] to 40 % less by Hoyer et al. [148], but the exact cost will depend on the applied design, of course. More advanced setups (SSF) are typically estimated to result in lower CAPEX [148].

2.5.5 Downstream processing

2.5.5.1 Ethanol

Ethanol purification is done by distillation techniques in technically all industrial applications. The process is simple, but its energy demand is a serious drawback. Pervaporation is also a possibility, but it is not commercially in use yet [139], although there are already techno-economic analysis proving that most probably it will be the dominant technology in the future [148]. The utilization of ceramic membranes for pervaporation has been reported to be successful for the filtration of cell biomass and for the removal of ethanol during the fermentation simultaneously [44]. After distillation a further dewatering step is needed, typically with a molecular sieve [149], before the ethanol can be used as a fuel for combustion engines.

It has been shown that under 40 g/l ethanol concentration the distillation is not energetically feasible because, in that case, 35 % of the heat that can be gained by burning the purified product is needed for purification. At 120 g/l ethanol concentration, this value is only 12.6 % (see Figure 2-18) [149]. Industrial experts indicated that 50 g/l ethanol is to be achieved after fermentation for realistic viability of the process [148].

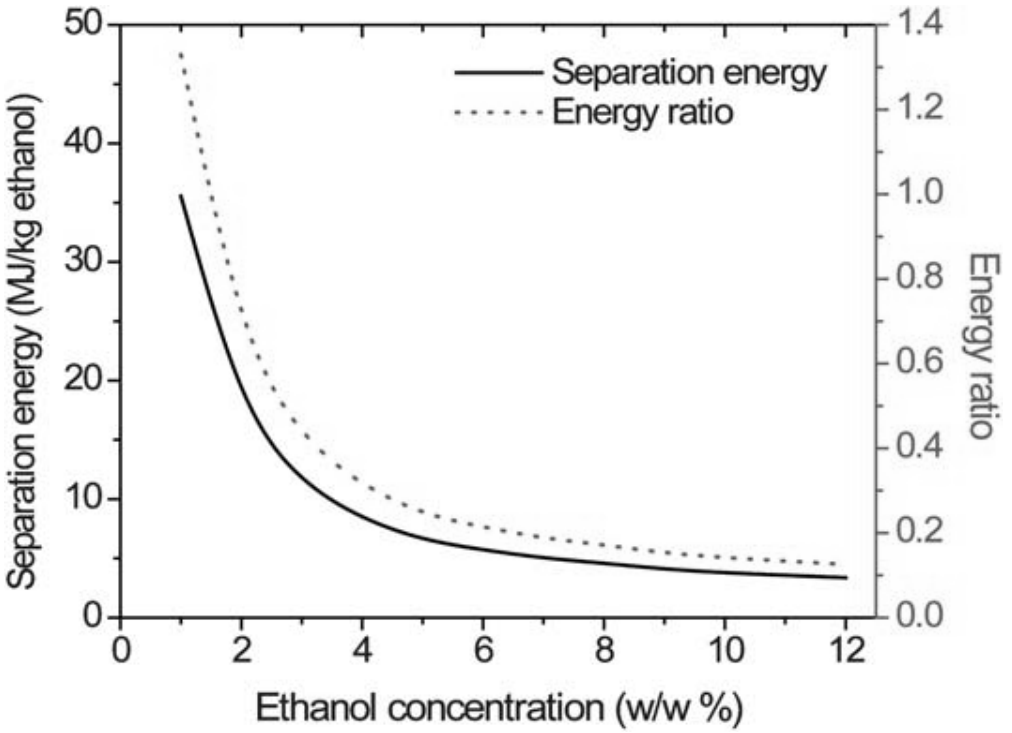

Figure 2-18: Energy demand of ethanol purification at different product concentrations [149].

2.5.5.2 Lactic acid

Lactic acid purification is much more complex, thus more expensive, contributing for approximately 50 % of the overall product selling price [150]. During purification gypsum is formed in 1:1 mass ratio, thus lime and sulfuric acid alone accounts for approximately 0.2 $/kg of the product price [141]. Purification contains two thermal-energy demanding steps: heating up the broth after raising the pH, e.g., lime addition, and evaporation of water (and other compounds) later. As sulfuric acid addition after liming generates significant heat, part of the energy can be instantly used. Final purification is done by crystallization, where according to industrial experts minimum 100 g/l product concentration is needed [71].

2.5.6 Detoxification

There is no defined maximum cost for detoxification, but it should as low as possible. The detoxification cost is also strongly dependent on synergies between hydrolysis, fermentation and downstream processing. For example, if during detoxification extra

compounds are removed, this can decrease post-processing costs, but this will be difficult to quantify. The gain in fermentation time or the decrease in the needed inoculum amount because of less toxic broth can be easier understood, investigated and calculated. Assuming a fixed fermentation tank, the needed fermentation time is the reciprocal of the annual production, hence the annual income [151]. A smaller fermenter tank will decrease CAPEX. The maximum inoculum size is around 20 v/v%, typically 5-10 % [71]. The inoculum is usually grown on glucose or sucrose in a seed train [136]. The amount of needed glucose or sucrose, in general, will increase linearly with the inoculum size, and increase the material costs. Thus, smaller inoculum size will decrease variable costs and CAPEX alike.

The synergy of detoxification with hydrolysis is the easiest to quantify (see Figure 2-19). Taking as an example an ethanol selling price of 0.74 \$/kg and an enzyme contribution of 21 % from Table 2-8 [132], then the enzyme cost is 0.1554 $\$/kg_{ethanol}$. Taking a theoretical 0.05 $\$/kg_{ethanol}$ detoxification cost, then the cost of cellulase and detoxification together is 0.2054 $\$/kg_{ethanol}$, when assuming no interaction in the scenario that the detoxification would result in 20 % cellulase activity reduction, then 25 % more cellulase would be needed (1/0.8=125 %) to achieve the same conversion. This means an increase of 0.039 $\$/kg_{ethanol}$, thus the effective cost of detoxification would be 0.089 $\$/kg_{ethanol}$, which is an increase of 79 % compared to the scenario with no interaction. On the other hand, if the detoxification would increase cellulase activity by 20 %, calculating with the same values as in the previous example (1/1.2=83 %), the needed cellulase amount can be decreased by 17 %, causing an additional savings of 0.026 $\$/kg_{ethanol}$. This would mean that the effective detoxification cost is 0.024 $\$/kg_{ethanol}$, i.e., 48 % lower than in the no interaction scenario. In theory, it is even possible that the effective detoxification cost becomes negative. Thus, it is shown that taking into account the synergies between hydrolysis and detoxification is very important.

Cavka et al. provided an example cost estimation for detoxification with sodium-sulfite detoxification in case of acid catalyzed steam exploded spruce based ethanol production [70]. The calculations showed that, in case of SSF with 12.5 % solid loading, 12.5 mM added sulfite increased cellulase activity and decreased the needed inoculum size. This concentration represents approximately 1.5 g/l, which corresponds to 0.02 $\$/l_{ethanol}$, that is 0.0253 $\$/kg_{ethanol}$. Inoculation volume was decreased by 80 %, e.g. 1 g/l from 5 g_{yeast}/l_{broth}, and cellulase activity was increased by 30 %. According to their calculation, altogether the treatment would reduce the final selling price of ethanol by

0.13 $/$l_{ethanol}$ or 0.16 $/$kg_{ethanol}$. Here, the sustainability aspects of the process should be mentioned. Sulfite would be used in significant quantities, calculating with 50 g/l ethanol titer and 1.5 g/l added sulfite, 3 m/m% of sulfite would be consumed compared to the mass of the product.

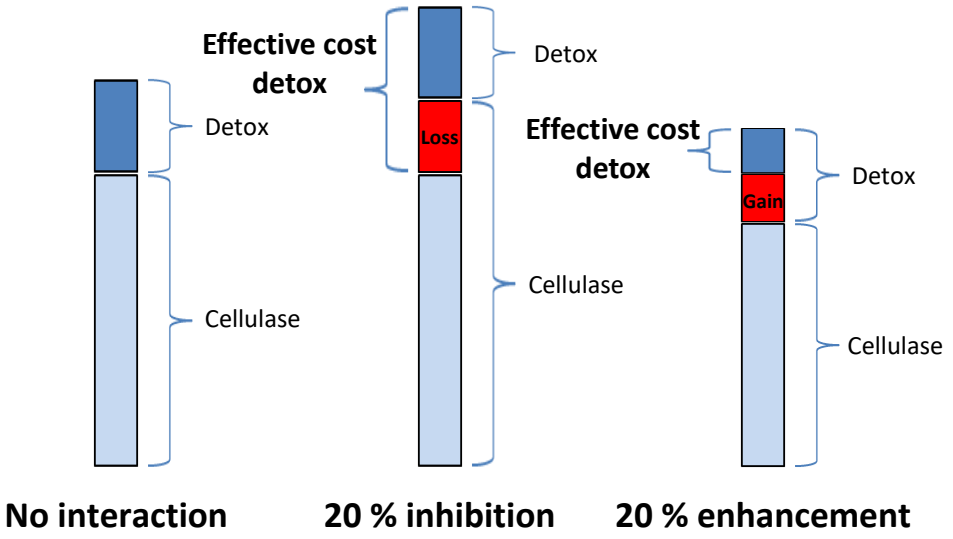

Figure 2-19: The evolution of effective detoxification cost in function of hydrolysis-detoxification interactions.

2.5.7 Conclusions

The expected/estimated contributions of some sub-costs to the minimum product selling price are summarized in Table 2-10. Downstream processing is not included as it significantly differs between ethanol and lactic acid. Both pretreatment (hydrothermal processes are meant here) and downstream processing are mature technologies, where significant cost changes are only expected from new technologies, i.e., organosolv for pretreatment or pervaporation for ethanol purification or electro dialysis for lactic acid downstream processing. Estimations vary based on technical parameters, i.e., the utilized material depending on pH, but besides that, lead to similar results. Substrate costs are completely market driven, ongoing investigations focus on estimating the future price, based on the demand growth, like the Billion-ton report [152]. By far the cellulase enzyme cost is the most uncertain, as neither the exact unit price, or future activity is known. Moreover, the inhibitors in the hydrolyzate

also inhibit the cellulase, thus detoxification can and will influence the needed cellulase amount.

Table 2-10: Summarizing the expected contribution of different sub-costs to the minimum selling price. Downstream not included, as it is significantly different for ethanol and lactic acid purification.

	Contribution to production costs [%]	Uncertainty	Cause	Research
Substrate	30-40	Moderate	Market price fluctuation	Better price prediction
Pretreatment	15-20	Low	Mature processes	New technologies
Cellulase enzyme	15-45	High	Future activity uncertain	Increase activity
Downstream	-	Low	Mature processes	New technologies

Chapter 3 LACCASE DETOXIFICATION: CHARACTERIZATION AND METHODOLOGY

3.1 Introduction

Laccase is known to decrease the phenolic inhibitor concentration in lignocellulosic hydrolyzates in a 'so-called' detoxification process (see Section 2.4.3), more specifically its biological/enzymatic means. Laccase detoxification was extensively studied before in literature, but its aspects concerning industrial applications are mostly missing: robust/simple measurements for monitoring and quantification, correlation between standard measurements and real substrates, and screening methods.

Fungal laccases tend to have a higher redox potential compared to that of bacterial origin, which makes them capable to oxidize a wider variety of substrates [153]. Steam exploded wheat straw was detoxified by bacterial laccase from *Streptomyces ipomoeae*. Treatment was performed at pH 8 and 50 °C for 24 h. A comparable treatment with *Trametes villosa* laccase was performed at pH 4 and 30 °C for 24 h. Experiments were conducted with solid fraction suspended in buffer. The added model inhibitors were vanillin, syringaldehyde, and p-coumaric and ferulic acids, from which bacterial laccase only reacted with syringaldehyde and ferulic acid, while fungal laccase removed also vanillin and p-coumaric acid. The results showed that phenols that are easier to oxidize tend to go through polymerization, while the others are more in favor to grafting (propagation of radicals, thus attaching to solid lignin if present). This is the reason why in case of fungal laccase treatment a slight increase in lignin content is reported. Similar results were reported by Kolb et al., i.e. *Trametes versicolor* laccase removed syringaldehyde, p-coumaric acid and ferulic acid in an hour, while vanillin was only removed after 24 h treatment, and 4-hydroxybenzaldehyde (HBA) did not vary its concentration within 1-week reaction time in the presence of laccase [154]. They achieved these results with single model phenolic substrates; however, when real hydrolyzate was used all soluble phenolics were removed to some extent, indicating that the formed radicals can react with HBA and vanillin, thus achieving some removal.

The results of De La Torre et al. showed that fungal laccase decreased phenolic content by 70-75 %, while bacterial laccase only with 35-37 % [153]. Similarly high phenolic removal rates were reported before with fungal laccases: e.g. 76 % when steam exploded rice straw was treated with *Coltricia perennis* laccase [155], and 92-95 %

when steam exploded wheat straw was treated with *P. cinnabarinus* laccase or *Coriolopsis rigida* laccase [156]. Bacterial laccase typically yields lower phenolic removal, 20–21 % in case of steam exploded wheat straw and MetZyme laccase [157]. It is visible in Table 3-1, that fungal laccases have much higher phenolic reduction, typically >70 %, than those of bacterial source, with removal around 20-30 %.

Table 3-1: Overview of articles published in laccase treatment of lignocellulosic hydrolyzates, references in original article [158].

Pretreated Material	Laccase Treatment	Effects	Benefits Produced
Steam-exploded rice straw	*Coltricia perennis*	Removal of phenolic compounds by 76 %	Increased saccharification yield by 48 %
Steam-exploded wheat straw	*Pycnoporus cinnabarinus* or *Trametes villosa*	Removal of phenols identified (vanillin, syringaldehyde, ferulic acid and p-coumaric acid) by 93–95 % with both laccases	Improved the fermentation performance of *Kluyveromyces marxianus* CECT 10875, shortening its lag phase and enhancing the ethanol yields
SO2 steam-pretreated willow	*Trametes versicolor*	Removal of phenolic compounds (93–95 %), revealing an oxidative polymerization mechanism by SEC analysis	Higher yeast growth, glucose consumption rate, ethanol productivity and ethanol yield using *Saccharomyces cerevisiae*
Dilute acid steam-pretreated spruce	*T. versicolor*	Removal of phenolic compounds by 93–95 %	Ethanol yield produced by *S. cerevisiae* comparable with that obtained after detoxification with anion exchange chromatography at pH 10
Steam-exploded wheat straw	Commercial bacterial laccase MetZyme®	Phenol reduction of 18 % (laccase alone) and 21 % (simultaneous laccase and presaccharification)	Improved the fermentation performance of *K. marxianus* CECT 10875 during SSF and PSSF processes, shortening the adaptation phases and the overall fermentation times
Water and acid-impregnated steam-	*T. versicolor or Coriolopsis rigida*	Removal of phenolic compounds by 93–95 % with both laccases	Reduction of the toxic effects on *S. cerevisiae*, resulting in higher yeast growth and improved ethanol production

exploded wheat straw			
Steam-exploded wheat straw	*P. cinnabarinus*	Phenol reduction around 67 % (laccase alone) and 73 % (simultaneous laccase and presaccharification)	Laccase detoxification allowed to obtain ethanol concentrations and yields with *K. marxianus* CECT 10875 comparable to those obtained with *S. Cerevisiae*
Steam-exploded wheat straw	*P. cinnabarinus*	Removal of phenolic compounds by 95 %	Improvement of cell growth and ethanol production of *S. cerevisiae* during SSF process
Steam-exploded sugarcane bagasse	*T. versicolor*	Approximately 80 % of the phenolic compounds removal	Improvements in ethanol yield and ethanol volumetric using a xylose-utilizing *S. cerevisiae*
Steam-exploded sugarcane bagasse	*Ganoderma lucidum 77002*	84 % of the phenolic compounds in prehydrolyzate	Ethanol yield was improved when *S. cerevisiae* was used on detoxified prehydrolyzate
Alkali-extracted sugarcane bagasse	*Aspergillus oryzae*	Not observed	Laccase improved the fermentation efficiency by 6.8 % for one-pot SSF and 5.7 % for SSF
Acid hydrolyzed from sugarcane bagasse	*Cyathus stercoreus*	Reduction of 77.5 % of total phenols	Improvements in the performance of *Candida shehatae* NCIM 3501
Steam-exploded wheat straw	*P. cinnabarinus*	Phenol reduction around 44 % (laccase alone) and 95 % (simultaneous laccase and presaccharification) at 12% (w/v) of substrate loading	Laccase detoxification triggered the fermentation by *K. marxianus* of steam-exploded material at 12 % (w/v), resulting in an ethanol concentration of 16.7 g/l during SSF process
Steam-exploded wheat straw	*P. cinnabarinus*	Reduction of total phenolic compounds by 50–80 %	Laccase detoxification allowed the fermentation of pretreated material at 20 % (w/v) of substrate loading using the evolved xylose-consuming yeast *S. cerevisiae* F12, producing more than 22 g/l during SSCF process
Steam-exploded wheat straw	*P. cinnabarinus*	Approximately 73–81 % of the phenolic compounds removal	Laccase detoxification improved cell viability of the evolved xylose-recombinant *S. cerevisiae* KE6-12, and increased the ethanol production up to 32 g/l when fed-batch SSCF process

			was used at 16 % (w/v) of substrate loading
Steam-exploded wheat straw	*P. cinnabarinus*	Phenols removal by 53 % during simultaneous laccase and presaccharification at 25 % (w/v) of substrate loading	Ethanol production of 58.6 g/l at 48 h with detoxified material at 25 % (w/v) of substrate loading during PSSF process with *S. Cerevisiae*
Dilute-acid spruce hydrolyzate	*T. versicolor* expressed in a recombinant *S. cerevisiae* strain	Reduction of low-molecular of phenolic compounds	Laccase-producing transformant was able to ferment at a faster rate than the control transformant
Organosolv pretreated wheat straw	*T. versicolor* immobilized on both active epoxide and amino carriers	Higher phenols removal (82 %) efficiency with laccase immobilized on active amino carrier	Better performance of *Pichia stipitis* during fermentation and reusability of immobilized laccase
Steam-exploded wheat straw	*T. villosa* or a bacterial laccase from *Streptomyces ipomoeae*	Phenol content reduction of 29 % and 90 % with bacterial and fungal laccases, respectively	Improvement performance of *S. Cerevisiae* during SSF and PSSF process

SEC, Size exclusion chromatography; SSF, simultaneous saccharification and fermentation process; PSSF, presaccharification and simultaneous saccharification and fermentation process; SSCF, simultaneous saccharification and co-fermentation process. Generally, laccases source is fungal, except in those cases where it is indicated.

3.2 Problem statement and goal

This chapter describes/develops the global measurement techniques applied throughout the PhD research, namely UV monitoring of laccase detoxification (new in the field, Section 3.3.1.2), simplified overall phenolic/inhibitor concentration HPLC measurements (major changes compared to literature, Section 3.3.1.1), structural carbohydrate content measurements (minor changes compared to literature, Section 3.3.2.2) and sugar/fermentation products concentration measurements (as in literature, Section 3.3.2.1). Furthermore, a general technique is developed for laccase screening by comparing standard laccase activity measurement (Section 3.6.1), vanillin-laccase reaction as a model substrate (Section 3.6.2) and XRF-laccase reaction

as a real substrate (Section 3.7). Except for vanillin-laccase reaction, the others were reported before, but the comparison was not done yet (Section 3.8).

The other experiments were all reported before, but they are necessary to perform to set the parameters/provide substrate for further experiments, namely autocatalyzed steam explosion (SE) of poplar wood and its partial optimization (Section 3.4), enzymatic hydrolysis of the substrate (Section 3.5).

3.3 Measurement techniques

In this section, the elaboration of all XRF and SF related measurement techniques is detailed. For each compound or group of compounds, first an overview of the possible measurements techniques is provided and it will be indicated why the specific technique was chosen. Later on, in the following chapters, only a brief description has been given in experiments where they were used.

3.3.1 Phenolic content measurement

In literature, several techniques to measure the phenolic content have been described. Most often, high-performance liquid chromatography (HPLC) with UV detection [154], [159], [160], mass spectrometry (MS) detection [161] or Folin–Ciocalteau method [162], [163] were applied, while visible (VIS) spectroscopy is usually reported for the phenolics that have an absorbance at visible wavelength (dyes) [164]–[166]. Each technique has its own strengths and weaknesses. Folin's method requires the addition of reagent, it does not provide information about the separate phenolics and it interferes with proteins and some other compounds, but the measurement is relatively fast and easy. VIS measurements are only useful for colored compounds, but it is an instantaneous measurement that does not require sample preparation (except filtration and/or sample dilution). Here it must be noted that since UV (254 or 280 nm) is relatively selective for condensed aromatic rings, it can be represented as the "color of the aromatic ring", as it is used in the same way as a VIS method. Interfering compounds are furans, proteins, non-phenolic aromatics and in general, everything that has a condensed ring, but it is not a phenolic inhibitor. HPLC methods are capable to separate different compounds, however, filtration is always needed (sample preparation), the measurement time is long, the equipment price and maintenance cost are higher and it is not trivial to determine the total phenolic concentration. HPLC-UV is more robust and has a lower cost than mass spectrometry (MS), however it needs standards for qualification and in general provides less information than the use of online libraries for MS chromatograms.

In this work, HPLC (two methods) as well as standard absorption at 280 nm were used for phenolic content determination, mainly because of availability and simplicity.

3.3.1.1 HPLC-UV measurements

A number of publications report HPLC-UV techniques for phenolic concentration determination. The most often a simple C18 column is used, which is a common, robust and low-cost column [154], [159]–[161], and a methanol/aqueous mobile phase, with the aqueous phase containing acetic acid [159], [160] or sometimes other dissolved compounds [154], [161]. Detection was at 254 nm [167], 280 nm [154] or at a range of 190 to 550 nm [160].

A number of compounds are reported to be found in steam exploded poplar hydrolyzates, i.e. p-hydroxybenzoic acid (HBA) and aldehyde, syringic acid and aldehyde, vanillin and vanillic acid [154], but it is evident that since steam explosion is, as a high temperature/pressure cracking, a non-selective process, all derivatives of these products are also found in the hydrolyzate [163]. Identifying them all is hard and time consuming. Nilvebrant et al. reported an HPLC-UV method for phenolics analysis in lignocellulosic hydrolyzates [107]. They defined the amount of phenolics as the sum of the area of peaks eluting after the furan peaks. Without further analysis of the products, this gives a summarized phenolic amount present in the sample.

Method

The technique of Nilvebrant et al. was modified for all inhibitor concentration HPLC measurements [107]. Samples were filtered through a 0.45 µm syringe filter, analyzed immediately or kept at -20 °C. HPLC-UV (Shimadzu SPD-M20A diode array detector, Shimadzu corp., Kyoto, Japan), with methanol and 1% v/v acetic acid solution (Sigma-Aldrich Corporation, St. Louis, MO, USA) as a mobile phase on a Luna 5 µm C18(2) 100 Å column (Phenomenex, Torrance, CA, USA) was used. Every analysis was performed at 1 ml/min flowrate.

For HPLC analysis, two different mobile phase gradients were used, with methanol and 1 % v/v acetic acid solution. Gradient A (fast method) was applied to have a fast analysis and to determine the total phenolics, as they elute as a region of unresolved peaks after the 5-(hydroxymethyl)-2-furaldehyde (HMF) peak. The gradient profile was 0-5 min 10 % methanol, 5-9.3 min gradient to 84.5 15.5 %, 9.3-9.4 min gradient to 100

%, 9.4-17 min 100 %. With Gradient B (detailed method, Figure 3-1), the elution was slower and it was used for detailed analysis of the samples with adequate peak resolution. The gradient profile was 0-15 min 10 %, 15-55 min gradient to 30 %, 55-70.1 min gradient to 100 %, 70.1-80 min 100 %.

In all the measurements, compounds are quantified in vanillin or syringaldehyde equivalents, which mean that it is respectively the concentration of vanillin or syringaldehyde that has the same UV absorbance as the compound. The absorbance at 280 nm corresponds to the $\pi \rightarrow \pi^*$ transition of the aromatic ring [168]. As phenolic inhibitors are small molecules, most of them have one aromatic ring.

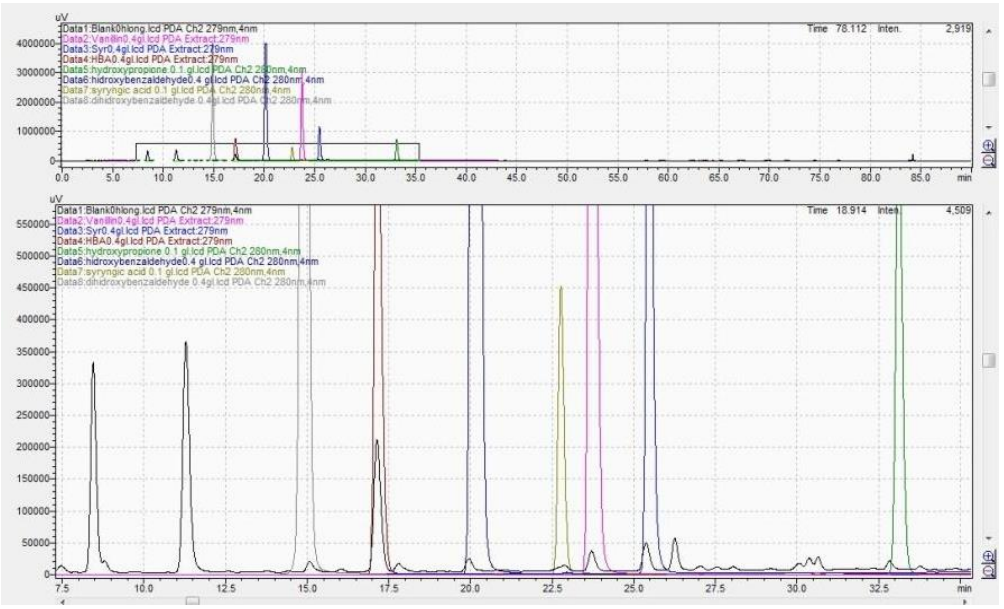

Figure 3-1: Detailed phenolic analysis using HPLC-UV method B.

3.3.1.2 UV Spectrophotometric measurements

A simple UV measurement can also give information about the phenolic content. It is a fast and low-cost method, but a number of products can interfere, with most importantly, the proteins and furans. If laccase reacts selectively with the phenolics in a sample, leaving every other UV absorbing compound unaffected, the absorbance change will be caused solely by the decrease of phenolic concentration [169]. If also other compounds are removed during detoxification (for example furfural), the UV absorbance can be used to determine the end-point of the reaction, but no information of the quantity/quality can be drawn. It had been noticed that, due to deprotonation of the phenolics, their spectra were usually dependent on the pH.

Method

For laccase-XRF analysis the sample was filtered through a 0.45 µm syringe filter, diluted 125 times (200 µl in 25 ml) with a NaOH pH 10.4 solution to stabilize the pH and measured by spectrophotometry (Genesys 10UV spectrometer, Thermo Fisher Scientific, Waltham, MA, USA) at 280 nm.

3.3.2 Carbohydrate concentration measurement

Sugar measurements are strongly needed, as they are the substrates for both ethanol and lactic acid fermentation; however, their chemical and physical properties make quantification difficult. Glucose and xylose do not have significant absorbance in UV-VIS range making detection difficult and the lack of capability for stronger interactions make their separation challenging. The widest spread methods are the 3,5-dinitrosalicylic acid (DNS) method to measure the reducing sugars, an enzymatic method and HPLC analysis. A DNS measurement is based on the reduction of the added DNS reagent, while the aldehyde function of reducing sugars is oxidized [170]. Enzymatic methods are based on the enzyme's selective reaction with one of the sugars resulting in colorimetric change, for example the oxidation of glucose by *glucose oxidase*. The measurement is selective to glucose; however, the enzyme kit is expensive. HPLC is the most widespread method as it gives selective and easily quantifiable results, however special columns are needed [68], [171]. After derivatisation of sugars, more measurement techniques become available, such as GC or alternative HPLC methods with common columns [172], however it requires an extra step and rather expensive equipment will still be needed.

3.3.2.1 HPLC-RI measurements

As mentioned before, it is difficult to separate sugars due to their inert nature. Two widespread columns are available: i.e. amine (HILIC) and a gel type H^+ cation exchange column (sugar column). Amine columns are cheaper, however often gradient elution is needed which makes Refractive Index (RI) detection difficult [173]. On the other hand, gel type sugar columns (Biorad [174], Transgenomic [175]) work with a single eluent in isocratic mode, measure all substrates and (side)products, both for fermentation and hydrolysis (glucose, xylose, acetic acid, methanol, ethanol and lactic acid) and no sample preparation is needed, only dilution and filtration. The drawback is the cost (around 1500 €, included guard column) and sensitivity of the column (only 700 injections guarantied). The detection is either refractive-index (RI, isocratic flow,

robust), evaporative light scattering detector (ELSD, non-linear, nitrogen is needed) or electrochemical detector (EC, magnitudes higher sensitivity and price, special eluent). The separation principle is not fully understood; it is supposed to be a combination of cation and ligand exchange together with size exclusion.

It has to be noted that gel sugar columns can measure also furans and some of the phenolics, both with an RI detector (lower sensitivity) or a coupled UV detector (high sensitivity), but the retention times are high (around 90 minutes). Mixing acetonitrile to the aqueous eluent makes it faster [175], however it is not advised by the manufacturer.

Method

The method given by the HPLC column provider was used without modification. The measurement setup was a HPLC (Hewlett Packard Series 1050, Palo Alto, CA, USA) with an ICSep COREGEL 87H column (Transgenomic, Omaha, NE, USA), equipped with a RI detector (Hewlett Packard 1047A, Palo Alto, CA, USA). The eluent was 8 mM sulfuric acid in demineralized water, at 55 °C, 0.5 ml/min. First measurements were made with an attached paper integrator (SHIMADZU C-R3A Chromatopac), afterwards it was changed to Geminyx software with an AD converter, and finally in-house written Labview software was used with the AD converter. The appendix contains a section about the HPLC measurement, as different setups were used.

3.3.2.2 Structural carbohydrate determination in the solid

Before enzymatic hydrolysis of the steam exploded solid substrate, it is necessary to measure its structural carbohydrate composition in order to calculate the hydrolysis efficiency and the remaining carbohydrate in the solid. The procedure is according to National Renewable Energy Laboratory (NREL) analytical procedure [175]. The principle of the method is a low temperature concentrated acid hydrolysis, followed by high temperature diluted acid hydrolysis, next to a blank sample. The measurement itself is a sugar concentration determination with the HPLC-RI method as described before (Section 3.3.2.1). Based on the obtained concentrations the sample's glucan and xylan contents are calculated.

Method

A simplified NREL method is used, where only the glucan and xylan is measured, the lignin is assumed to be the rest in the sample (thus ashes are also incorporated in lignin

content) [175]. The biomass sample was washed with demineralized water, and then dried at 40 °C for at least 24 h. Three parallels were measured for all samples. 300 mg of the sample was measured in a glass tube and 3.00 ± 0.01 ml of 72 % sulfuric acid was added. A separate glass stirring-rod was used for every tube, initially mixing the sample until it was thoroughly mixed. The tubes were covered watertight and placed in a water bath shaker set at 30 ± 3 °C and incubated for 60 ± 5 minutes. Samples were stirred every 15 minutes.

Upon completion of the 60 minute hydrolysis, tubes were removed from the water bath shaker. Pressure tubes were filled with 84.00 ± 0.04 ml deionized water (number of samples +1 tubes were used). The water from one pressure tube was removed, and the sample, including the material on the stirring rod, was carefully washed in this pressure tube with water from another one. This was done so the water remaining in the wet pressure tube is closely constant during every sample preparation. By the end one wet sample tube remained, which was not used further. The final sulfuric acid concentration was 4 %.

The tubes were sealed and placed in an autoclave for one hour at 121°C, together with three sugar recovery standards (SRS) (2 g/l glucose and xylose in 4 % sulfuric acid solution). After completion of the autoclave cycle, the hydrolyzates were slowly cooled to near room temperature before removing the caps. Calcium carbonate was added to the samples until they were foaming, after the foaming stops the pH will be around 7. After settling, the liquid phase was filtered with a 0.2 µm filter and measured for sugars by HPLC. For calculation of the exact concentrations, the peak areas were normalized by the areas measured in case of the current SRS standards and multiplied by 2 g/l (the concentration of the standards). For calculation of structural carbohydrates (glucan instead of glucose and xylan instead of xylose), the concentrations were corrected by 0.90 and 0.88 respectively (water molecule leaving when polymerized). The lignin content was assumed the rest of the mass after subtracting glucan and xylan content by neglecting the ash content, as it is less than a percent in the starting material [5].

3.4 Substrate preparation and characterization

Steam explosion (both autocatalyzed and catalyzed) is considered to be one of the most promising techniques to actual industrialization, because of easy upscaling, short treatment time, relative low chemical and energy demand and it is known to be effective for a wide range of substrates [176]. As the composition of the wood after

pretreatment varies depending on the treatment type, and several other parameters, it is important to characterize it prior to experiments [21].

3.4.1 Preparation

Poplar sawdust was donated by the sawmill Caluwaerts in Holsbeek, Belgium. The steam explosion was performed at Agro-BioTech in Gembloux, University of Liège (Figure 3-2). For every kg of sawdust, a liter of water was added, because otherwise the product would have been hard to remove from the reactor. This also decreased the concentration of products in the liquid phase to some extent (sugars, but also inhibitors). In the initial experiment (SE0), treatment was done at 25 bar (224 °C) for 3 minutes before explosion. Later, a wider range of treatment parameters were applied (

Table 3-2). As it was reported that longer pretreatment times (5-9 min) and lower temperatures (200-210 °C) are better for hemicellulose recovery [27], the temperature was decreased in the second session. Three batches (654, 655, 656) were later united as the ”SE united batch” and used for the bulk of the experiments. It must be noted that the temperature was steadily rising during the treatment, as the release valve was not sealing perfectly, except for run 653 (Figure 3-3) where the pressure was kept constant manually. The integrated severity factor was calculated for every batch [177], where **T** is the temperature in Celsius and **t** is the time in seconds.

$$S = log_{10} \int_0^t e^{\frac{T(t)-100}{14.76}} dt$$

Right after the treatment the slurry was centrifuged and stored at -20 °C as separate liquid (XRF) and solid fractions (GRF or SF). The solid fraction had 49.36±2.79 % dry content (Figure 3-4). It has to be noted that the XRF composition changed over time when it was left unfrozen, so the main volume was kept in three-liter batches, defrosted once, partitioned to 50-500 ml samples and refrosted again. It was defrosted a second time short before the experiments.

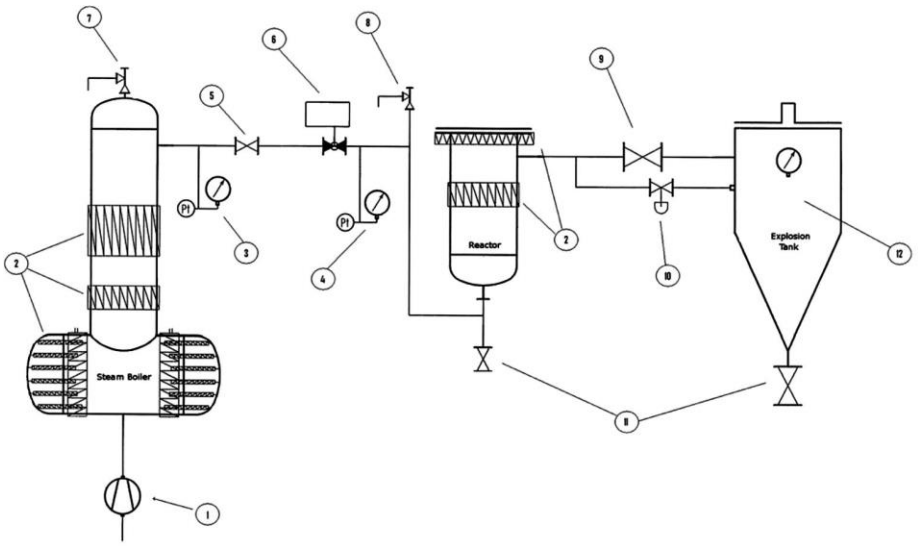

1. High pressure pump, 2. Heaters, 3. Gauges of steam boilers, 4. Gauges of reactor, 5. Isolation valve 6. Charging valve, 7. Safety steam boiler valve, 8. Safety reactor valve, 9. Explosion valve, 10. Purge valve, 11. Recovery valves, 12. Gauge of explosion tank

Figure 3-2: Scheme of steam explosion pilot plant in Gembloux [21].

Table 3-2: Steam explosion runs summarization. Including batch name, treatment time, temperature and calculated severity factor [21].

Batch	Time [min]	Temp [°C]	Severity [-]	Remarks
649	6.5	200	3.65	Reactor warmup
650	8	200	4.16	Higher treatment time
651	9	215	4.52	Higher time and temperature
652	7	200	4.07	Standard
653	9	200	3.89	Controlled pressure
654	7	200	3.92	SE united batch
655	7	200	3.93	SE united batch
656	7	200	3.99	SE united batch

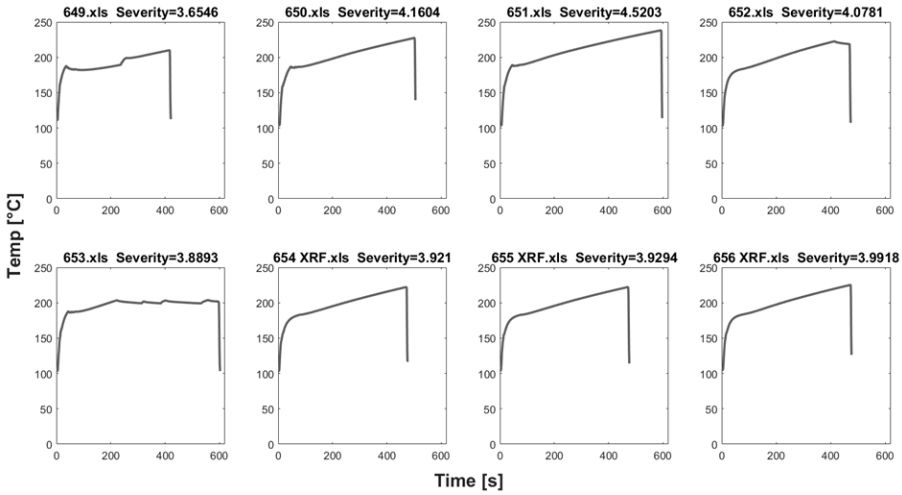

Figure 3-3: Temperature profile during steam explosion - runs 649, 650, 651, 652, 653 and three runs (654, 655, 656) that were later united as the ”SE united batch”.

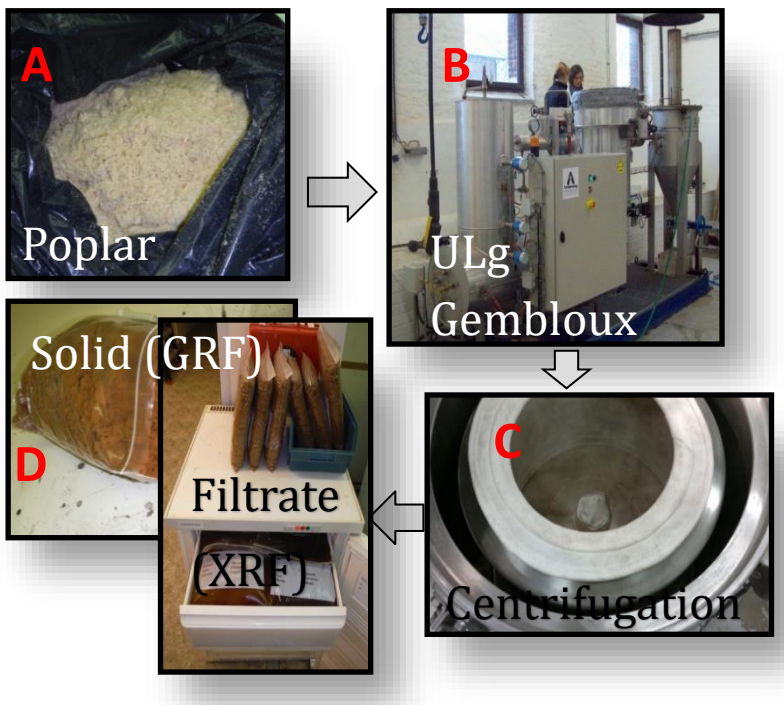

Figure 3-4: The pretreatment in pictures. Poplar sawdust (A), steam explosion (B), centrifugation (C) and the storage (D).

3.4.2 Composition of the solid fraction

Measuring the composition of the solid phase is essential for industrial application, as the hydrolysis efficiency ($g_{hydrolyzed}/g_{initial}$) is one of the most important cost-defining parameters next to carbon yield ($g_{product}/g_{substrate}$), volumetric productivity ($g_{product}/(l \cdot h)$) and titer ($g_{product}/l$). Samples were analyzed for their structural carbohydrates by acid hydrolysis, followed by HPLC-RI for sugars and HPLC-UV for inhibitors, as defined in Section 3.3.

Table 3-3: First steam explosion session (SE0) (25 bar or 225 °C, 3 min) – structural carbon composition of the solid fraction before and after steam explosion.

SE0 run	Starting material	Treated material
Glucan [%]	48.6	59.5
Xylan [%]	18.5	6.8
Arabinan [%]	1.2	0.0
Lignin [%]	31.7	33.7

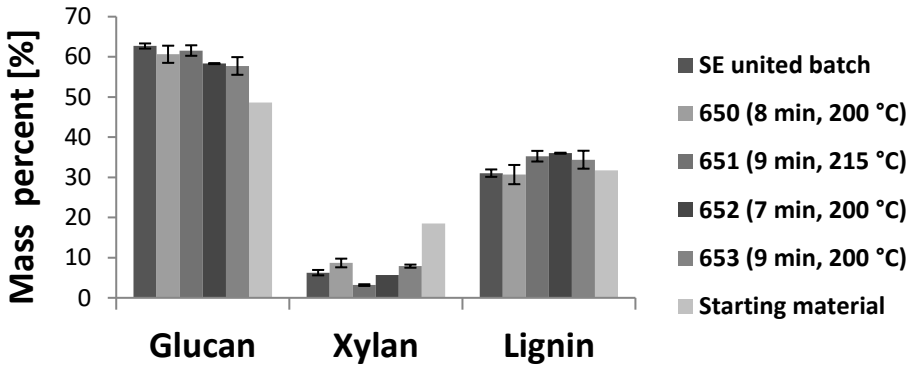

Figure 3-5: Structural carbohydrate measurements of the solid fraction from different steam explosion batches. Error bars are ±standard deviation from three measurements.

The parameters and conditions of the steam explosion runs were summarized before in

Table 3-2. Compared to the starting material, the xylan content of the solid fraction decreased significantly in every batch because of the hemicellulose hydrolysis (Table 3-3, Figure 3-5). The relative glucan content increased, mostly because of the overall

mass decrease due to hemicellulose hydrolysis, while the cellulose mainly remained intact, as was reported before [178]. The lignin content also increased in theory [178], but the measured differences are in the range of measurement errors. Lignin was hydrolyzed/degraded to a lesser extent, as will be observed from the XRF analysis later (see Section 3.7), and reported before [178]. In short, the amount of phenolics in the liquid phase does not confirm significant lignin solubilization. With standard deviations of the structural components varying between 0.1 and 2 absolute percent, considering that the sample injection of the HPLC itself has a standard deviation around 1 % and taking the complex nature of sample preparation into account, the results of the structural component measurement can be considered as precise. However, since the differences in percentages between different SE runs are typically also a few percent (with a maximum of 6 % absolute, see Figure 3-5), thus in the range of measurement errors, it is difficult to conclude statistically reliable facts, as in analytics 3xstd difference is considered to be the lower limit for reliable detection. Some general conclusions can be drawn however, Batch 651 has the lowest xylan content (Figure 3-5), which is expected, since it underwent the longest and highest temperature pretreatment (9 min at 215 °C). This consequently results in the highest lignin and cellulose percentages.

3.5 Enzymatic hydrolysis of steam exploded poplar substrate

3.5.1 Method

Hydrolysis of the five different SE batches (runs 650, 651, 652, 653 and SE united batch) was performed at 15 % solids loading, 2 m/v% cellulase loading (60 FPU/$ml_{product}$ of Optimase CX15L, DuPont, Wilmington, DE, USA), in a shaking water bath at 50 °C, 150 rpm and without external stirring for 48 h. The mixture's total mass of 20 g consisted of 3 g dry SF by using the equivalent wet SF, the added corresponding enzyme amount and was filled up with XRF until 20 g. The solid hydrolysis experiments from the SE united batch were also performed at 15 % solids loading (this is around 30 % SF in wet weight, see SF dry weight in Section 3.4.2), but at cellulase loadings of 2, 5, 10 and 20 m/v%. Again, the final mixture brought to 20 g by XRF. To determine the actual dry weight of SF added, the corresponding dry weight ratios of every stream explosion batch were used for correction. In one experiment, water was added instead of XRF to investigate the effect of inhibitors on the hydrolysis. During the hydrolysis experiments, liquid phase was sampled and analyzed with HPLC-RI for sugars and HPLC-UV for phenolics. First sample was taken after the mixture was homogenized;

thus, the reaction was already running for few minutes. Remaining solids after 48 h of hydrolysis were washed with three times solid volume demineralized water before structural carbohydrate measurements. Experiments were conducted in duplicate.

3.5.2 Results and conclusion

The initial carbohydrate concentrations were low in all cases, 0.6 g/l glucose and 0.2-0.3 g/l xylose (see Figure 3-7A and Figure 3-7B at 0 h), and no significant difference was visible between the different steam explosion batches. The inhibitor concentrations showed bigger variability both between batches and the standard deviation of the measurements was higher. In general higher severity (longer time and higher temperature) caused higher initial inhibitor concentrations [177]; the values of Batch 651 (9 min and 215 °C) are clearly the highest. Figure 3-6 shows the detailed phenolics analysis during two different steam explosion batches (one of the mildest and the most severe). It is visible that the formed compounds are the same, but their concentrations are different. It is expected that the phenolic profile (qualitative composition) is determined by the starting material and pretreatment technique rather than pretreatment parameters (time, pressure) (see Figure 3-6).

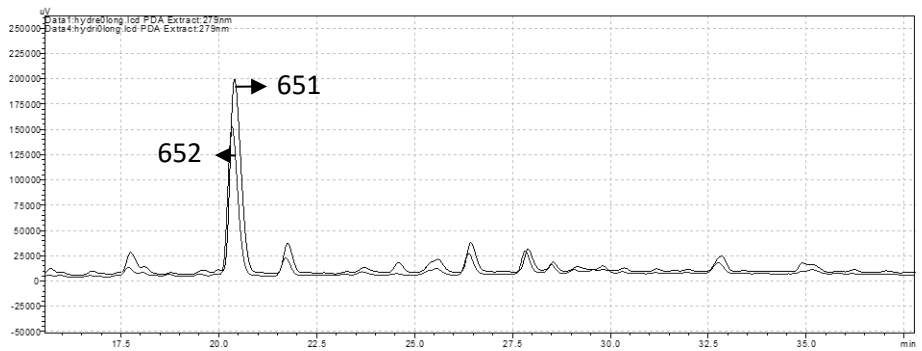

Figure 3-6: A detailed phenolic measurement of the XRF from batches 651 (longer treatment time, higher temperature) and 652 (shorter treatment time, lower temperature) shows how the amount of phenolics is depending on the treatment conditions but the exact compounds formed are the same.

During the hydrolysis experiment of four different steam explosion batches (Figure 3-7A), the glucose concentrations reached a final value around 9-12 g/l, this low value can be explained with the low cellulase loading (2 m/v%), glucan conversion was only 11 %. After hydrolysis, Batch 651 (steam explosion with highest pretreatment time and

temperature, 9 min and 215 °C) showed a higher glucose recovery compared to any other batch, i.e., around 25 % more, but also around 50 % less xylose concentration and almost a doubled furfural, HMF and phenolics concentration.

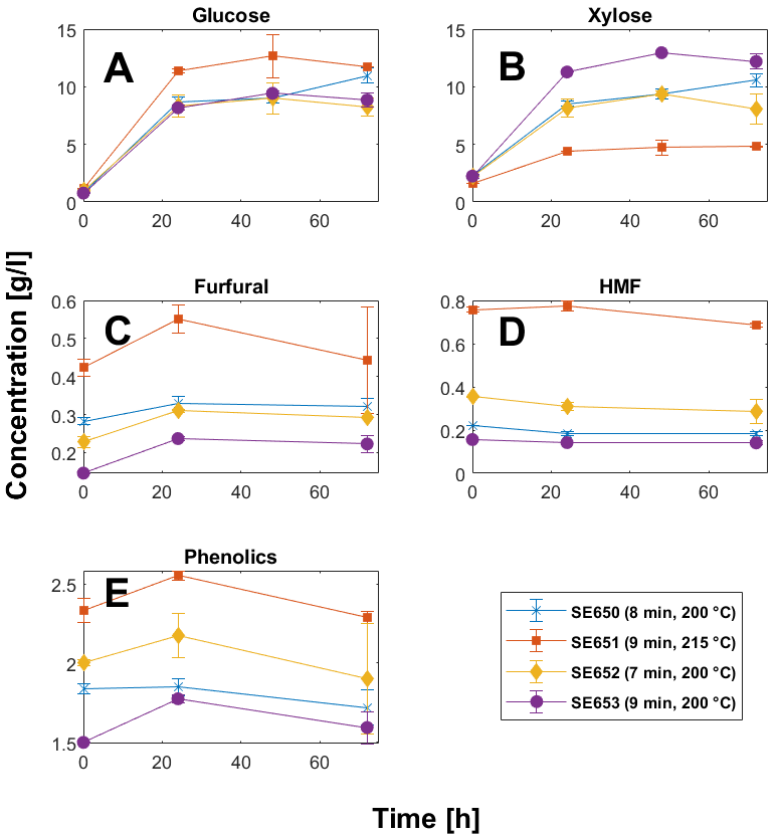

Figure 3-7: Hydrolysis experiments performed at high solid loading for four different steam explosion runs. The concentration evolution of five compounds was followed up: (A) glucose, (B) xylose, (C) furfural, (D) HMF and (E) phenolics. Standard deviation calculated from three samples.

In general, Batch 653 (manual pressure control at vapor pressure corresponding to 200 °C) produced comparable glucose recovery to the other batches (except for 651 which was 30 % higher), i.e., 50 % higher xylose recovery, 30 % lower furfural formation, significantly lower HMF and phenolic concentration. This batch is the relatively best if xylose is to be used, while if only glucose is utilized, a more severe pretreatment can be beneficial. This gives a hint that keeping the temperature low (around 200 °C) during steam explosion will be more important for efficient pretreatment than the treatment time [27].

Comparing xylose and furfural concentration of batches 651 and 653 (see Figure 3-7B and Figure 3-7C), it can be seen that the loss of 4 g/l xylose generated around 0.2 g/l furfural. This is partially explained by the difference in molar mass (150 to 81 g/mol), but there is still a 10-fold decrease remaining which is suspected to be caused by the evaporation of furfural during flash expansion. The phenolic inhibitor concentrations were usually slightly increasing during hydrolysis compared to initial concentrations (0-20 %) (Figure 3-7E), expectedly because of the release of inhibitors entrapped in the solid fraction matrix or because of desorption from the surface.

Analyzing the hydrolysis of the solids of the SE united batch (see Figure 3-8A) shows that increasing the enzyme amount clearly helped to increase the final glucose concentration. The relation between enzyme concentration and final glucose concentration is almost linear (see Figure 3-9), with at a 20 m/v% cellulase loading the curve is starting to bend due to substrate limitation and/or enzyme inhibition. At Figure 3-9 it seems like xylose hydrolysis yield saturates from 2 % added cellulase; however, this is just because the increase is not visible because of the relative higher glucose concentration. At Figure 3-8B it is visible that the final xylose concentration increases until 10 % added cellulase and saturates only after. It is not yet clear if it is because all accessible xylan was hydrolyzed by enzyme amounts equal to 10 % or that the hemicellulase enzyme was inhibited. Later it will be shown that the second case is valid in this section when discussing Figure 3-10, as significant amount of xylan was remaining in the solid phase. At Figure 3-8B, it can be seen that xylose concentrations stabilize before 20 h as hemicellulose is more sensitive to hydrolysis and a big portion of the xylose is dissolved in oligomer form that hydrolyzes in a few hours [31].

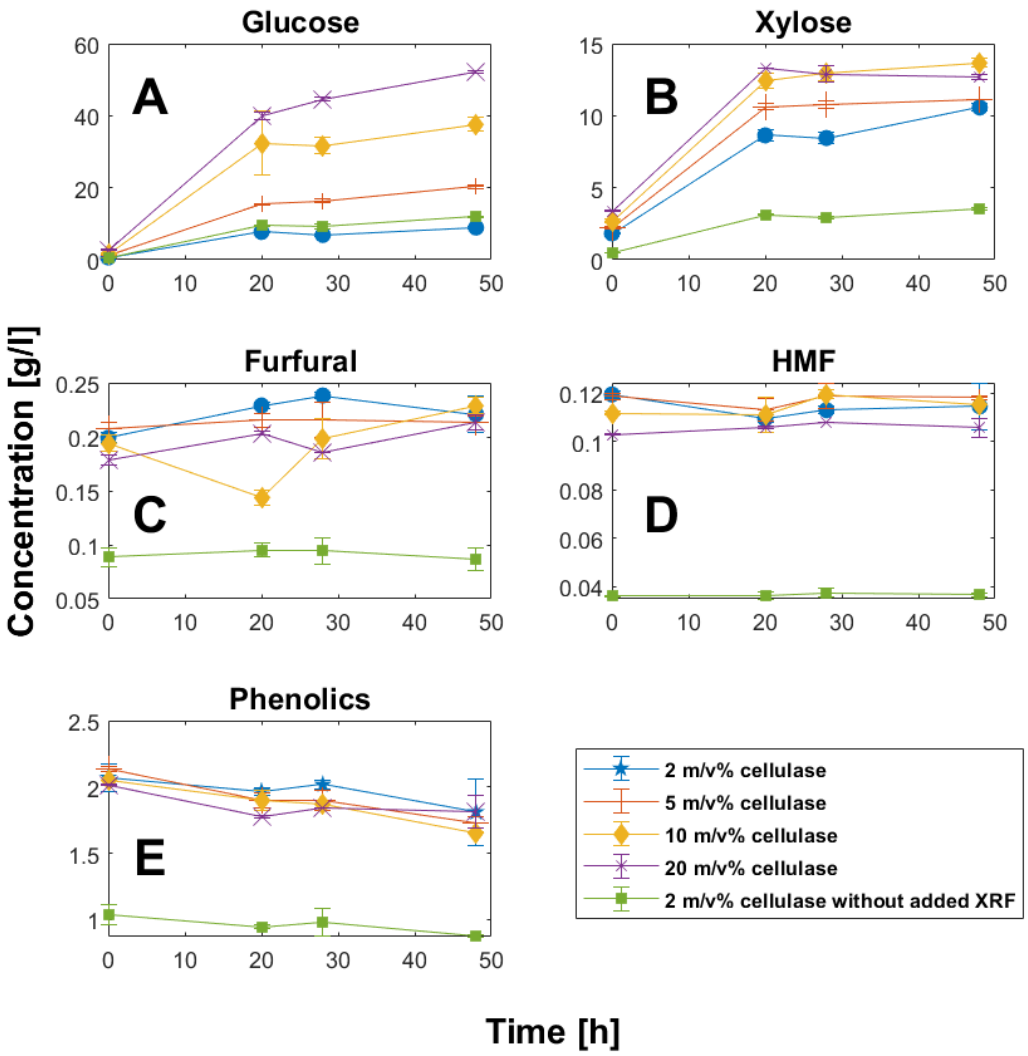

Figure 3-8: SE united batch hydrolysis experiments at 15 m/m% solid loading and different cellulase loadings of 2; 5; 10; 20 m/v%. One experiment was performed with water added instead of XRF to investigate adsorbed inhibitor amount and effect. The concentration evolution of five compounds were followed up: (A) glucose, (B) xylose, (C) furfural, (D) HMF and (E) phenolics. Different experiments are marked with different symbols. Error bars are ±standard deviation from three measurements.

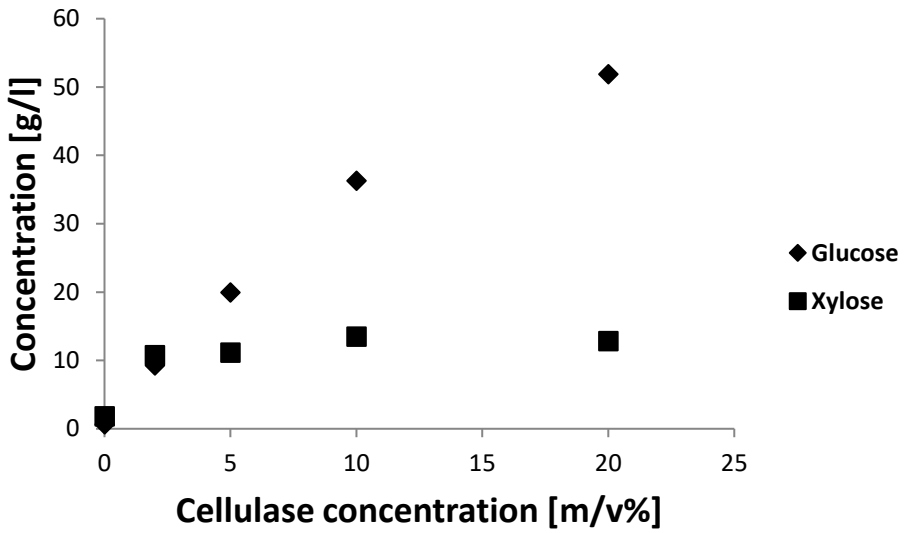

Figure 3-9: Final sugar concentration after 48 h of hydrolysis in function to added enzyme amount with XRF united batch.

A lot of variability can be observed, but generally, it seems that furfural increases until the first measurement point and then decreases (see Figure 3-8C), probably because of evaporation. The HMF concentration remained quite stable (see Figure 3-8D), while measured phenolics were decreasing slowly by time (see Figure 3-8E), expectedly because of evaporation and partially because of absorption coefficient difference caused by composition change as phenolic compounds can oxidize on air.

The experiment with added water instead of XRF produced slightly higher glucose yields compared to the XRF added experiment (12 versus 8.9 g/l, a 35 % increase). As a negligible amount of glucose is present in the XRF (0.6 g/l, initial value in Figure 3-8A), it is visible that the XRF composition hinders hydrolysis considerably (comparing experiment with/without added XRF inhibition is around 35 %). It has to be noted that from 20 g sample 6 g was the added solid, which contained around 3 g XRF liquid (50 % of solids DW). Calculating with approximately 14 g added XRF on top of these 3 g in other experiments, it can be seen that 3/17=17.5 % of XRF is also present in this case.

In Figure 3-8C-E, the inhibitors are always in a low concentration when water is added instead of XRF to the reaction mixture. However, when their ratio changes are compared in these experiments (furfural 0.09/0.20=0.45, HMF 0.04/0.12=0.33,

phenolics 1.03/2.07=0.55), it seems that they are present the XRF added experiment in much higher concentration than was expected from the XRF volume ratio in the initial reaction mixtures (0.175). From the evolution of the concentrations, it can be also concluded that, except maybe for furfural, the rest of the inhibitors are not trapped inside of the matrix, as their amounts do not significantly change and do not increase proportional to the rate of hydrolysis. The only logical solution is that after steam explosion, when both SF and XRF are in contact with each other, inhibitors are adsorbed on the solids in high concentration. Extensive washing would be needed to remove them. This is also the reason why the inhibitor concentration difference between the different experiments is lower than it would be expected from the XRF ratio, as if the concentration in the liquid phase decreases, compounds will desorb from the surface.

From the structural carbohydrate, measurements of the remaining solids after 48 h of hydrolysis (see Figure 3-10), it is visible that even the runs with 20 % added cellulase still contained 38 % glucan and 4 % xylan in the solid phase. This indicates that the saturation of the xylose concentration during hydrolysis after 10 % cellulase added (see final concentrations in Figure 3-8B), was not because of complete hydrolysis of hemicellulose but inhibition of enzyme, also glucan hydrolysis stopped because of enzyme related hindrance (deactivation, product inhibition, etc). The rest of the values are as expected, glucan and xylan percentage decreases with increasing enzyme amount (the difference is 0.8 % xylan between 2 % and 20 % enzyme experiment), while lignin percentage increases in the overall mass, as lignin is technically inert in the given conditions. It has to be emphasized that even with an economically unrealistic 20 % added enzyme around 2/3 of the glucan remained unhydrolyzed because of enzyme hindrance. As the enzyme is expensive, and 66 % of the valuable carbon source is still in the complex bounded form, it is deemed that this specific system (parameters, materials) is uneconomical in a separate hydrolysis and fermentation (SHF) process, as in this case the remaining unhydrolyzed sugars will not be utilized during fermentation and filtered out/thrown away later. As it was shown, inhibitors can significantly hinder hydrolysis, thus detoxification (e.g., laccase detoxification) techniques have a potential to enhance also hydrolysis, not only fermentation.

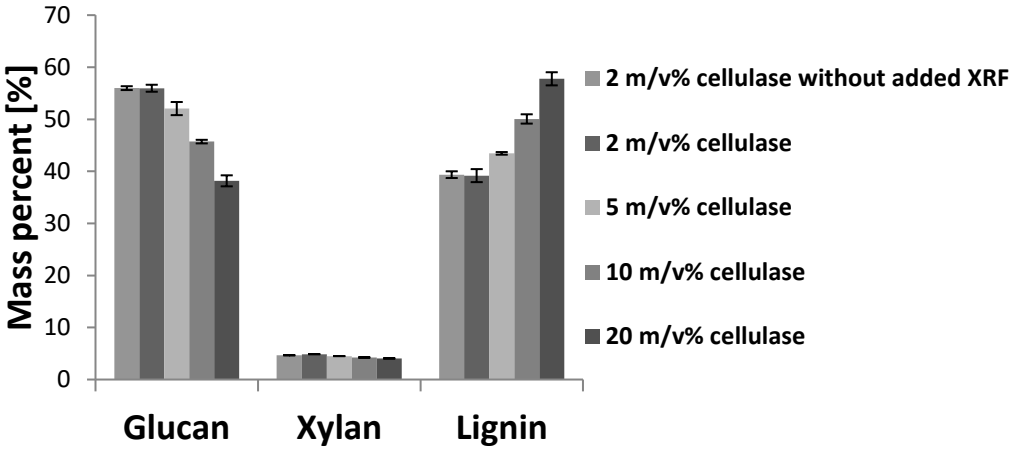

Figure 3-10: Structural carbon measurements of the remaining solid phase after hydrolysis with different cellulase ratios and with SE united batch. Error bars are ±standard deviation from three measurements.

3.6 Laccase characterization according to literature

This section introduces laccases, their standard activity measurement techniques according to literature, followed by an investigation of laccase reaction with vanillin, a model phenolic substrate. Thereafter the reaction with XRF, an industrially relevant substrate was investigated, followed by a benchmarking of laccases available on the market.

3.6.1 Laccase activity determination

It is important to have a fast activity determination method to map the best working conditions. The standard tests, however, strictly measure laccase activity on a specific substrate, thus extrapolating to another substrate (such as phenolics in XRF) is less certain and synergistic effects with the cellulase activity (very important if SSF is applied as the two enzymes have to work in parallel) are not quantified at all. Fast mapping is beneficial to gain fundamental information about pH and temperature dependencies, as these are important parameters in SSF. The typical temperatures are between the optimal cellulase working range (50 °C) and the optimal growth temperature for the microorganism (30-37 °C). The higher the temperature, the faster the reactions, and technically, it can be as high as 100 °C without significant extra energy requirement, as it is the temperature of the material right after the steam explosion. When looking at all of the subprocess, the lowest pH value is 3-4 (pH of the

material after autocatalyzed steam explosion), through pH 4.8 (during hydrolysis) until a maximum value of pH 6.5-7 (the case of bacterial fermentation). Any laccase detoxification performed at a pH value outside this range will require additional chemicals.

3.6.1.1 Method

The enzyme activity was measured, either with syringaldazine as a substrate [169] or by using ABTS as a substrate [179]. The concentrations were taken from standard methods; thus, it is expected that concentrations over V_{max} value, but this was not measured. ABTS is better soluble in water than syringaldazine, and the methanol that is used in the standard syringaldazine method inhibits the laccase enzyme [180]. The measurements were always done using 200 µl substrate, 100 µl enzyme solution and 1700 µl buffer. The absorbance change, monitored at the mentioned wavelength in the description, was followed with a Genesys 10 spectrophotometer (Thermo Fisher Scientific, Waltham, MA, USA) at every six seconds for four minutes and the initial linear phase was used for activity calculation. For activity determination, 0.1 M phosphate buffers between pH 5 and 8 and 0.1 M citrate buffers between pH 2 and 5 were used. All chemicals were purchased from Sigma-Aldrich (St. Louis, MO, USA).

Tests at a specific temperature were done as follows: the buffer and reagent were brought into a plastic cuvette, covered with a cap, and placed in an oven at the corresponding temperature. After several hours of equilibration, cuvettes were removed, the enzyme was added and mixed and the kinetics was measured instantly. The spectrophotometer was not temperature controlled.

Initially, the **syringaldazine** (4-hydroxy-3,5-dimethoxybenzaldehyde) test was used. (ε= 65 1/(mM·cm)). The absorbance was measured at 530 nm at 30 °C default (Soti et al., 2016). The syringaldazine solution had a concentration of 0.1 g/l in methanol. The **ABTS** (2,2'-azino-bis(3-ethylbenzothiazoline-6-sulphonic acid) (ε= 36.1/(mM·cm)) test is widely used, as the substrate has a high solubility in water, unlike syringaldazine. If not mentioned otherwise, it was performed with 5 g/l ABTS solution and monitored at 420 nm.

Through the course of the research, altogether five different laccases were tested:

1. *Trametes versicolor,* Sigma-Aldrich, 13.6 U/mg, powder form, 50 €/g price (50 000 €/kg). This is a high activity purified laccase, taken as a standard and used for most of the experiments. Because of its price, it is not relevant industrially. Referred to as Sigma laccase or **S**.
2. *Trametes species,* kindly offered by Company A, powder form, no further information available. Referred to as *Trametes* or **T**.
3. *Cerrena unicolor*, offered by Company A, granulate form, no further information available. Referred to as **U** or ***Unicolor***.
4. Commercial fungal laccase from Hangzhou Cyclic Chemical Co., Ltd. (Hangzhou, CH) 26 €/kg. This was the only laccase that had an exact high quantity price for it (in the range of tons). Referred to as **Ch**.
5. Bacterial laccase*,* offered by Company B, liquid crude extract and freeze-dried form, no purification. Referred to as bacterial or **B**.

3.6.1.2 Results and conclusions

Laccase activities were measured with the ABTS activity test in the relevant range of conditions for SSF, i.e. pH 3-5 and 30-50 °C (see Figure 3-11). Concentrations of the different enzyme solutions were adjusted to a similar activity range, which was successful in case of **U, T** and **Ch**. **S**, as a purified enzyme had a very high activity, even after applying high dilutions. In general, all fungal laccases had a better performance at a lower pH and higher temperature, except for the *Unicolor* laccase that showed a lower sensitivity towards the pH, producing similar activities over the applied pH range, while **Ch** was extremely sensitive to temperature as well as pH. Specific activity measurements (activity normalized by mass) at pH 5 and 50 °C showed that **S** had 3.7 times higher activity than **T**, which on his turn has 5.2 times higher activity than **U**, which has 237 times higher activity than **Ch** (see Figure 3-12). The above mentioned values are always used in comparison with each other, as pH changes the absorption characteristics of ABTS, thus comparing values at two different pH values is misleading, as well as it is known that the test underestimates the activity, thus the calculated value is not explicitly the reaction/time value defined in theory [179].

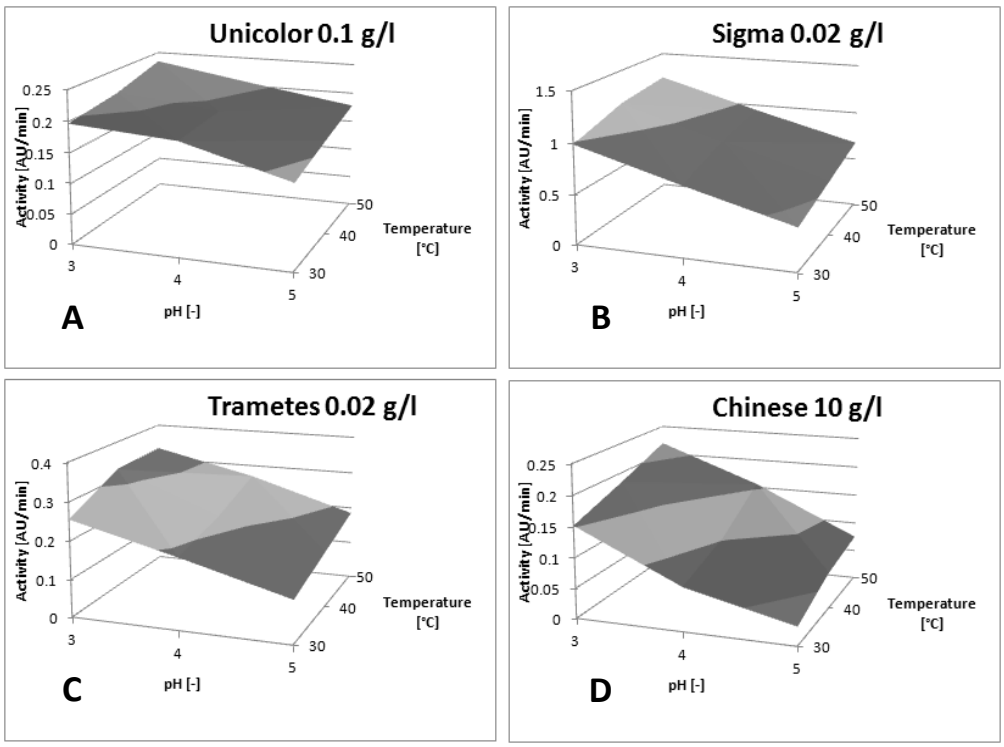

Figure 3-11: Activity of fungal laccases over the relevant working range (30-50 °C, pH 3-5) measured with ABTS substrate. Bacterial laccase had activity only at pH 8.

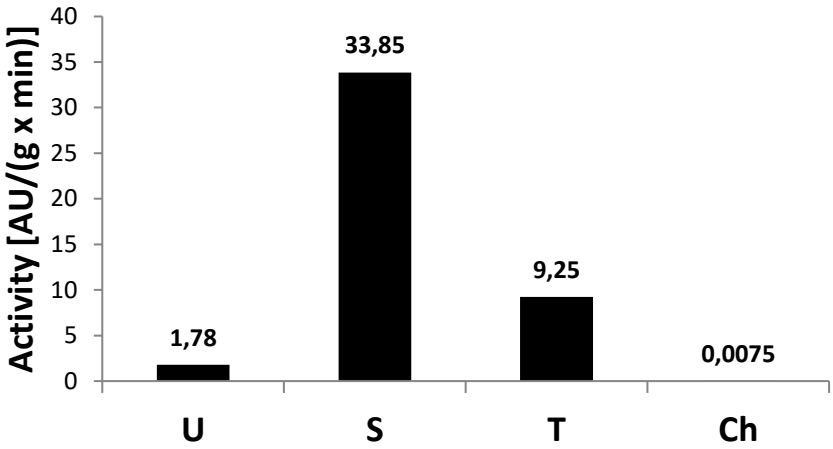

Figure 3-12: Specific activity of fungal laccases at pH 5 and 50 °C measured by ABTS substrate.

Bacterial laccase activity was measured with syringaldazine, in a 0.2 M phosphate buffer at pH 8, as it showed no activity over a pH range of 3-7, and a maximum activity

at pH 8. The enzyme was also temperature dependent, performing best at 50 °C. Higher pH values were not investigated, as it is known that saccharide monomers start to degrade from pH 9 and higher, hence it has no industrial relevance trying it. Measurements showed 121 mAU/min activity at a 4.29 m/V% crude enzyme dilution. The difference in molar extinction coefficients between ABTS and syringaldazine will cause a 1.8 times steeper slope for syringaldazine (65/36 mM·cm/mM·cm), which means that the measured ABTS change would be approximately 67.2 mAU/min. Strictly saying, this calculation is not correct as the absorbance characteristics depend on the pH, and the affinity/specificity of laccase towards the two substrates can differ. Taking the enzyme product concentration of the reaction solution (42.9 g/l) and the dry content of the enzyme product (38 m/m%) the specific activity would be around 0.0041 AU/(min·g_{dry}), which is almost half of that calculated for **Ch**. The similarities between the activities of the two industrial laccases confirm the results, and hints that the specific activity between industrial and purified enzymes can be easily in the range of tens if not hundreds. It must be emphasized that this is only a calculation, as the two measurements and parameters are not strictly comparable.

3.6.2 Laccase activity on vanillin as standard substrate

Vanillin, a phenolic aldehyde, was investigated as a model compound prior to XRF detoxification. It was chosen as it appears frequently as one of the phenolic inhibitors present in the hydrolyzate [181], [182]. The goal of this part of the measurement was to get familiar with laccase reactions and elaborate measurement techniques. Vanillin oligomerization appeared before in a number of articles. Constant et al. described the formation of two types of dimers by connecting two vanillin monomers through ether and carbon-carbon bounds or only one ether bound during thermocatalytic oxidation on noble metal catalysts [183]. Lahtinen et al. showed that in a vanillyl alcohol laccase system (and not the vanillin aldehyde) two main dimer products were formed, i.e. by an ether bound and a carbon-carbon covalent bound, and less vanillin was formed by oxidation of the hydroxyl group on the substrate [184]. They concluded that pH and temperature affect the profile of the reaction products (ratio of different products), but they did not investigate the product time evolution.

Our goal was to monitor the reaction, mainly the substrate evolution in time by spectrophotometry and compare it to HPLC-UV. UV-chromatography enabled additionally to measure the products and their evolution in time.

3.6.2.1 Method

For the reaction, 1.8 mg of vanillin substrate (>97 %, Sigma-Aldrich Corporation, St. Louis, MO, USA) was dissolved in 50 ml 0.1 M phosphate buffer of pH 6.9 in an Erlenmeyer, and placed in a water bath shaker at 30 °C and 150 rpm to equilibrate. The reaction was initiated by adding 5 ml of the enzyme solution to the mixture. For the vanillin reaction 0.6 U/ml (1 g/l) laccase solution was prepared from **S** with 0.1 M pH 6.9 potassium phosphate buffer, at least twelve hours before the measurement and stored at 4 °C. Follow-up was done by sampling regularly.

UV spectrometry and HPLC-UV measurement. Samples of the vanillin-laccase reaction were measured without filtration with UV spectrometry (Genesys 10UV spectrometer, Thermo Fisher Scientific, Waltham, MA, USA) or were filtered through a 0.45 µm syringe filter, either analyzed immediately by spectrometry or by HPLC-UV after adding 50 µl 1 mg/ml azide (Sigma-Aldrich Corporation, St. Louis, MO, USA) to a 3 ml aliquot to stop the reaction. HPLC-UV (Shimadzu SPD-M20A diode array detector, Shimadzu corp., Kyoto, Japan), with methanol and 1% v/v acetic acid solution (Sigma-Aldrich Corporation, St. Louis, MO, USA) as a mobile phase on a Luna 5 µm C18(2) 100 Å column (Phenomenex, Torrance, CA, USA). Every analysis was performed at 1 ml/min flowrate. The mobile phase gradient was: 0-5 min 10 % methanol, 5-35 min gradient to 50 %, 35-35.1 min gradient to 100 %, 35.1-40 min 100 %. The concentrations of the phenolics are expressed in vanillin equivalent, which is the concentration of vanillin that has the same peak area as the measured compound. The time required for filtration before azide addition and HPLC measurement was negligible compared to the time of the reaction. Azide was not added to the UV measurement due to its strong absorption in the UV range that would interfere with the spectrometric measurements of the phenolics. A blank sample was measured in the same way by mixing 3 ml of buffer with 50 µl of azide solution for HPLC and without azide for spectrometry.

Vanillin-laccase products identification with Preparative HPLC-MS. The fractionation of the sample was done with semi-preparative HPLC (Waters corp., Milford, MA, USA) with a binary pump, automatic injection sampler, diode array detector and triple quad detector mass spectrometer (TQD-MS, Waters corp., Milford, MA, USA) and an automatic fraction collector to isolate the HPLC fractions. The parameters of the MS detector were: 100 °C temperature, desolvation at 200 °C at 250 l/h gas flow and 50 l/h cone gas flow, the applied capillary/cone/extractor/RF lens voltages were 3k/60/3/0 V. The detector was working in positive mode. A Luna 5 µm C18(2) column with large internal diameter (250 x 10 mm) was used. The injection volume was 3 ml

and the elution rate was 3 ml/min, with methanol and 0.1 % acetic acid solution used in a gradient elution as follows: 0-15 min 50 % methanol, 15-20 min gradient to 100 %, 20-25 min 100 %. The fractions collected were dried in a vacuum centrifuge (RVC 2-18 Rotational Vacuum Concentrator, Martin Christ, Osterode am Harz, Germany) at 50 °C and 1200 rpm until the liquid was completely evaporated. 1 mg solids were brought into 1 ml water or methanol.

3.6.2.2 Results and conclusions

Preliminary experiments

Visual inspection of the vanillin-laccase reaction mixture revealed that it was transparent at the beginning of the experiment and turned to a slight opal yellow color after about one hour reaction time. The appearing yellow color of the laccase-vanillin reaction mixture is caused by the formed dissolved products, while the opal effect was expected to be caused by the formed particles, as the color remains and the opacity disappears after 0.45 µm filtration.

The vanillin concentrations, measured after filtration by UV and HPLC, decrease over time (see Figure 3-13), which was expected as the substrate was converted to oligomers. These products precipitate and the formed particles cause scattering. The unfiltered UV measurements first slightly increased and then faintly decreased, probably due to sedimentation afterwards. Since reaction monitoring by UV absorbance without filtering is not appropriate, no further experiments were done with unfiltered samples. The results of the filtered samples were promising so further experiments were conducted, and the UV-measurements and the HPLC concentrations followed a similar decreasing trend during the reaction.

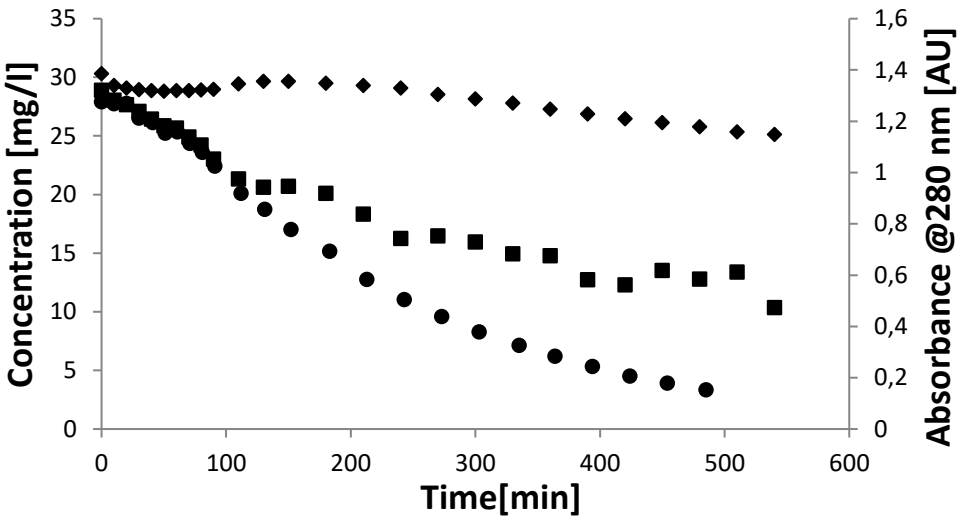

Figure 3-13: Vanillin concentration during reaction with laccase followed up by (◆) UV measurement without filtration, (■) UV measurement after filtration and (●) HPLC measurement.

UV-spectrophotometric measurements. Vanillin has absorption peaks at 280 and 315 nm and both could be used for reaction monitoring as they are declining with time (Figure 3-14). In these experiments 315 nm was used. After 360 minutes, the vanillin concentration measured by HPLC is under 10 % of the starting value, while the final absorbance is still about 40 % of the initial value. Part of this absorbance must be derived from the formed products as they have aromatic rings, but a scattering effect of particles with a size of 0.45 µm or smaller, can also play a role, as they are not filtered out.

HPLC measurements. A typical HPLC-UV chromatogram from a sample of the laccase-vanillin reaction taken after 180 min can be seen on Figure 3-15. The azide peak elutes at 4.5 min, the vanillin peak after 22.5 min. During the reaction two peaks appear at 35 and 35.5 min. The other peaks are the background derived from the buffer solution.

As soon as the reaction starts, the product peaks are appearing and increasing while the vanillin concentration as well as the summated HPLC peak area (see Figure 3-16), according to method detailed in Section 3.3.1.1, are decreasing. The total HPLC peak area is visualized to enable a better comparison with the measured UV spectrum and includes substrate, products and background, and excludes the azide peak. Product B

is formed faster than A during the course of the reaction, but later on its concentration decreases while A is still increasing until at least 300 minutes (Figure 3-16).

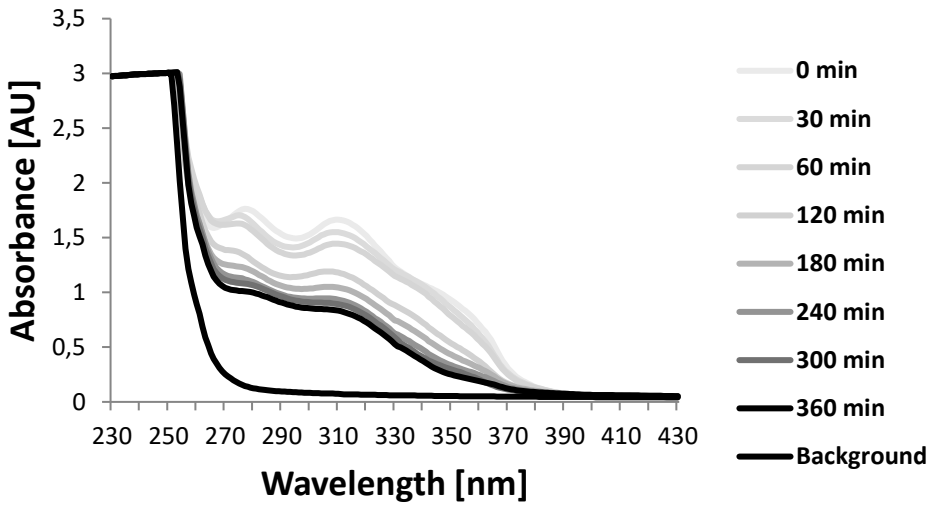

Figure 3-14: Absorbance spectrum decrease during Vanillin-laccase reaction.

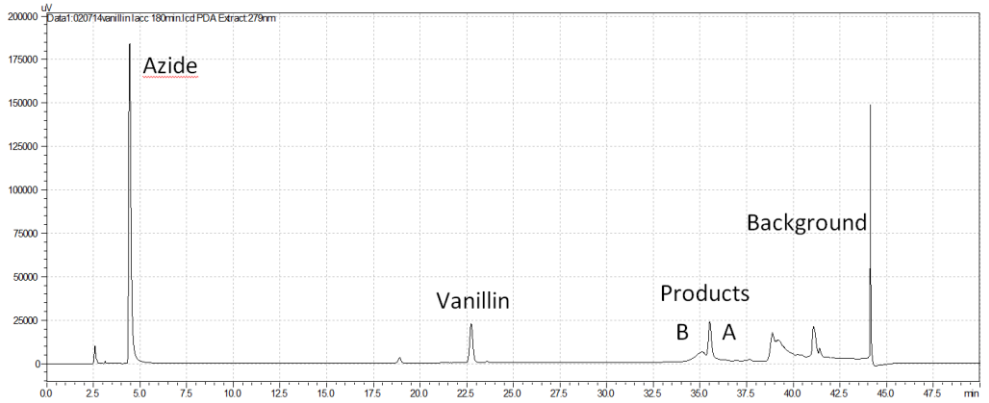

Figure 3-15: A typical HPLC chromatogram at 280 nm of the vanillin-laccase reaction from sample taken after 180 minutes with azide peak, vanillin peak and two product peaks B and A. Other peaks are background.

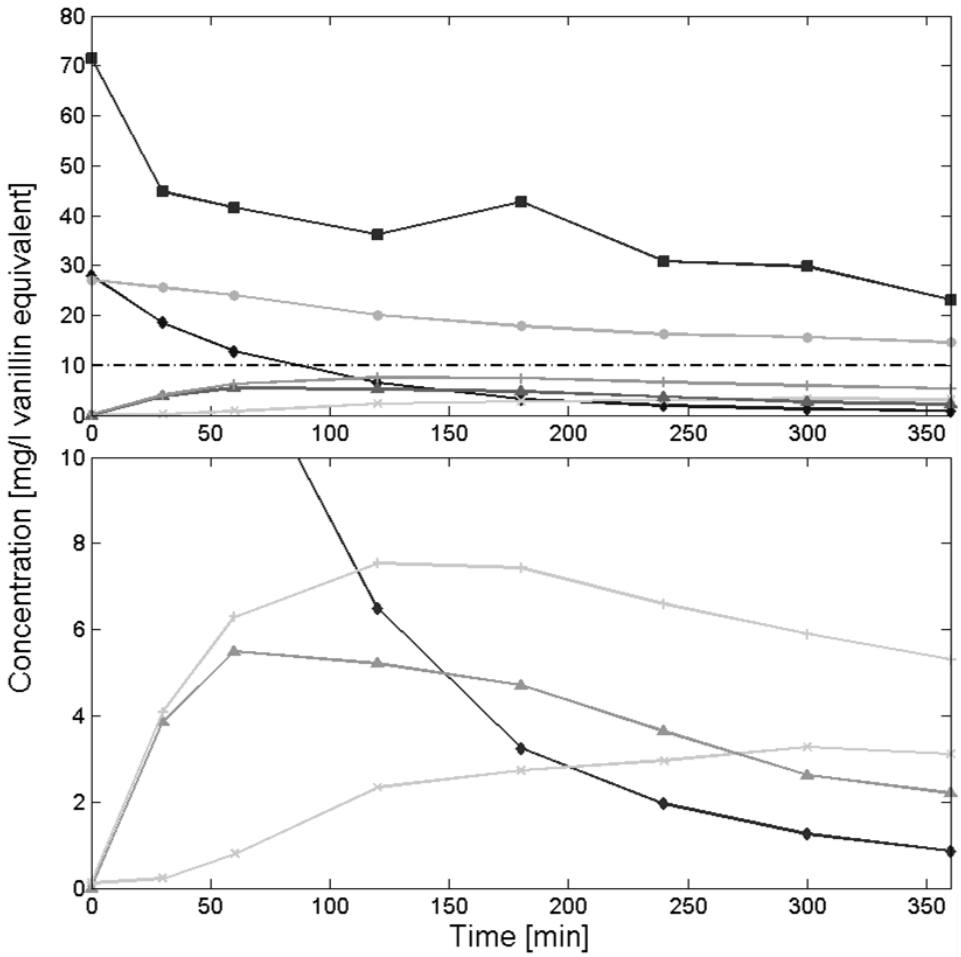

Figure 3-16: Concentration measurements during laccase vanillin reaction. The HPLC analysis of the reaction with (◆) the vanillin concentration, (x) product A, (▲) product B, (+) area of A and B products together, (■) is the total area of all peaks obtained from the sample. The concentration calculated from the UV spectrometric absorbance at 280 nm are marked with (●). Figure A covers the whole range, while Figure B is a detailed view in the 0-10 mg/l concentration range.

The number of products measured correlates well with the results of Lahtinen et al. [184], who investigated the vanillin alcohol-laccase reaction and found that the two main products were different dimers, one with an aromatic ring-aromatic ring bound and the other with an ether bound between the two aromatic rings, however the product concentration change in time was not investigated, as it is done in this work. From the evolution of both products in Figure 3-16, it seems that only product B is reacting further, while product A seems not to or at a much lower rate. The fate of the

reaction product from B is most probably polymerization and precipitation, as no additional product peaks appear.

Additionally, it is important to note that the absorption spectrum of vanillin is dependent on the pH of the solution, as often happens with phenolics [185]. The vanillin-laccase reaction was performed in buffer, so the pH remained stable during the UV measurements.

Product identification

HPLC-MS fractionation was performed in an attempt to separate the products and identify them. Chromatograms recorded during the fractionation of the vanillin-laccase reaction mixture are shown on Figure 3-17. The overall UV chromatogram, measured after 120 min of reaction time (Figure 3-17A), is closely related to Figure 3-15 that was obtained after 180 min at 280 nm. The first peak is vanillin at 11 min, whereas the second and third peaks are two product peaks at 18.5 min and 19.5 min, respectively. The absorption spectrum taken at a retention time of 19 min from the second product shows three main maxima at 206; 236 and 305 nm (Figure 3-17F). Figure 3-17B represents the mass spectrum monitored at 301 m/z, which is the deprotonated dimer mass.

From the fragmentation chromatogram (Figure 3-17E) filtered on 301 m/z, it was confirmed that the two products were dimers. This is the same as in the work of Lahtinen et al. [184]. The product peaks only differed in terms of intensity of fragments, but they had the same fragmentation pattern. The two main m/z-peaks, 285 and 286, found in the fragmentation chromatogram are expected to be the results of radical cleavages. Radical cleavage was suggested before by Cuyckens and Claeys in case of flavonoids [186]. They assumed that the negative charge on the neighboring phenolic ring enhances the stability of the remaining radical, thus a methyl radical will leave the molecule and a 286 mass unit negatively charged fragment is formed. The 285 fragment can be a result of a ring opening and a loss of extra H radical. As shown by Navarra, the free electron of radicals can delocalize to the oxygen of the phenol as well as in ortho-direction on the ring, though depending on the exact structure, other possibilities are described [187].

The mass spectrum at 151 m/z is visible on Figure 3-17C. This value is only appearing at the time the vanillin elutes, but it seems that no molecules of this size are obtained

after ionization of dimers. Figure 3-17D shows the overall mass spectrum during fractionation. The majority of the total mass present in the analytical sample is leaving the column after 4-10 minutes. No peak was found at 451 m/z, which would correspond to protonated trimers, although it is not clear if they are not produced, or if the low solubility makes them precipitate faster.

These findings are different to the results obtained for the phenol-peroxidase system by Yu et al. [188]. In their work all dimers were subjected to further polymerization by the *peroxidase* enzyme and the highest polymerization degree reached was that of a trimer. This was not true in our experiment (Figure 3-16) since only product B reacted further with laccase. Product B's concentration reached a maximum in 50 minutes and then started to decline.

According to the WATERNT™ software from the US Environmental Protection Agency, which estimates water solubility directly using a "fragment constant" method from the chemical structure, the dimer solubility decreases by 99 % compared to monomer, and trimer solubility decreased again with 98 % compared to dimers. Although the method is an approximation, the rates are an indication for the solubility decrease, and can explain why trimers were undetected in the solution.

After HPLC fractionation, the collected product samples were dried by vacuum centrifugation. The remaining solid was technically insoluble in both water and methanol. This suggests that the solid fraction underwent further reaction, possibly polymerization [189], or that the solubility of products is very low even in methanol.

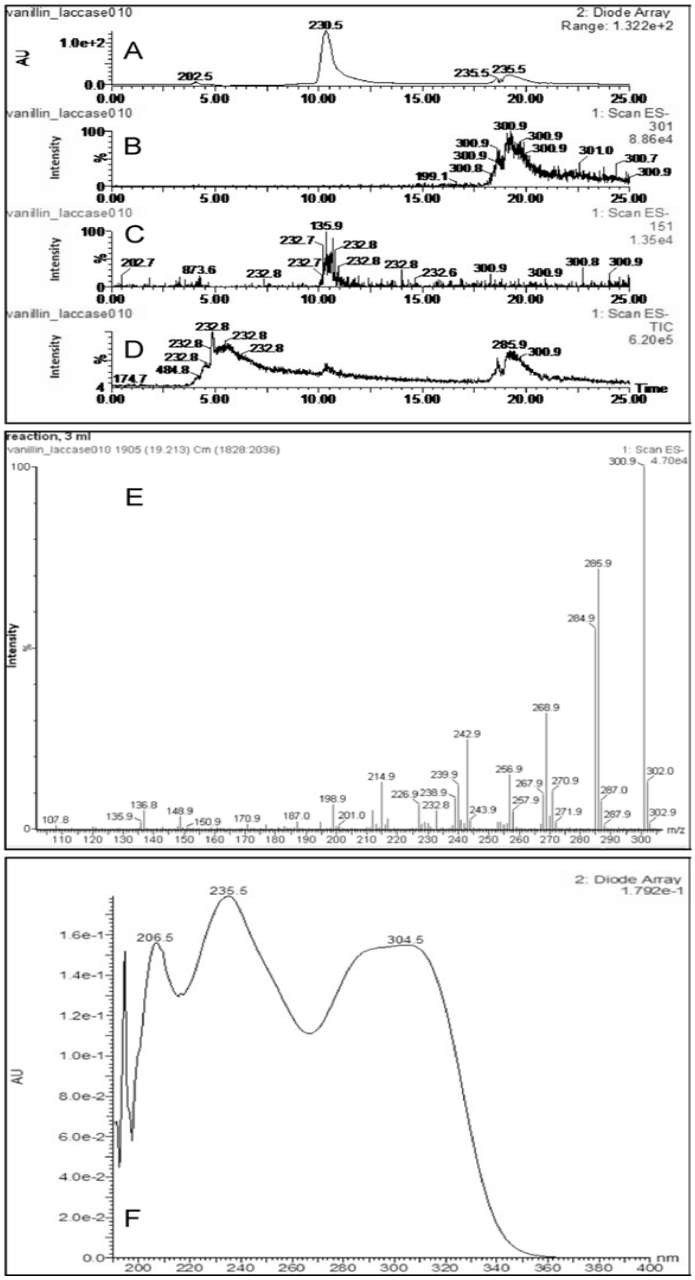

Figure 3-17: Preparative HPLC–MS chromatograms recorded during the purification of 3 ml sample. Graph A the general UV chromatogram, B the mass chromatogram at 301 m/z, C at 151 m/z, D the general mass chromatogram. Graph E is the mass spectrum taken from the product peak during fractionation and graph F is the UV spectrum of the product peak.

3.7 Laccase activity on the xylose rich fraction, detoxification

3.7.1 General investigation

Vanillin-laccase reaction is an XRF model system, which is good for understanding the process, whereas XRF is a real biological sample with a wide spectrum of compounds. XRF is obtained by lignocellulose pretreatment and contains sugars, but also lignin-derived phenolics that are toxic for the subsequent application of the sugars by microorganisms in fermentation. Spectrophotometric follow-up of the laccase detoxification reaction would be beneficial for industrial use, as it is simple, fast and robust.

3.7.1.1 Method

For XRF detoxification measurements, 29.5 and 3.3 U/ml (corresponding to 10 and 1.1 mg/ml respectively) Sigma laccase stock solutions were prepared in 0.1 M phosphate buffer of pH 6.9. The pH of XRF from the SE0 explosion run was brought to 7 with NaOH. Three different enzyme concentrations were used, i.e., 2.95, 0.3 and 0.03 U/ml. For an enzyme concentration of 2.95 U/ml (1.0 mg/ml), 5 ml of 29.5 U/ml (10 mg/ml) laccase solution was diluted to 50 ml with the XRF liquid. For 0.3 U/ml (0.1 mg/ml) enzyme concentration, 4.5 ml of 3.3 U/ml (1.1 mg/ml) laccase solution and 0.5 ml of buffer were diluted to 50 ml with XRF. For 0.03 U/ml (0.01 mg/ml) concentration, 0.5 ml of the 3.3 U/ml (1.1 mg/ml) and 4.5 ml buffer were diluted to 50 ml with XRF. The mixture was stirred at 150 rpm in a beaker at room temperature (22±2°C). Samples were collected and measured by HPLC-UV and spectrophotometry (methods in Section 3.1), after diluting 100 times with NaOH pH 10.4 solution to stabilize the pH.

Particle size measurements (Zetasizer Nano, Malvern Instruments Ltd., Worcestershire, UK) were performed with 2.95 U/ml laccase-XRF reaction solutions. Both enzyme and XRF solution were filtered (0.45 µm) separately before the reaction, and the two compounds were merged in an Erlenmeyer. Three samples were taken, at 0, 3 and 6 hours. The first sample was measured immediately; the other two samples were prepared in three different ways, i.e., without filtration, and with filtrations through a 0.45 µm and 0.2 µm syringe filter. Sampling was done in triplicate; each sample was subjected to 15 consecutive measurements; therefore, each data point is an average of 45 measurements.

3.7.1.2 Results

The hydrolyzate obtained after steam explosion had a pH value of 4 and was neutralized before the laccase reaction. During this, the color of the liquid turned to deeper brown. The reaction mixture was transparent at the start and turned milky over time. The speed of this change was faster at higher enzyme concentrations. During the reaction, slight acidification of the reaction mixture was observed by a decrease of pH by approximately 0.4 units.

UV-spectrophotometric measurements. The XRF had a single UV absorption peak at 280 nm corresponding to excitation of the aromatic π electron, which was decreasing fairly linearly over time at different rates depending on the enzyme dosage (Figure 3-18). It is important to note that the spectrum is strongly dependent on the pH, e.g., at pH 4 the peak is 32 % lower than at pH 10.4 for the sample taken at 0 min reaction time. Since the pH changes slightly during the reaction and the original samples absorbance is around 100, it was diluted 100 times in triplicate with NaOH solution to stabilize the pH and to achieve absorbance values under 2 units. Standard deviations from the triplicates were under 2.0 %. While filtering of the samples of the vanillin-laccase reaction caused a big difference in the spectrophotometric measurements (see Figure 3-13), the absorption difference between not filtering and filtering with 0.2 and 0.45 µm pore size was much lower for the XRF-laccase reaction. Compared to 0.2 µm filtered samples, filtering with 0.45 µm resulted in around 5 % higher absorbance and unfiltered samples gave 10 % higher values. This difference was stable during the course of the reaction. Probably this is due to the 100 times dilution of the XRF that reduces the particles concentration and hence the scattering effect.

Quantifying the different compounds from the UV spectrum of the spectrophotometer is impossible. It is known that furan-2-carbaldehyde (furfural) and HMF peaks have a significant absorbance at 280 nm, together with the targeted phenolics, so their presence is decreasing the sensitivity of the measurements (data not shown). In an industrial process, their concentration is minimized during pretreatment as they are formed by degradation of the processes' most valuable products, i.e., the monomer sugars.

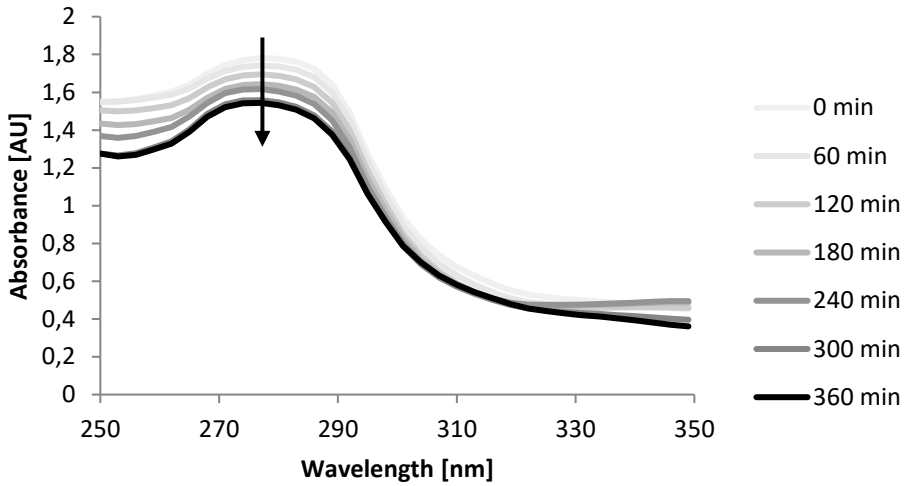

Figure 3-18: UV-spectrum change during *Trametes versicolor* laccase (Sigma)-liquid XRF reaction (1 g/l). Absorbance is decreasing over time at 280 nm.

HPLC measurements. The fast technique (Gradient A) identifies the following compounds, i.e., furfural, HMF and phenolics. Their initial concentration in the XRF gave rise to 12, 18 and 60 % of the UV absorbance respectively, but ratios measured may change with the pH due to the pH dependency of the extinction coefficient (data not shown). For 2.95 U/ml enzyme concentration, Figure 3-19 shows four chromatograms with Gradient B elution taken at different times (0, 3, 6, 24 h). Gradient B separates the phenolics to ten bigger peaks. From these, six peaks and afterwards, eight peaks disappeared after, respectively, 180 and 360 min reaction time. The two remaining peaks, i.e., the second and the fourth peak at 16 and 19 minutes, finally had 88 % and 83 % of their starting concentration respectively, and 47 % and 5 % of the starting total phenolics peak area (see Figure 3-20). From all the phenolic peaks, four were identified (see Table 3-4).

As discussed above, the decrease in phenolic peaks is clearly visible on Figure 3-19, but also formation of a broad flat peak can be distinguished at higher methanol concentrations in the mobile phase (more hydrophobic properties). Most probably, these are the product peaks of the reaction, i.e., dimers and potentially trimers. Their number can be estimated in the following way: if there are 10 different monomers and two bounding types (carbon-carbon and ether bound) are assumed, the number of possible dimer products is at a magnitude of hundreds, and the amount of different possible trimers are several thousands. It will be impossible to determine them

separately. As the polymerization degree rises, the aromatic ring will have a bigger impact on the properties and the side-chain functional groups that are bounded will have less, which explains the elution at higher hydrophobicity. In monitoring detoxification, these compounds will be measured as phenolics with both the 'fast' HPLC and the spectrophotometric measurements. However, research has proven that the polymerization products, obtained by enzyme treatment of phenolics, have reduced toxicity [190].

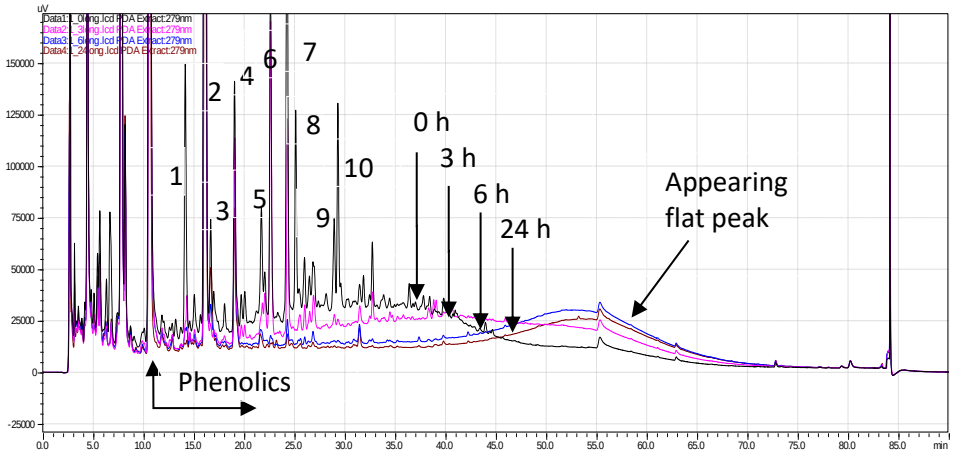

Figure 3-19: Measured HPLC chromatograms with Gradient B after 0 (—), 3 (—), 6 (—) and 24 h (—). The phenolics appear after the HMF peak at 12 minutes. Then main peaks were identified, numbered 1-9. The applied enzyme concentration was 2.95 U/ml.

The concentrations obtained by HPLC from the laccase-XRF reactions for the three different enzyme concentrations are presented in Figure 3-21. The HMF peaks increased slightly with the enzyme concentration, while furfural was slightly decreasing with a rate independent from the enzyme concentration (data not shown). The latter is caused by evaporation, as not the laccase enzyme caused the furfural decrease, but stirring and temperature did. Furfural decrease through vacuum evaporation was reported before in literature [191]. The grouped phenolics peaks were decreasing during the whole measurement at different rate and faster with higher enzyme dosage.

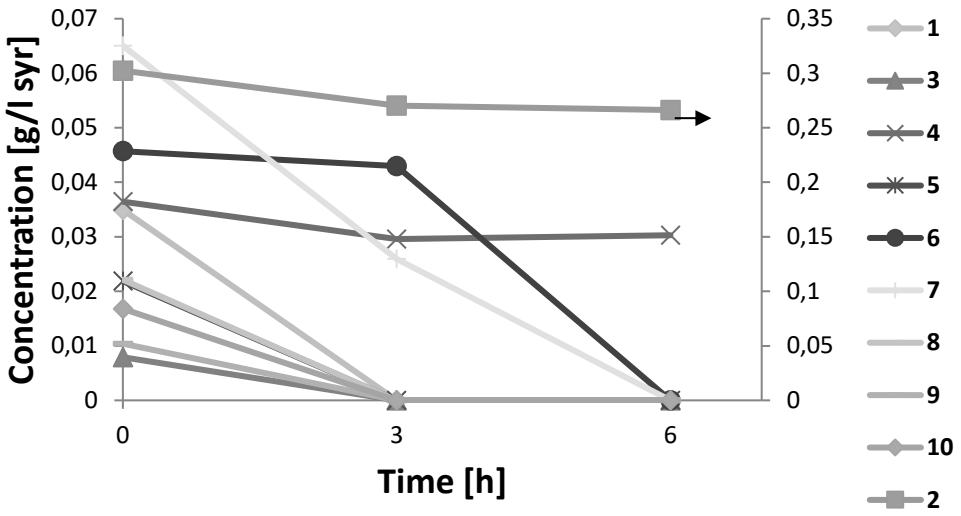

Figure 3-20: The concentration change of different phenolic compounds during *T. versicolor* laccase (Sigma)-XRF reaction.

Table 3-4: Phenolic compounds in the XRF from SE united Batch.

Retention time [min]	Area [-]	Area percent [%]	Model compound	Retention time [min]
8.57	3.8	0.54	-	-
9.42	10.3	1.47	-	-
10.30	21.5	3.07	3,4-DihydroxyBenzAldehyde	10.39
12.40	377.1	53.85	HydroxyBenzoicAcid	12.59
14.59	50.5	7.21	-	-
14.92	18.7	2.67	-	-
16.96	19.1	2.73	-	-
21.40	6.6	0.94	-	-
21.75	38.5	5.50	-	-
22.13	14.9	2.13	Vanillin	22.04
25.02	84.4	12.05	SyringAldehyde	24.96
26.76	11.5	1.64	-	-
28.08	4.5	0.64	-	-
28.26	4.9	0.70	-	-
30.20	10.9	1.56	-	-
31.13	3.5	0.50	-	-
32.26	15.7	2.24	-	-
34.42	3.9	0.56	-	-

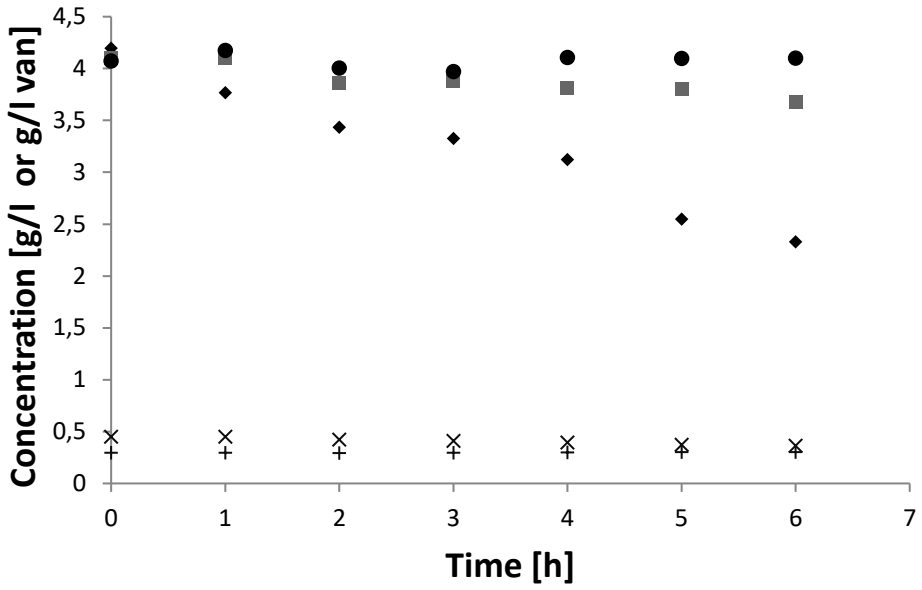

Figure 3-21: HPLC based concentration measurements of *T. versicolor* laccase (Sigma)-XRF reaction. Phenolic concentrations are marked with (●) 0.03, (■) 0.3 and (◆) 2.95 U/ml enzyme Concentration and are expressed in vanillin equivalent, (x) furfural and (+) HMF are the averages for the three measurements.

Comparing HPLC and spectrophotometric measurements. For both measurement techniques, the same samples were used to enable reliable comparison. Figure 3-22 shows the decrease of phenolics after three different reaction times for both HPLC and UV measurements for all three enzyme concentrations. Values are calculated from the vanillin calibration curve, and thus expressed in vanillin equivalents. After 6 hours of reaction with enzyme concentrations of 2.95, 0.3 and 0.03 U/ml, the total phenolics content, measured by HPLC, dropped with 1.9, 0.4 and 0.0 g/l respectively, which corresponds with 55 %, 89 % and 99 % of the initial concentration and reaction velocities of 0.30, 0.07 and 0.00 g/(l·h). For spectrophotometry, the velocity of the reaction calculated from the decrease of absorbance was 0.39, 0.23 and 0.06 g/(l·h) respectively with a remaining absorbance of 86 %, 91 % and 97 %. The absorbance decreases obtained by UV spectrophotometry are close to linear, as they are for the HPLC measurements, and as could be expected from the Michaelis-Menten equation for high substrate concentrations.

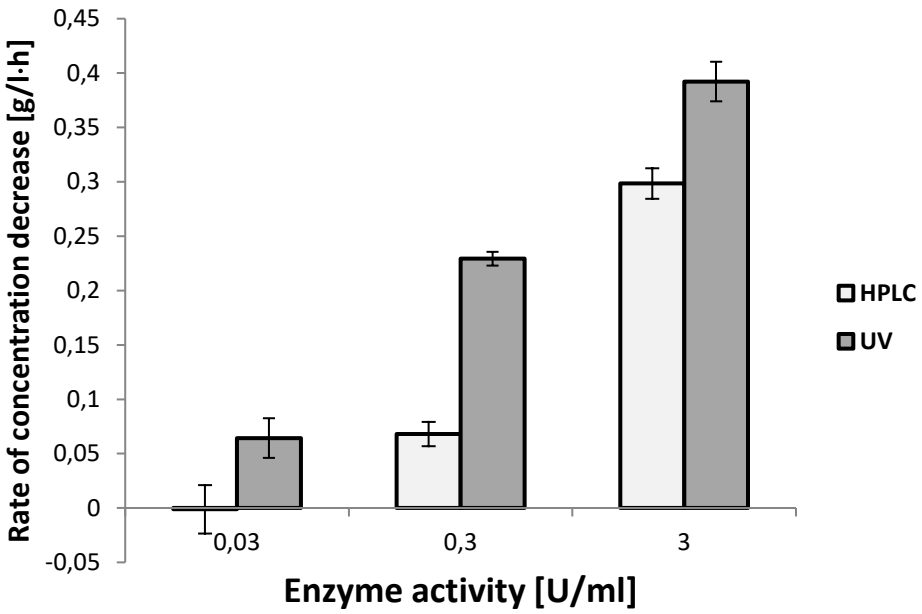

Figure 3-22: The rate of phenolic concentration decrease at three different enzyme concentrations and two different techniques: HPLC (□) and UV absorbance (■). Error bars are ±standard deviation from three measurements.

It can be seen that the enzyme activity measured as phenolics removed by time is not the same for HPLC and UV measurements. Although Figure 3-22 shows that for both measurement techniques, the enzyme activity increases with increasing enzyme concentration. A difference between the researched measurement techniques is that at the lowest enzyme dosage, where the HPLC measurement does not show any decrease in phenolics, the UV measurement (see Figure 3-22) shows a slight decrease. This error is expected to be caused by furfural evaporation, since it is the only compound that is decreasing significantly (see Figure 3-21). This will be the same for all three enzyme concentrations and can be considered to be in the range of the measurement error. It is known that different phenol measurement methods may result in different values. This was reported before when HPLC and Folin method were compared (around 20 % difference) [107] , although both methods are still considered valid. The results show that UV absorbency can be used to compare detoxification results and optimize processes.

Particle size distribution. Results measured with the Zetasizer Nano instrument have to be discussed with caution because the software is configured for monodisperse solutions, and after the reaction, most probably polydisperse solution was formed.

During the reaction, the first measurement point at zero hours showed that some particles were present. This was considered as the background. The samples obtained by different pore size filtrations after three- and six-hours reaction showed a significant number of particles at every size range, i.e., above 0.45 µm, under 0.45 µm as well as below 0.2 µm (see Table 3-5).

Table 3-5: Particle size measurements during the XRF-laccase reaction with 2.95 U/ml enzyme concentration. Samples were taken at 0, 3 and 6 h, with three different sample preparation: without filtration, with 0.45 µm and 0.2 µm pore size filtration. Each point is the average of 45 measurements. 'Derived count rate' is a measure for both particle concentration and size.

Time [h]	Filtration [µm]	Mean particle size [nm]	Std [nm]	Derived count rate [-]	Details [-]
0	0.2	2.0	0.98	702	polydisperse
	0.2	1.8	0.95	708	polydisperse
	0.2	1.4	0.75	749	polydisperse
3	non	661	269	139961	sedimenting
	non	550	100	135559	sedimenting
	non	837	336	132876	sedimenting
	0.45	188	71	6051	good quality
	0.45	195	85	6253	good quality
	0.45	201	93	6145	good quality
	0.2	2.1	1.1	1645	polydisperse
	0.2	2.8	1.2	1537	polydisperse
	0.2	2.5	1.1	1566	polydisperse
6	non	1244	320	305390	sedimenting
	non	1231	358	284748	sedimenting
	non	1493	381	278445	sedimenting
	0.45	4.4	1.4	11228	polydisperse
	0.45	8.6	2.6	11260	polydisperse
	0.45	7.2	2.7	11392	polydisperse
	0.2	10.2	9.5	5429	polydisperse
	0.2	14.4	12.8	5366	good quality
	0.2	9.2	9.5	5354	polydisperse

The 'derived count rate', that is a type of intensity parameter returned by the software for every measurement is correlated to both the size and concentration of the particles and can be used to compare concentrations in the same particle size-range. For the unfiltered samples, sedimentation appears which is also indicated by the software and can be seen from the increasing derived count rate by time, and thus the increasing concentration of particles (see Table 3-5). The filtered samples either produced good quality measurements or they were marked as polydisperse by the software. The mean particle diameter sometimes differs significantly between the three replicates. This is caused by the polydispersity. It can be concluded, that during the reaction the particle concentration is increasing in all three size ranges, as can be seen from the two to three folds bigger derived count rates. The mean particle size is growing in the unfiltered samples (approximately from 600 to 1200 nm) and in the 0.2 µm filtered samples (approximately from 2 to 11 nm). However, for the size range under 0.45 µm, the mean diameter is decreasing from around 200 to a rather low value, i.e., around 10 nm. A possible explanation is that the particles grew over the 0.45 µm limit from 3 h until 6 h reaction time and are filtered out, but this conclusion is very uncertain.

3.7.1.3 Conclusion

The results obtained in this work suggest that UV absorbance measurements can be used for end-point as well as enzyme activity determination (time evolution) of the laccase catalyzed reaction with phenolics as substrates. Direct calculation of precise, separate concentrations is often impossible even with HPLC, due to the number of substrates and formed products. Several difficulties appear, such as, changing ratios of the formed oligomer products during the course of the reaction, the remaining absorbance of the reaction products and the absorbency change caused by pH shift. Dilution with strong base before measurement solves the pH shift problem and is often required because of the high starting concentrations. Compared to HPLC measurements, spectrophotometric follow-up of the laccase-reaction is a possible substitute because HPLC measurement is slower, more expensive and harder to automate. Moreover, efficient optimization of the laccase-phenolics reaction for industrial application is allowed by this technique.

It was proven that during laccase-XRF reaction hydrophilic compounds are converted to more and more hydrophobic products as time goes on. The products are mostly in lower concentrations and are similar in terms of hydrophobicity, which can be explained with the higher aromatic content, compared to functional groups as the

polymerization degree rises. Generally, UV spectroscopy can be considered a valuable alternative for follow-up of phenolic removal during detoxification reactions.

3.7.2 Comparison of different laccase enzymes

As it was shown before, laccases are originating from different sources, either bacterial or fungal [192]. The differences appear in structure, substrate specificity, stability, working pH and temperature range, activity and their fermentative production time. The latter is the most important influencing factor in the enzyme price. As fungal fermentations are generally taking several days, the fungal enzyme price is significantly higher than bacterial, which is typically one day fermentation.

In this research, the following laccases were screened for their efficiency in hydrolyzate detoxification: *Trametes sp*. from Company A, *Unicolor sp.* from Company A, *Trametes versicolor* from Sigma*, Trametes sp*. from China and one from a bacterial source from Company B.

3.7.2.1 Method

Bacterial laccase

The bacterial laccase was supplied in liquid form; it had 38.1 ± 0.8 m% dry content, with 89.8 ± 0.3 % organic content, causing a final 34.1 ± 0.5 m/v% organic content. In the first experiment, 50 ml of XRF after enzyme addition was treated with 2.5 m/v% crude laccase (0.95 m/v% dry content) at room temperature and at pH 5. In the upcoming four experiments the laccase amount was doubled to 5.0 m/v% crude laccase (1.82 m/v% dry content) and one experiment was done by combining two temperatures (room temperature or 55 °C) and two pH values (pH 5 or pH 8 initial values). No pH control was applied during the experiments.

The setup was a three necked flask applied with a reflux condensator, an oil bath, temperature control, and a magnetic bulb. The enzyme was added through one of the openings when the XRF reached the desired temperature. Approximately 2 ml of sample was taken in desired intervals and analyzed by HPLC-UV. The final pH value was also measured at the end of each reaction.

In the last three experiments, a pH control was used as pH change was proven to be a significant parameter. The setup was modified in the following way (Figure 3-23): the

pH electrode was inserted in one of the free necks of the lombic; the base dosing tube was inserted in the other. The parameters of the controller (P=20 and I=3 originally) were decreased 100 times to match the much smaller liquid volume compared to fermenter volume. The added base was 2.5 M KOH. Laccase volume was decreased to half, 2.5 m/v% (0.95 m/v% dry).

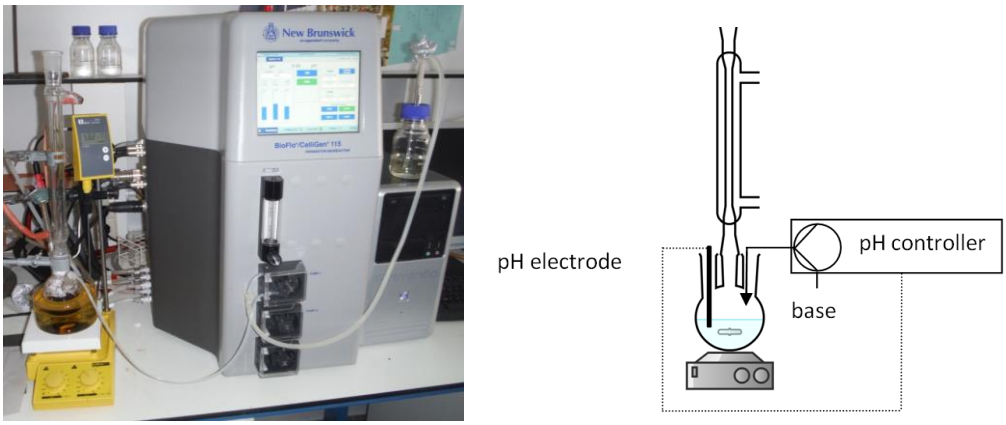

Figure 3-23: Picture (left) and scheme (right) of the detoxification setup with pH control.

Fungal laccases

As fungal laccases require an acidic pH to function, and it was proven that the reaction itself causes a pH drop (Section 3.7.1), no pH control is needed. To measure the laccase activity in conditions that are relevant for later SSF (Section 5.7), 2 m/v% of $CaCO_3$ was added to set the pH. The reaction was kept at a constant temperature by a temperature-controlled heating plate. As higher temperature is usually beneficial for detoxification, the reaction was tested at the temperature of lactic acid bacterial fermentation, which was found to be 40 °C (Section 5.7.1). As air input was proven to be useful to remove furfural and it is one of the substrates for the laccase reaction [193], the stirring was done by bubbling air through the reaction mixture with an aquarium pump. Experiments were performed in triplicate and 3 to 4 parallel runs could be started. A three-necked lombic was submerged in an oil bath, equipped with a reflux cooler (see Figure 3-24). Samples were taken regularly. In all experiments, one g laccase per liter reaction mixture was used, independent on the laccase source. The laccase comparison was done in triplicates for three different types (*Trametes sp.* from Company A, *Trametes versicolor* from Sigma and *Cerena unicolor* from Company A).

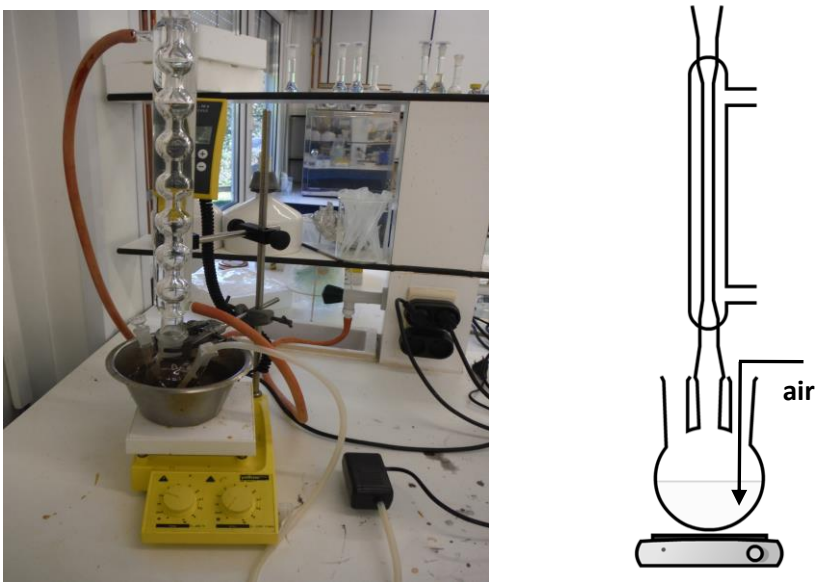

Figure 3-24: Picture (left) and scheme (right) of the setup used for fungal laccase detoxification of XRF.

3.7.2.2 Results and conclusion

Bacterial laccase

The HPLC results of the runs without pH control are detailed in Figure 3-25. On Figure 3-25A, only a slight removal of phenolics is shown at pH 5 and room temperature, meaning around 5 % decrease in 20 h in both cases. From the HPLC chromatogram, it was visible that the crude laccase extract contains compounds that are measured together with the phenolic compounds (Figure 3-26); this is the reason why on Figure 3-25A, the 5 m/v% laccase concentration experiment has around a 0.2 g/l syringaldehyde (SYR) equivalent higher initial phenolic concentration than the one with 2.5 m/v%. The phenolics removal happens relatively fast, i.e., in the first few hours; however, the removed amount is very low. The enzyme performed much better at pH 8 and room temperature (21 % removal), but a higher temperature of 55 °C also helped, i.e., 16 % removal in case of pH 5 and 32 % in case of pH 8. It is visible that the pH has a stronger effect on removal efficiency than temperature.

Furan values (see Figure 3-25C) are not changing significantly. It was seen that the pH decreased during the reaction (See Section 3.7.1.2). This can be explained by the

formation of acidic groups from alcohol and aldehyde groups. It could be noticed that the ending pH (see Figure 3-25B) was always around 5, except for the experiment at room temperature and pH 8, which ended around 6.30. This was expected to happen as laccase catalyzes a one electron oxidation, which can lead to the formation of acids from both alcohols and aldehydes [184]. These products will acidify the reaction mixture for experiments without active pH control. In case of fungal laccases this pH change is not a problem as their performance is better at acidic pH, but it can be problematic with bacterial laccase. The higher final pH in case of the reaction at room temperature and pH 8 is linked to the relatively lower removal; the reaction was in an earlier stage in terms of conversion, when fewer acids are formed yet. The change in the phenolic concentration composition was quite similar to that recorded with *T. versicolor* from Sigma (Figure 3-19), only the final concentrations were higher, i.e. less removal (see Figure 3-27D). It was also visible that lower hydrophobicity compounds were disappearing and more hydrophobic compounds were formed.

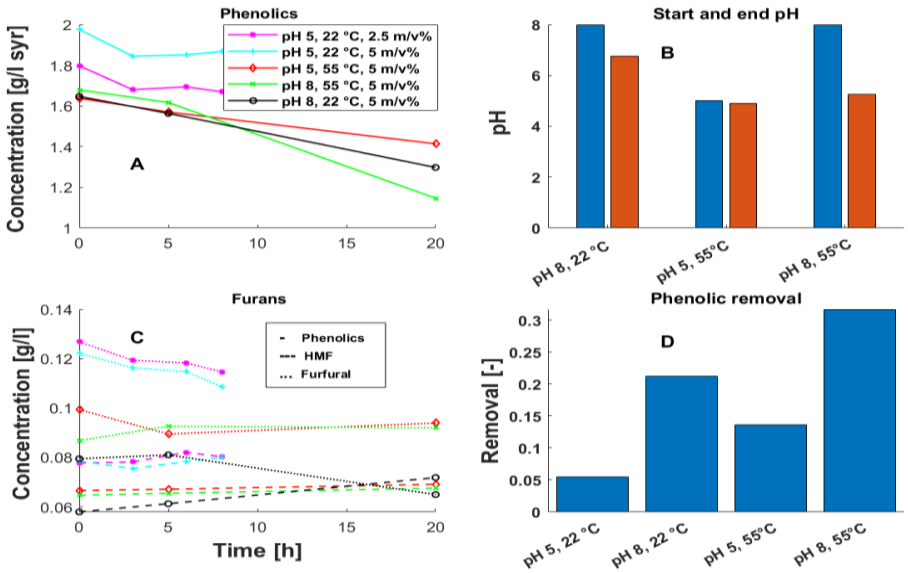

Figure 3-25: Summarization of XRF detoxification with bacterial laccase and without pH control. (A) Phenolic concentration evolution, (C) furan concentration evolution in time. Markers identify different experiments, lines different compounds: (—) represents phenolics, (--) HMF, (..) furfural concentrations. (B) Start and end pH of experiments. (D) Removed phenolic fraction in the experiment.

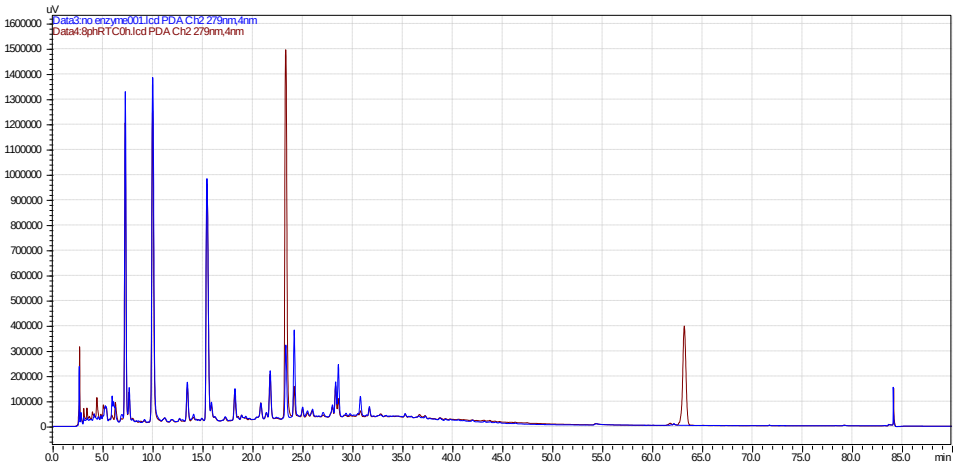

Figure 3-26: Difference in long HPLC method chromatogram between untreated XRF (blue) and XRF after bacterial enzyme addition (brown).

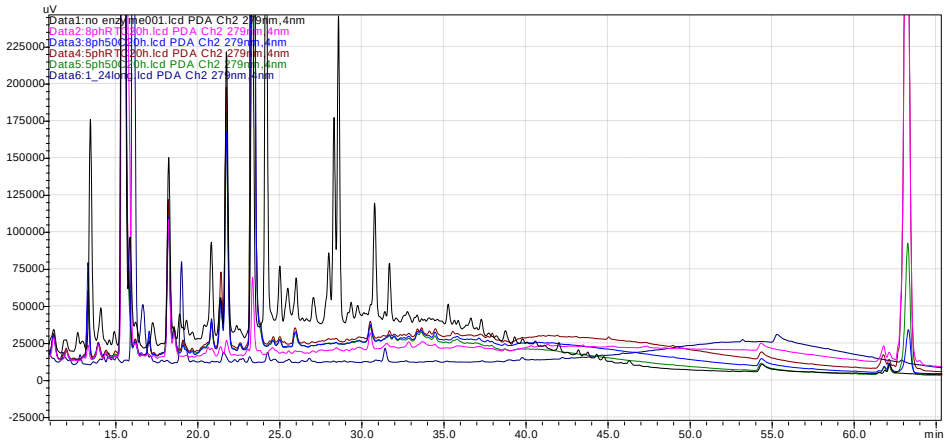

Figure 3-27: Difference between untreated XRF, *T. versicolor* (Sigma) and bacterial laccase treated XRF.

Results recorded with pH-controlled detoxification look significantly more appealing (Figure 3-28) as even the blank experiment without laccase caused approximately the same phenolic concentration than the best experiment in the non-pH-controlled detoxification with 30 % and 32 % decrease (Figure 3-25A and Figure 3-28A). At room temperature, the removal with pH control was 47 %, while at 50 °C, it was 58 %. It is also visible that the reference removal was significant with 30 % (Figure 3-28B REF), suggesting significant autodegradation of phenolics and/or dilution by pH control. If

the HMF concentration is checked (Figure 3-28C) it can be seen that it slightly drops caused by dilution instead of slightly increasing, which would be caused by evaporation. Calculating dilution from the HMF concentration decrease, in case of room temperature the dilution was less than 10 %, in case of reference detoxification, with 50 °C no laccase just pH control, it was slightly more than 10 %, while in case of 50 °C and laccase it was almost 20 %. This indicates that the pH drop happens also during autodegradation, not just laccase reaction; it is faster in case laccase is added (Figure 3-28B REF and other two curves). It is seen that in most cases the concentration of phenolics is stable after 24 h (Figure 3-28A), which indicates that if treatment could be overlapped with saccharification (allowing longer reaction times than 24 h), laccase concentration could be reduced to lower enzyme costs.

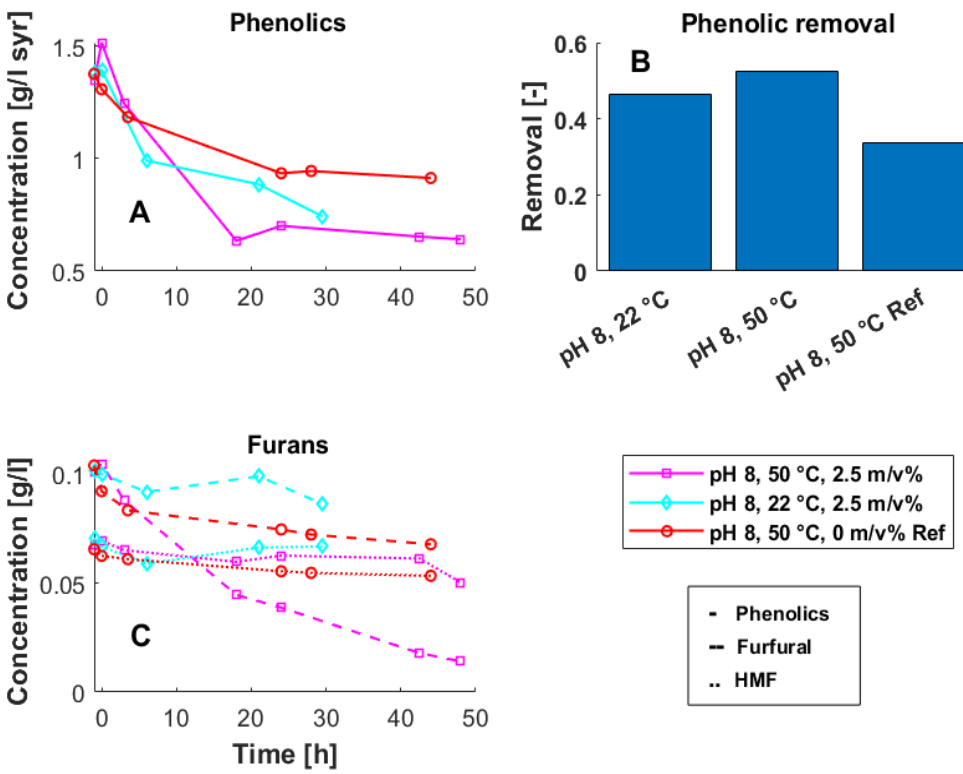

Figure 3-28: Overview of data from pH controlled bacterial laccase-XRF detoxification runs. (A) Phenolic concentration evolution, (C) furan concentration evolution in time. Markers identify different experiments, lines different compounds: (—) represents phenolics, (--) HMF, (..) furfural concentrations. (C) Removed phenolic fraction in the experiment.

Fungal laccases

In most of the experiments, a brown to reddish color shift was visible, because of the change in phenolic composition as was reported before [194]. This was the most pronounced in case of *C. unicolor* laccase, but it was visible in all cases. Foaming was also appearing regularly in the first 7 h, however not in every case, mostly with *C. unicolor* laccase (Figure 3-29). The cause is unknown; however, it could be connected to the fact that proteins can act as surfactants. The foaming was especially disturbing as it changes the system, part of the liquid will be in foam form, with less contact intensity, the top will be enriched in water as evaporating fumes will be condensed in the top layer, changing also the composition in the remaining liquid in the bottom where samples are taken. It is not easy to deal with it, as it is known that addition of antifoam changes the activity of laccase [195]. In an industrial process it is easier to deal with the problem by mechanical foam reducers, however, in this case it was not a possibility. In case of foaming, a new experiment was started.

Figure 3-29: The occurred foaming during some of the detoxification reactions.

As it is visible from the HPLC-UV chromatograms (long method) taken after 25 h for different laccases (Figure 3-30A), de main difference is the enzyme action on the hydroxybenzoic acid peak (at 20.5 minutes), which is present in the highest amount in the initial XRF. *Trametes* laccase removes hydroxybenzoic acid (HBA) with good

efficiency (but most probably through radical propagation via other compounds rather than direct action), while *C. unicolor* decreases it to a lesser extent. Furfural is completely removed in all cases (Figure 3-30A at 12.5 minutes), while HMF concentration is unchanged (at 9.5 minutes). Comparing the *Trametes* chromatogram after 24 h to the starting XRF chromatogram at 0 h (Figure 3-30B), it is visible that technically all phenolics and furfural are removed, but not HMF.

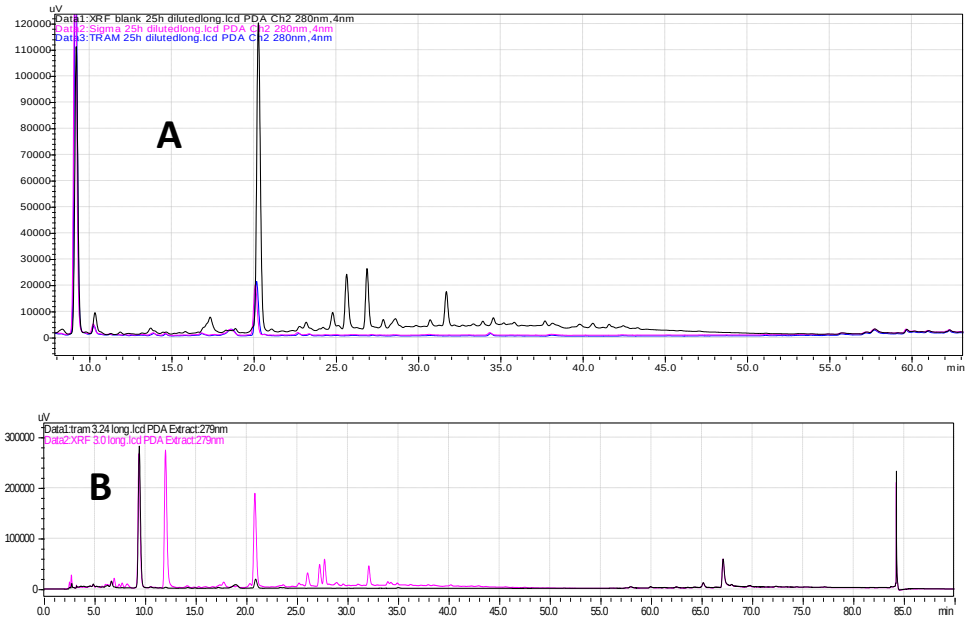

Figure 3-30: Difference between phenolic composition for different laccase types. (A) Composition after 25 h of blank XRF (black) and *Trametes* from Sigma (purple) and Company A *Trametes* (blue) laccase. (B) Composition after 24 h of blank XRF (purple) and Company A *Trametes* (black) laccase.

As it was mentioned, foaming was a problem appearing multiple times. One run was made without aeration (see Figure 3-31). No concentration change was visible (furans or phenolics), however it must be noted that in absence of air input no mixing was present. In the future, the experiment could be repeated with magnetic stirring.

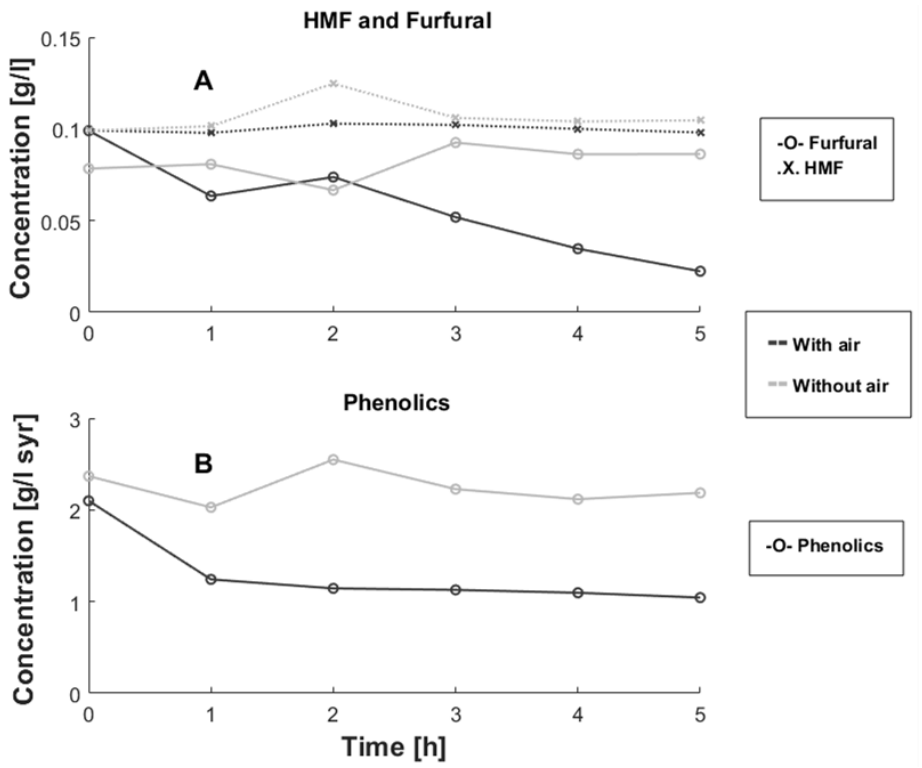

Figure 3-31: The change in concentrations of (A) furans and (B) phenolics in case of *C. unicolor* laccase detoxification, with (red) or without (green) supplied air.

All results of different fungal laccases, together with standard deviations, are summarized in Figure 3-32. Furfural concentrations were decreasing at exactly the same rate for all experiments (Figure 3-32A), including for the XRF blank with no added laccase, indicating that it is purely caused by its evaporation that is promoted by the aeration. After 7 h over 90 % furfural was removed and 100 % removal was achieved at 24 h. The HMF concentration increased slightly because of water evaporation (Figure 3-32B), as a few drops of water always remained in the condenser, decreasing slightly the solvent in the mixture, and thus increasing the concentrations. Phenolics concentration was decreasing for all laccases applied, however at slightly different rates (Figure 3-32C). The initial phenolics removal was rapid in all the cases, i.e., 57 % decrease was measured after 1 h in case of both *Trametes* laccases, and 3 h in case of *C. unicolor.* In the latter case, phenolics concentration stabilized at that time, achieving 65 % final removal. In contrast, *Trametes* detoxification went through a further linear removal in the first 3 h, and the phenolics concentration stabilized at 16 % of the initial

one. The two *Trametes* laccases were decreasing the phenolic concentration almost identically. The removal is also stabilizing at almost the same phenolic level, which indicates that the remaining phenolics were not substrates for further reaction. As both belonged to the same species it can be assumed that their behavior is close to each other, which means that approximately the same group of phenolics will remain in the mixture after the reaction is over (see Figure 3-30A).

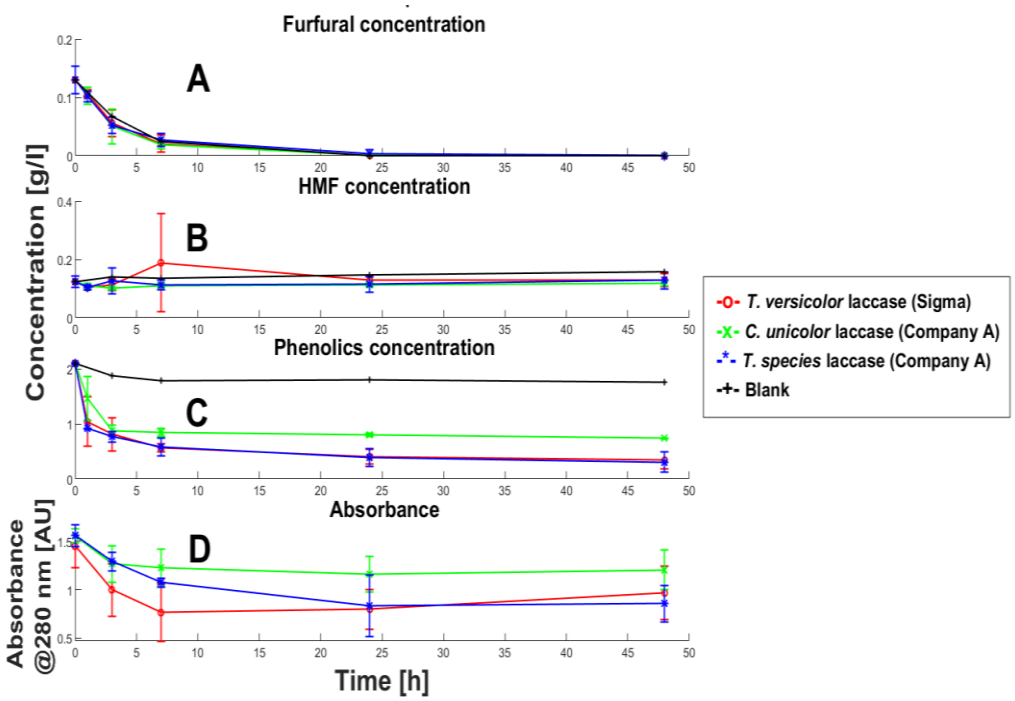

Figure 3-32: Summarization of concentrations ((A) furfural, (B) HMF and (C) phenolics) and (D) absorbance change during different fungal laccase detoxification reactions. Error bars are ±standard deviation from three measurements. Markers represent different experiments.

As was suspected before, absorbance decrease follows the detoxification reaction, stabilizing as soon as laccase reaction and furfural removal is over (Figure 3-32D). The overall process suggests that aeration is important for furfural removal, and HBA removal cannot be dealt with laccase reaction as even high activity Sigma *Trametes* laccase removes it rather slowly. If only laccase is meant to detoxify it, it can turn out expensive. Possible laccase should be used to remove the other phenolics, removing part of the HBA through radical propagation, and the rest with adsorption.

Comparison of fungal and bacterial laccases

The laccase detoxification experiments are summarized in Table 3-6. Fungal laccases were similar in terms of their optimal working parameters (acidic pH and higher temperature). *Trametes species/versicolor* laccase performed best in the detoxification, removing most of the phenolics (85 %), while *C. unicolor* and the bacterial laccase both were inferior, removing 58-65 %. This is caused by the difference in redox potential and substrate specificity of the laccases, some phenolics are left in the solution. It should be however noted, that in the economical point of view it is not expected to find a commercial laccase with comparable activity as purified *Trametes* laccase (Sigma). A smaller added activity can lead to the same detoxification in the end with longer treatment time, which will be important to decrease costs.

Table 3-6: Summarizing phenolic removals of laccase-XRF reactions.

Fungal laccases	pH [-]	T [°C]	Phenolics removal [-]	Pros	Cons
Blank	5.5	40	0.16	-High removal -pH in SSF range	-Purified products
T. versicolor (Sigma)	5.5	40	0.84		
C. unicolor (Company A)	5.5	40	0.65		
T. species (Company A)	5.5	40	0.85		
Bacterial laccase					
No pH control	5	55	0.14	-Industrial enzyme	-Low removal
	8	55	0.32		
	8	22	0.21		
pH control				-Relatively good removal -Industrial enzyme	-pH outside SSF range -Part of the removal is from autodegradation
Blank	8	50	0.30		
	8	50	0.58		
	8	22	0.47		

The performance of the bacterial laccase was lower than fungal laccases, the working pH was outside of the economically preferred range and the pH has to be actively

controlled. The stability of the enzyme is not that crucial in this specific case as the enzymes could not be recycled from the reaction mixture, the main parameter is to decrease the needed amount. If laccase immobilization is considered however, enzyme stability will be an important parameter.

3.8 General conclusions

Based on a literature overview about measurement techniques, suitable techniques for enzyme activity measurement (ABTS assay), phenolic and furan concentration measurement (HPLC-UV), free- and structural-carbohydrate and fermentation product determination (HPLC-RI) were chosen and introduced for the whole scope of the PhD research. Poplar wood was pretreated by autocatalyzed steam explosion at different treatment times and applied pressures. A test enzymatic hydrolysis was performed to investigate possible sugar titers and expected inhibitor levels. Results show that temperatures lower than 200 °C are needed to minimize xylose degradation and inhibitor formation, however glucose hydrolysis efficiency will be lower than at higher temperatures, as was reported before [27]. Suitable parameters were chosen and several steam explosion runs were performed to ensure standard substrate for the upcoming experiments (named as SE united batch). Methods to handle time-instable XRF were developed and presented.

Enzymatic hydrolysis was evaluated with the aforementioned SE united batch, which showed that industrially relevant sugar titers could not be reached in a single hydrolysis step, as well as that with exceptionally high cellulase concentration (20 m/v%) 2/3rd of the initial carbohydrates remained bounded. It was shown that inhibitor concentrations increase slightly during hydrolysis, which suggests that inhibitors are not entrapped in the matrix. Parallel hydrolysis experiments with added water instead of XRF showed that the inhibitors significantly hinder hydrolysis, while the concentration of phenolics present in the liquid suggested that the surface of the solid material physically adsorbs large amount of inhibitors, which are desorbed when washed.

A standard ABTS enzyme activity assay was used to map the activity of different laccase enzymes in the expected working temperature/pH range. In general, higher temperature is beneficial for activity; fungal laccases have an optimum at acidic pH, while the applied bacterial laccase performed best at a basic pH. Literature showed that comparison between the activities measured at different pH values is not

comparable even at theoretical level, as the molar extension coefficient of the substrate is changing with pH.

The laccase reaction was investigated on vanillin as a model phenolic compound. Results have shown that the substrate goes through an oligomerization, and precipitation caused by lower solubility of oligomers, which was later confirmed also in the case of XRF-laccase reaction, as both precipitate and more hydrophobic products were forming. UV spectrometry was shown to be useful for reaction monitoring, which was later confirmed with the XRF substrate.

The application of investigated laccases was evaluated for detoxification of the liquid phase from the SE united batch at pH values and temperatures close to the expected fermentation parameters. It was found that significant phenolics autodegradation is appearing at pH 8 and 50 °C, which could be utilized in a final industrial process. Results show that different types of laccases have a different affinity for phenolic compounds present in XRF, rendering the standard ABTS test useless for screening in this specific case, as it does not provide any information about the substrate specificity. Model compound-based laccase activity determination is an option, but preparing a good model substrate is tedious (exact composition of the XRF has to be determined and prepared which can be very difficult). Using the XRF directly was chosen, as it is readily given, composition is exactly that of the real substrate (a=a), provides instant information about laccase redox potential (how much and what kind of phenolics are left in the liquid), laccase activity (slope of decrease) and phenolic autodegradation.

The setup was accepted as a method for (relatively) fast screening. Aeration was found to be very effective in removing furfural from the broth. Its use should be considered in general applications (even if no laccase is used), and it is a must in laccase reactions as oxygen is one of the substrates of the enzyme [196].

Chapter 4 MAGNETIC CROSS-LINKED ENZYME AGGREGATES

4.1 Introduction

A possible way to decrease enzyme cost is immobilization, which allows catalyst recycling by filtration or centrifugation [197], but it also can increase the overall performance of the enzyme by improving the resistance to inhibitors and general stability, widening the pH or temperature working range, or even achieving enzyme purification during the process [198]. However, also the immobilization step has its costs and while improved stability is experienced with enzymes that are used in organic solvents, such as immobilized lipase [199], for laccase, enzyme deactivation is noticed due to the immobilization process [200]–[203]. Moreover, during the application of immobilized enzymes, mass transport phenomena can cause a lower overall activity.

Garcia-Galan et al. published a good overview of immobilization possibilities [198]. Techniques can be divided in methods using support materials (porous or nanoparticles) or without a support, as in case of CLEAs (Cross-linked Enzyme Aggregates) or CLECs (Cross-Linked Enzyme Crystals), and these two types can even be combined. Immobilized enzymes are typically recycled by filtration or centrifugation from the reaction medium. Therefore, applying the considerations published in the article [198] to the specific case of simultaneous saccharification, detoxification and fermentation, the following facts can be deduced about utilization of any enzyme during the process. (1) Even after maximum theoretical conversion of the solid substrate, solid parts would remain in the broth (lignin particles [169]) which will hinder catalyst filtration. Therefore, catalyst separation from the SSFD broth has to be done based on a different principle. (2) During the SSFD process, the formed particles can physically block the porous structure of the carrier material. (3) The enzymes used are always mixtures and rarely purified to decrease the costs. As CLECs are formed after crystallization of pure enzymes, this technology is not applicable. (4) Production of CLEAs is based on aggregation of enzymes and can be used for our application. Based on these considerations, magnetic Cross-linked Enzyme Aggregates (m-CLEAs) are investigated further in the concrete example of laccase enzyme, but the principles concluded are valid for enzymes in general. The carrier is non-porous, the enzymes are close to the surface and the separation can be done based on magnetic properties. It

has to be noted that the core should be ferromagnetic and not permanent magnetic, as the particles should not aggregate, only in presence of a magnetic field.

CLEAs are technically precipitated enzymes (by salting out or pH shift for example), which are thereafter cross-linked (see Figure 2-16), this way they will remain insoluble even after the reason of precipitation ceased to exist further (pH shifted back to initial value or the salt washed out from the solution) [130], [131], [197], [204]. CLEAs have almost 100 % protein loading as the only other component is the cross-linker used, and since the cross-linker is always an organic molecule, the organic loading of the catalyst is 100 %. Typically, glutaraldehyde is used in a few percent compared to the enzyme [205]. It is safe to assume that the cross-linker will not be in high amounts in the final catalyst. Additionally, external materials can be added to the solution before insolubilization, which will end up captured in the precipitate. This way the material can grant CLEAs special abilities (magnetic, static etc.). Laccase CLEAs were reported before in literature, in fact some authors achieved higher activity after immobilization (lower K_m and/or higher V_{max} values), for example for laccase used in decolorizing waste streams [206], [207].

A significant amount of literature is available about magnetic CLEAs, with different preparation methods, however with varying success. Since CLEAs are precipitated enzymes, their protein loading is almost 100 %, with the cross-linker contributing only for a minor part. Using magnetic cores, however, reduces protein loading significantly. Laccase was immobilized before on magnetically active mesoporous carbon with high enzyme loading (~50 m/m%) and relative high remaining activity (80-90 %) [200]. Horseradish peroxidase (anther phenol-oxidase) was immobilized on magnetic beads (~100 µm diameter) with a consecutive glutaraldehyde activation and immobilization. This led to low enzyme loading (~0.3 m/m%) but high retained activity (69 %) compared to free enzyme. However, immobilization improved working pH range, and thermal stability [201]. Laccase was immobilized on chitosan magnetic particles with increased V_{max}, but also increased K_m [208]. Kumar at al. immobilized laccase on magnetite nanoparticles and witnessed improved stability and pH working range. The catalyst reached 18 m/m% protein loading (measured from the difference between start and ending solution of immobilization), but a solution with a low enzyme concentration was used, 7 g/l which is 0.7 m/m%, compared to the industrial standard ~5-10 m/m% [209].

4.2 Problem statement and goal

The benefits of enzyme immobilization are clear, however, there are strict limitations in the investigated case of laccase detoxification of lignocellulose biomass. As will be shown in Section 6.1.3, enzyme load is a very important parameter [210], therefore only CLEAs have the potential for utilization in this specific case as their enzyme load is exceptionally high (over 50 m/m%). This enzyme load will be expressed as organic loading if the enzyme amount is determined by measurement of the organic content. Important improvements on the use of magnetic carriers in laccase immobilization were reported in literature, but they were not used for hydrolysis and detoxification of lignocellulose biomass substrates, let alone for simultaneous saccharification and detoxification and high solids conditions. Up to our knowledge, laccase CLEAs were never applied on lignocellulosic substrates for detoxification. Methods, to precisely measure CLEAs amounts are also missing from literature and, as will be shown in this chapter, it is not trivial.

In this chapter, it is aimed to fill the gap in literature concerning the m-CLEAs laccase utilization in XRF detoxification. It contains a method development for reliable m-CLEAs handling as well as detoxification experiments by bacterial laccase m-CLEAs.

4.3 Properties

The m-CLEAs used in this research were a kind gift from CLEA technologies (Delft, Netherlands), and were prepared from the free bacterial laccase of Company A that was applied in Section 6.4.1). As the m-CLEAs came in aqueous suspended form, it was not trivial how to reliably add exact amounts to the reaction mixture. If dried, they could lose their structure and activity. Therefore, firstly methods had to be developed to enable reproducible measurements of the enzyme amounts. Additionally, to compare the efficiency of free and immobilized enzyme, it was important to know the enzyme loading of the catalyst. The enzyme load, which can be measured during the immobilization process, was not known. Because of its immobilized state, the exact protein content would be difficult to determine, as the applied cross-linker was not known. Therefore, the organic loading was estimated by thermo-analysis. During this analysis, the treatment time and temperature are important as the iron can be oxidized ($Fe \rightarrow Fe_2O_3$), leading to a higher observed mass. The organic loading and the protein loading should fairly be the same, as mentioned in Section 4.1, i.e. the difference is the amount of cross-linker, which is present in much lower amounts than

the protein, typically a few percent [205]. The enzyme load will only differ from the protein load in case of enzyme inactivation.

4.3.1 Method

4.3.1.1 Precise measurement of m-CLEAs amount

The catalyst suspension, as delivered by CLEA Technologies, was mixed and approximately 8 g was poured in a porcelain crucible. The sedimentation of m-CLEAs was visible after few seconds (see Figure 4-1A); therefore the dry mass concentration of the m-CLEAs mixture can depend on the time and the place where the sample was taken. The sample was left for sedimentation for one minute and this was facilitated by placing a magnet right under the crucible. After decantation, the wet weight was measured and the catalyst was resuspended in demineralized water (after water addition the overall mass was the same as the mass before decantation). This sedimentation cycle and determination of the wet weight were repeated three times (see Figure 4-1) to calculate recycling efficiency from water. Thereafter the catalyst was dried for 24 h at 40 °C in an oven until constant weight to determine the dry content of the sediment. This dried material was used in the organic analysis later. All experiments were conducted in triplicate. The dry content of the initial solution was determined by subtracting the mass measured after drying from the initial mass. Recycling efficiency was calculated by dividing the mass of the current decanted wet catalyst by the mass of the catalyst after previous decantation (three points, as triplicate was measured).

Figure 4-1: (left) m-CLEAs sedimentation with a magnet. (right) Decantation of the liquid from the catalyst.

[122]

4.3.1.2 Organic loading

Iron powder obtained from Sigma (10 µm, >99.9 %) was used to determine at which temperature iron oxidizes, as this temperature is changing when the particle size decreases. 2 g iron powder was placed in a muffle furnace (Thermolyne, Thermo Scientific, Waltham, MA, USA) at 400 and 600 °C for 60 and 45 minutes respectively. Mass was measured before and after the treatment.

To determine the necessary treatment time for total oxidation of the organic matter in m-CLEAs the following steps were executed. Seven m-CLEAs samples, each representing around 2 g of original solution before decanting, were dried in an oven at 40°C for 24 h. Afterwards, they were treated at 400 °C in the muffle furnace for different time intervals. The mass decrease was calculated in function of the treatment time.

Based on the results, determination of the total organic content was performed by heat treatment at 400 °C for two hours. The samples, washed as described in the previous paragraph (Section 4.3.1.1), were measured for their organic content.

4.3.2 Results

4.3.2.1 Precise measurement of m-CLEAs amount

Figure 4-2A shows the wet weight of the catalyst after decantation relative to the mass of the original solution for the different cycles. The decanted fraction of the original m-CLEAs solution varied significantly around 40 m/m%, with a standard deviation of 2-4 absolute percent. This means an uncertainty of 5-10 relative percent, which can be considered significant. However, the recycling efficiency of the decanted fraction between washing rounds was remarkable, with averages ranging from 0.992 to 1.012 (a deviation between 0.6 and 2 %) in all three parallel experiments (see Figure 4-2B). This means that washing can be done several times without catalyst loss. The dry content of the original catalyst suspension and the dry content of the decanted wet catalyst was 6.4 ± 0.4 and 16.4 ± 0.5 m/m% respectively, which corresponds to a deviation of 6.25 and 3 % (see Figure 4-2C-D). As lower uncertainties are observed for measurements of the decanted fraction, it can be concluded that this fraction is easier to handle and offers significantly higher precision for dosing.

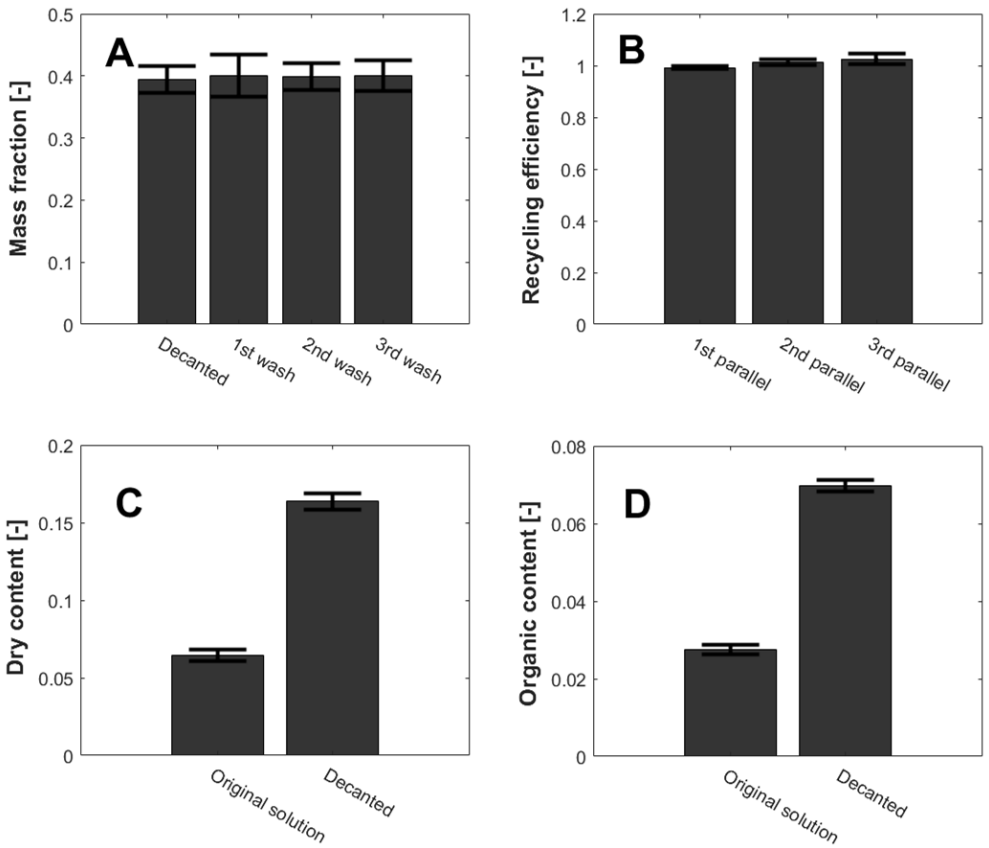

Figure 4-2: m-CLEAs dosing and composition details. (A) Mass recovery from original solution, (B) recycling efficiency after washing, (C) dry and (D) organic content off the original solution and the decanted fraction. Error bars are ±standard deviation from three measurements.

4.3.2.2 Organic loading

Table 4-1 presents the final mass of the iron powder compared to initial mass after a certain time on 400 and 600 °C. The sample mass increased by 13 % when treated at 600 °C in the muffle furnace, and only 0.6 % when it was heated at 400 °C, so the latter was chosen for further experiments as at this temperature the iron oxidation is considered negligible. The necessary treatment time for organic content determination of the m-CLEAs was determined by subjecting seven samples to 400 °C for different time intervals (see Figure 4-3). The mass stabilized after around 80 minutes; hence the treatment time was chosen to be 2 hours in which time all organic content will be considered as burnt completely.

Table 4-1: The mass change of heated iron powder on different temperatures.

Temp [°C]	400	600
Time [min]	60	45
Mass compared to start [%]	100.55	113.52

The samples used to determine the method for precise m-CLEAs mass addition (Section 4.3.1.1) were also analyzed on their organic loading. The original suspension and the decanted catalyst proved to have 2.8 and 7.0 m/m% organic loading respectively (Figure 4-2D), with the dry content itself having an organic loading of 42.7±0.7 m/m%. This value is high compared to the commercial polymer based immobilization techniques that usually result around 10 % organic loading [211], but it is in good correspondence with literature where 35-70 m/m% protein loadings were reported before [205]. It must be noted that most of protein loading measurements in researches are performed by measuring how much protein was removed during immobilization, which was not possible in this specific case (this method usually overestimates it). Taking the density difference between iron and enzymes aggregates into account, it is obvious that the vast majority of the volume of the catalyst particle is the precipitated enzyme.

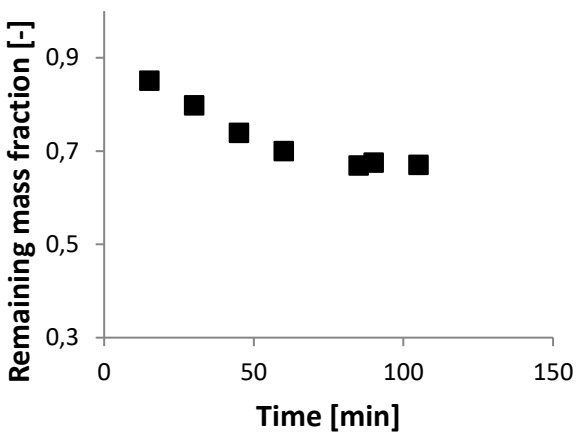

Figure 4-3: Decrease in decanted m-CLEAs catalyst mass during heat treatment at 400 °C.

4.4 Detoxification

Just as in the case of free laccase (Section 3.7), the real evaluation of laccase's detoxification capacity is the removal of phenolics from the actual XRF. m-CLEAs were tested at different temperatures and pH values to map the optimal and possible working range. Up to our knowledge no laccase CLEAs were applied to XRF before.

4.4.1 Method

The experimental set-up is shown in Figure 4-4. The reaction took place in three-necked flasks (100 or 250 ml), which were immersed in an oil bath. The system was supplied with a reflux condenser, a pH electrode and a tube to supply KOH alkali for pH control. m-CLEAs were washed three times with XRF prior to addition to XRF in order to minimize the dilution effect of the liquid present in the decanted catalyst. Experiments were performed with equal organic contents of laccase enzyme, which was the as-closest-as-possible solution to determine immobilization deactivation. The real common unit would have been an equal laccase protein content, but that was impossible to measure. As the organic content of the decanted m-CLEAs was 7 m/m%, and 38 m/m% in case of free bacterial laccase solution (Section 3.7.2.2), the mass of m-CLEAs with an equal organic content to the usually applied amount of free crude laccase, i.e. 2.5 m/v %, is 6.78 g of decanted m-CLEA to 50 ml XRF. The required decanted catalyst mass can be calculated as shown on Equation 4-1 and 4-2.

$$m_{CLEA} = \frac{V * c_{crude} * organic\ content_{crude}}{organic\ content_{CLEA}} \quad \textbf{4-1}$$

$$m_{CLEA} = \frac{0.05\ l * 25\ g/l * 0.38}{0.07} = 6.78g \quad \textbf{4-2}$$

Experiments were conducted at pH values of 5, 6, 7 and 8. The pH was kept at the desired value with the control system of a fermenter (BioFlow 115, New Brunswick) and by adding a concentrated KOH solution of 2.5 M to minimize the dilution effect. Dilution of the reaction mixture was quantified by measuring the mass of the remaining KOH solution. Samples were taken at regular time intervals and phenolic contents were measured with the short HPLC method (Section 3.3.1.1).

The effect of temperature is examined by performing three experiments at pH 6 i.e., at room temperature, 50 °C and 80 °C respectively. The temperature of the oil bath

was maintained at the given temperature ± 2 °C. Blank samples were measured in parallel with the same setup but without added m-CLEAs (pH regulation and stirring were active).

The suspension was stirred with a magnetic bulb at high speed. This caused part of the catalyst to bind to the bulb, as m-CLEAs are ferromagnetic, decreasing the contact efficiency of the catalyst. No air was supplied to the system.

Figure 4-4: Picture (left) and scheme (right) of the setup used for detoxification with m-CLEAs.

4.4.2 Result

m-CLEAs immobilized bacterial laccase removed phenolics faster than free bacterial laccase (Figure 3-28 and Figure 4-5). Points at -1 h represent the XRF composition before adding m-CLEAs and after pH setting. Figure 4-5A presents the evolution of the total phenolics content of all the experiments. Curves show immediate removal in the first half hour. In most cases, equilibrium was reached after 5 to 7 hours of reaction, but in some cases, the decrease lasted for around 24 hours after the start. Phenolic removal values were about 70 % against a removal of 34 % measured for the reference experiment without catalyst (see Figure 4-5A and Table 4-2). All measured phenolic concentrations decreased due to a significant dilution that was obtained by adding the alkali used for pH control, i.e., around 10 %. The significant phenolics removal of the reference can only partially been explained by this dilution. Therefore, most probably an auto-degradation of phenolics at pH 8 can be expected. Phenolics are known to be instable at high pH; this is the base of overliming as a detoxification technology [212]. From Figure 4-5B and Table 4-2, it can be concluded that the pH of the reaction is of low importance within the pH range of 6-8 (std 3 %), as very similar results were

acquired. At pH 5, m-CLEAs performed worse with 64 % removal (Figure 4-5E). According to the results presented in Figure 4-5C and F for experiments at pH 6, the temperature was visibly more important for phenolics removal performance. However, it can be noted that different XRF, with higher initial phenolic content was used at pH 6, 20 °C and 80 °C. The removal was 67-72 %, although the remaining phenolic concentration was still relatively high compared to experiments performed with the previous batch. As the experiments required significant preparation, and only two instruments were capable to control the pH by addition of alkali, performing parallel experiments was difficult. Two replicate experiments at pH 8 and 50 °C were performed (Figure 4-5D and G), however, they showed relatively close results, with only 2 % difference in phenolics removal.

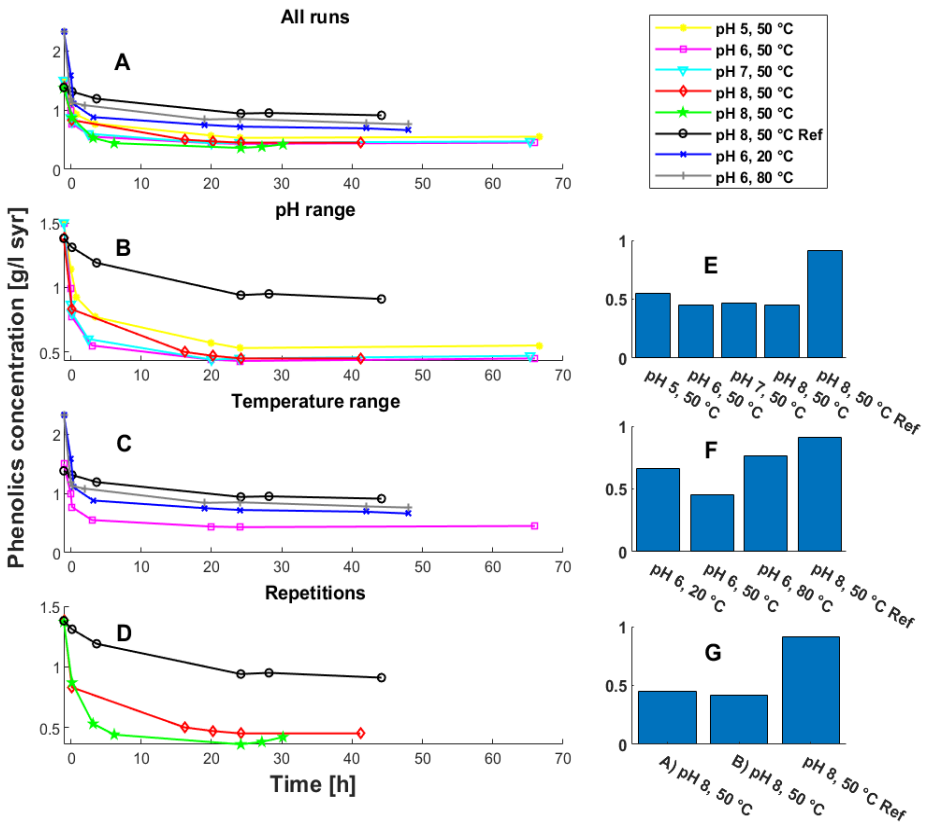

Figure 4-5: Summarizing graphs for m-CLEAs detoxification rounds. Phenolic concentration evolution for (A) for all runs, (B) at different pH values, (C) at different temperature and (D) for two repetitions. Markers mean different experiments. Bars show the ending phenolic concentration for (E) different pH values, (F) different temperatures and (G) repetitions.

Table 4-2: Summarizing phenolic removal of experiments.

	Temperature (°C)	pH control	Phenolic removal [%]
2.5% m-CLEAs	50	pH 5	64%
2.5% m-CLEAs	50	pH 6	70%
2.5% m-CLEAs	50	pH 7	69%
2.5% m-CLEAs	50	pH 8	67%
2.5% m-CLEAs	50	pH 8	69%
2.5% m-CLEAs	20	pH 6	72%
2.5% m-CLEAs	80	pH 6	67%
REFERENCE	50	pH 8	34%

However, the experimental results are based on phenolic removal and not on the formed product (radical, or dimer as the radical recoupling is very fast compared to enzymatic reaction) during enzymatic reaction. Therefore, in Section 4.5, it will be investigated if adsorption of phenolics on the carrier occurs. The rapid decrease in concentration, together with the low pH sensitivity can indicate that the measured decrease can be strongly influenced by adsorption, although stability increase during immobilization was reported before [201].

4.5 Adsorption

Based on the results in Section 4.4.2 adsorption of phenolics to m-CLEAs occurred when the catalyst was brought in contact with the XRF. The rate difference between the phenolic concentration decrease of free and immobilized catalyst suggests that removal in the latter case is caused by adsorption as it goes much faster (a few hours to reach stable value with immobilized enzyme and 48 h with free enzyme). Hence, adsorption measurements were conducted with deactivated catalyst to investigate the adsorption further.

4.5.1 Method

4.5.1.1 Adsorption experiments

Active and inactivated m-CLEAs were compared for their adsorption properties. Inactivation was done by autoclaving the catalyst at 20 bars for 30 minutes. 7 g of wet catalyst (0.49 g organic loading) was added to 10 ml of XRF and left for 30 min at room temperature, mixed in every 10 minutes. After that, a sample for HPLC analysis was taken and both the active and deactivated catalysts were recycled by decanting and applied for detoxification of XRF in four more rounds. Additionally, 1 g of the remaining

active catalysts (0.07 g organic loading) was subjected to 25 ml XRF for 15 minutes three times.

4.5.1.2 Desorption experiments

In the next experiment, the desorption phenomena were investigated on the inactivated catalyst at room temperature by first causing adsorption of the phenolics performing cycles of adding 0.53 g decanted inactive catalyst subsequently to five times 5 ml XRF, and thereafter to seven times 25 ml. Samples were taken and catalyst was recovered by decantation between each cycle. Finally, desorption was researched by washing the inactive recovered catalyst four times with 5 ml and once with 25 ml demineralized water. Samples taken after each cycle were analyzed by HPLC for phenolic inhibitors with both the short and long analysis method (Section 3.3.1.1).

4.5.1.3 Adsorption isotherm and working line

In the last set of experiments, 0.53 g of decanted active catalyst was brought in contact with, subsequently, five times 5 ml and seven times 25 ml XRF volumes at room temperature. In the first experiment, the catalyst was not separated from the mixture. Only fresh XRF was added to the batch in each round (final volume was 200 ml). In the second experiment, the catalyst was separated and recovered from the liquid by decantation between each addition of XRF. Finally, this last experiment was repeated at 45 °C instead of room temperature.

4.5.2 Result

Inhibitor removal, calculated from the HPLC phenolics concentrations of the experiments investigating **adsorption on active and deactivated m-CLEAs** (Section 4.5.1.1) are shown on Figure 4-6. The phenolic removal of active and deactivated catalyst performed nearly the same until a summed amount of 122 $ml_{XRF}/g_{organic}$ added in the different cycles, hereafter the active catalyst was not measured further. Deactivated catalyst had significant adsorption until 500 $ml_{XRF}/g_{organic}$ was added, while after 1000 $ml_{XRF}/g_{organic}$ little further removal can be observed (3 %, see Figure 4-6A and Table 4-3). The latter value (1000 $ml_{XRF}/g_{organic}$), corresponding to the concentration of1 g/l Sigma *T. versicolor* laccase, was used in Section 3.7.1 [169]. Furan removal was technically zero even after 60 $ml_{XRF}/g_{organic}$ (see Figure 4-6B-C).

Assuming (1) that the physical behavior, such as the adsorption capacity, of m-CLEAs will not change significantly if they are made in the same way by cross-linking, but

using other laccase enzymes, and (2) that the deactivation during immobilization would be the same for *Trametes sp.* laccase (Sigma) and *C. unicolor* laccase, Figure 4-6 can be used to estimate the adsorption effect of the m-CLEAs in general at a chosen enzyme concentration. Via a standard, i.e., *T. versicolor* laccase (Sigma), the same calculation can be made starting from a chosen enzyme activity instead of enzyme concentration.

Vertical lines on Figure 4-6 indicate the laccase amount with equal activity compared to 1 g/l *T. versicolor* (Sigma) laccase, $g_{organic}$ per ml_{XRF} based on their activities, expressed as the reciprocal $ml_{XRF}/g_{organic}$ ratios. For example, 1 g/l *T. versicolor* laccase (Sigma) is a purified protein with an organic loading of 1 $g_{protein}/g_{powder}$, it is applied in a concentration of 1 g/l (Section 3.7.1), which is 1 $g_{protein}$/1000 ml. The XRF amount per catalyst will be the reciprocal, thus 1000 $ml_{XRF}/g_{organic}$ as indicated on Figure 4-6. Free *T. versicolor* laccase (Sigma) had an activity of 33.85 ABTS AU/($g_{organic}$ x min), *C. unicolor* laccase had 19 times less activity, 1.78 ABTS AU/($g_{organic}$ x min) , which means that to add the same activity to the solution 19 times less XRF volume has to be used (1000/19 = 52.6 ml/$g_{protein}$), at which value the corresponding adsorption of 43 % phenolics removal is expected (see Figure 4-6A and Table 4-3). The activity values are in Section 3.6.1. The value of $ml_{XRF}/g_{organic}$ at which bacterial laccase m-CLEAs were used can be calculated as follows: 0.49 g organic loading equivalent of decanted m-CLEAs were added to 50 ml XRF, which gives 102 $ml_{XRF}/g_{organic}$ and 57% removal by adsorption (see Figure 4-6A and Table 4-3). In general, the less active the enzyme is, thus lower catalytic activity per mass organics, the higher the phenolic removal via adsorption gets, as higher catalyst mass will be needed for the same volume of XRF – thus the $ml_{XRF}/g_{organic}$ will decrease.

Table 4-3: Phenolic removal relative to untreated hydrolysate (0 %) due to adsorption of different laccases if used as m-CLEAs. The value of $ml_{XRF}/g_{protein}$ is calculated from enzyme activities on ABTS substrate for different free laccases.

	m-CLEAs ratio [$ml_{XRF}/g_{protein}$]	**Phenolic removal [%]**
Sigma laccase m-CLEAs	1000	3
Bacterial laccase m-CLEAs	102	43
***C. unicolor* laccase m-CLEAs**	52.6	57

It is visible on Figure 4-6A that the phenolic removal by bacterial m-CLEAs was mainly because of adsorption and dilution (43-55 %) and only 10-15 % was accounted for the

enzyme activity. At high activities (*T. versicolor* laccase from Sigma) the adsorption causes only 3 % of removal (Table 4-3). However, it has to be taken into account that industrial enzymes are usually not purified and have a lower activity per $g_{protein}$. Both HMF and furfural adsorption is technically zero even at the concentration where *C. unicolor* would be used (Figure 4-6B-C).

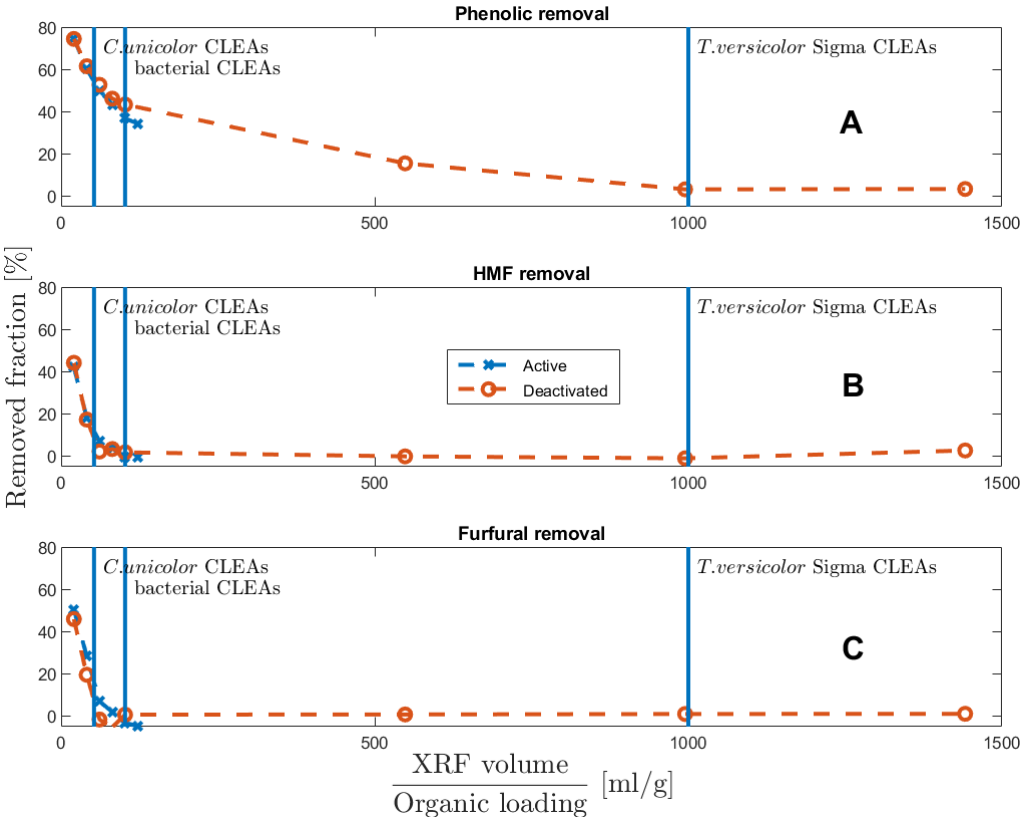

Figure 4-6: Adsorption phenomena of (A) phenolics, (B) HMF and (C) furfural at different XRF/ m-CLEAs ratios. The curves represent the measured data for (x) active and (o) deactivated catalyst, vertical lines the theoretical applied amount of different m-CLEAs enzymes based on their activity on ABTS substrate.

It can be concluded that adsorption to the immobilized catalyst is significant and is something that has to be investigated and taken into account. Chromatograms show significant adsorption on inactivated m-CLEAs (20-35 min), some phenolics are more affected (at RT 22, 29.5 min), some phenolics less (at RT 27, 29 min) (see Figure 4-7).

Compared to active carbon treatment (20 g/l C303 type, Desotec, Belgium) the removal is much lower.

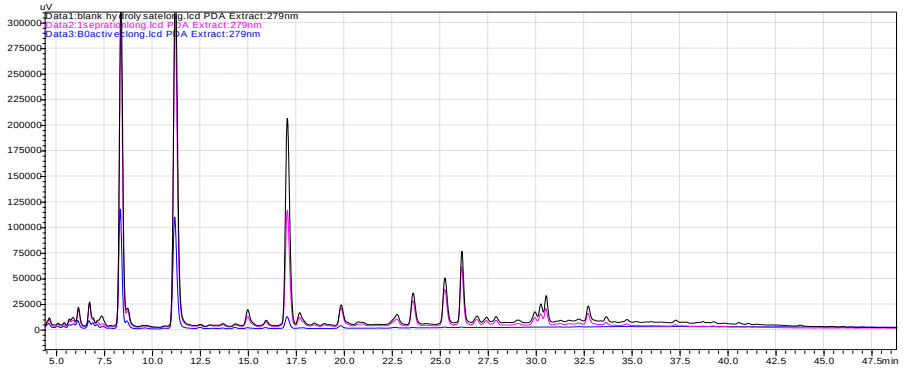

Figure 4-7: Comparison between long HPLC measurements of (—) untreated XRF, (—) active carbon and (—) m-CLEAs treated XRF.

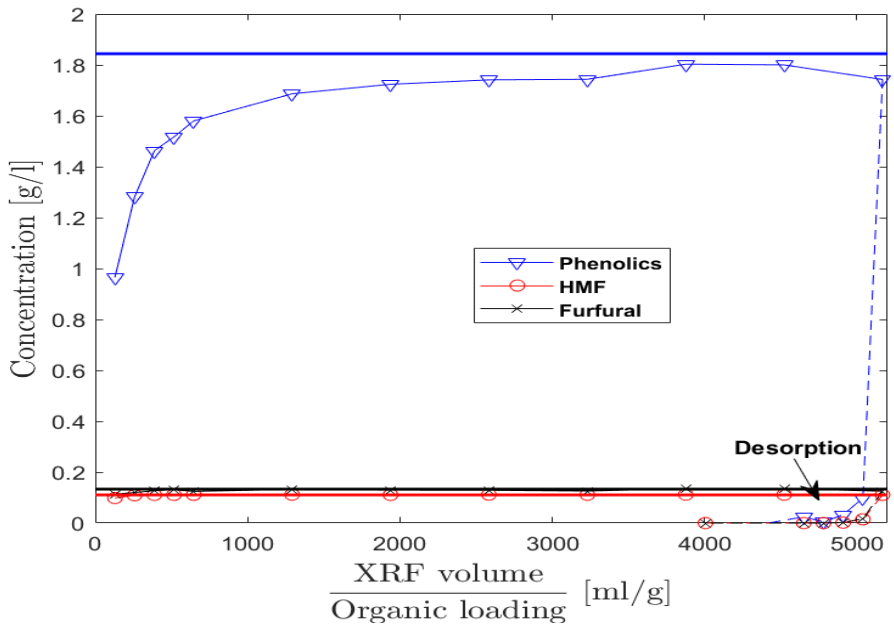

Figure 4-8: Adsorption and desorption on m-CLEAs catalyst. Concentrations of (Δ) phenolics, (x) furfural and (o) HMF during (—) adsorption and (--) desorption. Desorption x-axis goes from right to left. Horizontal lines represent starting concentrations in XRF.

Desorption experiments (see Section 4.5.1.2) showed minimal desorption, after two cycles of washing the measured phenolics concentration was in measurement error range. This indicated that the adsorption is irreversible, chemical rather than physical sorption (see Figure 4-8), as in case of physisorption the bounding is purely equilibrium based and washing would decrease the concentration of the compound in the bulk phase caused by desorption from the surface. Chemical sorption however is irreversible, as no desorption will occur during washing.

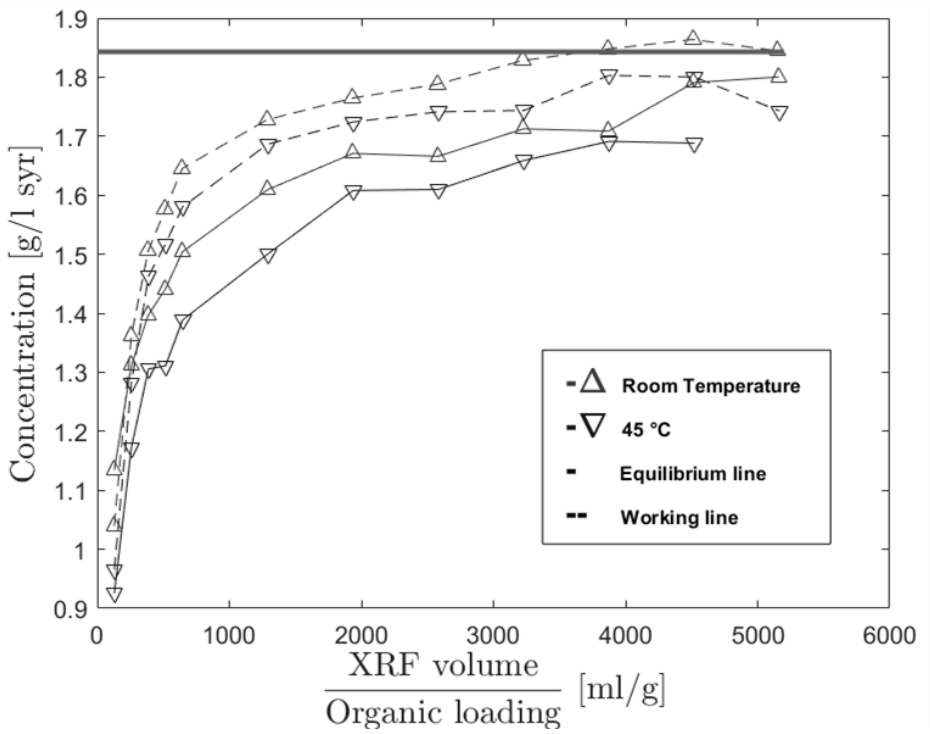

Figure 4-9: Adsorption at two different temperatures with m-CLEAs catalyst. (—) Represents experiments without separation, (--) represents experiments with catalyst separation and recycling.

When investigating the adsorption on m-CLEAs, first an **adsorption isotherm** was measured, a straightforward equilibrium curve (Langmuir, Freundlich etc.). It is obtained by using a fixed amount of adsorbent and shows the remaining concentration in the liquid at equilibrium [g/l] with respect to the amount of compound that is adsorbed per mass adsorbent [g/g]. In our case, measurement of the phenolic concentration was done by starting from a low XRF/m-CLEAs ratio and XRF was added

stepwise in 30 minutes intervals, without separating the catalyst from the liquid (see Section 4.5.1.3). In Figure 4-9, the remaining concentration in the liquid with respect to the different XRF volumes applied per amount of m-CLEAs is presented. The adsorbed mass of phenolics will be the difference between the equilibrium concentration and the original concentration (shown by the horizontal line at the top of the graph) multiplied with the volume of XRF. At high XRF volumes, the remaining concentration of phenolics will asymptotically approach the concentration of the blank XRF sample, because saturation of the catalyst will be reached, but never reach it as some phenolics will always be adsorbed on the surface, thus missing from the bulk liquid.

Next, the adsorption on m-CLEAs was investigated in the following way. When m-CLEAs were recycled, the liquid was separated from the catalyst and fresh XRF was added to start the next detoxification step. This represents the actual application of the catalyst, as it will be recycled from batch-to-batch. This is represented in the working line, which shows the phenolic concentration at equilibrium with respect to the added XRF volume (Figure 4-9). The phenolic concentration was obtained after addition of the recuperated m-CLEAs to an XRF volume/ m-CLEAs ratio of 129 (5 ml to 0.0378 $g_{organic}$) five times and seven times to a ratio of 646 (25 ml for the same mass). The x-axis shows the cumulated added XRF volumes in the different cycles. Physically, it means the m-CLEAs are always in contact with the same volume. It is straightforward that each batch volume, thus XRF/ m-CLEAs ratio, will have its own curve (25 ml/g and 200 ml/g can be significantly different) as theoretically different amounts of phenolics will be removed when different volumes XRF are added to the catalyst. Additionally, the starting point of the working line will be the same point as on the equilibrium curve, since the first batch is fresh catalyst with the corresponding amount of liquid added. In Figure 4-9 the starting points of the curves are different as the applied m-CLEAs masses are slightly different and the slope of the curve is big, thus small mass differences will result in relatively big remaining phenolic concentration differences. As in each subsequent step, fresh XRF is added and desorption is minimal, the measured remaining phenolic concentrations in the liquid phase will be higher than the equilibrium concentrations (the working line is “above” the equilibrium line). This can be understood by considering the following: as adsorption is a reversible process and the driving force of adsorption is the difference between the concentration at the surface of the adsorbent and the concentration in the liquid, the fresh XRF will always be the same higher initial concentration that will force more phenolics on the adsorbent material than if the fresh XRF is added to the already present XRF with a

decreased phenolic concentration. In the latter, the driving force will be smaller. For the same reason, the working line reaches the blank XRF concentration as soon as the m-CLEAs surface is saturated. Figure 4-9 shows the two curves, i.e., equilibrium (without separation of the m-CLEAs) and working line (with separation). It is furthermore visible that higher temperature enhances adsorption, a phenomenon appearing in case of chemisorption as higher temperature means higher reaction rates according to the Arrhenius equation. In case of physisorption, the opposite would occur, i.e. physical bounding forces will get weaker in case of higher temperatures, due to the higher kinetic energy of the molecules in the solution.

Therefore, it is clear that adsorption is even a more important phenomenon at the expected working temperature of SSF (40-50 °C) than on room temperature. Furthermore, due to the fact that for industrial enzymes the activity per g protein is usually lower than purified commercial research enzymes, more enzyme will be applied and, consequently, the applied XRF/ m-CLEAs ratio will be smaller. This makes adsorption a parameter that has to be quantified and calculated if the process will reach the application stage. On one of the datasets, Matlab modeling was performed to obtain a mathematical model, which can describe this reliably (Section 4.6).

4.6 Modeling

4.6.1 Goal and methodology

As it was shown in Section 4.5, adsorption is a significant phenomenon during laccase m-CLEAs and XRF reaction, so it is worthwhile to investigate it further. The goal of the model is to estimate the remaining phenolic concentration in function of XRF-catalyst ratios and recycling rounds, because their remaining concentration can decide whether extra detoxification steps will be needed. In a concrete process HPLC measurements are a possibility, but for theoretical designing/optimization this is not a possibility.

Two different datasets have been recorded (Figure 4-9), both presenting phenol concentration in function of XRF/m-CLEAs [ml/g] ratios or XRF volume [ml]. The so called ‘equilibrium line’ represents the situation when CLEAs are not separated from the liquid, i.e., fresh liquid is added to the mixture each time after reaching equilibrium. The other curve, called ‘working line’, contains the equilibrium concentrations of phenolics when the liquid was separated each time before addition of fresh XRF to the

m-CLEAs, i.e., exactly as what would happen if the m-CLEAs are recycled in an industrial application.

Methodologically the equilibrium curve is easier to measure and is expected to be the same for a given batch of catalyst, XRF and temperature. The working line is more difficult to measure and, additionally, it depends on the step-size of volume addition (**V/m**), which means potentially an infinite number of curves can be obtained for a given m-CLEAs /XRF/temperature system (see detailed explanation later). However, in an industrial setting, it is the working line curve that has importance and not the equilibrium curve. Therefore, it would be beneficial to investigate how to model the working line, and how the working line depends on the equilibrium line.

The dataset was recorded as described in Section 4.5.1 at 45 °C and an organic loading of 0.0319 g (equilibrium line) and 0.0387 g (working line). Therefore, the modeling was divided in two stages. Firstly, a fit for the equilibrium line (found to be the Freundlich isotherm) was determined, and, secondly, an empirical fit for the working line was constructed. All data processing was performed off-line using a commercial software package (MATLAB 2017.1, The MathWorks Inc., Natick, MA, 2017), and standard packages for optimization (minimum search).

4.6.2 Method

For modelling of the equilibrium and working line an experimental set was measured similar to the method described in Section 4.5.1. Wet m-CLEAs (1.11 g) were mixed with 10 ml XRF. After 30 mins at 45 °C, the solution was mixed and 5 ml of the whole mixture (catalyst and XRF) was pipetted to another Erlenmeyer lombic. This ensured that the starting point would be identical, however because of the fast sedimentation the mass of the two separated catalysts can be different. The actual catalyst mass was measured after decantation of the first 5 ml of the original solution, afterwards the corresponding $V_{XRF}/m_{m\text{-}CLEAs}$ was calculated based on the measured mass for both mixtures. For the equilibrium line measurements, the original content was 0.0319 $g_{protein}$, while for the working line measurements, this was 0.0387 $g_{protein}$. Each reaction cycle lasted for 30 min with mixing at 10 and 20 mins.

4.6.3 Modelling the adsorption isotherm

The well-known Freundlich isotherm takes the following form for solid liquid adsorption (Equation 4-3).

$$\frac{x}{m} = Kc_{eq}{}^{n} \quad \textbf{4-3}$$

where **x** is the adsorbed mass, **m** is the mass of the solid, **K** and **n** are constants, $\mathbf{c_{eq}}$ is the equilibrium concentration.

Using the fact that the adsorbed amount can be described with the volume and the concentration change in the liquid (Equation 4-4):

$$\frac{V}{m}(c_0 - c_{eq}) = Kc_{eq}{}^{n} \quad \textbf{4-4}$$

where $\mathbf{c_0}$ is the starting concentration.

After reorganizing the equation (Equation 4-5):

$$\frac{V}{m} = \frac{Kc_{eq}{}^{n}}{(c_0 - c_{eq})} \quad \textbf{4-5}$$

Alternatively, the mass, as it is constant in the experiment, can be included in **K** (Equation 4-6):

$$V = \frac{K'c_{eq}{}^{n}}{c_0 - c_{eq}} \quad \textbf{4-6}$$

where **K'** is a constant.

The equations give the relationship between the volume of XRF and the mass of m-CLEAs ratio (Equation 4-3) or the XRF volume (Equation 4-5) and the equilibrium concentration (Figure 4-9). Since in our case the V/m ratio is used, Equation 4-5 will be used further. Until this point, the equation derivation is mathematically correct, however it must be noted that the phenolics concentration used in this research is measured by UV absorbance as a mass equivalent calculated against a syringaldehyde standard, therefore not explicitly the exact phenolics concentration.

In this concrete adsorption isotherm, the volume is the independent and the concentration the dependent variable; therefore, it would be better to derive an equation that expresses the concentration explicitly. The difference in the power of $\mathbf{c_{eq}}$ (in Equation 4-5) makes this difficult. Instead, the graph presented as an inverted curve

(**V-c** instead of **c-V**) would allow that, from a given equilibrium concentration $\mathbf{c_{eq}}$, a concrete volume **V** could be calculated easily.

Similarly to the transformations done with the Freundlich isotherm (Equation 4-3), the same steps can be done with the Langmuir isotherm (Equation 4-7). The original model was defined for monolayer adsorption in case of gases, thus it defines a relation between partial pressure and surface saturation. The model can be also used for liquid-solid adsorption in the form of Equation 4-8.

$$\frac{V_{current}}{V_m} = \frac{Kp}{1 + Kp} \qquad \textbf{4-7}$$

Where $\mathbf{V_{current}}$ is the volume of the monolayer, $\mathbf{V_m}$ is the volume of the saturated monolayer, **K** is a constant and **p** is the partial pressure of the compound.

$$\frac{kV}{m}(c_0 - c_{eq}) = \frac{K'c_{eq}}{1 + K'c_{eq}} \qquad \textbf{4-8}$$

Where **V** is the volume of liquid, **m** the mass of the solid, **k** is a constant defining the relationship between the saturated monolayer and the adsorbed mass, $\mathbf{c_0}$ is the starting concentration, $\mathbf{c_{eq}}$ the equilibrium concentration and **K** is a constant.

Equation 4-8 can be expressed with **V/m** as dependent variable by dividing both sides by $\mathbf{c_0\text{-}c_{eq}}$ (Equation 4-9), and then dividing by **k** (Equation 4-10). Alternatively, **V** can also be expressed explicitly (Equation 4-11).

$$\frac{kV}{m} = \frac{K'c_{eq}}{(1 + K'c_{eq})(c_0 - c_{eq})} \qquad \textbf{4-9}$$

$$\frac{V}{m} = \frac{Kc_{eq}}{(1 + K'c_{eq})(c_0 - c_{eq})} \qquad \textbf{4-10}$$

$$\mathbf{V = \frac{mKc_{eq}}{(1 + K'c_{eq})(c_0 - c_{eq})}} \qquad \textbf{4-11}$$

Where **V** is the volume of liquid, **m** the mass of the solid, **k** is a constant defining the relationship between the saturated monolayer and the adsorbed mass, $\mathbf{c_0}$ is the starting concentration, $\mathbf{c_{eq}}$ the equilibrium concentration and **K, K'** are constants.

A fit of the adsorption isotherm in Figure 4-10, i.e., the dataset recorded with no XRF separation, was performed with the Freundlich model derived equation (Equation 4-5)

and the Langmuir model derived equation (Equation 4-10). The results are summarized in Table 4-4 and the resulting graphs are visualized (Figure 4-10). The Freundlich model gave a better fit compared to Langmuir (R^2=0.9711 instead of 0.9706). Therefore, Freundlich was used further, although the difference was really small, i.e. both seem to describe the measured data well.

Table 4-4: Results of equilibrium line fit. SSE is the sum of squared errors.

	SSE	K' or n	K	R^2
Freundlich	9.8194e+05	1.5652	206.64	0.9711
Langmuir	9.9834e+05	-0.2062	180.85	0.9706

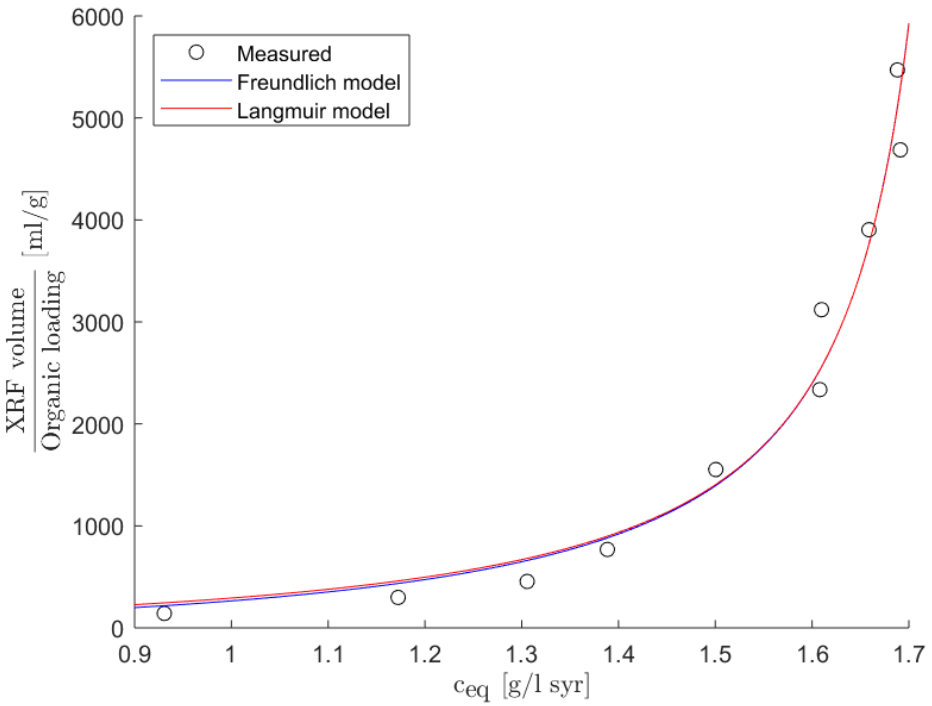

Figure 4-10: Measurement points and fitted (—) Freundlich/Langmuir model on the adsorption equilibrium line (o) measurement points with m-CLEAs and XRF.

After the parameters are calculated, the equation can be handled easier. Simulating the adsorption curve is straightforward, i.e., a vector of $\mathbf{c_{eq}}$ values is defined and the corresponding **V** values are calculated. However, it should be kept in mind that originally **V** is the independent variable and $\mathbf{c_{eq}}$ is the dependent as a concrete volume of XRF will be added to the m-CLEAs. Secondly, in our case, the volume can be

determined more precisely than the equilibrium concentration (volume measurement is more precise than syringaldehyde measured by the short HPLC method), therefore **V** values are more certain than $\mathbf{c_{eq}}$. This means that Equation 4-5 has to be used in the way that **V** values will be given and $\mathbf{c_{eq}}$ calculated. Since the difficulties to express the phenolics concentration explicitly still exist, Equation 4-5 was converted to a minimum search problem, which is executed relatively fast by Matlab. The expression can be rewritten to:

$$\frac{K{c_{eq}}^{n}}{(c_0 - c_{eq})} - \frac{V}{m} = 0 \qquad \textbf{4-12}$$

$$\left(\frac{K{c_{eq}}^{n}}{(c_0 - c_{eq})} - \frac{V}{m}\right)^2 = 0 \qquad \textbf{4-13}$$

Technically the equilibrium curve is calculated by solving the minimum value problem (Equation 4-13) at every value of **V**. This was the way the $\mathbf{c_{eq}}$ value was calculated for the corresponding **V** values in case of the equilibrium line further on (Section 4.6.4 and 4.6.5).

4.6.4 Modeling of the working line

The main difference between the equilibrium line and the working line is that the previous is measured by increasing the added XRF volume compared to a given amount of m-CLEAs, therefore all equilibrium lines for a given XRF (source, pretreatment parameters etc.) and m-CLEAs (enzyme, immobilization parameters etc.) will be the same, or they will be "overlapping". The working line represents the actual application situation, when given amounts of m-CLEAs are mixed with a given amount of XRF, the catalyst is filtered out and remixed with another batch of fresh XRF, and so on. It can be seen, that compared to the previous situation (equilibrium line), a new operation parameter is introduced, i.e., XRF volume/m-CLEAs mass, which means that for a given equilibrium line (varying XRF volume, constant m-CLEAs mass) infinite different working lines can be rendered in function of the $V_{xrf}/m_{m\text{-}CLEAs}$ ratio. The following properties are known for every different working line (constant $V_{xrf}/m_{m\text{-}CLEAs}$; constant XRF volume; constant m-CLEAs mass):

I. Each working line starts from the equilibrium line, or with other words, the first point of the working line will be always on the equilibrium line.
II. The concentrations on the working line will be always higher (or equal in case of the first point) than the equilibrium line.

III. The equilibrium line is continuous, while the working lines are discrete.
IV. The working line will reach the concentration of the blank sample and not approach it like the equilibrium line.

The first property (I.) can be understood by following a thought experiment. A working line experiment is performed at a given $V_{xrf}/m_{m\text{-}CLEAs}$ = **k** ratio. This means that the mixture will be first separated exactly at the k volume/mass, determined by that value, the first point of the working line starts from the equilibrium line.

The second property (II.) can be understood considering the following. The rate determining factor of adsorption is not the amount of liquid added, but the concentration difference between the actual bulk concentration of the liquid and the equilibrium concentration corresponding to the saturation level of the solid/catalyst. Keeping the same symbols and conclusions from the previous paragraph, the following applies: at every $V_{xrf}/m_{m\text{-}CLEAs}$ lower than **k,** the corresponding concentration is the same for the equilibrium line and working line. Let us call the corresponding bulk liquid equilibrium concentration $\mathbf{c_k}$ at the point where the ratio is **k**. At the **k** ratio, the mixture will be separated in case of the working line, and another batch of fresh XRF corresponding to the **k** ratio will be added (case 1). Let us assume that in case of the equilibrium line at **k** ratio, another **k** amount of XRF was added to the mixture without separation (case 2). The adsorbed amount on the surface of the solid/catalyst at the starting point (**k** point) will be the same in both case 1 and case 2, which means that the corresponding bulk liquid equilibrium concentration ($\mathbf{c_k}$) will be exactly the same. At the moment when the XRF is added however, the bulk concentrations will differ significantly, i.e., in case of working line (case 1), the new starting concentration will be $\mathbf{c_0}$ as fresh XRF is added, while in case of the equilibrium line (case 2,) the starting concentration will be $(\mathbf{c_0}+\mathbf{c_k})/2$, as the fresh XRF is added to the already present XRF. This will continue at every corresponding step: while the catalyst recycled according to the working line will always contact fresh XRF with $\mathbf{c_0}$ concentration, the catalyst measured according to the equilibrium line will contact the mixture of the previously "depleted" XRF and the fresh XRF. Therefore, the driving force, $\mathbf{c_{bulk}}\text{-}\mathbf{c_{saturation}}$, will always be higher in case of the working line (case 1) than in case of the equilibrium line (case 2). Since the driving force is higher, more phenolics will adsorb and the solid saturation level will be higher. Since a higher saturation level is connected to a higher equilibrium bulk concentration, described by the adsorption isotherm, and the latter

is exactly what is being measured, the working line will always be above the equilibrium line.

The third property (III.) is easy to understand, however it is only partially true. If the catalyst is used for a working line in a given **k** ratio (volume/mass), the first point will be recorded at the **k** value. After recycling the catalyst and adding new XRF, the next point will be at 2**k** value, the third point at 3**k** value, etc. 1.5**k**, for example, is not defined, in the same way as for example protein consumption by 1.5 man is not defined (although mathematically it can be calculated). This is true for the experiments described in Section 4.5.1.3. However, if the process is done in a fed batch mode and **k** is the ratio when the catalyst is separated from the mixture, there will be a starting **m** ratio (catalyst mass to added XRF), where **m**<**k**. Thereafter, new XRF is added to the mixture continuously until the ratio reaches the **k** value, then separated and recycled to a **k**+**m** ratio and separated again at 2**k**, recycled at 2**k+m** and separated at 3**k** etc. In this case the working line is not discrete anymore, but it will be defined in every [n*__k__+__m__,(n+1)*__k__**]** interval, where n is an integer.

The fourth property (IV.) comes from the third. If the thought experiment is continued, after many cycles in case of the working line experiment, there will be a point where only one molecule is adsorbed to the almost completely saturated surface. In the next round, none will adsorb and an equilibrium concentration equal to that of the initial $\mathbf{c_0}$ will be reached, thus the working line actually reaches $\mathbf{c_0}$ value. In case of an equilibrium experiment, the added XRF is mixed with the previous one, so if even a single molecule was adsorbed from it, the molecule will be still missing from the liquid, thus $\mathbf{c_0}$ equilibrium concentration cannot be reached, just approached. Keeping the previously defined symbols, it can be said that the working line concentration ($\mathbf{c_w(k,V)}$) will always be between $\mathbf{c_{eq}(V)}$ and $\mathbf{c_0}$, or $\mathbf{c_{eq}(V)}<\mathbf{c_w(k,V)}<\mathbf{c_0}$.

As no model has been defined for this kind of working line yet, an initial fit of the dataset with all measurement points was performed using the Freundlich and Langmuir type models, as defined in (Equation 4-5 and Equation 4-10) . The first problem with the fit comes from property IV., the working line concentration will reach the $\mathbf{c_0}$ concentration. Measurement errors will be also present, which means that potentially equal or higher concentrations than $\mathbf{c_0}$ will occur in the measurements (as in case of the last point of the given dataset). Both equations have a division by $\mathbf{c_0-c}$, which in this case will yield a small negative number or zero, which will result in a big negative number for **V**, which will cause an oscillation between big ±**V** values at $\mathbf{c_{eq}}$

values close to c_0, or a division by zero will cause a crash. Therefore, an initial correction was made before the fitting by leaving out values equal or greater than c_0. After the last point is left out the fit is still performing bad (see Figure 4-11), with R^2 of 0.050 and 0.102 for the Langmuir and the Freundlich model respectively. The bad performance of the models can be understood taking into account that both were developed for equilibrium measurements, not recycling as in case of the working line experiments.

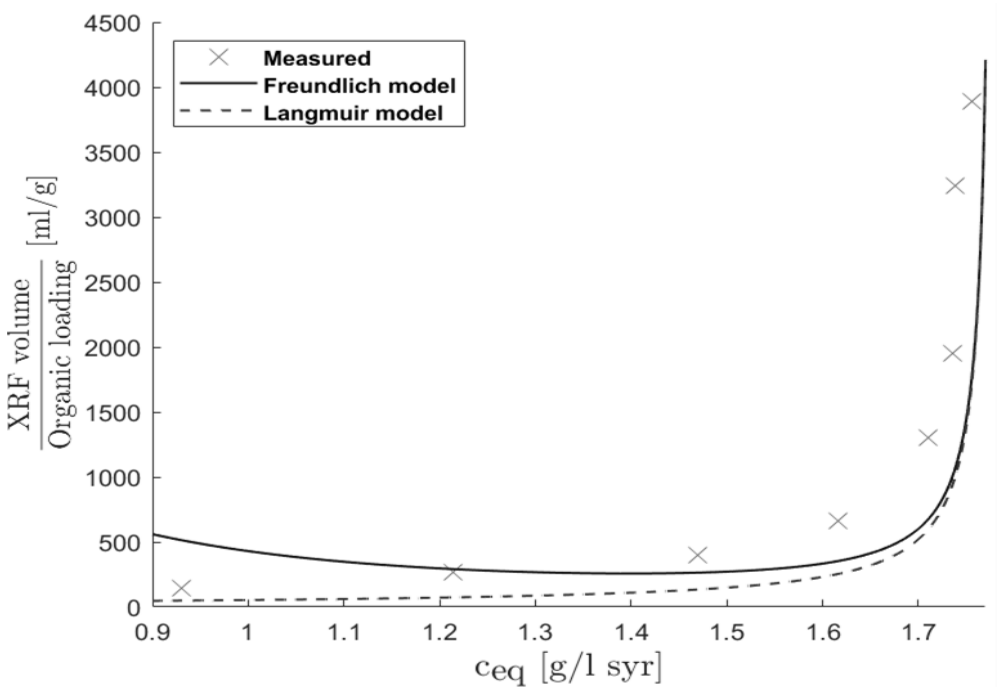

Figure 4-11: (--) Langmuir and (—) Freundlich model fit on working line (x) measurement points.

As an unlimited number of working lines for an equilibrium curve exists, it might be interesting to generalize them. An option to generalize the relation between c_w-**V** is to show how much portion of the c_0-c_{eq}**(V)** difference does c_w**(k,V)** actually covers (see Figure 4-12), and this factor will be called the c_{factor} (Equation 4-14)**.** The conversion from the c_{factor} to the working line concentration (c_w) is described by Equation 4-15**.** For example, a c_{factor} of 0.5 means that the c_w value is half way between c_{eq} at that point and c_0.

$$c_{factor}(k,V) = \frac{c_w(k,V) - c_{eq}(V)}{c_0 - c_{eq}(V)} \quad \textbf{4-14}$$

$$c_w(k,V) = c_{factor}(k,V) * (c_0 - c_{eq}(V)) + c_{eq}(V) \quad \textbf{4-15}$$

where $\mathbf{c_w}$ represents the concentration points at equilibrium during measurement of the working line.

Investigating Equation 4-14 and Equation 4-15, it is visible that the $\mathbf{c_{factor}}$ starts from 0, when $\mathbf{c_w}$ equals $\mathbf{c_{eq}}$, and will reach 1 when the adsorbent is saturated ($\mathbf{c_w} = \mathbf{c_0}$). This expression could be used for every working line (i.e., every **k** value) as it fulfills the criteria that $\mathbf{c_w}$ starts from the equilibrium line ($\mathbf{c_{eq}}$) and it goes to the initial blank concentration ($\mathbf{c_0}$). Technically, it is a transformation of the $\mathbf{c_w}$ variable to another $\mathbf{c_{factor}}$ variable. After the transformation, the **V** values were shifted to the origin by subtracting the minimum **V** value from all **V** values ($\mathbf{V}$-$\mathbf{V_{min}}$). This was to ensure that all working line curves are shifted to the same region, no matter which **k** value they have started from.

The transformation according to Equation 4-14 also has its cost. As **V** increases, both $\mathbf{c_w}$-$\mathbf{c_{eq}}$ and $\mathbf{c_0}$-$\mathbf{c_{eq}}$ will get smaller and smaller (Figure 4-12A), which means that random measurement errors, not significant if investigating the initial concentration values, can mean significant deviations when divided by small numbers ($\mathbf{\Delta c} \rightarrow 0$ when $\mathbf{V} \rightarrow \infty$). In case of $\mathbf{c_0}$-$\mathbf{c_{eq}}$, it is less a problem as the values are calculated from the already performed equilibrium fit, ensuring smooth evolution, but in case of $\mathbf{c_w}$ values, which are raw measurement data, including standard error, it can be a problem as visible in Figure 4-12B at the two points before the last. However, when the $\mathbf{c_{factor}}$ will be converted back to $\mathbf{c_w}$ the errors will decrease.

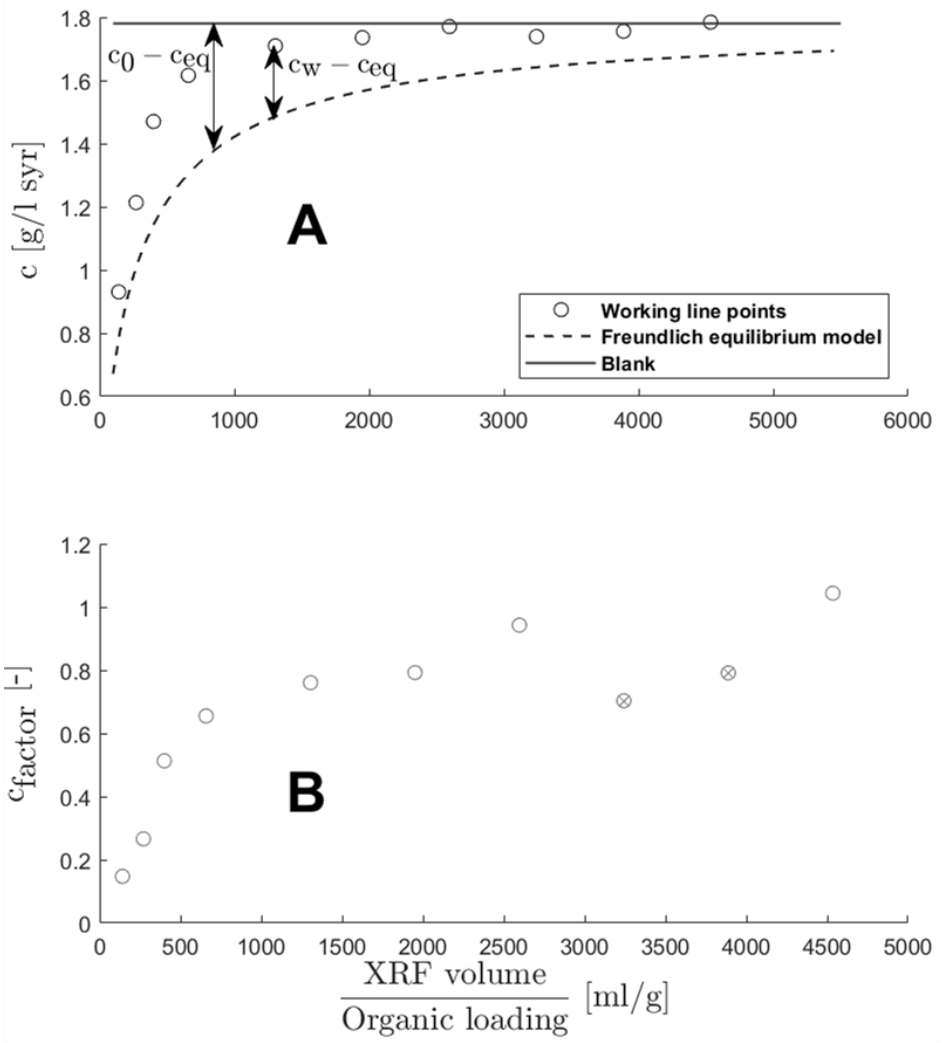

Figure 4-12: Visualizing c_{factor} calculation. (A) The measurement (o) points will be linearly transformed between the (--) equilibrium model and the (—) blank concentration. Points on the equilibrium line will be 0, points on the blank concentration 1. (B) (o) Points after transformation, (x) discarded points.

After $\mathbf{C_{factor}}$ transformation, shifting to the origin and excluding the two outliers two different models were fitted. Both were purely empirical. Empirical working line (WL) model 1 (see Equation 4-16) has an exponential part, which hard-codes the upper limit of 1 in the model, while Empirical WL-model 2 (see Equation 4-17) is an empirical equation with two parameters.

$$c_{factor} = 1 - e^{-\frac{V/m}{K}} \quad \textbf{4-16}$$

$$c_{factor} = \frac{KV/m}{K_2 + V/m} \quad \textbf{4-17}$$

where **K** and **K_2** are constants.

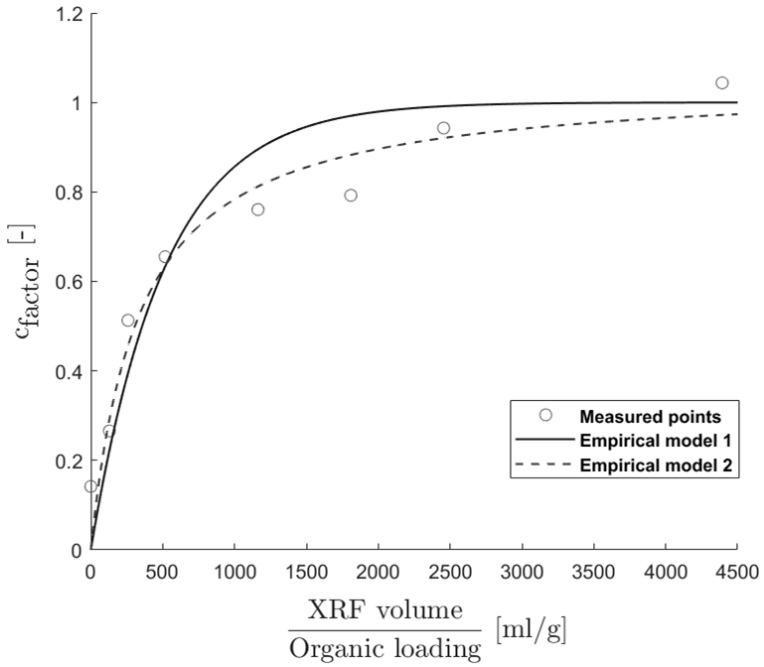

Figure 4-13: C_{factor} (o) points with two fitted empirical (—) (--) models.

The results of the fit are summarized in Table 4-5 and the curves visualized on Figure 4-13. WL model 2 performed significantly better with R^2=0.94, compared to 0.87 in case of Empirical model 1. It should be kept in mind that Empirical model 1 only had one fitted parameter while Empirical model 2 had two, thus the better fit is not surprising. The data set is too small to choose between the two, but in the current case, Empirical model 2 was used further.

Table 4-5: Results of c_{factor} fit. SSE is the sum square errors.

	SSE	R^2	K	K_2
Empiric 1	0.0921	0.8669	515.37	-
Empiric 2	0.0424	0.9388	1.0460	334.73

4.6.5 Constructing the summarized graph

For the next step, mainly because of the lack of data, it was assumed that the constants from the fitted empirical model (Equation 4-17) would remain the same at every recycling step size (**k**). The chances for this are very low, as most probably all constants will depend on **k**, i.e., **const(k)**, and additional models will be needed to describe this relation. However, to show how the fitted models can be used, the constants were assumed the same for every working line. Reproducing the equilibrium line is straightforward: a vector of **V** values was taken, and the corresponding $\mathbf{c_{eq}}$ values calculated according to Equation 4-13. In this specific case it would also be possible to take a vector of $\mathbf{c_{eq}}$ values and calculate **V** values according to Equation 4-5, as no exact **V** values are needed, only enough points to reproduce the full curve.

To simulate the working lines, a vector of different **k** values was chosen. For each **k** value and for **n** recycling steps, a vector of **V** values was generated, thus resulting in a **k-V** matrix, in such way that it will contain all **k*n** values in ascending order, where **n** is an integer. These are the points where that specific working line is defined, i.e. the volumes corresponding for the n_{th} recycling round. Theoretically, the vector contains infinite elements, but values greater than 6000 were discarded, as the last measured data point is at 5300. For each **V** value, the corresponding $\mathbf{c_{eq}}$ was calculated according to Equation 4-13, which will result in a $\mathbf{c_{eq}}$ vector equal to the dimension of **V** vector. Here, the use of Equation 4-5 is not an option as **V** values are defined, not $\mathbf{c_{eq}}$ values. A matrix of $\mathbf{c_{factor}}$ values are calculated according to Equation 4-17, at every point of the **k-V** matrix. Thereafter, a $\mathbf{c_w}$ value is calculated for each $\mathbf{c_{factor}}$ value according to Equation 4-15, and using the obtained $\mathbf{c_{factor}}$ and $\mathbf{c_{eq}}$ values. For visualization purposes full lines were plotted, not just the points corresponding to **V** vector, however this does not have a physical meaning, only the discrete points do exist. The schema of the calculations is shown in Figure 4-15. In the final step all data are plotted in Figure 4-14: the measured data, the simulated equilibrium curve, the simulated working lines both with a continuous line and visualizing only the points where the curve is defined. With the help of the figure, the adsorption phenomenon can be estimated: after the initial $V_{XRF}/m_{m\text{-}CLEAs}$ ratio is known for a reaction, the first point will be on the equilibrium graph. This shows which phenolic concentration can be expected in the broth after the adsorption equilibrium. The next point on the working line, starting from this point, will show which phenolic concentration is expected in the broth after the first recycling round etc.

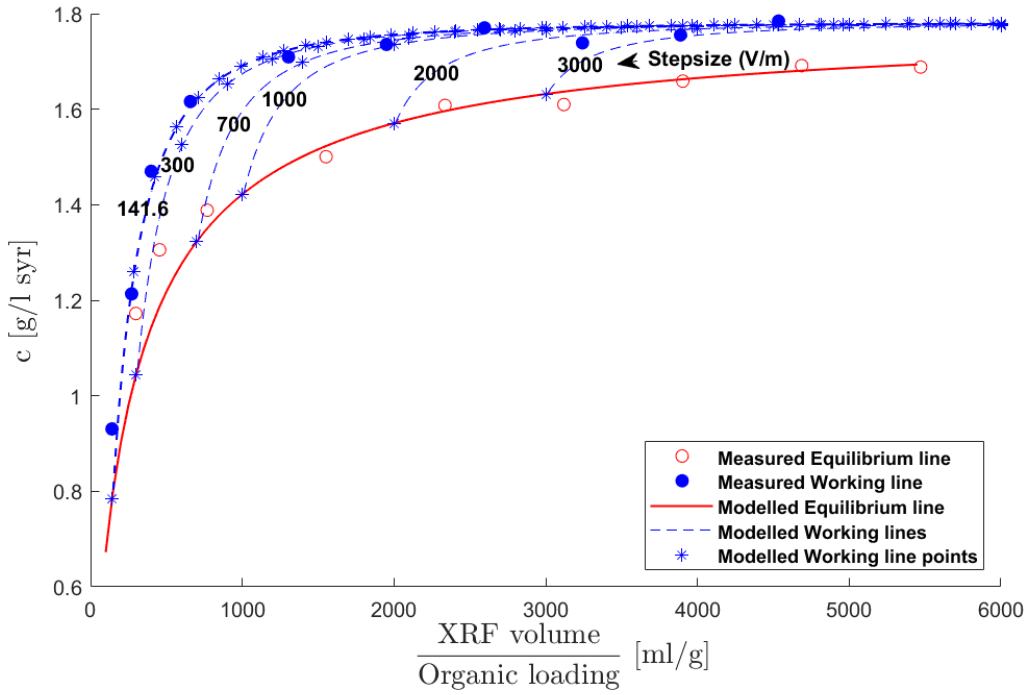

Figure 4-14: The complete model for adsorption estimation. Measured equilibrium line points (o) and working line points (●), modeled equilibrium line (—) and working lines (--) and the points where the working line is defined (*).

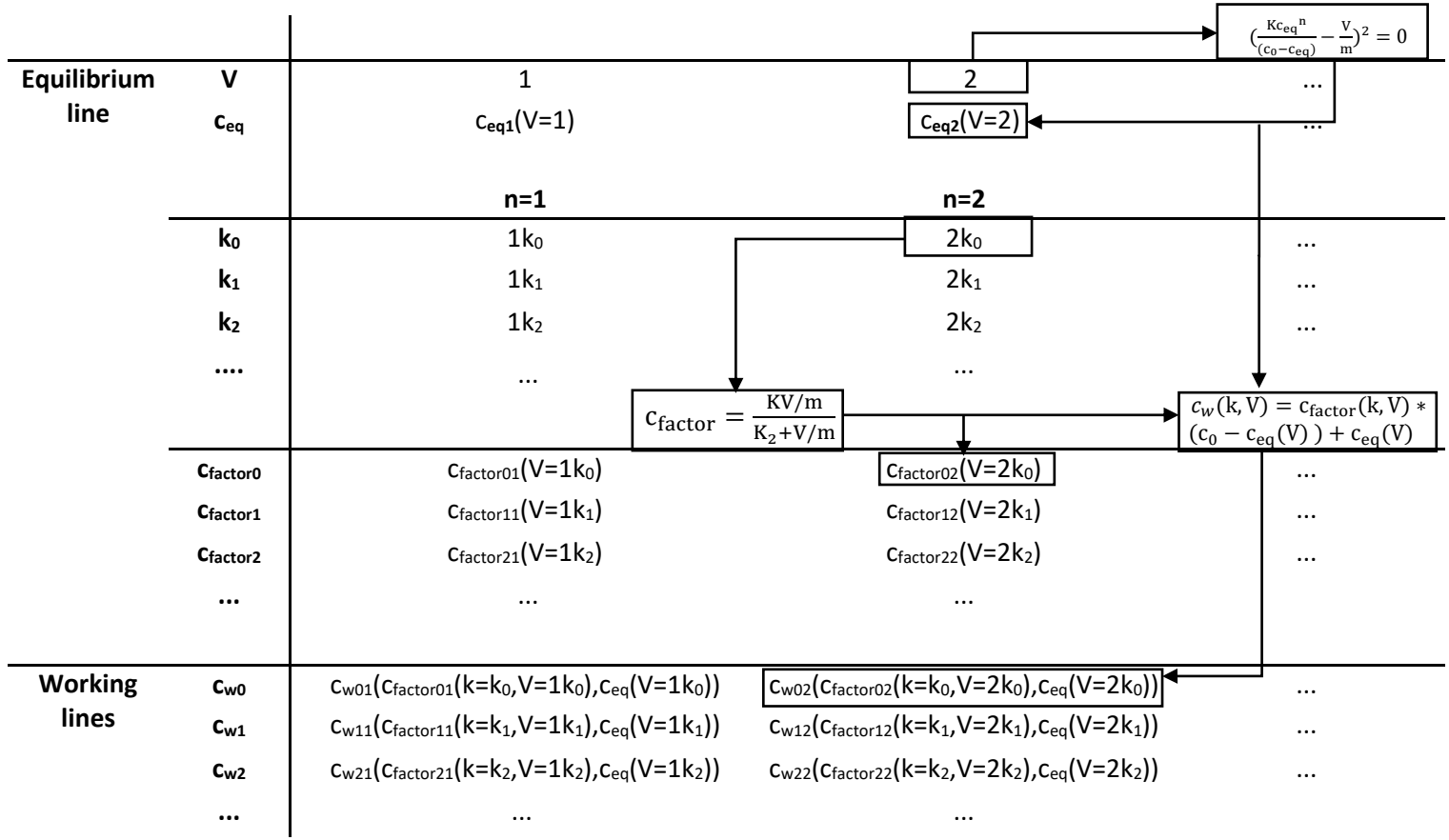

Figure 4-15: The schematic structure of the adsorption calculations of in case of XRF and m-CLEAs.

4.6.6 Conclusion

The phenolic adsorption on m-CLEAs follows the well-known Freundlich adsorption isotherm. When the catalyst adsorbs inhibitors, less laccase should be added for detoxification. Therefore, it is essential to approximate the needed catalyst amounts (calculated from free enzyme activity) and to know/quantify the catalyst's adsorption behavior. It has to be noted that the standard equilibrium measurements for an adsorption isotherm can produce significantly different concentrations compared to the possible industrial system with m-CLEA recycling (called the working line). Mixing 1 g catalyst with 100 ml XRF does not necessarily give the same results as mixing and recycling the catalyst 10 times with 10 ml XRF.

4.7 General conclusions

It was proven that m-CLEAs adsorb significant amounts of phenolics at volume/catalyst ratios that are relevant in case of industrial utilization (relatively high catalyst load from unpurified enzymes with relatively low activity) via irreversible chemisorption. In the first few recycling rounds, the enzymatic detoxification will be insignificant compared to adsorption. Technically speaking, this is not a problem as the inhibitors are still removed from the solution; in fact, it opens up new possibilities for applications. However, enzyme catalyst is too expensive to use it as an adsorbent, thus bacterial m-CLEAs laccase only for detoxification is not recommended. For adsorption of phenolics, active carbon would be more suitable (if of course laccase detoxification does not have additional positive effect). It can be investigated if cellulase m-CLEAs behave the same way, as cellulase is needed anyway in the process, and detoxification will be a welcomed "side effect".

It is important to measure the inhibitor concentration in the broth prior to fermentation to estimate the inhibition effect, and decide if actions should be taken to lower the concentration. This can be easily done by an HPLC measurement prior to fermentation, but if any m-CLEAs enzyme is used in the process, their addition alone will influence the concentrations depending on the amount and the generation of the catalyst (i.e. how many times was the catalyst recycled). As adsorption happens fast, i.e. in about an hour, and in the SSF process, inoculation will be shifted to a few hours (approximately 12 h) after enzyme addition, either cellulase or laccase, it is still possible to measure toxic compounds prior to inoculation. However, for designing the SSF process in more detail, a model is needed to calculate adsorption caused by m-

CLEAs as they influence detoxification costs. A model was constructed for that purpose. With a relatively few and simple measurement, an approximation can be made about the expected adsorption effect. Required measurements are an adsorption isotherm with the exact m-CLEAs and steam exploded substrate, and minimum two measurement points with the recycled m-CLEAs at the catalyst/volume ratio of the planned application. More points will increase the precision. Possible generalization of the model for other catalyst/volume ratios was mentioned in the text, but will require additional measurements to implement.

Chapter 5 **PROCESS INTEGRATION**

5.1 Introduction

Process integration in lignocellulose-to-chemicals conversion is a tool to decrease costs of production through simplification of equipment/control systems, overlapping processes, thus shortening production time and increasing productivity. An ideal process would mean that all the necessary materials, i.e., substrate, catalyst, microorganism, and conditioners, are placed in a single reactor at the desired conditions and that after a certain time the product could be removed. In reality, it is rarely possible; however, avoiding separation steps and slightly overlapping processes can still have significant benefits. As there are three main process steps, the possible overlapping combinations are simultaneous saccharification and detoxification (**SSD**), simultaneous fermentation and detoxification (**SFD**), and simultaneous saccharification and fermentation (**SSF**). The combination of all three processes at the same time is called simultaneous saccharification, fermentation and detoxification (**SSFD**). Microbial adaptation of the inoculum to the inhibitors in XRF can decrease lag phase thus cause higher volumetric productivity, and is a kind of overlapping/process integration of inoculum preparation and adaptation. The abbreviations might be different in literature. For example De La Torre et al. used presaccharification and simultaneous saccharification and fermentation (PSSF) instead of SSF when the two processes are not completely overlapped [153], but the principles are always the same.

The first benefits of process integration techniques appear in shortened process time, thus **higher volumetric productivity**, simplified reactor design (fewer reactor vessels, reduced separation steps) and auxiliary systems (e.g., piping, heat exchangers), simplified process control, thus **lower capital investment costs (CAPEX)**. From previous results, own results and literature alike, we know that the steps of hydrolysis, detoxification and fermentation typically take days. Saccharification needs minimum 24 h, typically 48 or 72 h (see Section 3.5), laccase treatment takes usually 24 h (see Section 3.7.2.2), while bacterial fermentation is around 24 h and fungal fermentation takes 24-72 h (see later in this chapter). If the technological solution for the fermentative biomass-to-chemicals production would strictly contain consecutive steps, the overall production time will be several days, possibly even a week, thus lowering volumetric productivity. Furthermore, overlapping processes have the additional advantage that they will result in longer reaction times for the subprocesses

in general: in case of separate 24 h hydrolysis and fermentation the overall reaction time is, e.g., 48 h, but if the processes are completely overlapped, keeping the processing time constant, both hydrolysis and fermentation have 48 h of reaction time. Longer reaction time means that for the same conversion lower starting concentrations of catalyst (e.g., enzyme or inoculum) can be used, not considering possible counteractions. This is important since enzymes contribute to the process costs significantly.

The factors determining the success of the simultaneous process are the possible interactions between the discussed process steps and the tolerance to the altered consensus environmental conditions. Processes will have different optimal parameters (temperature and pH in case of hydrolysis and fermentation, aeration in case of laccase detoxification and fermentation), while in a simultaneous process, there can be only one single value for every environmental parameter at a given moment, which means that at least one process does not have optimal parameters.

In the upcoming sections the current state of art on simultaneous processes, both for ethanol and lactic acid fermentations will be discussed. In both of these two processes, saccharification and detoxification are in common as both use the same carbohydrates as substrate for subsequent fermentation. This means SSD is technically the same in both cases, not taking the different strain's inhibitor resistance in to account. As we will see in Section 0, the required economical substrate loading is also identical, which means the reactor setup (stirring, viscosity details) will also be the same. SSF, SFD and SSFD will differ; however, there is also a significant difference when different microorganisms producing the same product are applied as both fungi and bacteria strains are known for both ethanol and lactic acid fermentations. The general remarks apply for both possible fermentations.

5.1.1 Simultaneous saccharification and detoxification

Reported SSD results with laccase detoxification are somewhat controversial. Generally low redox potential (mainly bacterial) laccases are beneficial or neutral to hydrolysis, while high redox potential laccases (mainly fungal) are neutral or negative to hydrolysis [158]. This was explained by the fact that only those phenolics that are oxidized by high redox laccases are prone to undergo radical propagation, which will lead to some of the phenolics attaching to the solid lignin matrix, increasing lignin content of the solid phase, thus hindering hydrolysis. It has to be noted that

publications about SSD with bacterial laccases are very recent, typically from the last three years.

Steam exploded wheat straw was detoxified by bacterial laccase from *Streptomyces ipomoeae* [153]. Treatment was performed at pH 8 and 50 °C for 24 h. In comparison, a treatment with *Trametes villosa* laccase was performed at pH 4 and 30 °C for 24 h. Experiments were conducted with the solid fraction after steam explosion separated from XRF, suspended in buffer. Saccharification experiments showed that bacterial laccase treatment did not interfere with subsequent hydrolysis of pretreated wheat straw, while fungal laccase treatment decreased both glucose and xylose recovery by 6-7 %.

Recently a laccase-like enzyme was isolated from the bacterium *Thermobifida fusca*, named Tfu1114. It is capable to oxidize phenolics; however, it has no activity on ABTS, a standard substrate for laccases. The structure is rather unusual, as it contains only one copper ion instead of the standard four. It was also shown that it enhances hydrolysis two folds when it was added to a designer cellulosome, i.e., resulting in a multienzyme complex containing cellulases, hemicellulases as well as laccase. These kinds of complexes increase efficiency due to the proximity of synergistically acting enzymes [213].

5.1.2 Simultaneous saccharification and fermentation

SSF was first mentioned in a patent from 1976 [147]. From all discussed overlapping processes, it is considered to be the best method to overcome cellulase end product inhibition [147], [158]. According to some calculations it can also decrease the CAPEX value by 20 % [147]. The fermentation will be less prone to contaminations compared to separate processes as glucose, the main substrate for most microbial strains, is almost immediately consumed and the product is formed [145]. Of course, to contaminations consuming the fermentation product, ethanol or lactic acid, the system will still be sensitive.

Around 40 g/l of ethanol titer was reported on steam exploded woody type of biomass (spruce, poplar) at high solid loading (around 10 % dry content) with *S. cerevisiae* [147]. Ohgren et al. compared separate saccharification and fermentation (Separate hydrolysis and fermentation, SHF) with SSF on steam pretreated corn stover at 8 % solid loading with adapted *S. cerevisiae* microorganism, and found that even SSF with undetoxified hydrolyzate gave higher titers than SHF with detoxified hydrolyzate [214].

Lactic acid production via the SSF method is also studied, but to a much lesser extent than bioethanol production. Alfalfa (grass type), rice bran, cassava bagasse were used as substrates, reaching 28-83 g/l final lactic acid titer [59]. Industrially relevant titers in case of lactic acid are above 100 g/l [71]. Lactic acid SSF fermentations performed on steam exploded corn stover at extremely high solid loading (30 %) were reported with 101 g/l titer and 77 % yield, which values reach the industrially relevant regime [215].

Although the beneficial effects of laccase treatment prior to fermentation are thoroughly researched [158], up to our knowledge simultaneous fermentation and detoxification (SFD) is not reported in literature. Strictly saying, this is the process where hydrolysis is done separately, thereafter the solid is removed and the liquid is inoculated at the same time as laccase is added to the solution. SSFD, where all three processes are overlapped is much more frequently studied (see later Section 5.1.3). The reason is most probably that the benefits of SFD are minor, i.e., it does not help to overcome cellulase product inhibition and solid separation will still be necessary, although it can give insights on laccase reaction and microorganism interactions when compared to SSFD.

5.1.3 Simultaneous saccharification, fermentation and detoxification

Moreno et al. published several articles about laccase application in SSF experiments, however all of them on wheat straw substrate. *S. cerevisiae* bioethanol production in SSF experiments with steam exploded wheat straw (7 % dry content) subjected prior to *P. cinnabarinus* laccase treatment showed slower glucose formation in the first 6 hours compared to the control without laccase pretreatment. However, glucose concentration started decreasing right after inoculation, compared to control where glucose concentration only started decreasing after 48 h. After 72 h, all free glucose was consumed and the experiments with laccase treatment showed 30 % higher ethanol titer [156]. The same experiments, i.e. *S. cerevisiae* SSF with steam exploded wheat straw subjected prior to *P. cinnabarinus* laccase treatment, but at high substrate loading (17, 20, 25 % dry content), showed that the positive effect of laccase treatment was more significant with increasing solid loading [175]. SSFD experiments performed with *S. cerevisiae* on steam exploded wheat straw at 16 % solid loading showed three times higher ethanol titer (30 g/l) after 168 h compared to the control SSF without laccase treatment. *P. cinnabarinus* laccase was added 21 h after inoculation. The

fermentation time was long (7 days) [216]. SSFD experiments performed with *Kluyveromyces marxianus* CECT 10875 on steam exploded wheat straw at 10 % solid loading were performed with bacterial laccase (Company B). After a laccase treatment of 16-24 h the cellulase was added, and inoculated at the same time or after 8 h. All experiments with laccase showed a reduced lag phase and equal or higher sugar recovery compared to control samples without added laccase [157]. SSFD experiments conducted with added bacterial laccase from *Streptomyces ipomoeae* or added fungal laccase from *Trametes villosa* on steam exploded wheat straw showed that the final ethanol yields were comparable for both laccases. Laccase treatment caused a slightly faster glucose consumption compared to the control experiment. However, the used dry content (6 %) is far from that of the optimum for industrialization (15 %) [153].

5.1.4 Adaptation of the inoculum

Adaptation is not a classic overlapping process, as the prior mentioned examples are, however it can be treated as one if the process is investigated more detailed than the simplified pretreatment/hydrolysis/fermentation/downstream scheme. The fermenting microorganism inoculation culture is usually prepared in synthetic growth medium prior to fermentation and added to the hydrolyzate when fermentation starts. Thereafter the microorganisms go through an adaptation phase (lag phase), during which time minor growth and product formation are visible; this lag phase is expected to be the reason for lower overall volumetric productivities during hydrolyzate fermentation [86]. If adaptation occurs during inoculum preparation, i.e., inoculum preparation and adaptation overlapped, it will lead to a shorter fermentation time and higher volumetric productivities during fermentation. Even if the overall time of inoculum preparation and fermentation would not be shortened, there would still be a benefit, as the inoculum preparation is usually done in around 5-10 times lower volume and often simpler reactor design than the final fermentation vessel, a less expensive equipment would be occupied for the adaptation time.

The technique for adaptation is the addition of toxic hydrolyzate or toxic compounds present in the hydrolyzate to the inoculation medium, in one-step, multistep or continuous addition. Adaptation of *S. cerevisiae* was shown to be important in SSF experiments by Nielsen et al. [217]. The adapted inoculum resulted in higher fermentation rates in hydrolyzate than the unadopted parent. This was partly due to the faster conversion of HMF by the adapted yeast. Keller et al. [218] also demonstrated that *S. cerevisiae* D5A and K-1 strains could adapt and grow in Douglas fir acid hydrolyzate (15 % solids) with a reduced lag phase.

5.2 Problem statement and goal

This chapter describes the possibility of overlapping different process steps. Methods and setups to handle viscous liquids at lab scale, which are rarely reported in literature, are introduced. In addition, a low-cost, lab-scale inoculum adaptation method is described. As the ultimate goal of detoxification is to increase efficiency of consecutive fermentations (titer, volumetric productivity, and carbon yield), test fermentations were performed with untreated, detoxified and synthetic medium with different microorganisms, i.e., *Saccharomyces cerevisiae*, *Scheffersomyces stipitis* and different *Lactobacillus species*. Based on the initial experiments general conclusions are drawn and possible directions for future research discussed.

5.3 Initial test fermentations

A few experiments were performed to have an approximate idea about the effect of the inhibitors in the XRF on the growth of *S. cerevisiae* and *S. stipitis*, as well as the effect of laccase detoxification on the subsequent fermentation.

5.3.1 Methods

Effect of inhibitors

Water bath fermentation experiments were performed with *Scheffersomyces stipitis* CBS 5773. The inoculum medium was yeast extract-peptone-dextrose (YPD) (20 g/l dextrose, 20 g/l peptone, 10 g/l yeast extract, Sigma-Aldrich Corporation, St. Louis, MO, USA). A 100 ml Erlenmeyer flask, containing 25 ml YPD medium was inoculated with two loopful amounts of the defrosted stock culture. The Erlenmeyer flasks were incubated in a shaking water bath (150 rpm, Julabo SW22, Seelbach, Germany) at 33 °C for 48 h.

Synthetic fermentation medium was YPD with 20 g/l added xylose. XRF from the SE0 batch was supplemented with the nutrients yeast extract and peptone, in the same concentration as in YPD media, and supplemented with an additional 20 g/l xylose. Inoculation concentration was 10 v/v%. After homogenization, one ml inoculated fermentation medium was added in each sterilized tube and was placed in the water bath at 30 °C, pH 5. After sampling, the tube was discarded. Because of the high surface/volume ratio, this method is not meant to measure volatile compounds (ethanol), but sugars and cell count can be measured with low standard deviations, as

they are not volatile. Samples were drawn at regular time intervals and analyzed by plating.

Plating was done as follows: sample preparation was performed in a sterile manner. Eppendorf tubes were prepared in advance, containing 900 µl of YPD, and stored in the fridge at 4 °C. Dilution cycles were performed by adding 100 µl of the sample into the Eppendorfs. The liquid was homogenized, and 100 µl from this broth was used further for the next dilution. Each dilution cycle meant ten times reduction in the cell count in the sample. 50 µl of properly diluted sample was spread on a Petri dish and put in an incubator at 30 °C for two days, and then colonies were counted.

Bioreactor experiments were carried out in a 2 l BioFlo 110 Fermenter and a 7.5 l BioFlo/Celligen 115 Fermenter (New Brunswick, New Jersey, USA), see Figure 5-1. Bioreactor experiments are performed under more controlled conditions than water bath experiments, but they require more material and invested time for a single run and it is difficult to run parallel experiments, as the inoculum will be different for every run.

The preparations of the bioreactors were done as follows: 1 M sodium hydroxide, 1 M sulfuric acid solution and tubes used for sampling were prepared and autoclaved. The oxygen electrode was inserted in the reactor. Every inlet, outlet and necessary tubes of the bioreactors were sealed adequately with silicone tubes and clips, except one for pressure release during sterilization. Filters were covered by aluminum foil before sterilization in the autoclave. YPD medium was poured in the reactor before sterilization. XRF was poured into the autoclaved reactor after sterile filtration. Autoclaving was performed for 60 min at 121 °C.

After all sterile medium compounds were in the fermenter, the control unit was switched on. The pH electrode was calibrated. Temperature, stirring (150 rpm), pH control and aeration were left to stabilize overnight. The oxygen electrode was calibrated shortly before the start of the experiment. Hereto, the electrode connection was detached to set zero and attached again to set 100 %, as the liquid was saturated with oxygen after overnight aeration. For fermentation thereafter, the aeration was switched off at the start of the experiment. Sterilized antifoam (Antifoam 204, Sigma-Aldrich Corporation, St. Louis, MO, USA) was added (0.9 ml/l) to each bioreactor to avoid foam formation. After everything was set, the prepared inoculum was added in a sterile manner at 1 v/v% inoculation concentration and the experiment was started. Samples were withdrawn in a sterile way with an attached 50 ml syringe.

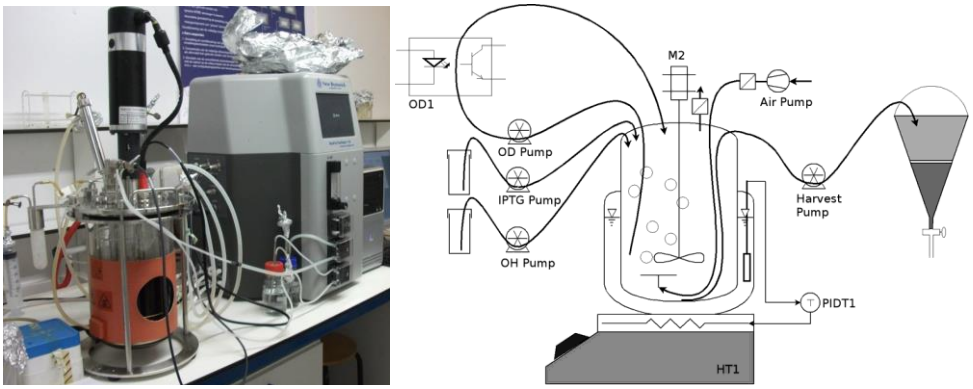

Figure 5-1: Bioreactor picture (left) and an example schema (right) used for some of the liquid fermentations.

Effect of laccase detoxification

The laccase treatment effect was investigated with *Saccharomyces cerevisiae* MUCL 49179 fermentations in a bioreactor as described in this section earlier. The medium was the same as described in the previous paragraph (YPD), but without added xylose. Laccase treatment was performed by adding 1 g *T. versicolor* laccase per liter 24 h prior to the inoculation of the reactor with 1 v/v% inoculum. Samples were taken regularly, analyzed for cell count and inhibitor concentration with HPLC-UV analysis, as described in Section 3.3.

Growth data obtained from experiments with undetoxified and laccase treated hydrolyzates were simulated with the Baranyi-Roberts equation (Equation 5-1 and 5-2 [219]) and the fitted μ_{max} parameters were compared. Lag time (t_{lag}) was calculated based on the formula Equation 5-3. All data processing was performed off-line using a commercial software package (MATLAB 2017.1, The MathWorks Inc., Natick, MA, 2017).

$$\frac{d\ln N(t)}{dt} = \mu_{max}\frac{Q(t)}{1+Q(t)}1 - e^{\ln N(t) - \ln N_{max}} \quad \textbf{5-1}$$

$$\frac{dQ(t)}{dt} = \mu_{max}Q(t) \quad \textbf{5-2}$$

$$t_{lag} = \frac{1}{\mu_{max}} \ln\left(1 + \frac{1}{Q(0)}\right) \quad \textbf{5-3}$$

where N is the cell count, μ_{max} the maximum specific growth rate, N_{max} the maximum cell concentration and Q the physiological state of the cells at time *t*.

5.3.2 Results and discussion

Effect of inhibitors

Preliminary experiments with *Scheffersomyces* XRF fermentation showed high inhibition compared to the control fermentation with synthetic medium (see Figure 5-2). Bioreactor experiments with 1 % inoculum showed inhibition of growth (lag phase) for over 24 hours after a short 3 h initial growth phase, while the control fermentation was growing after a one-hour lag phase and reached a stationary growth phase at 15-16 ln (CFU/ml) in about 10 hours. As it has often been referred to in literature, higher inoculum concentrations usually increase the cell recalcitrance towards toxic effects [220], so fermentations were carried out with a 10 % inoculum in a shaking water bath. It can be seen that the control experiment reached a maximum in about 7 hours, with about tenfold higher cell count than with a lower inoculum in the bioreactor. On the other hand, the XRF water bath fermentations by that time went through a 150-thousand-fold decrease in cell concentration, and the lag phase lasted until at least 24 hours. In this case, it was visible that the XRF was highly inhibiting to *S. stipitis* in both water bath and reactor experiments.

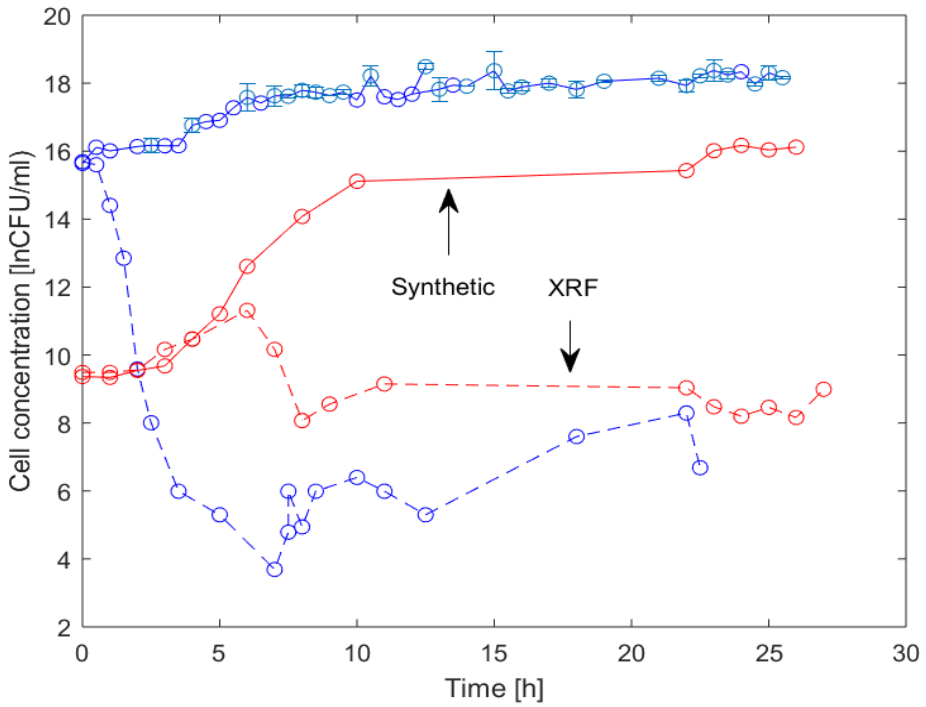

Figure 5-2: Inhibition effect of XRF on *Scheffersomyces stipitis* fermentation in water bath (—) or bioreactor fermentation (—). Full lines represent synthetic media, dashed lines XRF media.

Effect of laccase detoxification

The comparison of *Saccharomyces cerevisiae* bioreactor fermentation on untreated and laccase treated hydrolyzate (see Figure 5-3) showed that the laccase treatment removed part of the phenolics, 30 % according to the measurements (see phenolics on Figure 5-3A and B), and the concentration did not change significantly during the fermentations. The measurements were done after nutrition addition, which contains proteins that interfere with the measurements, so the removal was most probably higher. The changes of phenolic content during the fermentation are small and can be caused either by measurement errors or by the metabolism of the microorganisms, as it is known that they can reduce phenolic aldehydes to alcohols but not metabolize them further [221]. HMF and furfural were consumed faster from the laccase treated medium than from the control untreated hydrolyzate. Furfural is always metabolized before HMF. Furfural conversion starts at the same time as the growth, while HMF conversion starts when furfural concentration is nearly zero.

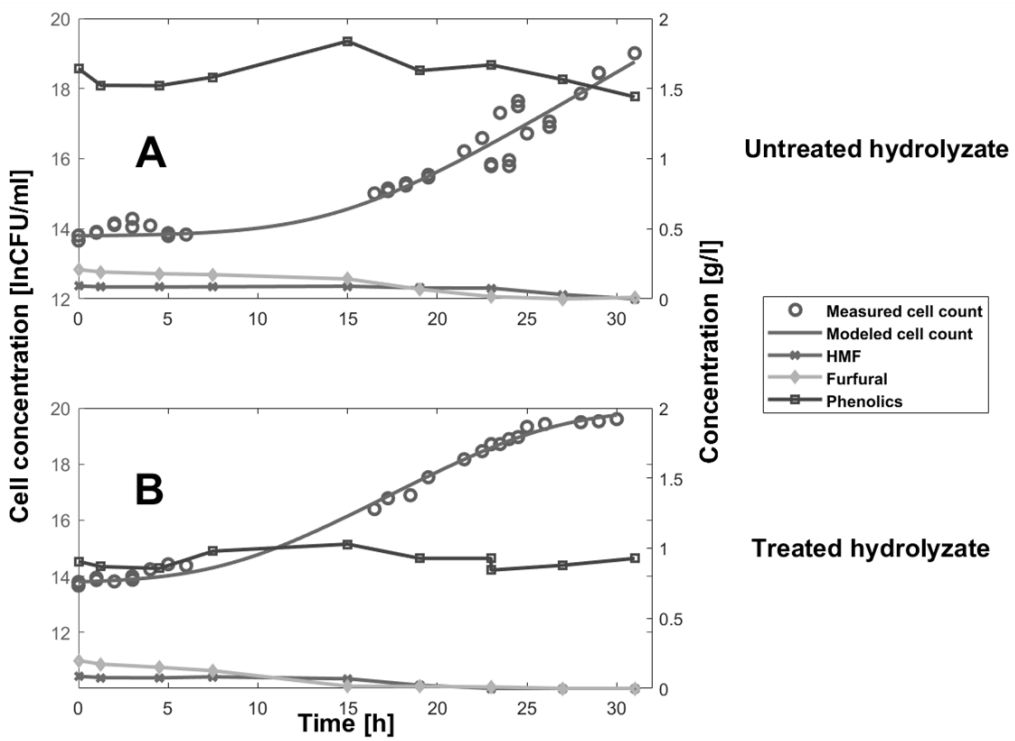

Figure 5-3: Inhibition effect of (A) untreated and (B) laccase detoxified XRF on *Saccharomyces cerevisiae* fermentation. (x) Marks HMF, (◊) furfural, (□) phenolics concentration, (o) the measured cell concentrations, while (—) the modeled cell concentrations.

Precise conclusions about the lag phase cannot be drawn as points are missing from the relevant phase, but seemingly the yeast started to grow after a short lag phase of 5 h on laccase treated hydrolyzate (see Figure 5-3B), compared to a lag phase of 10 h in case of no laccase pretreatment (see Figure 5-3A). This is in agreement with before reported literature for a variety of microbial strains and laccase detoxification [221]. After 10 h of lag phase, the strain seems to be adapted to the untreated hydrolyzate and shows the same performance in growth and furan removal. After modeling, the difference in the estimated maximum specific growth rate, μ_{max} was, not significant (0.300±0.038 h^{-1} and 0.348±0.023 h^{-1} for growth curves from untreated and treated hydrolyzate respectively). However, it has to be noted that *Saccharomyces cerevisiae* is known to be one of the most robust microorganisms in fermentation technology, thus it is expected that the difference between the untreated and treated media will be greater in case of other strains [222].

5.4 Inoculum adaptation

Hereby a low-cost set-up was constructed for an automated fed-batch inoculum adaptation to the compounds in the XRF hydrolyzate. The system is discussed in detail in Appendix. Adaptation was performed with untreated XRF and active coal treated hydrolyzate from the XRF of SE0 batch with *Lactobacillus pentosus* LMG 9210 strain.

5.4.1 Methods

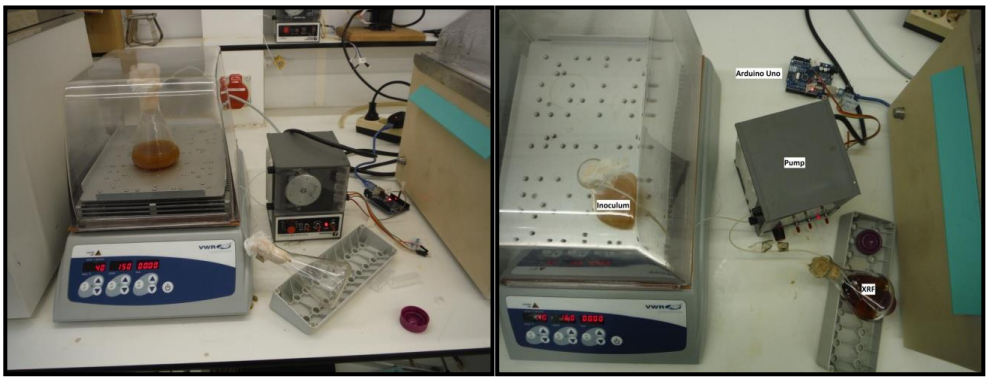

Figure 5-4: Setup used for inoculum adaptation from front- (left) and top-view (left). The inoculum is incubated in a shaking incubator, while an Arduino controlled pump adds XRF stepwise according to the time profile.

The growth medium was 50 ml of premixed standard De Man, Rogosa and Sharpe medium (MRS) (BIOKAR diagnostics, Solabia group, Pantin, France) diluted with demineralized water. After adding 10 g/l $CaCO_3$ the medium was sterilized at 121°C for 20 minutes. It was inoculated with 50 µl stock culture and incubated at 37°C and 150 rpm in a shaking incubator for 24 h (Incubating Mini Shaker, VWR International, Radnor, PA, USA).

Adaptation inoculum preparation

Two XRF fractions (30 ml, to make sure that 25 ml liquid will be available) were supplemented with 30 g/l glucose but no nitrogen sources. Charcoal detoxification was carried out on one of the fractions by adding 4 m/v% of charcoal (C303 type, Desotec, Roeselare, Belgium) and shaking for 30 minutes. Afterwards, charcoal was filtered from the hydrolyzate with a Buchner funnel. The composition of the two fractions is presented in Table 5-1. 25 ml of both untreated and charcoal treated XRF were sterile

filtered in a pre-sterilized Erlenmeyer and sealed with a cotton plug (see Figure 5-4). The tubes of the peristaltic pump (Pharmacia LKB pump P-1, Stockholm, Sweden) were sterilized, assembled and one side inserted in the XRF-containing lombic outside of the shaker (see Figure 5-4), so that the end of the tube is at the lowest point of the Erlenmeyer under the liquid, thus XRF liquid will be completely pumped out.

50 ml premixed standard MRS (BIOKAR diagnostics, Solabia group, Pantin, France) growth medium was prepared with demineralized water. After adding 10 g/l $CaCO_3$ the medium was sterilized at 121°C for 20 minutes. It was inoculated with 50 µl stock culture, mixed and separated to two 25 ml portions in two sterile lombics with a sterile pipette. The other side of the tube from the peristaltic pump was inserted in the inoculum containing Erlenmeyer, so that the end of the tubing does not touch the wall of the beaker or the liquid surface (the tube is used to add the XRF to the inoculation medium). Prior to the start of the experiment, the tubes were filled completely with XRF (by manually controlling the pump). The inoculum containing lombic was placed in a shaking incubator (Incubating Mini Shaker, VWR INTERNATIONAL, RADNOR, PA, USA) at 37 °C and 150 rpm and the timer started.

The XRF addition to the inoculum was started 5.25 h after inoculation and finished at 24 h, increasing the XRF content (measured in v/v%) linearly in 30 min steps so the final XRF content of the inoculation medium will be 33 % (see Section Appendix for details). The whole inoculum preparation was finished after 72 h.

Table 5-1: Composition of XRF from SE0 batch used for adaptation.

Hydrolyzate	Glucose (g/l)	Xylose (g/l)	HMF (g/l)	Furfural (g/l)	Phenolics (g/l_{syr})
Untreated	29.6	4.8	0.10	0.10	0.55
Charcoal	26.3	4.2	0.00	0.00	0.05

Subsequent fermentation

For the subsequent fermentation experiments five ml of the adapted inoculum was centrifuged and the pellet suspended in 50 ml untreated XRF with 30 g/l glucose added. The broth was placed under the same conditions as the inoculum (37 °C and 150 rpm). Samples were taken regularly and analyzed for sugars and products.

5.4.2 Results and discussion

As expected, the addition of XRF slowed down the glucose consumption significantly (see Figure 5-5A). The pump started the addition after 5.25 h, at the moment when the growth is still in log phase. Later addition at the exponential phase could have been more favorable, as higher cell concentration usually causes faster adaptation. In general, charcoal treated hydrolyzate showed less inhibition compared to untreated, but neither of them depleted the glucose before the 72 h cycle ended. The standard inoculum followed a sigmoid curve and reached full-grown state before 48 h.

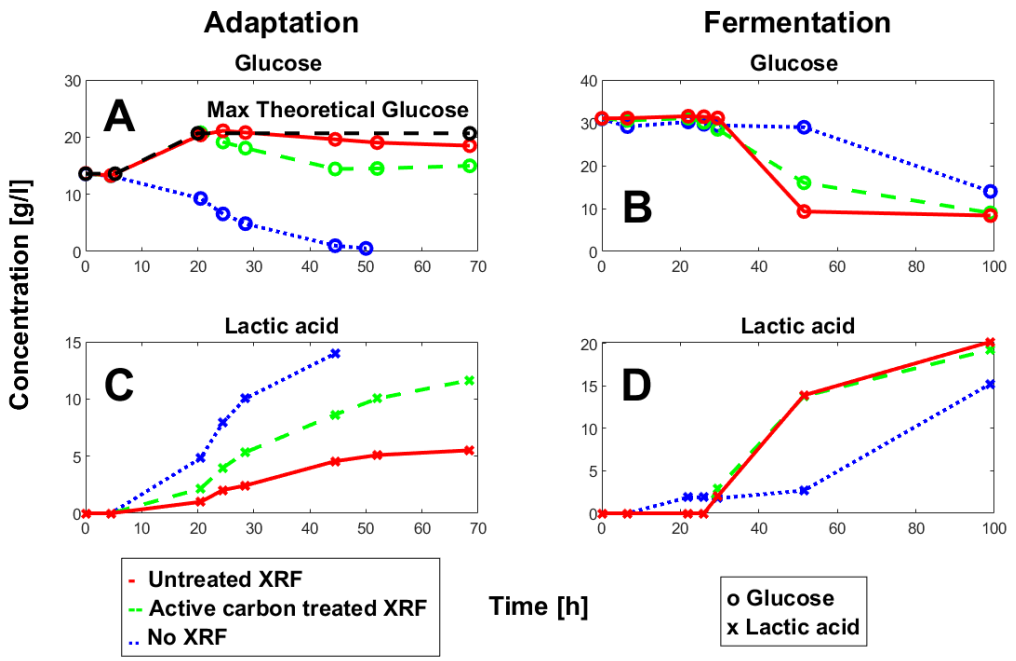

Figure 5-5: Comparison of (o) glucose and (x) lactic acid concentration evolution during (A, B) inoculum adaptation with (--) active carbon treated, (—) untreated XRF and (..) the reference cell growth in MRS medium, followed by subsequent (C, D) XRF fermentation.

The subsequent fermentation also showed interesting results (see Figure 5-5B). Since not all glucose was fermented, but 5 ml of inoculum was centrifuged for all three experiments, it can be suspected that the cell count in the adapted inocula was significantly lower than that of the standard inoculum, which is in good correspondence with published results with *S. cerevisiae* in SSF [217]. However, both adapted inocula performed better than the unadopted inoculum; visibly shorter lag

and higher ending product concentration, as it was published with *S. cerevisiae* in SSF co-fermentation [217]. This trial showed the viability of this simple adaptation method for XRF fermentation by the *Lactobacillus pentosus* strain, thus it was further optimized and used for experiments. The additional gain for this kind of adaptation is that it is fully automated, thus can be left for the weekend, and when the fermentation experiments start on Monday, the inoculum will be adapted and ready to use.

5.5 Simultaneous fermentation and detoxification

The main advantage of simultaneous fermentation and detoxification process integration would be the treatment time reduction compared to the separate processes. The goal of this experiment is to investigate the effect of detoxification reaction during fermentation, as no report was found about it in literature. Possibly, interactions that can occur are that the microorganisms can alter the phenolics, e.g. by oxidation or reduction, leading to a modified V_{max} and K_M values of the laccase reaction [221], the formed metabolites (fermentation products, furan metabolites etc.) can alter the enzyme functionalities, or the products formed by laccase reaction can interfere with the microbial growth.

5.5.1 Methods

Fermentation experiments were performed with *Scheffersomyces stipitis* in a water bath as described in Section 5.3.1. XRF (SE0 batch) was supplemented with 20 g/l glucose, 20 g/l xylose and nutrients, in the same concentration as in YPD medium and 1 g/l of *T. versicolor* Sigma laccase was added at the same time. The temperature was set to 30 °C, the pH was 5 and 150 rpm was applied. Three different inoculum concentrations were tested and the cell count was followed up in time. The control fermentations were performed at the same conditions and in the same medium, but without added laccase.

5.5.2 Results and discussion

In Figure 5-6, the curves show that without laccase treatment a lag phase/cell deactivation occurs immediately after inoculation. The effect is more severe at the lowest inoculum concentration, no growth was visible even after 24 h. For experiments with laccase addition all three inoculum sizes: 15; 13 and 11 ln(CFU/ml) went through a sharper deactivation, around 100-150 fold cell concentration decrease, than in case of untreated samples, lasting approximately 5-10 h, which agrees with the laccase reaction reaching stable phenolic concentrations (see Section 3.7.1.2). The cell

concentration starts to increase immediately after this initial deactivation, with higher growth rate than in the untreated hydrolyzate, except for the highest inoculum concentration where the growth rate is approximately the same for both laccase treated and untreated hydrolyzate. The faster cell growth is expected, as this is a known effect of detoxification. The initial inactivation can be explained by the fact that laccase induces radical formation which can be lethal to the cells.

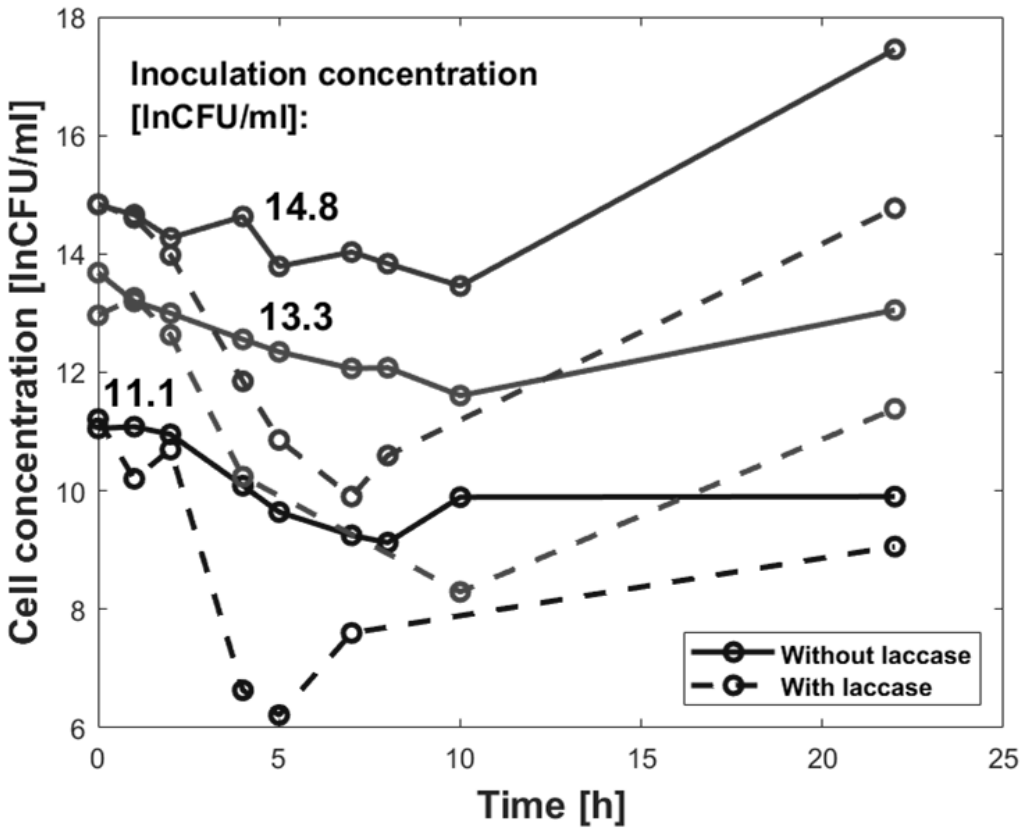

Figure 5-6: Simultaneous fermentation and detoxification (SFD) with *S. stipitis* and Sigma *Trametes versicolor* laccase on XRF, at three different inoculation concentration. Measured cell concentrations (--) with laccase treatment and (—) without added laccase.

There can be a difference between low and high redox potential laccases (bacterial versus fungal) as a recent publication explains [158], outside of the fact that higher redox laccase will cause more reactions through the detoxification process it also generates radicals with higher radical propagation potential, which might be more lethal to microorganisms. As a conclusion, it can be stated that starting the

fermentation together with laccase treatment at exactly the same time is not encouraged; detoxification should start a few hours prior to the inoculation, using the parameters used in this experiment about 5-7 hours earlier.

5.6 Simultaneous saccharification and detoxification

The main advantage of the simultaneous saccharification and detoxification process integration would be the treatment time reduction compared to separate processes and, possibly, higher yields, because, next to the fermenting microorganism, the phenolics can inhibit the cellulase enzyme too [103]. The goal of this experiment is to investigate the effect of detoxification reaction to simultaneous hydrolysis.

5.6.1 Methods

The solid fraction, containing lignin and (hemi)cellulose, and the liquid fraction, containing mainly xylose and inhibitors of the steam exploded (SE0) poplar were used in these experiments. 42.55 g of SF (corresponding to 15 % dry content in the final reaction mixture) was placed in a 500 ml Erlenmeyer flask. 1.5 m/m% of free bacterial laccase, 3.75 m/m% decanted m-CLEAs from bacterial laccase and/or 1.5 m/m% cellulases, Multifect (55 FPU/ml) or Optimase (60 FPU/ml) from Genencor (DuPont, Wilmington, DE, USA), were added to the solids according to Table 5-2. The Erlenmeyer was filled with XRF or distilled water until 130 g. The lombic was placed in a water shaker bath at 50 °C and 150 rpm. Nine experiments were performed in triplicates.

Table 5-2: Summary of all the SSD experiments.

Exp no.	Liquid	Starting pH [-	Cellulase	Laccase
A1	XRF	5	Multifect CX	-
A2	XRF	5	Multifect CX	free
A3	XRF	8	Multifect CX	free
B1	water	6.76	-	free
B2	water	6.76	Optimase CX	-
B3	water	6.76	Optimase CX	free
C1	water	6.76	Optimase CX	m-CLEAs
C2	water	6.76	Optimase CX	free + m-CLEAs
C3	water	6.76	Optimase CX	free

5.6.2 Results and discussion

Results are presented on Figure 5-7. Bacterial laccase enhanced hydrolysis in all cases compared to the blank hydrolysis performed with cellulase alone. Compared to blank (A1), additional laccase produced 89 % higher glucose yield at pH 5 (A2), while starting the reaction from pH 8 gave 120 % higher glucose yield (A3). Water, instead of XRF, performed worse (Figure 5-7B), possibly because of the less favorable pH, i.e., 6.76 instead of 5, as the control cellulase hydrolysis (B2) also gave a 22 % lower glucose yield than A1. Laccase supplementation during hydrolysis produced 82 % higher glucose yield (B2), while laccase alone did not produce any free glucose (B1). This proves that, although the laccase helps hydrolysis significantly, it does not have cellulase activity. Experiments with m-CLEAs (Figure 5-7C) showed that adding m-CLEAs caused approximately a 25 % increase in glucose concentration (C1) compared to blank hydrolysis performed with cellulase alone (B2). Addition of bacterial laccase (C3) gave 62 % higher yield compared to the control (B2) and 29 % compared to addition of m-CLEAs (C1), while the two together (C2) gave 114 % higher yield compared to the control (B2) and 72 % higher than m-CLEAs alone (C1). B3 and C3 were the only two completely identical experiments and their results differed by 9 %, which suggests that the reproducibility of the experiments was good (from B3 the last point was discarded). Investigating literature, It has to be noted that hydrolysis increase caused by bacterial laccase was also reported shortly after our research was conducted [157]. Usual reports prior that were about decreased hydrolysis yield with fungal laccases [223].

Comparing results between different pH values, added water (Figure 5-7B-C) and XRF (Figure 5-7A), the control hydrolysis with only added cellulase (A1 and B1) at pH 5 gave 28 % higher final sugar yield than at pH 6.76, which is expected as pH 5 is more favorable to cellulase. Hydrolysis experiments with free laccase addition (A2 and B3) resulted in a 31 % lower glucose yield at pH 6.76, which is approximately the same difference than the 28 % between the two control hydrolysis experiments with cellulose alone (A1 and B1). In Figure 5-7C, combined free and m-CLEA laccase (C2) gave 114 % higher sugar concentration than the control hydrolysis (B2). When comparing the B3 experiment with free laccase addition and C1 with only m-CLEAs added with respect to the control (B2), respectively 68 % and 24 % increase in sugar concentration was obtained. This shows that the effect of both laccases can be synergistic, i.e., 68 +29 = 97 %, which is lower than the 114 % glucose concentration

increase in case of C2 when both are added together compared to control with cellulase only (B2). However, the addition of equal organic contents resulted in a 24 % increase by m-CLEAs, which is 39-35 % of the glucose concentration increase of hydrolysis with added free laccase (61 and 68 % increase). This value could be considered the deactivation during immobilization. In literature deactivation values are reported over a wide range, for example laccase immobilized on magnetic mesoporous carbon was reported to maintain 20-90 % of the relative activity depending on the parameters [200]. However, it must be emphasized that the measured deactivation via hydrolysis enhancement is not only caused by lower enzyme activity due to the immobilization (deactivation, wrong orientation etc.) but also diffusion limitations and activity decrease due to contact limitations between enzyme and substrate, etc.

Generally, it can be concluded that bacterial laccase enhances hydrolysis, which is beneficial to costs, as technically part of the enzyme used for hydrolysis can be substituted with another enzyme that detoxifies for the subsequent fermentation in the meanwhile.

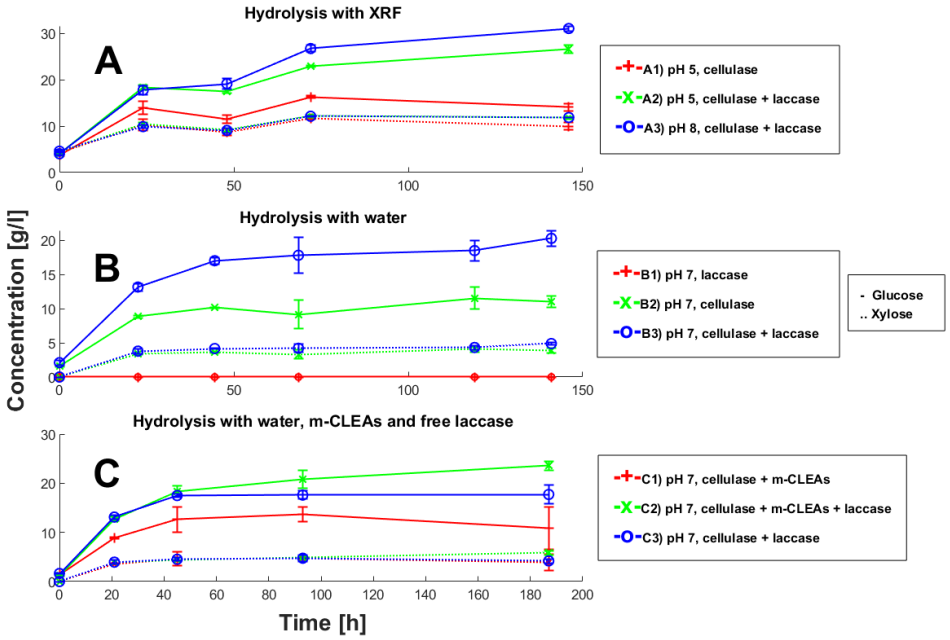

Figure 5-7: (—) Glucose and (..) xylose concentration evolution during SSD experiments with free or m-CLEAs laccase, in (A, B, C) three different triplicate combinations. Markers represent different experiments Error bars are ±standard deviation from three measurements.

5.7 Simultaneous saccharification and fermentation

SSF is the standard, well-documented technique for process integration in lignocellulose based fermentative chemical production [44], [147]. The main gain is unquestionably in avoiding end-product inhibition of cellulase via carbohydrate consumption by the simultaneous conversion in the microorganism's metabolism. Other benefits are shortened processing time compared to separate processes, simpler configuration (closer to one pot design) and some articles even claim that the process is more resistant to contamination due to the low glucose concentration throughout the process [44]. The goal of this section is to get to know the SSF system better, as it will be further improved in Section 5.8.

5.7.1 Growth temperature

One of the big challenges about SSF is choosing a consensus temperature. The enzyme usually has a higher optimal working temperature, than most of the microorganisms [147]. Cellulase activity usually decreases drastically at lower temperature. That is why attention was shifted towards fermentation by thermophilic yeasts [95] or bacteria [64]. The goal of this section is to investigate the maximal growth temperature (the maximum temperature when the microorganism is still growing) of *Lactobacillus pentosus* LMG 9210, used later in Section 5.8.

5.7.1.1 Methods

Experiments were performed on MRS growth medium; in the same way as the inoculation culture was prepared (described in Section 5.4.1). Three different growth temperatures were investigated, i.e., 37 °C, 45 °C and 50 °C. Shake flasks were placed in a shaking incubator at 150 rpm. Samples were taken at 24 h after inoculation. Relative concentrations of glucose were calculated based on starting glucose HPLC-RI (described in Section 3.3) area peak.

5.7.1.2 Results and discussion

As can be seen on Figure 5-8, during the fermentation at 37°C, all the glucose was consumed and a high amount of lactic acid was produced in 24 h. This is equivalent to almost 80 % of the starting glucose concentration area. At 45 and 50 °C however, no measurable glucose consumption occurred, i.e., *L. pentosus* seems not to grow at these temperatures. Later experiments (not shown) showed that the maximum growth temperature of *L. pentosus* was 42 °C. Therefore, 40 °C was chosen in the

experiments in order to leave a safety range for possible temperature fluctuations caused by non-ideal thermostatisation.

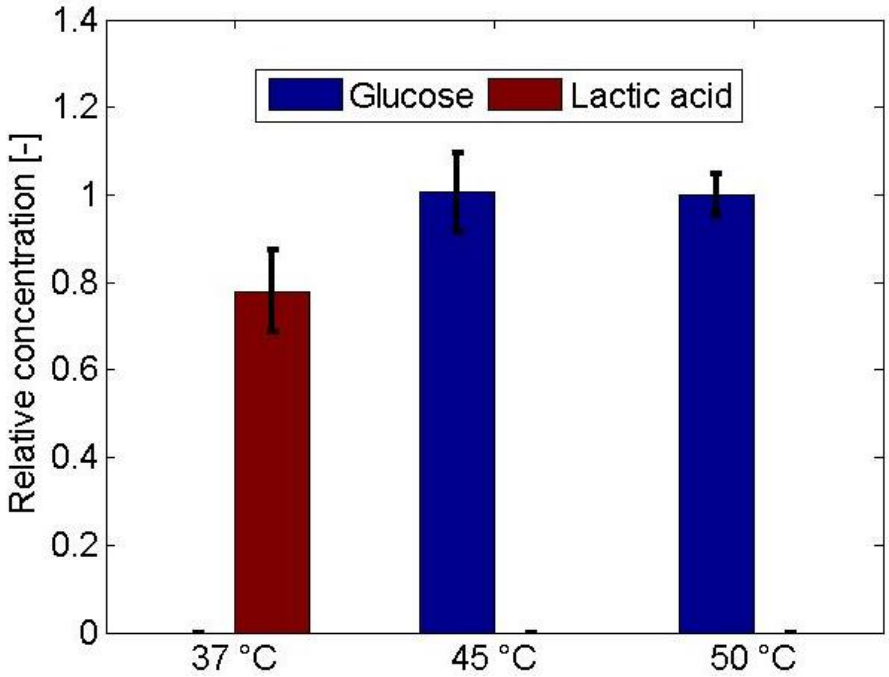

Figure 5-8: *Lactobacillus pentosus* maximum growth experiments at three different temperatures. Error bars are ±standard deviation from three measurements.

5.7.2 SSF experiment

5.7.2.1 Methods

For all lignocellulosic simultaneous saccharification and fermentations performed in this PhD research, the inoculum was adapted to the reactor conditions prior to inoculation, as described Section 5.4. This was done by first inoculating 50 ml of $CaCO_3$ buffered (2 m/v%) MRS medium with 50 µl of *L. pentosus* stock culture. The shake flask was then placed in an incubator at 40 °C and shaken at 120 rpm. After 12 h, the gradual addition of 50 ml of XRF was started with a peristaltic pump, controlled by an Arduino UNO microcontroller, over 36 hours with a linearly increasing XRF ratio in the inoculum (V_{xrf}/V_{total}%). Inoculation preparation was performed altogether for 72 h. The initial volume of MRS medium and the added volume of XRF resulted in a final inoculation volume of 100 ml.

SSF experiments were performed in a two-liter double wall reactor with an overhead stirrer (502D, LH fermentation, UK). The stirrer was modified with two metal bars to stir viscous fluids (see Figure 5-9) and a water bath was used to keep the reactor temperature constant. Sterilization was not applied, as the XRF was proven to be too toxic for most contaminants (no sugar consumption visible after days in a non-sterile environment), and heat treatment would change the composition of both XRF and solid fraction.

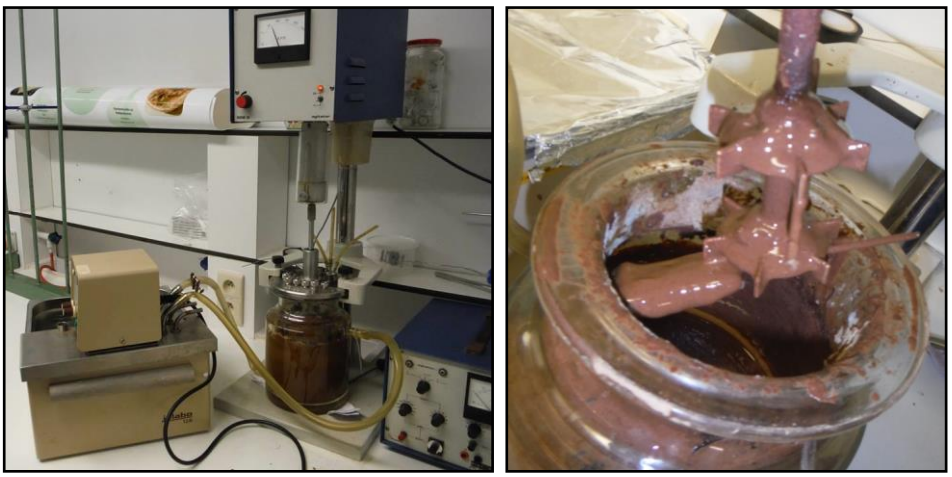

Figure 5-9: Setup used for viscous medium fermentations (left) and the rotor with the attached magnet (right).

400 g SF (200 g dry) of solid fraction and XRF were placed in the reactor. Calcium carbonate, antifoam and the same compounds as in MRS medium were added, except for the glucose. The mixture was then filled up with XRF until 1241.4 g (see Table 5-3). Stirring and temperature control was turned on, and after the temperature was constant, the cellulase added. Inoculation was done by pouring 100 ml of adapted inoculum in the fermenter. Samples were taken regularly and analyzed by HPLC. All together three SSF experiments were done with *L. pentosus*. Due to the extreme conditions of the high solids fermentation, only one experiment provided results. The experiment will be referred to as SSF1.

Samples were taken twice a day. Each time, approximately 20 g of slurry was spooned out and filtered by using a Buchner filter and Wattman No. 1 filter paper. Part of the liquid obtained was used for plating; the remaining part was filtered through a 0.45

µm syringe filter and used for HPLC analysis. The filter cake was used for structural carbohydrate determination (see Section 3.3) after washing three times with demineralized water and drying.

Table 5-3: Composition of starting broth in SSF1 experiment.

SSF1	General percentage [%]	Mass [g]
Solid dry (SF)	15.8	200
CaCO3	1.58	26.6
MRS nutrition	3	37.6
Optimase CX15L	2	26.6
Laccase	0	0
Tween80	0.1	1.3
Mass after XRF addition	100	1268

5.7.2.2 Results and discussion

The mixture's viscosity was visually decreasing as the hydrolysis proceeded (see Figure 5-10), with a slight color shift to lighter brown. The viscosity decrease was witnessed before in Section 5.6.2 and Section 3.5. It can be concluded that the special stirring is only necessary in the first 24-48 h. Afterwards, as the fibers break down to particles, a simple Rushton impeller would work.

During the SSF1 experiment, the glucose concentration was steadily rising, except at 30 hours, i.e., immediately after inoculation (see Figure 5-11A). At the moment of inoculation, the substrate concentration decreased as the inoculum was an XRF/water (MRS) mixture and part of the substrate was already consumed by the microorganism, thus diluting the whole broth. The rise that can be observed between 70 and 80 h is not significant as the deviations are in the range of the standard deviation (1-2 g/l). The lactate concentration was different from zero at the start of the experiment and slightly increases after inoculation. The first is unexpected, most probably the added MRS contained a compound with retention time very close to lactic acid. The second is most probably caused by the formed lactic acid product in the inoculum.

Figure 5-10: Mixture consistency after 2 h (left) and 48 h (right) after start of the experiment. Viscosity was not quantified.

The phenolics concentration, as measured by HPLC, decreases slightly (see Figure 5-11B), however there are no measurement data from the first day. The decrease can be caused by several factors: evaporation/oxidation of phenolics in contact with air, pH shift of the fermentation or by laccase reaction. It was obvious that some reaction was ongoing as the color of the mixture shifted from brown to red. However, the total decrease in phenolics concentration is around 10 % or 0.5 g/l with standard deviation of about 5 %. The absorbance increases slightly, around 20 %, but the standard deviations of absorbance measurements are low (see error bars on Figure 5-11B). The increasing UV measurements cannot be explained by increasing furan concentrations, as they were decreasing (see Figure 5-11C). The furfural concentration decreases by time, while HMF is also decreasing slightly most probably because of metabolization by *L. pentosus*. No lactic acid was produced during the experiments. In general, it can be concluded that 96 h is not enough to conduct an efficient lactic acid production by SSF with undetoxified hydrolyzate under the given conditions.

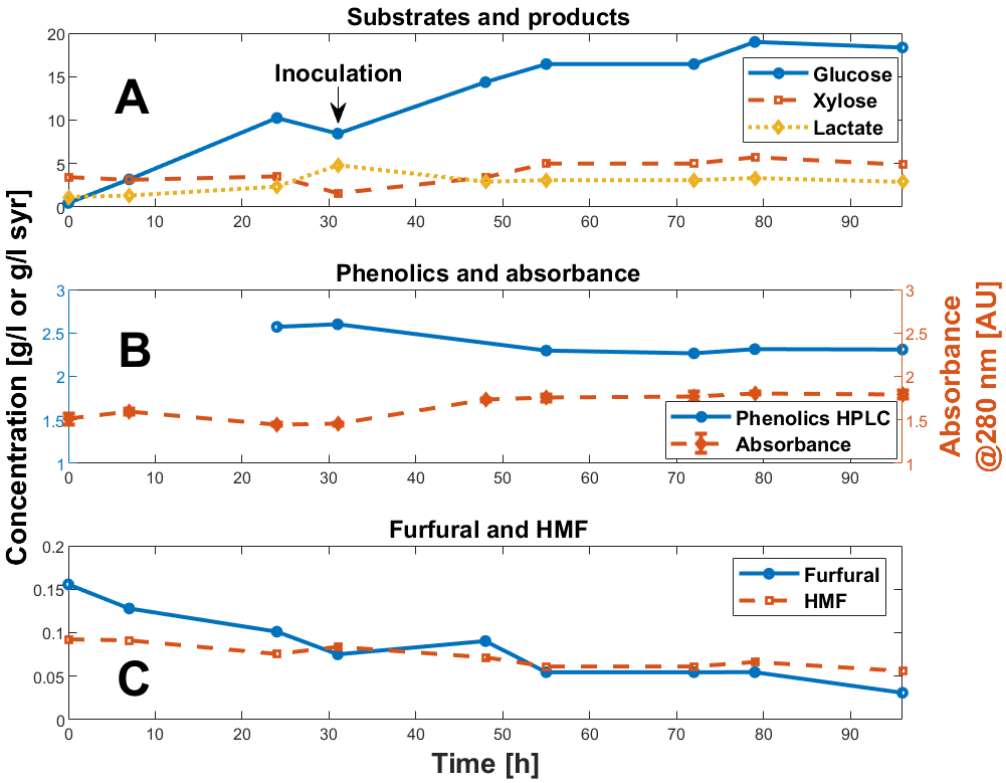

Figure 5-11: Time evolution of (A) substrates, product, (B) phenolics and absorbance and (C) furan concentrations during SSF1 experiment. Different compounds are marked with different lines and markers.

5.8 Simultaneous saccharification, fermentation and detoxification

SSFD experiments are the real interest of the current research as they integrate most of the necessary sub-processes, i.e., hydrolysis, fermentation and detoxification, in a single pot reaction. The consistency of the broth remains the same as in SSF (Section 5.7.2.2), so initial high viscosity stirring is needed. Incorporating the knowledge from previous experiments, the detoxification was started together with the hydrolysis (Section 5.6.2) and inoculation was shifted to avoid cell death due to laccase reaction (Section 5.5.2). The pros and cons discussed in every section all apply for this all in one-pot process too.

5.8.1 Methods

In total, four SSFD experiments were performed. The setup, described in Section 5.7.2.1, was used for all experiments. Inoculum adaptation was also applied for each of the fermentations, as discussed in Section 5.4 and time values were modified as reported in Section 5.7.1.1, namely the addition of XRF starts at 12 h after inoculation and is added linearly for 36 h. The final inoculation volume was 100 ml, corresponding to 7-8 v/m% of the total fermentation broth. Samples were taken regularly, analyzed by HPLC and UV absorbance. For the last experiment, also plate counting was performed. The general composition of the broth at the start of the experiment consisted of 400 g wet SF (15-16 %), 30 g MRS nutrition without glucose, 20 g Optimase CX15L, 1.14 g *C. unicolor* laccase (Company A), 0.8 g antifoam, for exact values see Table 5-4. The experiments differed in their amount of calcium-carbonate added and, in three of the experiments, 6 g active carbon was added (see Table 5-4). *C. unicolor* laccase was used for every detoxification run. It is best to avoid antifoam, as it is known to inhibit gas-liquid mass transfer [224], thus possibly decreasing the laccase regeneration rate through lower dissolved oxygen concentration; however foaming made the addition necessary. The broth was aerated during all experiments, but only until inoculation.

Table 5-4: Composition of all SSFD runs at the beginning of the experiment.

	SSFD1 (¤)	SSFD2	SSFD3	SSFD4 (¤¤)
LAB	*L. pentosus*	*L. pentosus*	*L. pentosus*	*L. amylotrophycus*
SF [g]	401	400	400	400
CaCO3 [g]	40	190	116	121
MRS nutrition [g]	39	32	0	28
Optimase CX15L [g]	20	20	20	20
***C. unicolor* laccase [g]**	1.145	1.14	1.14	1.01
Active carbon [g]	0	6	5.85	6.01
Antifoam [g]	0.8	0.8	0.8	0.8
Mass after XRF addition [g]	1343	1263	1210	1215

(¤) 8 h pre detoxification before hydrolysis

(¤¤) Evaporation loss was corrected with demineralized water

For three of the SSFD experiments *L. pentosus* was used and for the fourth one *Lactobacillus amylotrophycus* DSM 20534. These experiments will be referred to as

SSFD1, SSFD2, SSFD3 and SSFD4. In the fourth run (SSFD4) the reactor was detached from the water pump and placed on a balance to check the weight loss due to evaporation before every sample taking, it was then supplemented with distilled water and homogenized before the actual sample was taken. SSFD1 inoculation was done 8 h after the start of the hydrolysis, while the other three experiments had 14 h of pre-SSD (simultaneous saccharification and detoxification period).

5.8.2 Results and discussion

The decrease of the viscosity, as was described in case of SSF1 (see Section 5.7.2), was observed again with liquefaction after 18-24 h. Due to laccase addition, the mixture went through a color shift from brown to red in the first 12 h, then back to brown gradually by time. In the first experiment, no antifoam was used initially, but strong foaming made it necessary to add it, and it was added in every upcoming experiment. $CaCO_3$ was used to bring the pH close to a value of 6.5, as lactic acid production gets inhibited at low pH values, typically under 5 [59]. The use of chalk is preferred for a number of reasons. It is generally low cost, the remaining Ca^{2+} ions are much less inhibiting than Na^+ or K^+ ions [59] and it can be easily removed by addition of sulfuric acid as the formed gypsum is technically insoluble in aqueous environment. This is why most of the traditional purification processes are based on this [59]. Furthermore it acts like a buffer for acidifying reactions as once the pH drops below a certain pH the calcium-carbonate (and a water molecule) decomposes to $Ca(OH)_2$ and carbon dioxide (see Equation 5-4). The latter leaving the mixture in a gaseous form, and the remaining $Ca(OH)_2$ reacts with acidic compounds, increasing the pH [225]. In practice, the increasing chalk addition during experiments only elevated the pH to 5.5 from the initial 4.5-5, even at 10 m/m%. Further increase could be achieved by addition of lime; however, this is far from trivial (Section A.3).

$$CaCO_3+2H_2O \rightarrow Ca(OH)_2+H_2CO_3 \rightarrow Ca(OH)_2+H_2O+CO_2 \uparrow \qquad \textbf{5-4}$$

The summarized results for all four SSFD runs are presented in Figure 5-12. Glucose concentrations (see Figure 5-12A0, with detailed graph in Figure 5-12A1) started from close to zero and reached maximal value between 42-92 h. In the hydrolysis experiments the glucose concentration saturated in the same range (see Figure 5-7). Xylose concentration was close to the final value after around 14 h, as was also the case in most of the hydrolysis experiments, saturating between 3-5 g/l (section 5.6.2 and Figure 5-7). No significant xylose consumption was measured in any of the experiments. The furfural concentration was decreasing steadily with the same rate

until aeration was on (see Figure 5-12B). SSFD1 had only 8 h aeration, compared to 14 h in the other three cases; it is visible that the furfural concentration only decreases until this time. Furfural removal was caused by air stripping as discussed in Section 3.7.2.2. Evolution of HMF concentration was varying between experiments. It was mostly stable in case of SSFD1 from 0 until 72 h, while HMF was decreasing earlier in the process in the other three cases. The initial decrease was because of added active carbon (at 14 h) rather than metabolism. Phenolic concentration measurements yielded useful results in only two of the four measurements (see Figure 5-12C), i.e. SSFD3 and SSFD4, and they showed a similar behavior in time with approximately stable phenolic concentration. There was visible lactic acid production, which is connected to microbial growth, only in two experiments, SSFD2 and SSFD4, with a lag phase of 92 h and 110 h. This late microbial growth, is unusual, the longest lag phase found in literature was 32 h with *Pediococcus acidilactici* DQ2 on corn stover [215], but typically by 24 h the growth is visible like in the case of *Lactobacillus plantarum* MSUL 903 on corn stover [71], [226]. None of the trend lines is strictly decreasing, indicating that phenolics were not removed from the liquid by the laccase reaction in the same way as it was reported in Section 3.7.2.2. The reasons for this could be the presence of the solid fraction, microorganism or antifoam. Unfortunately, no literature was found, where the phenol concentration was followed up during SSFD. Moreno et al. published several papers on the topic, but either laccase was used prior to SSFD [157], [227] or the phenolic concentration was not followed in time [157], [175]. No literature was found about the comparison between laccase detoxification in XRF alone and in the whole slurry, however it was reported before that laccase treatment caused quantifiably phenol reduction on the whole slurry [227]. The presence of solids can easily alter the reaction that was investigated with laccase and liquid XRF due to different viscosity, enzyme/substrate adsorption to the solid surface or radical reaction with the solid particles. In case of high redox laccase, the radicals with high propagation potential will react with the solid matrix, grafting to it, instead of activating another soluble phenolic substrate, thus decreasing quantifiable phenolic removal. The correlation between the UV absorbance measurements and the phenolics concentrations as measured by HPLC was strong (see Figure 5-12C), indicating that UV measurements can be also useful for monitoring during SSF and SSFD.

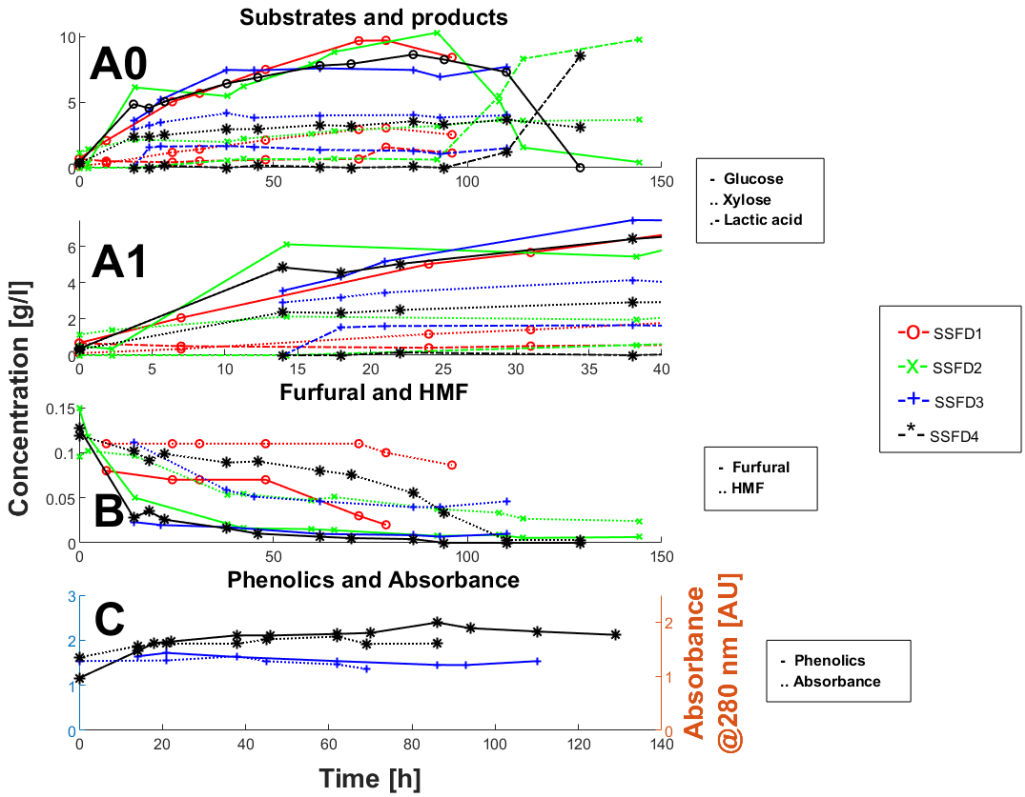

Figure 5-12: Time evolution of (A0, A1) substrates and product, (B) furan and (C) phenolics concentration and absorbance during four SSFD experiments. Different compounds are marked with different lines, different SSFD experiments with different markers.

The lactic acid production has to be improved undoubtedly (Figure 5-12A0). It was expected that the microorganism would consume all glucose in less than 24 h, as it was an adapted inoculum and, to obtain the maximum cell concentration, it only needed to reach ten times higher concentrations compared to initial state (7-8 v/m% inoculum). However, in case of SSFD1 no glucose consumption/lactate production was observed until 100 h. The maximum glucose concentration during all four SSFD experiments ranged between 8-10 g/l (Figure 5-12A0), significantly lower than 15 g/l obtained during hydrolysis experiments with cellulase and with added XRF (see Figure 5-7A1). The difference can be caused by metabolism of the fermenting microorganism, but it is unlikely as no lactic acid production was measured. SSF1 results are in good correspondence with the results performed by cellulase at pH 5 (see Figure 5-7) as glucose concentration reaches approximately 17 g/l concentration. The difference between SSF1 and SSFD experiments is the presence of *C. unicolor* laccase, thus it can be concluded that the lower glucose concentration is caused by laccase.

After the first experiment, several changes to the experimental setup were applied: aeration time increased to reduce furfural concentration, additional chalk was supplied to increase the pH to 6 which is closer to the optimum of the *Lactobacillus* strain and additional active carbon was added to reduce the HMF concentration. SSFD2 was the first experiment done with these modified parameters, but it still did not show significant lactic acid concentration increase until 92 h, the experiment was extended through the weekend. Although lactic acid concentration increase was definitely visible by the next measurement point, i.e., 16 h later at 108 h, and most glucose was consumed by 114 h, the late lactic acid production is disappointing. At 142 h glucose was completely consumed and lactic acid yield was over 90 % of the theoretical yield. The third experiment was a replication, but again, no lactic acid production was observed in the first 108 h. As *L. pentosus* was only used for its capability to consume pentoses, and no pentose consumption was shown during any of the three experiments, another more robust strain was chosen, i.e., *L. amylotrophycus* with the same inoculum adaptation method as with *L. pentosus*. This time, the cell concentration was determined by plate counting, as this is the only method that gives information about the viable cells in the broth. The liquid used for colony counting was obtained by filtering the fermentation broth through a Buchner funnel with the solids remaining in the cake above the filter paper, which can easily alter results, as part of the colony forming units will be filtered out, thus providing lower CFU values. However, it was expected that the filtered-out portion of the cells would be approximately constant. The plate counting showed that the viable cell count was one CFU/50 µl even after 24 h, which is 10 h after the inoculation (see Figure 5-13). No matter how toxic the broth is, from a full-grown and adapted inoculum it would be expected that plenty of cells were viable after 10 h since glucose was released and readily available, based on the adaptation experiments (Section 5.4). Cell concentration increased only afterwards. Further investigations led to the recognition that the shaking incubator used for inoculum preparation was malfunctioning time-by-time, stopping the air and temperature homogenization during adaptation. It was shown that the microorganisms were growing at 42 °C, but 45 °C was lethal to them (Section 5.7.1.2), and the temperature swing in the incubator occasionally exceeded 45 °C. It is not known when the malfunction did exactly happen, somewhere during the SSF and SSFD experiments.

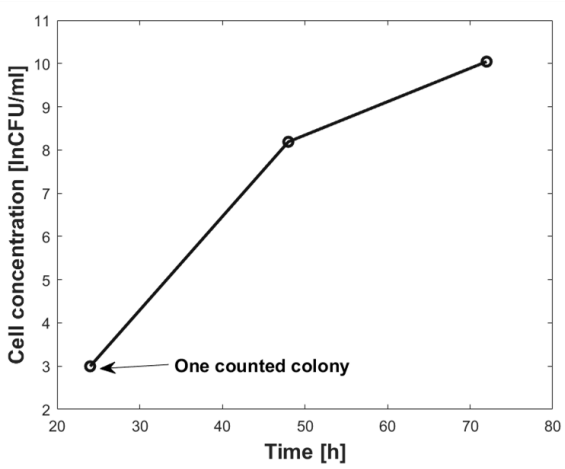

Figure 5-13: Viable cell concentration during SSFD4 with *L. amylotrophycus*.

Comparing hydrolysis speed between SSF1 and any of the SSFD experiments (see Figure 5-11A and Figure 5-12A), it is visible that the cellulase activity was strongly inhibited by the laccase reaction. In the earlier case glucose concentration went up to 17 g/l (see Figure 5-11A), while the latter reached maximum 12 but mainly 8-10 g/l (see Figure 5-12A).

5.9 General conclusions

It was shown that the inhibitors in XRF do significantly elongate fermentation time (Section 5.3.2) and that laccase treatment can, for some extent, compensate for this (Section 5.3.2). It was also shown that aeration removed all furfural (Section 0) as it happened in case of experiments with XRF and laccase (Section 3.7.2.2), and was published before by our group [169]. HMF concentration unfortunately was not altered by neither aeration nor laccase treatment, but only by the microorganism's metabolism or active carbon addition (Section 0). An example method and low-cost setup was presented for lab-scale inoculum adaptation, which decreased the sensitivity of the inoculum to the toxic compounds in XRF significantly (Section 5.4). It was reported before that with increasing toxicity (i.e. increasing inhibitor concentration, i.e. increasing solid loading) the standard deviation of the fermentations increased [217]. Moreover it was shown that at industrially relevant high substrate loading (starting from approximately 15 m/m%) the behavior of microorganisms changes, cell death enhances and lag phase increases drastically [175], [217], [227]. It was reported before that higher concentration of added inhibitors strengthen the inoculum in case of *S. cerevisiae*, but also increases variability/standard

deviation in adaptation [217]. It should be further assessed if it is more beneficial to adapt the inoculum by addition of lower volumes of XRF and lower standard deviation but possibly less adapted inoculum, or the use of higher XRF volume addition.

Simultaneous saccharification and detoxification (SSD) experiments showed that bacterial laccase significantly enhanced the cellulase activity, while fungal laccase reduces it (Section 5.6.2 and Section 0). According to a recent publication this is due to phenolic grafting of radicals with high propagation potential to the lignin matrix only induced by high redox potential (mostly fungal) laccase [158]. Results also indirectly suggest that immobilization to m-CLEAs causes a significant deactivation (Section 5.6.2), as the cellulase activity enhancing effect of laccase was smaller when using m-CLEAs in equal organic content compared to free laccase. Deactivation during immobilization was reported before in literature several times and a detailed overview was given in Section Chapter 1. It is not known if evaluating the ability to increase the hydrolysis truly quantifies the laccase enzyme activity towards phenolics, as the exact mechanism of the hydrolysis enhancing is not described yet in detail. Therefore, deriving the inactivation by immobilization from a difference in hydrolysis increase by free and immobilized laccase is questionable. If the effect involves surface-reactions, the measured and calculated deactivation by the decreased hydrolysis enhancing yield of immobilized enzyme compared to free enzyme, can be significantly higher than it would be measured in cases when the substrate is soluble and no surface-reactions are involved.

It was also proven that laccase treatment and fermentation should be shifted in time, 12 h seems enough, to avoid viable cell count decrease caused by radicals (Section 5.5.2). This method was reported in literature before, under the name PSSF (presaccharification and simultaneous saccharification and fermentation), but no reasoning was given and the laccase reaction induced cell inactivation was not mentioned [175]. The phenolic concentration evolution was shown to be completely different in case of SSD (Section 5.6.2) and SSFD (Section 0) compared to that recorded during the initial laccase screening on XRF (Section 3.7.2.2). This finding induces that screening has to be done in presence of the solid phase, which will require special equipment. It was also shown that calcium carbonate addition was unable to elevate the pH until 6 (Section 0), so a lime addition method has to be developed. The achieved titers were too low for any industrial application (Section 0), but it has to be noted that reliable results from the fermentation part could not be drawn.

Chapter 6 TECHNO-ECONOMIC ANALYSIS

6.1 Introduction

Cost estimation is a crucial, but very difficult task even for mature technologies, not to mention if the process is not yet applied or widespread. When conducting a techno economic analysis, the costs can be generally divided into capital investment (CAPEX) and operating costs (OPEX). The former is a one-time investment (land, building, machinery), whose ratio to the total costs often decreases by up-scaling (increase of production quantity), while the latter is linearly increasing (or at least correlates) with production quantity (typically raw materials, chemicals). In the long run, the production price will be close to OPEX, which means that the paid-off production lines will produce close to the variable costs, thus it is also interesting to investigate CAPEX and OPEX separately.

In the next subchapters, the necessity of high initial substrate loading will be explained, thereafter a literature overview about cellulase and laccase prices is given, and finally, an overview about the CLEAs immobilization and the recuperation of laccases and cellulases is presented.

6.1.1 Initial substrate concentration and minimal titers

The needed initial substrate concentration can be back-engineered from the downstream processing (Section 2.5.5) as the initial substrate and final product titer requirement are strongly linked. It was shown that the minimum concentration needed for effective downstream processing is 50 and 100 g/l product respectively for ethanol and lactic acid [71]. Equation 6-1 shows how to calculate the initial substrate concentration in general. Table 6-1 contains the values for the calculations. Monomer conversion factor indicates the mass of polymer obtained by complete polymerization of 1 g monomer, theoretical fermentation values are for homo-fermentations, realistic fermentation yields were 95 % for glucose and 70 % for xylose of theoretical yields and 80 % for hydrolysis yield. The result is 12.5 m/v% and 12.8 m/v% initial substrate loading in theoretical case for ethanol and lactic acid fermentation respectively, and 17.8 m/v% and 18.2 m/v% in more realistic case. Typical cost estimations work with 15-20 % substrate loading (see Table 2-8). This means a very viscous mixture, which can make immobilized catalyst recovery difficult.

$$c_{sub} = c_{titer}\left(\frac{c_{cel}Y_{hidGlu}Y_{fermGlu}}{Y_{monomerGlu}} + \frac{c_{hemcel}Y_{hidXyl}Y_{fermXyl}}{Y_{monomerXyl}}\right)^{-1} \quad \textbf{6-1}$$

where c_{sub} is the initial substrate concentration, c_{titer} the final titer after fermentation, $Y_{monomer}$ is the monomer to polymer conversion factor (constant 0.9 for glucose and 0.88 for xylose), c_{cel}/c_{hemcel} is the cellulose/hemicellulose concentration in the substrate, Y_{hid} is the hydrolysis yield, Y_{ferm} is the fermentation yield.

The realistic initial substrate loading requirements are around the typical dry content values of the whole slurry after steam explosion, usually around 20 m/v%. This leads to the conclusion, that after the steam explosion, a dilution to decrease the inhibition effect of XRF is not economically viable, thus the slurry has to be utilized directly. In case of dry dilute acid pretreatment, which is technically a type of steam explosion, however, significant dilution can be applied as the solid ratio of the slurry is 50 m/m% [71].

Table 6-1: Values used for initial substrate calculation.

	Theoretical		Realistic	
	Cellulose	Xylan	Cellulose	Xylan
Content in poplar [-]	0.5	0.2		
Monomer conversion factor [-]	0.9	0.88		
Hydrolysis yield [-]	1	1	0.8	0.8
Eth fermentation yield [-]	0.51	0.51	0.4845	0.357
Lac fermentation yield [-]	1	1	0.95	0.7

6.1.2 Enzyme price

Cellulase

Enzyme prices are hard to estimate as detailed by Klein-Marcuschamer [228]. There is so little information available, that often authors give an estimated price without indicating sources or models. These prices range from 1.5 \$/kg_{prot} up to 6 \$/kg_{prot} (see Table 2-8) from researchers, but industrial experts say the current prices can go up to the range of 200-2000 \$/kg_{prot} [211], with a theoretical minimum of 1.25 \$/kg in case of soy protein [228]. Enzyme prices correspond to about 15-25 % of the final selling price of the product (see Table 2-8), but technically most estimations use

future/expected prices and activities, thus the enzyme uncertainty has significant effect on the overall cost estimation. The main sources of enzyme prices are models [132], [135], [137], [228] or information from the enzyme producers, Novozymes and Genencore, or public institutes [136]. The Department of Energy in the USA stated in 2009 that the cost of enzyme with the current technology is about 0.35 $/gal_{ethanol}$ (0.12 $/kg_{ethanol}$) and it is expected to drop to 0.12 $/gal_{ethanol}$ (0.04 $/kg) by 2012. Industrial experts state that even 0.35 $/gal_{ethanol}$ is too optimistic, and it is more likely 0.5 $/gal_{ethanol}$ (0.17 $/kg_{ethanol}$) [136]. Considering the uncertainty of the enzyme cost the best decision seems to use the whole range for cost estimations as Liu et al. did for lactic acid production (see Table 2-8). Using the range of 1.25 to 23.30 $/kg_{protein}$ the selling price of lactic acid varied from 0.48 to 1.17 $/kg, and the cellulase cost from 8 to 62 %, the latter calculated with current enzyme prices [71].

A model for price calculation of cellulase enzyme production from raw materials to final concentrated enzyme product was published [228]. The model was based on available data and a simple process flow incorporating seeding the inoculum, fermentation, filtering, incinerating the cells and concentrating the enzymes to 150 g/l (also transport, taxes, wages etc. are included). The model estimates the production cost of cellulase from steam exploded poplar to be 10.14 $/kg in the base case, from which 49 % is facility dependent, 27 % the cost of raw material, and the rest includes utilities, wages, transportation, consumables and waste treatment. From raw material cost, glucose, NH_4OH and poplar are the dominant with a share of 33, 28 and 27 %, respectively. It is shown that the relative high cost of the enzyme itself is caused by both the expensive equipment and high OPEX (nearly 50-50 %). Excluding fixed costs, the price is still about 5 $/kg [228], which would be the case with a fully paid back production line. These estimations are useful as several enzymes could (and must) be used for a lignocellulose biomass based SSF process including different cellulases (endo-, exocellulase, hemicellulase etc.) and laccases [169].

There is a constant discussion about whether it is more cost effective to produce enzymes on site or buy them on the market. Typically independent sources state that it is approximately equal [37] or cheaper (30 % [229] up to 70 % [230]). By logical thinking, we can say that this should be the case if the two technologies (on-site and off-site) are strictly the same as on-site production will spare post processing costs, i.e. concentration, stabilizing, bottling and transportation. In the meanwhile, the process can be integrated in the refinery by combined waste treatment, cell incineration and heat integration, reducing CAPEX. Companies dealing with off-site enzyme production

have to rely on superior technology such as better microorganisms and more advanced fermentation technology in order to be competitive, or sell licenses for on-site production.

Laccase

No price estimation is available about laccase. From the current market enzyme prices, the laccase from China was the only enzyme with a reasonable price in big quantities, although still very high (34 $/kg) [141]. The other laccases were either received as sample from companies or their price was clearly not the bulk market price (*Trametes versicolor* laccase from Sigma for 57 $/g). Hence making price estimations is difficult. The cost of the use of laccase in an SSF process is purely the price of the enzyme and aeration, as no extra steps are needed, and aeration is low cost.

6.1.3 Immobilization

A possible way to decrease enzyme cost is immobilization, which allows catalyst recycling by filtration or centrifugation [197]. It can also increase the overall performance of the enzyme by improving the resistance to inhibitors and general stability, widening the pH or temperature working range. Even enzyme purification was reported during the process if the immobilization is achieved by bounding specific functional groups, as other compounds not containing the specific group will be left in the solution [198]. However, also the immobilization step has its costs and while improved stability is experienced with enzymes that are used in organic solvents, such as immobilized lipase [199], for laccase, enzyme deactivation is noticed due to the immobilization process [200]–[203]. Moreover, during the application of immobilized enzymes, mass transport phenomena can cause a lower overall activity. Garcia-Galan et al. published a good overview of immobilization possibilities [198]. Techniques can be divided in methods using support materials (porous or nanoparticles) or without a support, as in case of CLEAs (Cross-linked Enzyme Aggregates) or CLECs (Cross-Linked Enzyme Crystals), and these two types can even be combined. Immobilized enzymes are typically recycled by filtration or centrifugation from the reaction medium. Therefore, applying the considerations published in the article [198] to the specific case of simultaneous saccharification, detoxification and fermentation, the following facts can be deduced about utilization of any enzyme during the process. (1) Even after maximum theoretical conversion of the solid substrate, solid parts would remain in the broth (lignin particles [169]) which will hinder catalyst filtration. Therefore, catalyst

separation from the SSFD broth has to be done based on a different principle. (2) During the SSFD process, the formed particles can physically block the porous structure of the carrier material. (3) The enzymes used are always mixtures and rarely purified to decrease the costs. As CLECs are formed after crystallization of pure enzymes, this technology is not applicable. (4) Production of CLEAs is based on aggregation of enzymes and can be used for our application. Based on these considerations, magnetic Cross-linked Enzyme Aggregates (m-CLEAs) are investigated further in the concrete example of laccase enzyme, but the principles concluded are valid for enzymes in general. The carrier is non-porous, the enzymes are close to the surface and the separation can be done based on magnetic properties. It has to be noted that the core should be ferromagnetic and not permanent magnetic, as the particles should not aggregate, only in presence of a magnetic field.

Since simultaneous use of laccase and cellulase enzymes is a possibility, co-immobilization can also be considered. In literature, some examples of co-immobilized enzyme systems exist. For example, Chmura et al. reported about combi-CLEAs [148]. In this case several different enzymes are co-immobilized, although no cellulase or laccase is involved in the study. A more recent example on the co-immobilization of *lipase* and *galactosidase* was reported by Peirce et al. [231], showing that even enzymes with different inactivation characteristics can be co-immobilized and the one faster deactivating selectively removed from the carrier. The stable enzyme was first immobilized on agarose support, thereafter the catalyst treated with ionic polymer and the second enzyme weakly immobilized via ion exchange. The latter can be removed selectively if it is deactivated. It should be noted that the applied cellulase complex is already a mixture containing a number of different enzymes. However, co-immobilization of the cellulase complex and laccase can be an interesting topic for further investigation.

Techno-economic investigations on enzyme immobilization are rare, and none was found investigating the efficiency of recycling from an often-difficult liquid such as high solid loading (10-20 m/m%) SSF fermentation broth. A published cost estimation [232] used a price of 900 $/kg for immobilized catalyst in a packed column process, which is a realistic pessimistic estimation (commercial price), while a lower estimate from Novozymes is 500 $/kg catalyst with 5 % enzyme loading [211]. Both correspond to a specialty polymer as carrier material and relatively low enzyme loading.

The organic loading of the catalyst is a crucial parameter. As it was shown in the experiments with varying cellulase amount (Section 3.5) and published in cost estimations (see Table 2-8), around 5 m/v% of 10 % protein content crude cellulase enzyme product will need to be added to the broth, which means added 5 $g_{protein}/l_{broth}$. If the organic loading is a relatively high 50 m/m% and no deactivation is taken into account, this will be 1 m/v% added catalyst to the broth, keep in mind, next to 20 % dry content substrate already in the broth. If the organic loading of the catalyst is 10 m/m%, de added mass has to be 5 m/v%. If the enzyme activity increases, the enzyme load can of course be reduced.

Cellulase

A significant amount of literature is available about the application of magnetic CLEAs, or similar immobilization methods, from laccases or cellulases, however with varying reported remaining enzyme activity. Cellulase was immobilized on Fe_2O_3 nanoparticles (final catalyst size ~100 nm, 16 m/m% enzyme loading) with simultaneous cross-linking and immobilization. Remarkably, a high remaining activity (99 %) was measured with a soluble standard substrate, i.e., sodium carboxymethylcellulose, with a loss of only 8 % activity in 15 cycles and 33 % in 20. Also, real substrate (corncob) was applied in a low concentration (<1 m/m%) and a high catalyst-substrate ratio (25 m/m%), where 62 % of hydrolysis yield was achieved. Recirculation was not reported [233]. Liao et al. immobilized cellulase on polyvinyl alcohol /Fe_2O_3 (270 nm), the enzyme retained 91 % filter paper activity. When they applied the catalyst on microcrystalline cellulose substrate at low concentration (2.5 m/v%) in a ball mill, it lost 60 % activity in four cycles. In these experiments the enzyme was not separated from the mixture, but the whole solid part was recycled [202]. By Alftrén and Hobley cellulase was covalently immobilized on different paramagnetic particles (1 µm diameter, ~1 m/m% enzyme loading, ~50 % remaining activity). The catalyst was tested on pretreated wheat straw at low substrate loading (2 m/v%) and after magnetic recycling the activity decreased by 20 % [203].

Laccase

Laccase was immobilized before on magnetically active mesoporous carbon with high enzyme loading (~50 m/m%) and relative high remaining activity (80-90 %), however even with 2,2'-azino-bis(3-ethylbenzothiazoline-6-sulphonic acid) (ABTS, a soluble

substrate) it has lost 30 % and 50 % activity respectively [200]. Horseradish peroxidase (oxidoreductase as laccase enzyme) was immobilized on magnetic beads (~100 µm diameter) by applying a consecutive glutaraldehyde activation and immobilization. This led to low enzyme loadings (~0.3 m/m%) but high retained activity (69 %) compared to free enzyme. However, immobilization improved the working pH range, and thermal stability. Immobilized enzyme recirculation was not investigated [201]. Up to our knowledge, immobilized laccase was never tested on lignocellulose biomass before, and definitely not on high solid loading SSF broth.

6.2 Problem statement and goal

This chapter is intended to provide a better understanding of enzyme use in lignocellulose-to-chemicals process, and more specifically SSF(D). Although the cellulase price has significant uncertainty, as it was shown in Section 6.1.2, cellulase is applied as an example, because estimations/models/publications are available, unlike for laccase. Where possible, conclusions will be drawn for laccase utilization, based on the obtained results.

m-CLEAs as an immobilization method was investigated for its utilization potential in the SSF process by measuring the recovery efficiency of the catalyst from the fermentation broth at lab scale. Preparation of m-CLEAs from cellulase and laccase enzymes was reported before in literature, but they were rarely applied for lignocellulose biomass substrates, let alone for simultaneous saccharification and detoxification at high solids loading (see Section 6.1.3).

Minimum sugar revenue (MSR) was estimated for hardwood based sugar production, based on an existing model [144], and compared to corn derived MSR. The price estimation was performed in function of the possible range of enzyme unit price and enzyme activity increase, both in case of free and m-CLEAs immobilized cellulase. For MSR estimation with immobilized cellulase, the deactivation parameter measured previously (see Section 0) was used. Monte Carlo simulations were used to calculate the uncertainty of the analysis at different enzyme unit prices; thereafter the parameter sensitivity was estimated at four different scenarios for all utilized model inputs.

The possible future enzyme unit price was assessed via a known published enzyme cost estimation model from Klein-Marcuschamer [228]. First, the production cost decrease was evaluated by using shorter fermentation times, as it would be expected

in a bacterial fermentation instead of fungal. Then, the possible decrease of enzyme price by inoculum recycling was investigated.

6.3 Methods

In this chapter, three topics are investigated. First, recycling experiments were done to recuperate m-CLEAs from the SSF broth, a heterogeneous mixture with high solid ratio. Thereafter the hardwood based minimum sugar revenue (MSR) was estimated in function of the utilized enzyme unit price and possible future increase in enzyme activity (see details later). Thirdly the production cost of the enzyme is estimated, starting from the model of Klein-Marcuschamer [234] for fungal enzyme production (detailed later), by using shorter fermentation times, caused by utilizing bacteria instead of fungi, and by recycling inoculum.

6.3.1 Experiments on immobilized enzyme recovery

Experiments on immobilized enzyme recovery of m-CLEAs laccase from simultaneous detoxification and saccharification reaction mixture were performed. The immobilized enzyme, m-CLEAs was a kind gift from CLEA Technologies (Delft, NL), made from a thermostable bacterial laccase, with an organic loading of 38 m/m% and based on glutaraldehyde cross linking from the crude laccase product. Immobilization was performed as described in Lopez et al. (2002) and Sheldon et al. (2016). No more information was given from the company. The experiments were solely focused on the recuperation possibilities of the m-CLEAs from a thick liquid. Recuperation efficiency was based on m/m%. Recovery experiments were performed using an LH Fermenter 500 (LH Fermentation ltd., Reading, UK) and a neodymium magnet (4x2x0.4 cm). The reaction mixture consisted of 12 m/m% steam exploded poplar (Soti et al., 2013), 0.13 m/v% organic loading equivalent m-CLEAs (19.1 g wet catalyst) and 2 m/v% cellulase liquid product (0.24 m/m% dry load) (Optimase CX15L, DuPont, Wilmington, DE, USA). The reactor setup (see Figure 6-1) was modified by attaching metal rods on the rotor for high viscosity mixing. m-CLEAs were separated from the bioreactor after 24 h of hydrolysis when the broth was liquefied, i.e., converted from wet solids into a thick liquid.

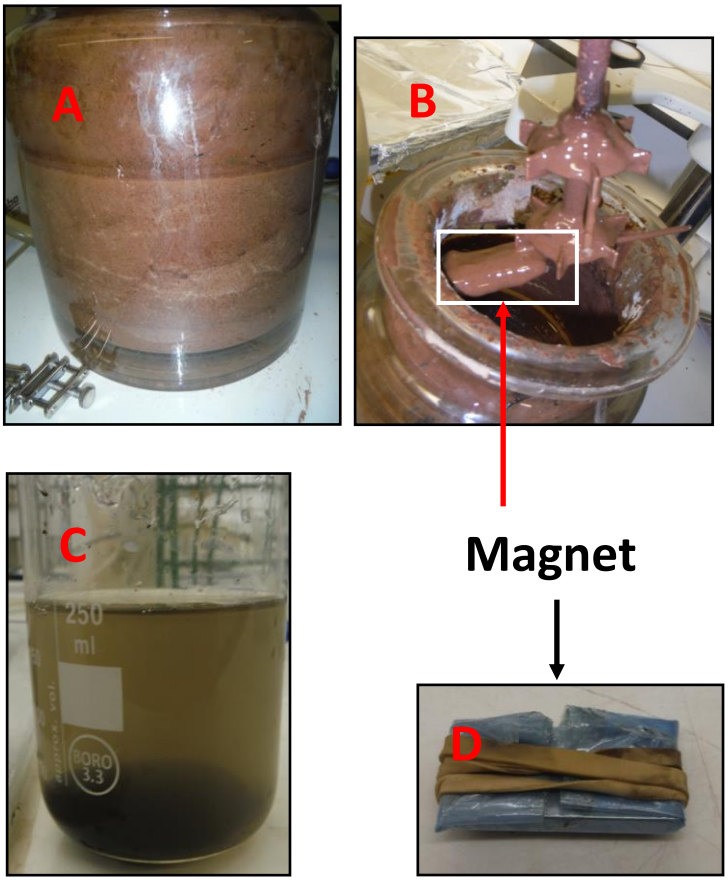

Figure 6-1: The setup and process used for recovery measurements. The mixture, when the separation was started (A), the magnet in a protective foil (D) is attached to the rotor (B). The beaker (C) contains the recovered catalyst during the washing process.

Hereto, the magnet was attached to the rotor, stirring speed linearly decreasing from 500 to 0 rpm in 30 min. In this way, it was expected that higher agitation rates caused better mixing and thus improved the contact of the catalyst to the magnet, but also intensify the disturbance of the attached catalyst layer, as the catalyst remaining on the magnet is a mixture of iron, enzyme and lignocellulose particles, thus the magnetic field is weaker layer by layer. Lower agitation rates would result in less layer disturbance but also less contact and mixing. The optimum agitation rate was not determined, but it was expected that by linearly decreasing the rpm over a long time the agitation rate will go through the optimum (collect the most catalyst possible), and on a lower value it will maintain the collected material as the breakaway effect is decreasing. Afterwards the material containing the catalyst was released from the magnet, washed in 200 ml demineralized water and subsequently separated from the

washing liquid by the magnet again. The mass of the remaining material was measured. This washing cycle was repeated 16 times, i.e., until the washing liquid was transparent (all lignocellulose material was washed out). Two parallel experiments were performed. The measured recycling efficiency was used in the later cost estimations.

6.3.2 Estimation of minimum sugar revenue

MSR estimation is a convenient tool to benchmark different sugar sources, as it is general, not dependent on fermentation, but it might miss some of the interactions, because it is independent from fermentation. The cost estimation of hardwood based minimum sugar revenue (MSR) was based on the publication of Reeb et al. [144]. The values used for calculations are visible in Table 6-2. The best hardwood-based scenario, thus the lowest MSR, was taken from the publication, 272 $/t$_{carbohydrate}$ in case of autocatalyzed steam explosion followed by enzymatic hydrolysis with 75 % yield, pellets produced by residues and co-location with a pulp mill instead of green field investment. Supercritical water extraction gave better results, but the obtained values were much more uncertain than in the case of autohydrolysis. CAPEX was directly taken from the publication (110 $/t$_{carbohydrate}$) by subtracting the substrate (126 $/t$_{carbohydrate}$) and enzyme cost (55 $/t$_{carbohydrate}$) from the published MSR in case of hardwood-based sugar production. Based on the criteria of Independent Projects Analysis (IPA, www.ipaglobal. com) CAPEX meet the ± 35 % precision.

Based on the calculations in the article, 11 kg$_{protein}$ cellulase was used for every t$_{carbohydrate}$, as the enzyme cost was 55 $/t$_{carbohydrate}$, and the enzyme unit price 5 $/kg$_{protein}$ [144]. This value incorporates every process parameter (sugar degradation during pretreatment, incomplete hydrolysis etc.). The price of the enzyme (unit price, $/kg$_{protein}$) and the activity ratio (FPU$_{future}$/FPU$_{current}$) were the investigated variables. The range of unit prices was taken between the current price (23 $/kg$_{protein}$ [71]) and 2 $/kg$_{protein}$, the activity between the current activity (1) and an estimated activity if the cellulase would be used in the same concentration as amylase is used for starch (0.5 g$_{protein}$/kg$_{starch}$ [236]), as a mature/optimized enzyme cocktail. The hydrolysis experiment that reached 20 g/l glucose concentration after 24 h contained 5 m/m% cellulase (50 g) per 200 g wood. Calculating with 10 m/m% protein content in the enzyme product, the protein/wood ratio is 25 g$_{protein}$/kg$_{wood}$, and 35 g$_{protein}$/kg$_{carbohydrate}$, which is 70 times higher than the ratio used in case of amylases.

Raw hardwood prices were obtained from the Billion ton report [237], they included preprocessing and transportation to the refinery. Average price and standard deviation were calculated form an annual quantity-price chart with Monte-Carlo simulation, by choosing 10000 random annual quantities and the corresponding lignocellulosic cost. Gaussian distribution was assumed and the mean and standard deviation values calculated from the 10000 values, which gave 78.5 ± 6.5 $/t$_{lignocellulose}$. Calculating with 70 m/m% biomass sugar content [144] the estimated price of carbohydrates is 112.1 ± 9.3 $/t$_{carbohydrate}$. Corn grain derived MSR, based on the past five years deviation, was taken as 230 ± 50 $/t$_{carbohydrate}$ [144].

Immobilized enzyme system

The price of m-CLEAs preparation was estimated to be 10 $/kg$_{protein}$, as the iron powder would cost 1-1.2 $/kg [141] and the glutaraldehyde solution 2 $/kg [141]. As the catalyst contains approximately 40 m/m% organic loading the mass corresponding to 1 kg of protein is 2.5 kg catalyst, containing 1.5 kg iron, if the mass of glutaraldehyde is neglected. The iron itself corresponds to 1.5-1.8 $/kg. The variable cost will be probably around 5 $/kg, and the same value of CAPEX was estimated. Recycling efficiencies (obtained from experiments detailed in Section 6.3.1) and enzyme deactivation (based on Section 5.1.1), were used to estimate the immobilized enzyme utilization costs.

The calculation of immobilized enzyme cost can be written as Equation 6-2. The amount of enzyme needed is known from the article of Reeb et al. (11 kg/t$_{carbohydrate}$) [144] with the difference that the catalyst price is the addition of enzyme and immobilization price (calculated in $/kg$_{protein}$), and the enzyme amount has to be recalculated with the deactivation caused by immobilization . Only the catalyst that could not be recovered has to be replenished to allow the same enzyme activity for each batch. The added amount in each round of reuse is the catalyst that could not be recycled, i.e. *(1-Recirc)*. This amount has to be corrected with one factor, reflecting the enzyme loss and deactivation during the immobilization process, i.e., $Deact_{immob}$, which was taken to be 50 %. However in some reports this deactivation was measured to be only 10-20 % [238]. It is very likely that the enzyme stability and the pH working range are improved after immobilization. This will also be incorporated in the variable $Deact_{immob}$, expectedly decreasing it because inhibitors present in the hydrolysate can also inhibit enzymes (e.g., inhibition of cellulases by phenolics), thus the immobilization can grant the enzyme better inhibitor resistance. The pH applied during

SSF can differ from the optimal pH of the enzyme; again, immobilization can yield in less activity loss caused by the pH shift.

$$Cost_{immob} = Mass_{free\ enzyme} \times \left(Price_{enzyme} + Price_{immob}\right) \times \frac{1 - Recirc}{1 - Deact_{immob}} \quad \textbf{6-2}$$

By investigating Equation 6-2, some general remarks can already be given, i.e., the saving is higher if the ratio of immobilization price to enzyme price is lower, if the recycling efficiency (*Recirc*) is higher or if the deactivation by immobilization (*Deact*) is lower. Furthermore, if the recycling efficiency is not higher than the loss by deactivation, the process cannot be cost effective under any circumstances.

An important remark on the application of these equations is that instead of deactivation of the enzyme during immobilization, the enzyme can obtain an increased activity, due to the favorable environmental conditions. In that case, the factor $Deact_{immob}$ will be a negative number.

Monte Carlo simulation

Monte Carlo simulations were performed in function of enzyme activity increase at three different enzyme unit prices, 5 \$/$kg_{protein}$ most frequently appearing in cost estimations [144], 10 \$/$kg_{protein}$ as estimated by Klein-Marcuschamer [234] and approximate current price 20 \$/$kg_{protein}$. For most cases, the standard distribution was taken, except for corn grain derived MSR (not used for calculations, just for comparison) and the CAPEX distribution. Each simulation contained 10000 iterations, where all values were independently generated. The confidence intervals for free enzyme based MSR was calculated by fitting Gaussian to measurement points at each enzyme activity increase value (x-axis), and investigating ± 1 δ (68.2 %). In case of immobilized enzyme, an empirical confidence interval was used (70 %).

A variable-by-variable uncertainty analysis was performed at two scenarios: assuming 15 \$/$kg_{protein}$, thus a little decrease in unit production costs and an activity factor of 1, current activity, and 10, tenfold increase. A Monte Carlo simulation was done for each variable in both scenarios by choosing 10000 values from the distribution and keeping all other parameters the same. The sensitivity is calculated based on the empirical 70 % confidence interval for each simulation.

All data processing was performed off-line using a commercial software package (MATLAB 2017.1, The MathWorks Inc., Natick, MA, 2017). Prices applied during cost calculations were taken from Alibaba [141].

Table 6-2: The values used for MSR estimations and Monte Carlo simulations.

	Mean value	Deviation	Distribution	Unit	Reference
MSR corn grain	230	50	Uniform	$/$t_{carbohydrate}$	[144]
Hardwood	112.1	9.3	Gauss	$/$t_{carbohydrate}$	Monte Carlo based on [237]
CAPEX	110	38.5	Uniform	$/$t_{carbohydrate}$	[144]
Immobilization cost	10	2	Gauss	$/$kg_{protein}$	Own estimation
Deactivation	0.5	0.1	Gauss	-	Own experiments
Recirculation	0.9	0.05	Gauss, rejecting values above 1	-	Own experiments

6.3.3 Enzyme price estimation

Enzyme price estimation was based on the model of Klein-Marcuschamer [234] with some specific modifications made by using SuperPro Designer (Intelligen, Scotch Plains, NJ, USA). The model was based on available data and a simple process flow incorporating seeding the inoculum, fermentation, filtering, incinerating the cells and concentrating the enzymes to 150 g/l (also transport, taxes, wages etc. are included). The process was kept as was published, modifications were made to investigate how the price would change if the inoculum was recycled (thus eliminating the seeding tanks) or the fermentation time shortened.

6.4 Results

6.4.1 Recycling efficiency of immobilized laccase

It is common that yields of only 20-30 g/l reducing sugars per 100 g wood are obtained after hydrolysis of pretreated wood [239]. Therefore, the solid content after hydrolysis is still significant. During the simultaneous saccharification and detoxification

experiments in our laboratory, it was observed that the initial wet solid fermentation mixture was changed into a smooth thick liquid after 12-24 h. m-CLEAs recycling was performed from demineralized water as a standard and from SSF hydrolysis medium as a possible industrial substrate. Enzyme recovery has been expressed in m/m% because of the adsorption of phenolics on the CLEAs, which hampers the measurement of the decrease in phenolics due to laccase activity separately from the decrease due to adsorption phenomena. Results of the recovery showed that the catalyst could be easily recycled from demineralized water with 99.5 m/m% efficiency, but 88 m/m% of the immobilized catalyst could be still recovered even from the thick liquid containing remaining lignocellulose solid particles (16 washing cycles were required to separate the catalyst from the solid part).

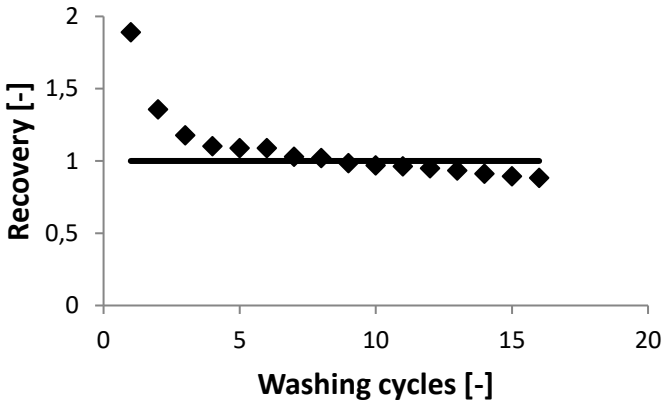

Figure 6-2: Mass recovered by magnet in first recovery step in function of washing cycles (♦) and line indicating the mass of initially added m-CLEAs (—).

Figure 6-2 shows the decrease in mass of the separated m-CLEAs catalyst, including some lignocellulose material, during the washing cycles. It has to be noted that this washing is only needed for analytical purposes. In an industrial application, the separated unwashed catalyst will directly be reused in the next batch. The mass of recovered catalyst before washing was almost double that of the initial mass because of the presence of lignocellulose slurry that was removed from the reactor at the same time (see Figure 6-2). It can be seen that the final catalyst recovery from the broth was 88 m/m% after only one separation step.

6.4.2 Estimation of minimum sugar revenue

Minimum sugar revenue estimation is a convenient tool to compare different carbohydrate sources universally, as it is fermentation-independent. The base of comparison is corn grain derived carbohydrate, which is the current base of fermentations in the Northern Hemisphere [144]. Figure 6-3 shows the estimated hardwood based MSR in function of cellulase unit price and enzyme activity increase in case of free (red) and immobilized (blue) enzyme in 3D (A, B) and top view (C). The more expensive technique is visibly the free enzyme, as that surface is “on the top”. For exact comparison, Figure 6-4 will be used. The current corn derived MSR is marked with a black line, while the confidence interval is the area of darker red color, to understand the shape of the interval see later Figure 6-4. It is visible that the current MSR for poplar wood at high enzyme unit prices (Figure 6-3A in the back corner) is higher than 400 $/$t_{carbohydrate}$, thus even more expensive than white sugar, not to mention corn grain derived carbohydrate. Taking current enzyme activity (Enzyme activity increase factor = 1), the unit price has to drop until 7 $/$kg_{protein}$ to reach the highest MSR of corn derived sugar. However, relatively small activity increase, tenfold, can render the hardwood-based sugar production competitive. Relatively small is meant in comparison to the ratio in which amylases are used, of course.

The point (or technically the line), where the cost of free and immobilized enzyme utilization meet is at 2.5 $/$kg_{protein}$ independent from the enzyme activity, as Equation 6-2 does not contain activity. Under this unit price, free enzyme utilization is expected to be more cost effective, above this immobilized enzyme. It will be shown later that this unit price most probably be never reached; thus, immobilization seems promising at first glance.

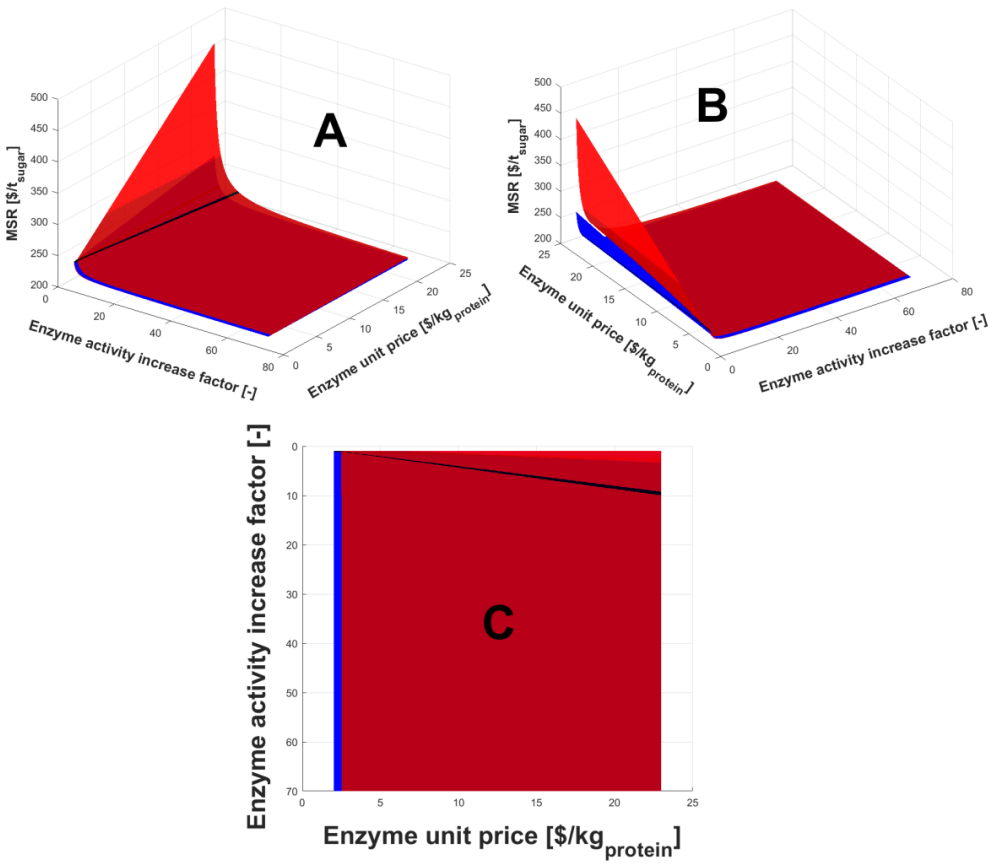

Figure 6-3: Estimated minimum sugar revenue (MSR) in function of enzyme unit price and activity increase compared to current cellulase in 3D (A, B) and top view (B). Red surface is the free cellulase, blue surface is the immobilized enzyme. Dark red color is the MSR regime of corn-derived sugar, while the black line is the current price of corn-derived sugar.

To investigate and visualize the uncertainty of the calculations, Monte Carlo simulations were performed at three enzyme unit prices (see Figure 6-4): the current price (C), approximately 20 $/kg$_{protein}$ [71], 10 $/kg$_{protein}$ (B) as estimated by Klein-Marcuschamer [234] and 5 $/kg$_{protein}$ (A) frequently appearing in cost estimations [144]. It should be noted however, that the 5 $/kg$_{protein}$ is calculated based on Novozymes, who stated that the cellulase cost will be 0.5 $/gallon$_{ethanol}$ [144], thus these calculations are very indirect uncertain, calculating from current enzyme activity and needed enzyme amount.

In all three cases as the activity increases, the MSR converges to the sum of CAPEX and substrate costs, approximately 205 $/t$_{carbohydrate}$, as enzyme costs become negligible. Immobilization is more cost effective above 2.5 $/kg$_{protein}$, however, at 5 $/kg$_{protein}$ the difference is small (<8 % in MSR at current activity), it will not worth it to deal with the complexity increase of preparation/utilization of immobilized catalyst. At 10 and 20 $/kg$_{protein}$ price, the difference is 20 and 36 % in MSR. These are significant saving factors, but the difference in MSR% decreases as the activity increases, as the difference, the ratio of immobilized/free enzyme cost remains constant, but the ration of enzyme cost in MSR decreases.

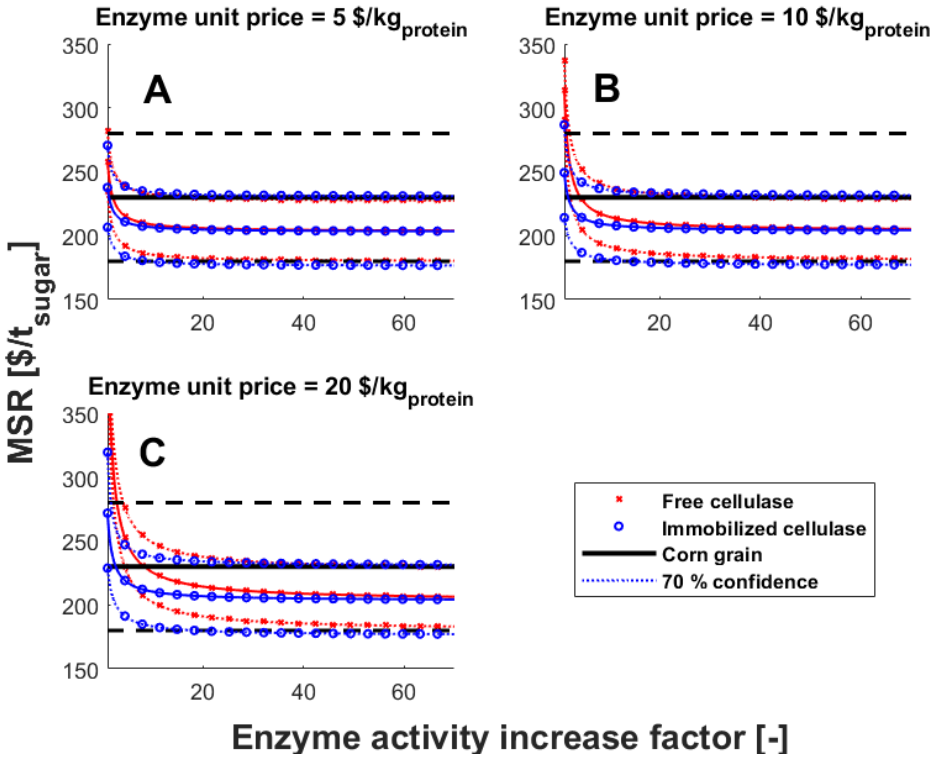

Figure 6-4: Monte Carlo simulation of minimum sugar revenue (MSR) in function of enzyme activity increase at three different enzyme unit prices: 5 (A), 10 (B) and 20 (C) $/kg$_{protein}$ in case of free cellulase (x) and in case of immobilized enzyme (o). Confidence intervals (..) are at 70 % level, calculated from 10000 simulations. Black horizontal lines are the corn grain derived MSR.

The activity increase ratio, when the free enzyme reaches the interval of corn derived MSR and mean value of corn derived MSR is correspondingly: [-,2] in case of 5 $/kg$_{protein}$, at this enzyme unit price it would be competitive at higher corn grain prices.

[1.5,4] in case of 10 $/kg$_{protein}$, thus it needs a few folds improvement for economic viability. [3,8] in case of 20 $/kg$_{protein}$, thus it needs more improvement to economic viability. The same values for immobilized enzyme activity increase at 5, 10 and 20 $/kg$_{protein}$ are [-, -], [-, 1.1] and [-, 1.6], thus m-CLEAs cellulase, theoretically would be viable even with current prices assuming the highest corn grain price, and a few folds activity increase is needed to reach current corn MSR cost – again, theoretically. It is also worth mentioning that the lower bond of corn derived MSR and hardwood derived MSR are almost the same, it is difficult to compete with cheap corn price even at most optimistic process values.

The parameter sensitivity was evaluated for four scenarios: free/immobilized cellulase utilization at current enzyme activity and in case of tenfold activity increase at 15 $/kg$_{protein}$ enzyme unit price (see Table 6-3). In both cases, immobilized enzyme system had lower MSR, 30 % saving at current activity and 70 % at higher activity. The CAPEX is a major uncertainty causing approximately 10 % change in MSR. Recirc parameter was also a significant parameter, with 10 % influence on MSR at current activity. At tenfold activity increase however, all enzyme related uncertainties are disappearing as the enzyme cost will be small compared to CAPEX and substrate costs.

Table 6-3: Parameter sensitivity investigation in case of 15 $/kg$_{protein}$ enzyme unit price and activity factor of [1,10] for free and immobilized cellulase utilization.

	Activity factor [-]	**1**	**Activity factor [-]**	**10**
	Free	**Immobilized**	**Free**	**Immobilized**
MSR [$/t]	368	258	220	209
Sensitivity [%]				
Lignocellulose	2.1	3.0	3.6	3.8
CAPEX	7.2	10.3	12.3	12.9
Immob cost	-	1.8	-	0.2
Deact	-	4.7	-	0.6
Recirc	-	10.5	-	1.3

Although MRS estimation is a convenient and general tool to compare the potential of broad range of substrates, it completely lacks fermentation, thus it cannot incorporate the positive effect of detoxification on microbial growth. The positive effect of

detoxification, the enhancement of hydrolysis, however could be incorporated, as it appears as a reduction in necessary cellulase amount (see Equation 6-3).

$$Cost_{detox} = cost_{laccase} - cost_{cellulase} * f_{enhancement} \quad \textbf{6-3}$$

The enhancement factor was measured in Section 5.6.2, but every other parameter is uncertain: cellulase cost was just investigated and the difficulties highlighted, while about laccase costs no estimation is available. As the process is not economical currently, the only case that could have viability is $f_{enhancement} > 1$, assuming that laccase and cellulase unit prices are the same, because it would mean that adding laccase helps hydrolysis more than adding the same amount of cellulase. Here it should be mentioned that adding laccase and starting the hydrolysis from pH 8 provided 120 % higher final glucose concentrations than the reference hydrolysis without laccase at pH 5 (Figure 5-7A1 and A3), thus it is worth further investigation. In other cases, the enhancement factor was between 30-90 %. If the cellulase cost would decrease however, there would be great potential in laccase utilization.

6.4.3 Enzyme price

The previously mentioned model (section 6.3.3) [228] was used as an estimation of the general costs for extracellular enzyme production. Parameter sensitivity was investigated to see how the price would change in case of different enzyme production. It has to be noted that the model is based on wood degrading microorganisms, as poplar is one of the carbon sources.

Assuming 24 h fermentation, instead of 192 h, or 96 h in case of seed tanks (Figure 6-5B), would decrease the production cost of cellulase from 10.14 $/kg to 8.65 $/kg, with 32 % raw material related costs and 48 % facility dependent, 1.5 $/kg decrease. Switching to bacterial fermentation usually shortens fermentation time, however 24 h is optimistic. It can be seen that 8 folds of decrease in fermentation time only leads to 15 % drop in production cost.

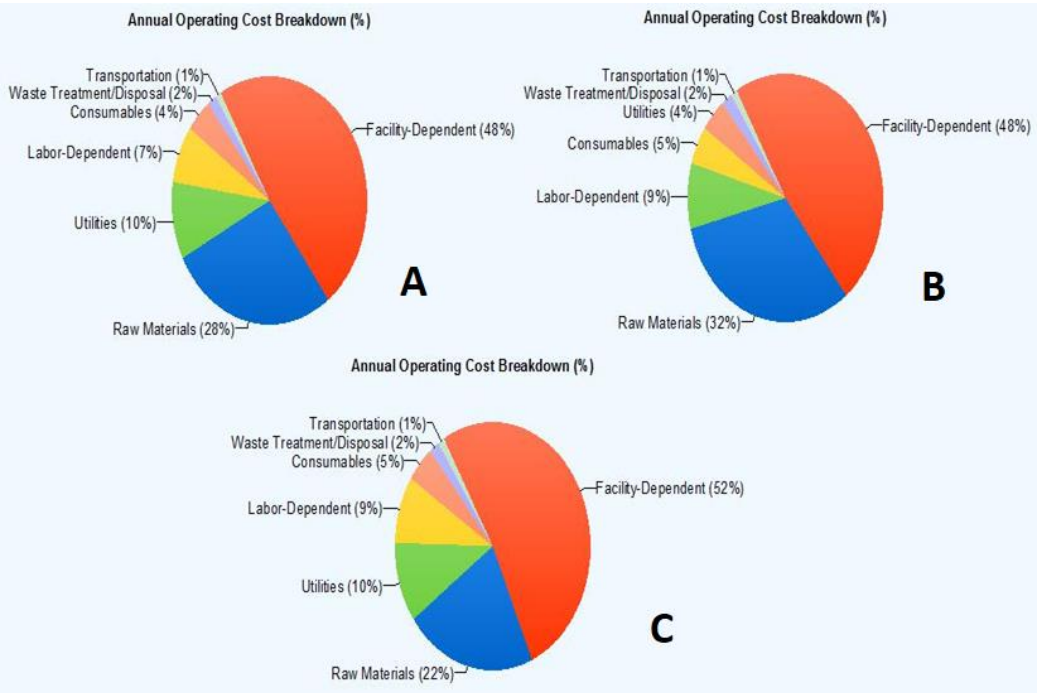

Figure 6-5: Annual cost breakdown of enzyme production for reference case (A), shorter fermentation time (B) and inoculum recycling (C).

It is not easy to decrease raw material costs for enzyme production. One possibility is to increase the yield of enzyme production, since this way less carbon source would be used per unit of enzyme produced. This would also decrease fermenter and downstream processing costs at the same time. However, increasing enzyme yield further will be difficult because calculations are already done based on an optimized cellulase production process. The second possibility is to recycle the inoculum, which would mean technically substituting the glucose carbon source that is applied for culturing the inoculum with cheaper poplar. In the meantime, it would make seed tanks unnecessary, which represent around 9 % of CAPEX. This way the production price was decreased from 10.14 to 8.63 $/kg, from which 51 % is facility dependent and 21 % raw material dependent (see Figure 6-5C). Altogether, this means 14.9 % decrease in final price. From the raw materials part, poplar and ammonium hydroxide together take around 40 % of the costs. In this remaining production price, the raw materials account for 1.81 $/kg and 4.3 $/kg is assigned to all variable costs, which can be considered as very low. Issues, such as the seeding of the fermentation tank once

at the start of the first fermentation or genetic stability of the microorganisms were not taken into account.

From the calculations, the expected minimum unit price of enzymes is around 10 $/kg$_{protein}$, which is in correspondence to an enzyme price range of 10-20 $/kg$_{protein}$ available online for a variety of different dried products [141]. The future cost reduction of the use of enzymes is expected from an increase in the activity of the individual enzymes instead of a decrease in the unit price.

6.5 Conclusion

The driving force of enzyme recycling is the difference between the enzyme price and the immobilization price. The current enzyme prices are far from the calculated minimums reported in literature. Some estimations [228] and market prices of mature enzymes [141] suggest that the enzyme unit price will not decrease below 10-15 $/kg$_{protein}$. Minimum sugar revenue (MSR) estimations based on a published model [144] show that at current enzyme price and activity the hardwood based MSR is not competitive with corn based MSR (+70 %), but about tenfold enzyme activity increase would render it economically viable at the current enzyme unit price.

It was shown that m-CLEAs can be successfully recovered (≈90 m/m%) from high substrate loading in a viscous SSF broth. MSR estimations for m-CLEAs immobilization instead of free cellulase utilization showed promising results. At the expected enzyme unit prices, it could have potential. Close to the current enzyme price of 20 $/kg$_{protein}$, m-CLEAs cellulase can be already competitive when corn prices are high, while with 1.6-fold activity increase it can be economically feasible even with the current corn prices. In case of a unit price of 10 $/kg$_{protein}$, only one-fold increase in activity is needed to reach economic feasibility with the current corn prices.

Parameter sensitivity estimation showed that CAPEX uncertainty has the biggest effect on final MSR, approximately 10 %. In case of immobilization, the recirculation efficiency was the other major contributor followed by the deactivation parameter, with respectively 10 % and 5 % effect on MSR. Upon a tenfold increase in activity, the enzyme related uncertainties would be reduced to the range of one percent and CAPEX will remain the most uncertain parameter.

Until the process itself is not economically viable, there is no possibility for laccase utilization, unless laccase enhances hydrolysis more than the same amount of added

cellulase, see the reasoning of Figure 2-19. When the relative cost of cellulase in the process will drop however, laccase will have a great potential because of its hydrolysis enhancing capability and detoxification effect.

For further refinement of the model, the recovery parameter should be evaluated at a bigger scale, to see if the 90 % recovery factor could still be reached in case of higher volumes. Furthermore, decrease in activity in function of recycling rounds should be measured and incorporated in the model, as well as the detoxification effect of m-CLEAs due to significant removal of inhibitors by adsorption. To estimate the positive effect of detoxification on the microbial growth, another model system will be necessary, as MSR calculation does not deal with the subsequent fermentation.

Chapter 7 GENERAL DISCUSSION AND CONCLUSIONS

7.1 Global conclusions

Different aspects of laccase utilization in steam-exploded poplar-based fermentation were investigated. Laccase-vanillin, a model compound, experiments showed that monomer molecules go through random polymerization via radical coupling, and dimers precipitate, due to their lower solubility in aqueous media. Software simulations suggest that the sharply decreasing solubility in case of phenolic dimers compared to monomers is general, thus this is the mechanism of detoxification.

Laccase-XRF (liquid xylose rich fraction) detoxification experiments showed that laccases differ in terms of redox potential, that is which phenols they react with. HBA (4-hydroxymethylbenzoic acid) was not affected with even high activity *Trametes versicolor* laccase from Sigma, although its concentration decreased to some extent during the reaction when radicals were forming, because of radical propagation. Air bubbling is necessary during laccase utilization to help enzyme regeneration; in the meanwhile, furfural is removed from the solution by air stripping. HMF (5-hydroxymethylfurfural) concentrations were only affected by active carbon treatment or cell metabolism.

Fungal laccases performed superior in terms of phenolic removal from XRF (>60 %) and working pH (acidic, in the range of SSF parameters). The bacterial laccase caused lower phenolic removal (max 60 %) and the working pH of 8 is not ideal for SSF. Furthermore, the pH has to be kept with active control (thus addition of chemicals), as the reaction acidifies the solution. Significant phenolic autodegradation (≈30 %) was encountered at pH 8.

Experiments were performed with bacterial m-CLEAs (magnetic Cross-Linked Enzyme Aggregates) laccase. CLEAs type of immobilized enzymes have exceptional high enzyme loading (≈40 m/m%) compared to other immobilization techniques (5-10 m/m%). High enzyme loading is a necessity in application, where the enzyme will be used in relatively high concentration (>1 m/m%). Magnetic properties are also important, as from a heterogenic SSF broth the catalyst cannot be recovered with filtration. XRF detoxification experiments showed that, compared to free bacterial laccase, the phenolic removal was rapid (an hour instead of 24 h), and less pH dependent (identical at pH 6-8). Further experiments showed that the removal was

caused by chemisorption rather than enzymatic activity, and adsorption will be dominant until few recycling rounds. A model was constructed to quantify adsorption effect in function of applied m-CLEAs concentration and recycling rounds based on few experiments. m-CLEAs recovery experiments proved that 90 m/m% of the catalyst can be recycled from a high substrate loading (<10 %) fermentation broth on lab-scale.

Different process integration possibilities were investigated by combining the three investigated process steps of lignocellulose-based fermentation, i.e., saccharification (S), detoxification (D) and fermentation (F). Simultaneous fermentation and detoxification (SFD) experiments showed that laccase reaction decreases viable cell concentration due to the formed radicals, thus detoxification should be done prior to fermentation. SSD experiments showed that bacterial laccase enhances hydrolysis (90-120 % depending on the parameters), even in m-CLEAs form (approximately 50 % lower than with free laccase). Hydrolysis enhancement is rarely reported in literature, most laccases decrease sugar titer, as cellulase is a major factor in the production costs, these results are promising. SSFD experiments need further optimization; the late cell growth has to be overcome. Phenolic evolution during SSD and SSFD did resemble the Michaelis-Menten type of evolution recorded in XRF-laccase reactions, suggesting that the presence of the solid phase altered the reaction significantly, thus XRF-laccase detoxification cannot be used for screening experiments.

Minimum sugar revenue (MSR) estimations showed that an approximate 8-fold cellulase activity increase would be needed to be compatible with current corn derived sugar at current enzyme unit price (20 $/kg$_{protein}$), while in case of m-CLEAs cellulase 1.6-fold increase could be sufficient. At 10 $/kg$_{protein}$ cellulase unit price 4-fold increase in case of free and 1.1-fold increase in case of m-CLEAS cellulase would be sufficient for feasibility. The model of Klein-Marcuschamer and current amylase prices suggest that the enzyme unit price will not decrease under 10-15 $/kg$_{protein}$. Currently cellulase has to be used about 70-fold higher ratio than amylase/starch ratio. While this level will be difficult to reach, as lignocellulose is a more complex/recalcitrant material, 10-fold decrease in the utilized ratio seems plausible.

Although m-CLEAs utilization seems promising, the model used for m-CLEAs estimation is rather simple, further research should be done to investigate the activity decrease during recycling rounds, the recovery yield in bigger scale, and the cost of immobilization. The high enzyme loading, remarkable recovery of m-CLEAs from the

fermentation broth, together with their adsorption capacity, makes them well suited for industrialization. Magnetic separation of m-CLEAs' was proven to be efficient, but whether enzyme immobilization should be used at all will depend on further research investigating the stability during recovery cycles.

Laccase utilization, until cellulase cost does not decrease, would only be possible if the hydrolysis enhancement would be >100 %, thus it would decrease cellulase costs. Cellulase-laccase interaction should be assessed already during screening of laccase. Since cellulase and laccase are both enzymes, they can be combined in a single product after determining their ideal ratio. It was shown that the presence of solids significantly alters the laccase-catalyzed phenolics reaction, thus the ideal screening would be done directly in a SSFD experiment to compare the yields, or at least an SSD.

According to the results, the best practice for SSFD would be to start with added bacterial laccase and cellulase at pH 8, 50 °C and aeration. Until a certain time (to be optimized later), the pH has to be kept at 8, afterwards the pH control stopped and the reaction itself will shift the pH back to fermentation-range. The temperature should be decreased to SSF range and the aeration stopped when the sugar concentration increase starts to decrease, and inoculation done in such a time that the exponential phase is reached when the sugar concentration starts to saturate. Adapted inoculum should be used as its superior performance was proved. The SSF temperature should be sub-lethal to the microorganism, but more in favor of hydrolysis than fermentation. Cellulase activity is limiting (linear) compared to cell-growth (exponential). The steps on how to determine the parameters is discussed in Section 7.3.

7.2 Situating the research

This research was started in 2012 and the experimental part finished in 2016. Novozymes CellicCTEC3 HS application document [240] contains the process description of SSF with pre hydrolysis, named hybrid hydrolysis and fermentation (HHF). This specific document is from 2017, could be that the process was included few years prior, but it is visible that it appeared as standard during the time of this research. Moreno's paper [157] about SSF with bacterial laccase, and the enhancing effect on hydrolysis was published after the end of the experimental chapter and much later than the time these concrete experiments were performed. The exact bacterial laccase used in the experiments is a new product of the company, not yet on the market. The idea of the m-CLEAs immobilization method was also very new, the company and our

research group came to the idea nearly simultaneously. The remarkably high catalyst recovery from the SSF broth was unexpected for both of us. Immobilized enzyme cost estimation was not published in literature before, as well as the method for adsorption estimation model during recycling rounds.

7.3 Future steps for industrial application

The reduction in cellulase costs is not expected to happen rapidly, thus most probably 2G ethanol production will not be feasible economically in the near future without either external parameters (tax reduction, carbon quota) or significant increase in 1G substrate stock price. Biotechnology is expensive. Many trials are needed for screening. These two parameters hinder development, lowering costs and used material amounts, designing simple equipment and in general open-source attitude would be welcomed in the field.

The proposed future directions are addressing the fields of cost reduction and enzyme utilization. Other options are finding better laccases via screening, cost reduction of screening and further investigating m-CLEAs for SSF process.

For immobilization further assessment of immobilization deactivation, stability during recycling rounds and recycling efficiency is needed. An option for increasing activity is to decrease particle size, but this decreases recycling efficiency, thus activity and recycling should be investigated in pair. Laccase screening has to be performed as close as the exact utilization as possible, thus at least during SSD or preferably SSFD. A single run of SSFD in a reactor requires around one kg of material and around a week of fermentation time, and because of the price of the fermenter, replications are difficult to perform. Appendix contains an open source, lab-scale equipment description for SSD or SSFD, where a reactor would cost around 50 € and 100 g of substrate is enough for an experiment, thus several parallels can be run simultaneously. Appendix also contains a description for lime addition; this can be used for bigger reactors to utilize lime instead of NaOH or KOH, closer to the parameters used in industry. Finally, a method to estimate close optimal parameters for a big reactor run from the results measured during smaller reactor experiments is presented in Section 0.

SSFD mathematical calculation

This section describes a method to calculate the close optimal parameters for SSFD, based on small SSFD experiments. The following principles were taken into consideration: **reach titer** (given), **reach certain volumetric productivity or fermentation time** (independent) and **reduce costs (enzyme)** (dependent). The titer comes from the product purification step, 100 g/l for lactic acid. The volumetric productivity or the fermentation time (the two are equivalent as V_{prod}=titer/time), is a subjective parameter, how long should a fermentation take. Shorter time will require more enzymes (raises variable costs); longer time will require more/bigger fermenters for a unit of product flux (raises CAPEX). After the titer and fermentation time is chosen, the cellulase concentration can be calculated.

As significant portion of the product selling price comes from cellulase, it is wise to decrease its (needed) amount. Two things could be done: use cellulase optimum parameters (T, pH) if possible, avoid anything that inhibits it (laccase, end-product inhibition). From the first term it is visible that the initial parameters for the hydrolysis should be that of (or close to) cellulase optimum. Coming from the second term it is visible that any laccase that inhibits cellulase activity is problematic (*C. unicolor* laccase), while anything that helps it is welcomed (bacterial laccase); to quantify it fast screening SSD can be done. Coming from the second term it is also visible that for optimum performance glucose should be consumed once end-product inhibition is becoming significant, or with other words, the microorganism growth should reach exponential growth phase when end-product inhibition would start.

Fermentation can (and will) require different temperature and pH compared to hydrolysis. As the microorganism growth is exponential, except for a short period at the time during lag phase, but the hydrolysis rate is (close) linear to cellulase amount, it is evident that the fermentation time will be dependent on the cellulase action rather than the microorganism. With other words, the microorganism in general can consume the sugars much faster than cellulase can produce them. Therefore, the fermentation parameters (P_{ferm}= [temperature, pH]) should be chosen as closer to hydrolysis optimum (P_{hydro}) as possible, but still durable for the microorganism, optimal growth is not determining.

P_{ferm} can be determined, but it is not as good as if it would be determined via SSF/SSFD. The time (t_{growth}) when the microorganism should be in exponential phase can be calculated based on the following principles: hydrolysis rate will be lower (equal in best

case) at P_{ferm}, so ideally t_{growth} is the moment when the end product inhibition will decrease the hydrolysis rate at P_{hydro} to the maximum hydrolysis rate at P_{ferm}, before that it does not make any sense to change. Alternatively, a threshold can be used, for example, when the hydrolysis yield goes under 0.8 of the maximum hydrolysis rate at P_{ferm}. To determine $t_{inoculation}$, the lag phase should be deduced, for which example SSFD fermentation is needed. This will alter the hydrolysis also as from $t_{inoculation}$ time the parameters are changed from P_{hydro} to P_{ferm}, but the difference caused by this will alter t_{growth} minimally.

There are three important parameters in combination with inoculation: $t_{inoculation}$, $V_{inoculation}$ and t_{growth}. t_{growth} comes out of the previous calculation, while there can be potentially infinite numbers of $t_{inoculation}$- $V_{inoculation}$ pairs belonging to a single t_{growth} value. Industrially $V_{inoculum}$ should be between 1-10 v/v%, and the corresponding $t_{inoculation}$ should be determined by measuring few SSFD runs at different values (example 0.01, 0.05, 0.10). The curve should be monotone increasing, but linearity cannot be assumed. With this method, most of the parameters are determined in the close to optimal range.

Experimental wise it is better to choose $t_{fermentation}$ as initial input parameter, as it should fit in five working days, but investigation wise it would be interesting to see a map with different enzyme concentrations, as they are the most cost determining components.

REFERENCES

[1] A. J. Amstrong and J. Hamrin, *The Renewable Energy Policy Manual*. 1999.

[2] L. Wu, T. Moteki, A. A. Gokhale, D. W. Flaherty, and F. D. Toste, "Production of Fuels and Chemicals from Biomass: Condensation Reactions and Beyond," *Chem*, vol. 1, no. 1, pp. 32–58, Jul. 2016.

[3] S. Q. Tian, R. Y. Zhao, and Z. C. Chen, "Review of the pretreatment and bioconversion of lignocellulosic biomass from wheat straw materials," *Renewable and Sustainable Energy Reviews*, vol. 91. Elsevier Ltd, pp. 483–489, 01-Aug-2018.

[4] M. Balat, "Production of bioethanol from lignocellulosic materials via the biochemical pathway: A review," *Energy Convers. Manag.*, vol. 52, no. 2, pp. 858–875, Feb. 2011.

[5] A. Limayem and S. C. Ricke, "Lignocellulosic biomass for bioethanol production: Current perspectives, potential issues and future prospects," *Progress in Energy and Combustion Science*, vol. 38, no. 4. pp. 449–467, Aug-2012.

[6] L. Olsson and B. Hahn-Hägerdal, "Fermentation of lignocellulosic hydrolysates for ethanol production," *Enzyme Microb. Technol.*, vol. 18, no. 5, pp. 312–331, Apr. 1996.

[7] S. H. Mood *et al.*, "Lignocellulosic biomass to bioethanol, a comprehensive review with a focus on pretreatment," *Renew. Sustain. Energy Rev.*, vol. 27, pp. 77–93, Nov. 2013.

[8] "Startseite | Max-Planck-Institut für Kohlenforschung." [Online]. Available: https://www.kofo.mpg.de/de. [Accessed: 13-Feb-2019].

[9] Z. Jin, K. S. Katsumata, T. B. T. Lam, and K. Iiyama, "Covalent linkages between cellulose and lignin in cell walls of coniferous and nonconiferous woods," *Biopolymers*, vol. 83, no. 2, pp. 103–110, Oct. 2006.

[10] V. Menon and M. Rao, "Trends in bioconversion of lignocellulose: Biofuels, platform chemicals & biorefinery concept," *Prog. Energy Combust. Sci.*, vol. 38, no. 4, pp. 522–550, Aug. 2012.

[11] P. Sannigrahi, "Poplar as a feedstock for biofuels: a review of compositional characteristics," *Biofuels, Bioprod. …*, pp. 209–226, 2010.

[12] J. Wang, J. Feng, W. Jia, S. Chang, S. Li, and Y. Li, "Lignin engineering through laccase modification: A promising field for energy plant improvement," *Biotechnol. Biofuels*, vol. 8, no. 1, 2015.

[13] S. Berthet *et al.*, "Disruption of LACCASE4 and 17 Results in Tissue-Specific Alterations to Lignification of Arabidopsis thaliana Stems," *Plant Cell*, vol. 23, no. 3, pp. 1124–1137, Mar. 2011.

[14] M. Özparpucu *et al.*, "Unravelling the impact of lignin on cell wall mechanics: a comprehensive study on young poplar trees downregulated for CINNAMYL

ALCOHOL DEHYDROGENASE (CAD)," *Plant J.*, vol. 91, no. 3, pp. 480–490, 2017.

[15] M. de L. S. Saleme *et al.*, "Silencing CAFFEOYL SHIKIMATE ESTERASE affects lignification and improves saccharification," *Plant Physiol.*, p. pp.00920.2017, 2017.

[16] R. Van Acker *et al.*, "Different Routes for Conifer- and Sinapaldehyde and Higher Saccharification upon Deficiency in the Dehydrogenase CAD1.," *Plant Physiol.*, vol. 175, no. 3, pp. 1018–1039, Nov. 2017.

[17] M. A. Abdel-Rahman, Y. Tashiro, and K. Sonomoto, "Lactic acid production from lignocellulose-derived sugars using lactic acid bacteria: Overview and limits," *J. Biotechnol.*, vol. 156, no. 4, pp. 286–301, Dec. 2010.

[18] N. Sarkar, S. K. Ghosh, S. Bannerjee, and K. Aikat, "Bioethanol production from agricultural wastes: An overview," *Renew. Energy*, vol. 37, no. 1, pp. 19–27, Jan. 2012.

[19] N. Mosier *et al.*, "Features of promising technologies for pretreatment of lignocellulosic biomass," *Bioresour. Technol.*, vol. 96, no. 6, pp. 673–686, Apr. 2005.

[20] H. Jørgensen, J. B. Kristensen, and C. Felby, "Enzymatic conversion of lignocellulose into fermentable sugars: challenges and opportunities," *Biofuels, Bioprod. Biorefining*, vol. 1, no. 2, pp. 119–134, Oct. 2007.

[21] P. Alvira, E. Tomás-Pejó, M. Ballesteros, and M. Negro, "Pretreatment technologies for an efficient bioethanol production process based on enzymatic hydrolysis: a review," *Bioresour. Technol.*, vol. 101, pp. 4851–4861, 2010.

[22] P. Kumar, D. M. D. Barrett, M. J. Delwiche, and P. Stroeve, "Methods for pretreatment of lignocellulosic biomass for efficient hydrolysis and biofuel production," *Ind. Eng. Chem.*, vol. 48, no. 8, pp. 3713–3729, 2009.

[23] M. Prussi, S. Ferrero, L. Oriani, P. Ottonello, P. Torre, and F. Cherchi, "Review of pretreatment processes for lignocellulosic ethanol production, and development of an innovative method," *Biomass and Bioenergy*, vol. 46, pp. 25–35, Nov. 2012.

[24] J. Q. Bond *et al.*, "Production of renewable jet fuel range alkanes and commodity chemicals from integrated catalytic processing of biomass," *Energy Environ. Sci.*, vol. 7, no. 4, pp. 1500–1523, Mar. 2014.

[25] T. Pielhop, J. Amgarten, P. R. Von Rohr, and M. H. Studer, "Steam explosion pretreatment of softwood: The effect of the explosive decompression on enzymatic digestibility," *Biotechnol. Biofuels*, vol. 9, no. 1, pp. 1–13, 2016.

[26] C.-M. S. and P. R. von R. Thomas Pielhopa, Gastón O. Larrazábalb, Michael H. Studerc, Simone Brethauerc, "Lignin repolymerisation in spruce autohydrolysis pretreatment increases cellulase deactivation," *Int. J. Psychosoc. Rehabil.*, vol. 20, no. 2, pp. 25–33, 2016.

[27] S. Di Risio, C. Hu, and B. Saville, "Large-scale, high-solids enzymatic hydrolysis of steam-exploded poplar," *Biofuels, Bioprod. …*, vol. 5, pp. 609–620, 2011.

[28] Y. He, L. Zhang, J. Zhang, and J. Bao, "Helically agitated mixing in dry dilute acid

pretreatment enhances the bioconversion of corn stover into ethanol," *Biotechnol. Biofuels*, vol. 7, no. 1, pp. 1–13, 2014.

[29] A. Boussaid and A. Esteghlalian, "Steam pretreatment of Douglas-fir wood chips," *Twenty-First Symp. …*, vol. 84, 2000.

[30] Y. Zhang, X. Fu, and H. Chen, "Pretreatment based on two-step steam explosion combined with an intermediate separation of fiber cells--optimization of fermentation of corn straw hydrolysates.," *Bioresour. Technol.*, vol. 121, pp. 100–4, Oct. 2012.

[31] S. . Shevchenko, K. Chang, J. Robinson, and J. . Saddler, "Optimization of monosaccharide recovery by post-hydrolysis of the water-soluble hemicellulose component after steam explosion of softwood chips," *Bioresour. Technol.*, vol. 72, no. 3, pp. 207–211, May 2000.

[32] W. K. El-Zawawy, M. M. Ibrahim, Y. R. Abdel-Fattah, N. A. Soliman, and M. M. Mahmoud, "Acid and enzyme hydrolysis to convert pretreated lignocellulosic materials into glucose for ethanol production," *Carbohydr. Polym.*, vol. 84, no. 3, pp. 865–871, Mar. 2011.

[33] H. Kobayashi, H. Kaiki, A. Shrotri, K. Techikawara, and A. Fukuoka, "Hydrolysis of woody biomass by a biomass-derived reusable heterogeneous catalyst," *Chem. Sci.*, vol. 7, no. 1, pp. 692–696, Dec. 2016.

[34] R. Kumar, S. Singh, and O. V. Singh, "Bioconversion of lignocellulosic biomass: biochemical and molecular perspectives," *J. Ind. Microbiol. Biotechnol.*, vol. 35, no. 5, pp. 377–391, May 2008.

[35] J. S. Van Dyk and B. I. Pletschke, "A review of lignocellulose bioconversion using enzymatic hydrolysis and synergistic cooperation between enzymes—Factors affecting enzymes, conversion and synergy," *Biotechnol. Adv.*, vol. 30, no. 6, pp. 1458–1480, Nov. 2012.

[36] E. Palmqvist and B. Hahn-Hägerdal, "Fermentation of lignocellulosic hydrolysates. I: inhibition and detoxification," *Bioresour. Technol.*, vol. 74, no. 1, pp. 17–24, Aug. 2000.

[37] J. Olofsson, Z. Barta, P. Börjesson, and O. Wallberg, "Integrating enzyme fermentation in lignocellulosic ethanol production: Life-cycle assessment and techno-economic analysis," *Biotechnol. Biofuels*, vol. 10, no. 1, pp. 1–14, 2017.

[38] Y. Zheng, Z. Pan, and R. Zhang, "Overview of biomass pretreatment for cellulosic ethanol production," *Int. J. Agric. Biol. Eng.*, vol. 2, no. 3, pp. 51–68, 2009.

[39] J. R. Almeida, T. Modig, A. Petersson, B. Hähn-Hägerdal, G. Lidén, and M. F. Gorwa-Grauslund, "Increased tolerance and conversion of inhibitors in lignocellulosic hydrolysates bySaccharomyces cerevisiae," *J. Chem. Technol. Biotechnol.*, vol. 82, no. 4, pp. 340–349, Apr. 2007.

[40] F. M. Gírio, C. Fonseca, F. Carvalheiro, L. C. Duarte, S. Marques, and R. Bogel-Łukasik, "Hemicelluloses for fuel ethanol: A review," *Bioresour. Technol.*, vol. 101, no. 13, pp. 4775–4800, Jul. 2010.

[41] B. Erdei, B. Frankó, M. Galbe, and G. Zacchi, "Glucose and xylose co-fermentation of pretreated wheat straw using mutants of S. cerevisiae

TMB3400," *J. Biotechnol.*, vol. 164, no. 1, pp. 50–58, Mar. 2013.

[42] E. Palmqvist, H. Grage, N. Q. Meinander, and B. Hahn-Hägerdal, "Main and interaction effects of acetic acid, furfural, and p-hydroxybenzoic acid on growth and ethanol productivity of yeasts.," *Biotechnol. Bioeng.*, vol. 63, no. 1, pp. 46–55, Apr. 1999.

[43] B. Erdei, B. Frankó, M. Galbe, and G. Zacchi, "Separate hydrolysis and co-fermentation for improved xylose utilization in integrated ethanol production from wheat meal and wheat straw," *Biotechnol. Biofuels*, vol. 5, no. 1, p. 12, Mar. 2012.

[44] S. K. Saggi and P. Dey, "An overview of simultaneous saccharification and fermentation of starchy and lignocellulosic biomass for bio-ethanol production," *Biofuels*, no. September 2016, pp. 1–13, 2016.

[45] J. Hou, F. Suo, C. Wang, X. Li, Y. Shen, and X. Bao, "Fine-tuning of NADH oxidase decreases byproduct accumulation in respiration deficient xylose metabolic Saccharomyces cerevisiae," *BMC Biotechnol.*, vol. 14, no. 1, pp. 1–10, 2014.

[46] S. Krahulec, R. Kratzer, K. Longus, and B. Nidetzky, "Comparison of Scheffersomyces stipitis strains CBS 5773 and CBS 6054 with regard to their xylose metabolism: implications for xylose fermentation.," *Microbiologyopen*, vol. 1, no. 1, pp. 64–70, Mar. 2012.

[47] C. P. Kurtzman, J. W. Fell, and T. Boekhout, *The yeasts : a taxonomic study*. Elsevier Science, 2011.

[48] F. K. Agbogbo, G. Coward-Kelly, M. Torry-Smith, and K. S. Wenger, "Fermentation of glucose/xylose mixtures using Pichia stipitis," *Process Biochem.*, vol. 41, no. 11, pp. 2333–2336, 2006.

[49] A. D. Moreno, D. Ibarra, I. Ballesteros, A. González, and M. Ballesteros, "Comparing cell viability and ethanol fermentation of the thermotolerant yeast Kluyveromyces marxianus and Saccharomyces cerevisiae on steam-exploded biomass treated with laccase," *Bioresour. Technol.*, vol. 135, pp. 239–245, May 2013.

[50] J. P. Buyondo and S. Liu, "Lactic acid production by lactobacillus pentosus from wood extract hydrolysates," *J-for*, vol. 1, no. 3, pp. 38–47, 2011.

[51] A. M. Boguta, F. Bringel, J. Martinussen, and P. R. Jensen, "Screening of lactic acid bacteria for their potential as microbial cell factories for bioconversion of lignocellulosic feedstocks," *Microb. Cell Fact.*, vol. 13, no. 1, p. 97, Dec. 2014.

[52] K. Hofvendahl and B. Hahn–Hägerdal, "Factors affecting the fermentative lactic acid production from renewable resources1," *Enzyme Microb. Technol.*, vol. 26, no. 2–4, pp. 87–107, 2000.

[53] G. Bustos, A. B. Moldes, J. M. Cruz, and J. M. Domínguez, "Production of fermentable media from vine-trimming wastes and bioconversion into lactic acid by Lactobacillus pentosus," *J. Sci. Food Agric.*, vol. 84, no. 15, pp. 2105–2112, Dec. 2004.

[54] A. Ishizaki, T. Ueda, K. Tanaka, and P. F. Stanbury, "L-lactate production from

xylose employingLactococcus lactis IO-1," *Biotechnol. Lett.*, vol. 14, no. 7, pp. 599–604, Jul. 1992.

[55] M. A. Patel *et al.*, "Isolation and characterization of acid-tolerant, thermophilic bacteria for effective fermentation of biomass-derived sugars to lactic acid.," *Appl. Environ. Microbiol.*, vol. 72, no. 5, pp. 3228–35, May 2006.

[56] M. Oshiro *et al.*, "Kinetic modeling and sensitivity analysis of xylose metabolism in Lactococcus lactis IO-1," *J. Biosci. Bioeng.*, vol. 108, no. 5, pp. 376–384, Nov. 2009.

[57] J. A. Reis, A. T. Paula, S. N. Casarotti, and A. L. B. Penna, "Lactic Acid Bacteria Antimicrobial Compounds: Characteristics and Applications," *Food Eng. Rev.*, vol. 4, no. 2, pp. 124–140, Jun. 2012.

[58] A. J. Wolfe, "Glycolysis for Microbiome Generation," *Microbiol. Spectr.*, vol. 3, no. 3, Jun. 2015.

[59] Y. Wang, Y. Tashiro, and K. Sonomoto, "Fermentative production of lactic acid from renewable materials: Recent achievements, prospects, and limits," *J. Biosci. Bioeng.*, vol. 119, no. 1, pp. 10–18, 2015.

[60] G. P. Philippidis and T. K. Smith, "Limiting factors in the simultaneous saccharification and fermentation process for conversion of cellulosic biomass to fuel ethanol," *Appl. Biochem. Biotechnol.*, vol. 51–52, no. 1, pp. 117–124, Sep. 1995.

[61] S. Hari Krishna, T. Janardhan Reddy, and G. V. Chowdary, "Simultaneous saccharification and fermentation of lignocellulosic wastes to ethanol using a thermotolerant yeast," *Bioresour. Technol.*, vol. 77, no. 2, pp. 193–196, Apr. 2001.

[62] "Cellulosic ethanol Novozymes Cellic® CTec3 - Secure your plant's lowest total cost," 2009.

[63] M. S. Ou, N. Mohammed, L. O. Ingram, and K. T. Shanmugam, "Thermophilic Bacillus coagulans Requires Less Cellulases for Simultaneous Saccharification and Fermentation of Cellulose to Products than Mesophilic Microbial Biocatalysts," *Appl. Biochem. Biotechnol.*, vol. 155, no. 1–3, pp. 76–82, May 2009.

[64] M. S. Ou, L. O. Ingram, and K. T. Shanmugam, "L: (+)-Lactic acid production from non-food carbohydrates by thermotolerant Bacillus coagulans.," *J. Ind. Microbiol. Biotechnol.*, vol. 38, no. 5, pp. 599–605, May 2011.

[65] P. V. Iyer and Y. Y. Lee, "Product inhibition in simultaneous saccharification and fermentation of cellulose into lactic acid," *Biotechnol. Lett.*, vol. 21, no. 5, pp. 371–373, 1999.

[66] M. J. Torija, N. Rozès, M. Poblet, J. M. Guillamón, and A. Mas, "Effects of fermentation temperature on the strain population of Saccharomyces cerevisiae.," *Int. J. Food Microbiol.*, vol. 80, no. 1, pp. 47–53, Jan. 2003.

[67] A. Gladis, P. M. Bondesson, M. Galbe, and G. Zacchi, "Influence of different SSF conditions on ethanol production from corn stover at high solids loadings," *Energy Sci. Eng.*, vol. 3, no. 5, pp. 481–489, 2015.

[68] K. Ohgren, O. Bengtsson, M. F. Gorwa-Grauslund, M. Galbe, B. Hahn-Hägerdal,

and G. Zacchi, “Simultaneous saccharification and co-fermentation of glucose and xylose in steam-pretreated corn stover at high fiber content with Saccharomyces cerevisiae TMB3400.,” *J. Biotechnol.*, vol. 126, no. 4, pp. 488–98, Dec. 2006.

[69] F. Nielsen, G. Zacchi, M. Galbe, and O. Wallberg, “Sequential Targeting of Xylose and Glucose Conversion in Fed-Batch Simultaneous Saccharification and Co-fermentation of Steam-Pretreated Wheat Straw for Improved Xylose Conversion to Ethanol,” *Bioenergy Res.*, vol. 10, no. 3, pp. 800–810, 2017.

[70] A. Cavka, C. Martín, B. Alriksson, M. Mörtsell, and L. J. Jönsson, “Techno-economic evaluation of conditioning with sodium sulfite for bioethanol production from softwood,” *Bioresour. Technol.*, vol. 196, pp. 1–7, Nov. 2015.

[71] G. Liu, J. Sun, J. Zhang, Y. Tu, and J. Bao, “High titer l-lactic acid production from corn stover with minimum wastewater generation and techno-economic evaluation based on Aspen plus modeling,” *Bioresour. Technol.*, vol. 198, pp. 803–810, Dec. 2015.

[72] J. Zhang and J. Bao, “A modified method for calculating practical ethanol yield at high lignocellulosic solids content and high ethanol titer,” *Bioresour. Technol.*, vol. 116, pp. 74–79, 2012.

[73] L. R. Lynd, W. H. Van Zyl, J. E. McBride, and M. Laser, “Consolidated bioprocessing of cellulosic biomass: An update,” *Curr. Opin. Biotechnol.*, vol. 16, no. 5, pp. 577–583, 2005.

[74] Q. Xu, A. Singh, and M. E. Himmel, “Perspectives and new directions for the production of bioethanol using consolidated bioprocessing of lignocellulose,” *Curr. Opin. Biotechnol.*, vol. 20, no. 3, pp. 364–371, Jun. 2009.

[75] B. Hahn-Hägerdal, M. Galbe, M. F. Gorwa-Grauslund, G. Lidén, and G. Zacchi, “Bio-ethanol – the fuel of tomorrow from the residues of today,” *Trends Biotechnol.*, vol. 24, no. 12, pp. 549–556, Dec. 2006.

[76] S. Kok, R. Lobbes, A. De Jong, and B. De Vegt, “Process for the removal of undesired flavour and odour components from potassium lactate,” US7588790B2, 02-Sep-2004.

[77] A. M. Baniel *et al.*, “Lactic acid production, separation and/or recovery process,” US5510526A, 1996.

[78] J. Van Breugel, J. Van Krieken, A. C. Baró, J. M. Vidal Lancis, and M. Camprubi Vila, “Method of industrial-scale purification of lactic acid,” US6630603B1, 21-Mar-2000.

[79] J. Van Krieken, “Method for the purification of an alpha-hydroxy acid on an industrial scale,” US7002039B2, 14-Sep-2001.

[80] P. Coszach, J.-C. Bogaert, P.-A. Mariage, A. Chianese, and M.-P. Parisi, “Method of purifying lactic acid by crystallization,” US8471062B2, 18-Nov-2009.

[81] A. Chandel, S. da Silva, and O. Singh, “Detoxification of lignocellulosic hydrolysates for improved bioethanol production,” *Biofuel Prod. …*, 2011.

[82] J. . Parajo, H. Dominguez, and J. . Dominguez, “Biotechnological production of

xylitol . Part 3: operation in culture media made from lignocellulose hydrolysates," *Bioresour. Technol.*, vol. 66, pp. 25–40, 1998.

[83] E. Palmqvist and B. Hahn-Hägerdal, "Fermentation of lignocellulosic hydrolysates. II: inhibitors and mechanisms of inhibition," *Bioresour. Technol.*, vol. 74, no. 1, pp. 25–33, Aug. 2000.

[84] S. I. Mussatto and I. C. Roberto, "Alternatives for detoxification of diluted-acid lignocellulosic hydrolyzates for use in fermentative processes: a review.," *Bioresour. Technol.*, vol. 93, no. 1, pp. 1–10, May 2004.

[85] L. J. Jönsson and C. Martín, "Pretreatment of lignocellulose: Formation of inhibitory by-products and strategies for minimizing their effects," *Bioresour. Technol.*, vol. 199, pp. 103–112, Jan. 2016.

[86] M. Yajima and K. Yokotsuka, "Volatile compound formation in white wines fermented using immobilized and free yeast," *Am. J. Enol. Vitic.*, vol. 52, no. 3, pp. 210–218, 2001.

[87] A. K. Chandel, S. S. Silva, and O. V. Singh, "Detoxification of Lignocellulose Hydrolysates: Biochemical and Metabolic Engineering Toward White Biotechnology," *BioEnergy Res.*, vol. 6, no. 1, pp. 388–401, Aug. 2012.

[88] A. H. Stouthamer, "The search for correlation between theoretical and experimental growth yields," *Quayle, J R (Ed) Int. Rev. Biochem. Vol*, vol. 21 Micr, no. Ed, p. Baltimore, Md , Usa Illus P1-48, 1979.

[89] C. Verduyn, E. Postma, W. A. Scheffers, and J. P. Van Dijken, "Effect of benzoic acid on metabolic fluxes in yeasts: A continuous-culture study on the regulation of respiration and alcoholic fermentation," *Yeast*, vol. 8, no. 7, pp. 501–517, Jul. 1992.

[90] H. A. Krebs, D. Wiggins, M. Stubbs, A. Sols, and F. Bedoya, "Studies on the mechanism of the antifungal action of benzoate.," *Biochem. J.*, vol. 214, no. 3, pp. 657–63, Sep. 1983.

[91] A. Ullah, R. Orij, S. Brul, and G. J. Smits, "Quantitative analysis of the modes of growth inhibition by weak organic acids in Saccharomyces cerevisiae.," *Appl. Environ. Microbiol.*, vol. 78, no. 23, pp. 8377–87, Dec. 2012.

[92] J. P. Delgenes, R. Moletta, and J. M. Navarro, "Effects of lignocellulose degradation products on ethanol fermentations of glucose and xylose by Saccharomyces cerevisiae, Zymomonas mobilis, Pichia stipitis, and Candida shehatae," *Enzyme Microb. Technol.*, vol. 19, no. 3, pp. 220–225, Aug. 1996.

[93] S. Ando, I. Arai, and K. Kiyoto, "Identification of Aromatic Monomers in Steam-Exploded Poplar and Their Influences on Ethanol Fermenta- tion by Saccharomyces cerevisiae," vol. 64, no. 6, pp. 567–570, 1986.

[94] S. Larsson, A. Quintana-Sáinz, A. Reimann, N.-O. Nilvebrant, and L. J. Jönsson, "Influence of Lignocellulose-Derived Aromatic Compounds on Oxygen-Limited Growth and Ethanolic Fermentation by Saccharomyces cerevisiae," in *Twenty-First Symposium on Biotechnology for Fuels and Chemicals*, Totowa, NJ: Humana Press, 2000, pp. 617–632.

[95] A. D. Moreno, D. Ibarra, J. L. Fernández, and M. Ballesteros, "Different laccase detoxification strategies for ethanol production from lignocellulosic biomass by

the thermotolerant yeast Kluyveromyces marxianus CECT 10875," *Bioresour. Technol.*, vol. 106, pp. 101–9, Feb. 2012.

[96] H. B. Klinke, A. B. Thomsen, and B. K. Ahring, "Inhibition of ethanol-producing yeast and bacteria by degradation products produced during pre-treatment of biomass," *Appl. Microbiol. Biotechnol.*, vol. 66, no. 1, pp. 10–26, Nov. 2004.

[97] P. Villa *et al.*, "Influence of phenolic compounds on the bioprocess of xylitol production by Candida guilliermondii," in *Esbes-2 European symposium on biochemical engineering science, Porto*, 1998.

[98] A. V. Tran and R. P. Chambers, "Ethanol fermentation of red oak acid prehydrolysate by the yeast Pichia stipitis CBS 5776," *Enzyme Microb. Technol.*, vol. 8, no. 7, pp. 439–444, Jul. 1986.

[99] N. E. Watson, B. A. Prior, P. M. Lategan, and M. Lussi, "Factors in acid treated bagasse inhibiting ethanol production from d-xylose by Pachysolen tannophilus," *Enzyme Microb. Technol.*, vol. 6, no. 10, pp. 451–456, Oct. 1984.

[100] P. Alvira, M. Ballesteros, and M. J. Negro, "Progress on Enzymatic Saccharification Technologies for Biofuels Production," in *Biofuel Technologies*, Berlin, Heidelberg: Springer Berlin Heidelberg, 2013, pp. 145–169.

[101] L. J. Jönsson *et al.*, "Detoxification of wood hydrolysates with laccase and peroxidase from the white-rot fungus Trametes versicolor," *Appl. Microbiol. Biotechnol.*, vol. 49, no. 6, pp. 691–697, Jun. 1998.

[102] E. Ximenes, Y. Kim, N. Mosier, B. Dien, and M. Ladisch, "Deactivation of cellulases by phenols," *Enzyme Microb. Technol.*, vol. 48, no. 1, pp. 54–60, Jan. 2011.

[103] E. Ximenes, Y. Kim, N. Mosier, B. Dien, and M. Ladisch, "Inhibition of cellulases by phenols," *Enzyme Microb. Technol.*, vol. 46, no. 3–4, pp. 170–176, Mar. 2010.

[104] A. Cavka and L. J. Jönsson, "Detoxification of lignocellulosic hydrolysates using sodium borohydride," *Bioresour. Technol.*, vol. 136, pp. 368–376, May 2013.

[105] C. C. Geddes, I. U. Nieves, and L. O. Ingram, "Advances in ethanol production," *Curr. Opin. Biotechnol.*, vol. 22, no. 3, pp. 312–319, Jun. 2011.

[106] M. J. Taherzadeh, C. Niklasson, and G. Lidén, "On-line control of fed-batch fermentation of dilute-acid hydrolyzates," *Biotechnol. Bioeng.*, vol. 69, no. 3, pp. 330–338, Aug. 2000.

[107] N. O. Nilvebrant, a Reimann, S. Larsson, and L. J. Jönsson, "Detoxification of lignocellulose hydrolysates with ion-exchange resins.," *Appl. Biochem. Biotechnol.*, vol. 91–93, pp. 35–49, Jan. 2001.

[108] R. H. Leonard and G. J. Hajny, "Fermentation of Wood Sugars to Ethyl Alcohol.," *Ind. Eng. Chem.*, vol. 37, no. 4, pp. 390–395, Apr. 1945.

[109] J. W. Miller, "Adsorption Technology: A Step-by-Step Approach to Process Evaluation and Application," *J. Environ. Qual.*, vol. 15, no. 1, p. 94, 1986.

[110] S. I. Mussatto, "Influência do tratamento do hidrolisado hemicelulósico de palha de arroz na produção de xilitol por Candida guilliermondii," *São Paulo*,

2002.
[111] J. C. Parajó, H. Domínguez, and J. M. Domínguez, “Study of charcoal adsorption for improving the production of Xylitol from wood hydrolysates,” *Bioprocess Eng.*, vol. 16, no. 1, p. 39, 1996.
[112] J. C. Parajó, H. Domínguez, and J. M. Domínguez, “Charcoal adsorption of wood hydrolysates for improving their fermentability: Influence of the operational conditions,” *Bioresour. Technol.*, vol. 57, no. 2, pp. 179–185, Aug. 1996.
[113] S. S. d. Silva *et al.*, “Xylitol production by Candida guilliermondii FTI 20037 grown in pretreated sugar cane bagasse hydrolysate.” London (United Kingdom) James & James, 1998.
[114] W. G. Lee, J. S. Lee, C. S. Shin, S. C. Park, H. N. Chang, and Y. K. Chang, “Ethanol Production Using Concentrated Oak Wood Hydrolysates and Methods to Detoxify,” in *Twentieth Symposium on Biotechnology for Fuels and Chemicals*, Totowa, NJ: Humana Press, 1999, pp. 547–559.
[115] S. I. Mussatto and I. C. Roberto, “Hydrolysate detoxification with activated charcoal for xylitol production by Candida guilliermondii,” *Biotechnol. Lett.*, vol. 23, no. 20, pp. 1681–1684, 2001.
[116] A. D. Moreno, D. Ibarra, I. Ballesteros, J. L. Fernández, and M. Ballesteros, “Ethanol from laccase-detoxified lignocellulose by the thermotolerant yeast Kluyveromyces-Effects of steam pretreatment conditions, process configurations and substrate loadings,” *Biochem. Eng. J.*, vol. 79, pp. 94–103, Oct. 2013.
[117] M. Alkasrawi, A. Rudolf, G. Lidén, and G. Zacchi, “Influence of strain and cultivation procedure on the performance of simultaneous saccharification and fermentation of steam pretreated spruce,” *Enzyme Microb. Technol.*, vol. 38, no. 1–2, pp. 279–286, Jan. 2006.
[118] M. Fernández-Fernández, M. Á. Sanromán, and D. Moldes, “Recent developments and applications of immobilized laccase,” *Biotechnol. Adv.*, vol. 31, no. 8, pp. 1808–1825, Dec. 2013.
[119] L. Munk, A. K. Sitarz, D. C. Kalyani, J. D. Mikkelsen, and A. S. Meyer, “Can laccases catalyze bond cleavage in lignin?,” *Biotechnol. Adv.*, vol. 33, no. 1, pp. 13–24, Jan. 2015.
[120] H. Lange, S. Decina, and C. Crestini, “Oxidative upgrade of lignin – Recent routes reviewed,” *Eur. Polym. J.*, vol. 49, no. 6, pp. 1151–1173, Jun. 2013.
[121] P. Baldrian, “Fungal laccases – occurrence and properties,” *FEMS Microbiol. Rev.*, vol. 30, no. 2, pp. 215–242, Mar. 2006.
[122] J.-A. Majeau, S. K. Brar, and R. D. Tyagi, “Laccases for removal of recalcitrant and emerging pollutants,” *Bioresour. Technol.*, vol. 101, no. 7, pp. 2331–2350, Apr. 2010.
[123] J. Rogalski and A. Dawidowicz, “Immobilization of laccase from Cerrena unicolor on controlled porosity glass,” *J. Mol. …*, pp. 29–39, 1999.
[124] C. S. Karigar and S. S. Rao, “Role of microbial enzymes in the bioremediation of pollutants: a review.,” *Enzyme Res.*, vol. 2011, p. 805187, Sep. 2011.
[125] P. Widsten and A. Kandelbauer, “Laccase applications in the forest products

industry: A review," *Enzyme Microb. Technol.*, vol. 42, no. 4, pp. 293–307, Mar. 2008.

[126] S. Rodríguez Couto and J. L. Toca Herrera, "Industrial and biotechnological applications of laccases: A review," *Biotechnol. Adv.*, vol. 24, no. 5, pp. 500–513, Sep. 2006.

[127] D. Yinghui, W. Qiuling, and F. Shiyu, "Laccase stabilization by covalent binding immobilization on activated polyvinyl alcohol carrier," *Lett. Appl. Microbiol.*, vol. 35, no. 6, pp. 451–456, Dec. 2002.

[128] N. Miletić, A. Nastasović, and K. Loos, "Immobilization of biocatalysts for enzymatic polymerizations: Possibilities, advantages, applications," *Bioresour. Technol.*, vol. 115, pp. 126–135, Jul. 2012.

[129] M. Asgher, M. Shahid, S. Kamal, and H. M. N. Iqbal, "Recent trends and valorization of immobilization strategies and ligninolytic enzymes by industrial biotechnology," *J. Mol. Catal. B Enzym.*, vol. 101, pp. 56–66, Mar. 2014.

[130] R. A. Sheldon, "Cross-linked enzyme aggregates (CLEA®s): stable and recyclable biocatalysts," *Biochem. Soc. Trans.*, vol. 35, no. 6, pp. 1583–1587, 2007.

[131] R. A. Sheldon and S. van Pelt, "Enzyme immobilisation in biocatalysis: why, what and how," *Chem. Soc. Rev.*, vol. 42, no. 15, pp. 6223–6235, 2013.

[132] F. K. Kazi *et al.*, "Techno-economic comparison of process technologies for biochemical ethanol production from corn stover," *Fuel*, vol. 89, no. SUPPL. 1, pp. S20–S28, Nov. 2010.

[133] Z. Jian *et al.*, "Biodetoxification of toxins generated from lignocellulose pretreatment using a newly isolated fungus, Amorphotheca resinae ZN1, and the consequent ethanol fermentation," *Biotechnol. Biofuels*, vol. 3, no. 1, p. 26, Nov. 2010.

[134] E. Joelsson, B. Erdei, M. Galbe, and O. Wallberg, "Techno-economic evaluation of integrated first- and second-generation ethanol production from grain and straw," *Biotechnol. Biofuels*, vol. 9, no. 1, pp. 1–16, 2016.

[135] A. Wingren, J. Söderström, M. Galbe, and G. Zacchi, "Process considerations and economic evaluation of two-step steam pretreatment for production of fuel ethanol from softwood," *Biotechnol. Prog.*, vol. 20, no. 5, pp. 1421–1429, 2004.

[136] A. A. D. Humbird, R. Davis, L. Tao, C. Kinchin, D. Hsu, "Process Design and Economics for Biochemical Conversion of Lignocellulosic Biomass to Ethanol," 2011.

[137] P. Sassner, M. Galbe, and G. Zacchi, "Techno-economic evaluation of bioethanol production from three different lignocellulosic materials," *Biomass and Bioenergy*, vol. 32, no. 5, pp. 422–430, 2008.

[138] K. Gubicza, I. U. Nieves, W. J. Sagues, Z. Barta, K. T. Shanmugam, and L. O. Ingram, "Techno-economic analysis of ethanol production from sugarcane bagasse using a Liquefaction plus Simultaneous Saccharification and co-Fermentation process," *Bioresour. Technol.*, vol. 208, pp. 42–48, 2016.

[139] A. K. Chandel, O. V. Singh, G. Chandrasekhar, L. V. Rao, and M. L. Narasu, “Key drivers influencing the commercialization of ethanol-based biorefineries,” *Journal of Commercial Biotechnology*, vol. 16, no. 3. pp. 239–257, 2010.

[140] “Ethanol Market and Pricing Data - February 20, 2018 - U.S. GRAINS COUNCIL.” [Online]. Available: https://grains.org/ethanol_report/ethanol-market-and-pricing-data-february-20-2018/. [Accessed: 17-May-2019].

[141] “Manufacturers, Suppliers, Exporters & Importers from the world’s largest online B2B marketplace-Alibaba.com.” [Online]. Available: https://www.alibaba.com/. [Accessed: 22-Jun-2017].

[142] AGRI G 4 Committee for the Common Organisation of Agricultural Markets, “Sugar Market situation,” 2019.

[143] barchart, “Corn Mar ’19 (XBH19) Futures Price Quote - Barchart.com.” [Online]. Available: https://www.barchart.com/futures/quotes/XBH19. [Accessed: 14-Feb-2019].

[144] C. Reeb *et al.*, “Techno-economic analysis of various biochemical conversion platforms for biosugar production: Trade-offs of co-producing biopower versus pellets for either a greenfield, repurpose, or co-location siting context,” *Biofuels, Bioprod. Biorefining*, vol. 12, no. 3, pp. 390–411, May 2018.

[145] Y. Sun and J. Cheng, “Hydrolysis of lignocellulosic materials for ethanol production: a review,” *Bioresour. Technol.*, vol. 83, no. 1, pp. 1–11, May 2002.

[146] A. Wingren, M. Galbe, and G. Zacchi, “Techno-economic evaluation of producing ethanol from softwood: comparison of SSF and SHF and identification of bottlenecks.,” *Biotechnol. Prog.*, vol. 19, no. 4, pp. 1109–17, 2003.

[147] K. Olofsson, M. Bertilsson, and G. Lidén, “A short review on SSF – an interesting process option for ethanol production from lignocellulosic feedstocks,” *Biotechnol. Biofuels*, vol. 1, no. 1, p. 7, May 2008.

[148] K. Hoyer, M. Galbe, and G. Zacchi, “Influence of fiber degradation and concentration of fermentable sugars on simultaneous saccharification and fermentation of high-solids spruce slurry to ethanol,” *Biotechnol. Biofuels*, vol. 6, no. 1, p. 145, 2013.

[149] W. D. Huang and Y. H. Percival Zhang, “Analysis of biofuels production from sugar based on three criteria: Thermodynamics, bioenergetics, and product separation,” *Energy Environ. Sci.*, vol. 4, no. 3, pp. 784–792, 2011.

[150] A. Komesu, M. R. Wolf Maciel, and R. Maciel Filho, “Separation and Purification Technologies for Lactic Acid – A Brief Review,” *BioResources*, vol. 12, no. 3, pp. 6885–6901, Aug. 2017.

[151] E. Heinzle, A. P. Biwer, and C. L. Cooney, “Development of sustainable bioprocesses.” John Wiley & Sons, 2006.

[152] A. D. Resources, “2016 BILLION-TON REPORT,” vol. I, no. July, 2016.

[153] M. De La Torre *et al.*, “Comparison of the efficiency of bacterial and fungal laccases in delignification and detoxification of steam-pretreated lignocellulosic biomass for bioethanol production,” *J. Ind. Microbiol. Biotechnol.*, vol. 44, no. 11, pp. 1561–1573, Nov. 2017.

[154] M. Kolb, V. Sieber, M. Amann, M. Faulstich, and D. Schieder, “Removal of monomer delignification products by laccase from Trametes versicolor.,” *Bioresour. Technol.*, vol. 104, pp. 298–304, Jan. 2012.

[155] D. Kalyani, S. S. Dhiman, H. Kim, M. Jeya, I. W. Kim, and J. K. Lee, “Characterization of a novel laccase from the isolated Coltricia perennis and its application to detoxification of biomass,” *Process Biochem.*, vol. 47, no. 4, pp. 671–678, 2012.

[156] A. D. Moreno, D. Ibarra, P. Alvira, E. Tomás-Pejó, and M. Ballesteros, “Exploring laccase and mediators behavior during saccharification and fermentation of steam-exploded wheat straw for bioethanol production,” *J. Chem. Technol. Biotechnol.*, vol. 91, no. 6, pp. 1816–1825, Jun. 2016.

[157] A. Moreno, D. Ibarra, A. Mialon, and M. Ballesteros, “A Bacterial Laccase for Enhancing Saccharification and Ethanol Fermentation of Steam-Pretreated Biomass,” *Fermentation*, vol. 2, no. 2, p. 11, 2016.

[158] Ú. Fillat, D. Ibarra, M. Eugenio, A. Moreno, E. Tomás-Pejó, and R. Martín-Sampedro, “Laccases as a Potential Tool for the Efficient Conversion of Lignocellulosic Biomass: A Review,” *Fermentation*, vol. 3, no. 2, p. 17, 2017.

[159] K. Shuttleworth and J. Bollag, “Soluble and immobilized laccase as catalysts for the transformation of substituted phenols,” *Enzyme Microb. Technol.*, vol. 8, pp. 171–177, 1986.

[160] A. Salis, M. Pisano, and M. Monduzzi, “Laccase from Pleurotus sajor-caju on functionalised SBA-15 mesoporous silica: Immobilisation and use for the oxidation of phenolic compounds,” *J. Mol. …*, vol. 58, pp. 175–180, 2009.

[161] J. Ihssen, M. Schubert, L. Thöny-Meyer, and M. Richter, “Laccase catalyzed synthesis of iodinated phenolic compounds with antifungal activity.,” *PLoS One*, vol. 9, no. 3, p. e89924, Jan. 2014.

[162] A. Blainski, G. C. Lopes, and J. C. P. de Mello, “Application and analysis of the folin ciocalteu method for the determination of the total phenolic content from Limonium brasiliense L.,” *Molecules*, vol. 18, no. 6, pp. 6852–65, Jan. 2013.

[163] M. Jurado, A. Prieto, A. Martínez-Alcalá, A. T. Martínez, and M. J. Martínez, “Laccase detoxification of steam-exploded wheat straw for second generation bioethanol.,” *Bioresour. Technol.*, vol. 100, no. 24, pp. 6378–84, Dec. 2009.

[164] P. Peralta-Zamora and C. Pereira, “Decolorization of reactive dyes by immobilized laccase,” *Appl. Catal. B …*, vol. 42, pp. 131–144, 2003.

[165] P. Champagne and J. Ramsay, “Reactive blue 19 decolouration by laccase immobilized on silica beads,” *Appl. Microbiol. Biotechnol.*, vol. 19, pp. 819–823, 2007.

[166] J. Osma, J. Toca-Herrera, and S. Rodríguez-Couto, “Transformation pathway of Remazol Brilliant Blue R by immobilised laccase,” *Bioresour. Technol.*, vol. 101, pp. 8509–8514, 2010.

[167] J. M. Bollag, K. L. Shuttleworth, and D. H. Anderson, “Laccase-mediated detoxification of phenolic compounds.,” *Appl. Environ. Microbiol.*, vol. 54, no.

12, pp. 3086–3091, 1988.
[168] S. Kumar, “Spectroscopy of Organic Compounds,” 2006.
[169] V. Sóti, N. Jacquet, S. Apers, A. Richel, S. Lenaerts, and I. Cornet, “Monitoring the laccase reaction of vanillin and poplar hydrolysate,” *J. Chem. Technol. Biotechnol.*, vol. 91, no. 6, pp. 1914–1922, Jun. 2016.
[170] A. Gutiérrez *et al.*, “Demonstration of laccase-based removal of lignin from wood and non-wood plant feedstocks,” *Bioresour. Technol.*, vol. 119, pp. 114–22, Sep. 2012.
[171] W. H. Chen, C. C. Tsai, C. F. Lin, P. Y. Tsai, and W. S. Hwang, “Pilot-scale study on the acid-catalyzed steam explosion of rice straw using a continuous pretreatment system,” *Bioresour. Technol.*, vol. 128, pp. 297–304, 2013.
[172] P. N. Wahjudi, M. E. Patterson, S. Lim, J. K. Yee, C. S. Mao, and W.-N. P. Lee, “Measurement of glucose and fructose in clinical samples using gas chromatography/mass spectrometry,” *Clin. Biochem.*, vol. 43, no. 1–2, pp. 198–207, Jan. 2010.
[173] P. Lehtonen and R. Hurme, “LIQUID CHROMATOGRAPHIC DETERMINATION OF SUGARS IN BEER BY EVAPORATIVE LIGHT SCATTERING DETECTION,” *J. Inst. Brew.*, vol. 100, no. 5, pp. 343–346, Sep. 1994.
[174] J. M. Laplace, J. P. Delgenes, R. Moletta, and J. M. Navarro, “Cofermentation of glucose and xylose to ethanol by a respiratory-deficient mutant of Saccharomyces cerevisiae co-cultivated with a xylose-fermenting yeast,” *J. Ferment. Bioeng.*, vol. 75, no. 3, pp. 207–212, Jan. 1993.
[175] P. AAlvira, A. D. Moreno, D. Ibarra, F. Sáez, and M. Ballesteros, “Improving the fermentation performance of saccharomyces cerevisiae by laccase during ethanol production from steam-exploded wheat straw at high-substrate loadings,” *Biotechnol. Prog.*, vol. 29, no. 1, pp. 74–82, Jan. 2013.
[176] A. A. Modenbach and S. E. Nokes, “The use of high-solids loadings in biomass pretreatment-a review,” *Biotechnol. Bioeng.*, vol. 109, no. 6, pp. 1430–1442, 2012.
[177] N. Jacquet *et al.*, “Influence of steam explosion on the thermal stability of cellulose fibres,” *Polym. Degrad. Stab.*, vol. 96, no. 9, pp. 1582–1588, Sep. 2011.
[178] L. R. Lynd, P. J. Weimer, W. H. van Zyl, and I. S. Pretorius, “Microbial Cellulose Utilization: Fundamentals and Biotechnology,” *Microbiol. Mol. Biol. Rev.*, vol. 66, no. 3, pp. 506–577, Sep. 2003.
[179] C. Johannes and a Majcherczyk, “Laccase activity tests and laccase inhibitors.,” *J. Biotechnol.*, vol. 78, no. 2, pp. 193–9, Mar. 2000.
[180] S. Afreen *et al.*, “A novel multicopper oxidase (laccase) from cyanobacteria: Purification, characterization with potential in the decolorization of anthraquinonic dye,” *PLoS One*, vol. 12, no. 4, p. e0175144, Apr. 2017.
[181] M. Cantarella, L. Cantarella, A. Gallifuoco, A. Spera, and F. Alfani, “Effect of inhibitors released during steam-explosion treatment of poplar wood on subsequent enzymatic hydrolysis and SSF.,” *Biotechnol. Prog.*, vol. 20, no. 1, pp. 200–6, 2004.
[182] P. T. Pienkos and M. Zhang, “Role of pretreatment and conditioning processes

on toxicity of lignocellulosic biomass hydrolysates," *Cellulose*, vol. 16, no. 4, pp. 743–762, Jun. 2009.

[183] S. Constant, M. Robitzer, F. Quignard, and F. Di Renzo, "Vanillin oligomerization as a model of side reactions in lignin fragmentation," *Catal. Today*, vol. 189, no. 1, pp. 123–128, Jul. 2012.

[184] M. Lahtinen and P. Heinonen, "On the factors affecting product distribution in laccase-catalyzed oxidation of a lignin model compound vanillyl alcohol: experimental and computational," *Org. …*, pp. 5454–5464, 2013.

[185] A. Manole, D. Herea, H. Chiriac, and V. Melnig, "Laccase activity determination," *Cuza Univ. Sci. …*, no. 11, 2008.

[186] F. Cuyckens and M. Claeys, "Mass spectrometry in the structural analysis of flavonoids.," *J. Mass Spectrom.*, vol. 39, no. 1, pp. 1–15, Jan. 2004.

[187] I. RIVA, Sergio(Istituto di Chimica del Riconoscimento Molecolare C.N.R. Milano, "LACCASE MEDIATED OXIDATION OF PHENOLIC DERIVATIVES," 2014.

[188] J. Yu, K. E. Taylor, H. Zou, N. Biswas, and J. K. Bewtra, "Phenol Conversion and Dimeric Intermediates in Horseradish Peroxidase-Catalyzed Phenol Removal from Water," *Environ. Sci. Technol.*, vol. 28, no. 12, pp. 2154–2160, Nov. 1994.

[189] K. Rittstieg, a Suurnakki, T. Suortti, K. Kruus, G. Guebitz, and J. Buchert, "Investigations on the laccase-catalyzed polymerization of lignin model compounds using size-exclusion HPLC," *Enzyme Microb. Technol.*, vol. 31, no. 4, pp. 403–410, Sep. 2002.

[190] G. Ward, Y. Hadar, and C. G. Dosoretz, "Lignin peroxidase-catalyzed polymerization and detoxification of toxic halogenated phenols," *J. Chem. Technol. Biotechnol.*, vol. 78, no. 12, pp. 1239–1245, Dec. 2003.

[191] S. Larsson, A. Reimann, N.-O. Nilvebrant, and L. J. Jönsson, "Comparison of Different Methods for the Detoxification of Lignocellulose Hydrolyzates of Spruce," *Appl. Biochem. Biotechnol.*, vol. 77, no. 1–3, pp. 91–104, 1999.

[192] D. M. Mate and M. Alcalde, "Laccase: a multi-purpose biocatalyst at the forefront of biotechnology," *Microb. Biotechnol.*, vol. 10, no. 6, pp. 1457–1467, 2017.

[193] A. Steevensz, M. M. Al-Ansari, K. E. Taylor, J. K. Bewtra, and N. Biswas, "Comparison of soybean peroxidase with laccase in the removal of phenol from synthetic and refinery wastewater samples," *J. Chem. Technol. Biotechnol.*, vol. 84, no. 5, pp. 761–769, May 2009.

[194] I. Pardo, X. Chanagá, A. I. Vicente, M. Alcalde, and S. Camarero, "New colorimetric screening assays for the directed evolution of fungal laccases to improve the conversion of plant biomass," *BMC Biotechnol.*, vol. 13, 2013.

[195] F. Bettin, Q. Montanari, R. Calloni, T. A. Gaio, M. M. Silveira, and A. J. P. Dillon, "Production of laccases in submerged process by Pleurotus sajor-caju PS-2001 in relation to carbon and organic nitrogen sources, antifoams and Tween 80," *J. Ind. Microbiol. Biotechnol.*, vol. 36, no. 1, pp. 1–9, 2009.

[196] J. P. Ghosh, K. E. Taylor, J. K. Bewtra, and N. Biswas, "Laccase-catalyzed removal

of 2,4-dimethylphenol from synthetic wastewater: Effect of polyethylene glycol and dissolved oxygen," *Chemosphere*, vol. 71, no. 9, pp. 1709–17, Apr. 2008.

[197] R. Sheldon, "Enzyme immobilization: the quest for optimum performance," *Adv. Synth. Catal.*, 2007.

[198] C. Garcia-Galan, Á. Berenguer-Murcia, R. Fernandez-Lafuente, and R. C. Rodrigues, "Potential of different enzyme immobilization strategies to improve enzyme performance," *Adv. Synth. Catal.*, vol. 353, no. 16, pp. 2885–2904, 2011.

[199] J. Gao, L. Shi, Y. Jiang, L. Zhou, and Y. He, "Formation of lipase Candida sp. 99–125 CLEAs in mesoporous silica: characterization and catalytic properties," *Catal. Sci. Technol.*, vol. 3, no. 12, p. 3353, Nov. 2013.

[200] Y. Liu *et al.*, "Immobilization of laccase on magnetic bimodal mesoporous carbon and the application in the removal of phenolic compounds.," *Bioresour. Technol.*, vol. 115, pp. 21–6, Jul. 2012.

[201] G. Bayramoğlu and M. Y. Arica, "Enzymatic removal of phenol and p-chlorophenol in enzyme reactor: horseradish peroxidase immobilized on magnetic beads.," *J. Hazard. Mater.*, vol. 156, no. 1–3, pp. 148–55, Aug. 2008.

[202] H. Liao, D. Chen, L. Yuan, M. Zheng, Y. Zhu, and X. Liu, "Immobilized cellulase by polyvinyl alcohol/Fe2O3 magnetic nanoparticle to degrade microcrystalline cellulose," *Carbohydr. Polym.*, vol. 82, no. 3, pp. 600–604, 2010.

[203] J. Alftrén and T. J. Hobley, "Immobilization of cellulase mixtures on magnetic particles for hydrolysis of lignocellulose and ease of recycling," *Biomass and Bioenergy*, vol. 65, pp. 72–78, 2014.

[204] I. Matijošyte, I. W. C. E. Arends, S. de Vries, and R. a. Sheldon, "Preparation and use of cross-linked enzyme aggregates (CLEAs) of laccases," *J. Mol. Catal. B Enzym.*, vol. 62, no. 2, pp. 142–148, 2010.

[205] M. Tudorache, A. Nae, S. Coman, and V. I. Parvulescu, "Strategy of cross-linked enzyme aggregates onto magnetic particles adapted to the green design of biocatalytic synthesis of glycerol carbonate," *RSC Adv.*, vol. 3, no. 12, p. 4052, 2013.

[206] M. Vršanská, S. Voběrková, A. M. Jiménez Jiménez, V. Strmiska, and V. Adam, "Preparation and optimisation of cross-linked enzyme aggregates using native isolate white rot fungi Trametes versicolor and Fomes fomentarius for the decolourisation of synthetic dyes," *Int. J. Environ. Res. Public Health*, vol. 15, no. 1, pp. 1–15, 2018.

[207] Z. A. Sinirlioglu, D. Sinirlioglu, and F. Akbas, "Preparation and characterization of stable cross-linked enzyme aggregates of novel laccase enzyme from Shewanella putrefaciens and using malachite green decolorization," *Bioresour. Technol.*, vol. 146, pp. 807–811, 2013.

[208] N. A. Kalkan, S. Aksoy, E. A. Aksoy, and N. Hasirci, "Preparation of chitosan-coated magnetite nanoparticles and application for immobilization of laccase," *J. Appl. Polym. Sci.*, vol. 123, no. 2, pp. 707–716, Jan. 2012.

[209] V. V. Kumar, S. Sivanesan, and H. Cabana, "Magnetic cross-linked laccase aggregates - Bioremediation tool for decolorization of distinct classes of

recalcitrant dyes," *Sci. Total Environ.*, vol. 487, no. 1, pp. 830–839, 2014.

[210] L. Cao, "Immobilised enzymes: Science or art?," *Curr. Opin. Chem. Biol.*, vol. 9, no. 2, pp. 217–226, 2005.

[211] O. K. Jesper Brask, Claus C. Fuglsang, "General information relating to the cost of enzymes." .

[212] M. Cantarella, L. Cantarella, A. Gallifuoco, A. Spera, and F. Alfani, "Comparison of different detoxification methods for steam-exploded poplar wood as a substrate for the bioproduction of ethanol in SHF and SSF," *Process Biochem.*, vol. 39, no. 11, pp. 1533–1542, Jul. 2004.

[213] L. Davidi *et al.*, "Toward combined delignification and saccharification of wheat straw by a laccase-containing designer cellulosome," *Proc. Natl. Acad. Sci.*, vol. 113, no. 39, pp. 10854–10859, Sep. 2016.

[214] K. Öhgren, R. Bura, G. Lesnicki, J. Saddler, and G. Zacchi, "A comparison between simultaneous saccharification and fermentation and separate hydrolysis and fermentation using steam-pretreated corn stover," *Process Biochem.*, vol. 42, no. 5, pp. 834–839, 2007.

[215] K. Zhao *et al.*, "Simultaneous saccharification and high titer lactic acid fermentation of corn stover using a newly isolated lactic acid bacterium Pediococcus acidilactici DQ2," *Bioresour. Technol.*, vol. 135, pp. 481–489, 2013.

[216] A. D. Moreno, E. Tomás-Pejó, D. Ibarra, M. Ballesteros, and L. Olsson, "Fed-batch SSCF using steam-exploded wheat straw at high dry matter consistencies and a xylose-fermenting Saccharomyces cerevisiae strain: effect of laccase supplementation," *Biotechnol. Biofuels*, vol. 6, no. 1, p. 160, Nov. 2013.

[217] F. Nielsen, E. Tomás-Pejó, L. Olsson, and O. Wallberg, "Short-term adaptation during propagation improves the performance of xylose-fermenting Saccharomyces cerevisiae in simultaneous saccharification and co-fermentation," *Biotechnol. Biofuels*, vol. 8, no. 1, pp. 1–15, 2015.

[218] F. A. Keller, D. Bates, R. Ruiz, and Q. Nguyen, "Yeast Adaptation on Softwood Prehydrolysate," in *Biotechnology for Fuels and Chemicals*, Totowa, NJ: Humana Press, 1998, pp. 137–148.

[219] P. Baranyi, J. Roberts, T.A. McClure, "A non-autonomous differential equation to model bacterial growth," *Food Microbiol.*, 1993.

[220] L. J. Jönsson, B. Alriksson, and N.-O. Nilvebrant, "Bioconversion of lignocellulose: inhibitors and detoxification," *Biotechnol. Biofuels*, vol. 6, no. 1, p. 16, Jan. 2013.

[221] A. D. Moreno, D. Ibarra, P. Alvira, E. Tomás-Pejó, and M. Ballesteros, "A review of biological delignification and detoxification methods for lignocellulosic bioethanol production," *Crit. Rev. Biotechnol.*, vol. 8551, no. 3, pp. 342–354, 2014.

[222] Z. L. Liu, P. J. Slininger, and S. W. Gorsich, "Enhanced Biotransformation of Furfural and Hydroxymethylfurfural by Newly Developed Ethanologenic Yeast Strains," *Appl. Biochem. Biotechnol.*, vol. 121, no. 1–3, pp. 0451–0460, 2005.

[223] A. Oliva-Taravilla *et al.*, "Unraveling the effects of laccase treatment on enzymatic hydrolysis of steam-exploded wheat straw," *Bioresour. Technol.*, vol. 175, pp. 209–215, 2015.

[224] A. Morão, C. I. Maia, M. M. R. Fonseca, J. M. T. Vasconcelos, and S. S. Alves, "Effect of antifoam addition on gas-liquid mass transfer in stirred fermenters," *Bioprocess Eng.*, vol. 20, no. 2, p. 165, 1999.

[225] T. Akatsuka, T. Mochizuki, and T. Koike, "Buffering Effects of Calcium Carbonate as Clarified by Sevelamer Hydrochloride Monotherapy," *Ther. Apher. Dial.*, vol. 12, no. 3, pp. 216–225, Jun. 2008.

[226] K. Chookietwattana, "Lactic Acid Production from Simultaneous Saccharification and Fermentation of Cassava Starch by Lactobacillus Plantarum MSUL 903," *APCBEE Procedia*, vol. 8, no. Caas 2013, pp. 156–160, 2014.

[227] A. D. Moreno, E. Tom??s-Pej??, D. Ibarra, M. Ballesteros, and L. Olsson, "In situ laccase treatment enhances the fermentability of steam-exploded wheat straw in SSCF processes at high dry matter consistencies," *Bioresour. Technol.*, vol. 143, pp. 337–343, 2013.

[228] D. Klein-Marcuschamer, P. Oleskowicz-Popiel, B. A. Simmons, and H. W. Blanch, "The challenge of enzyme cost in the production of lignocellulosic biofuels," *Biotechnol. Bioeng.*, vol. 109, no. 4, pp. 1083–1087, 2012.

[229] Y. Hong, A.-S. Nizami, M. Pour Bafrani, B. A. Saville, and H. L. MacLean, "Impact of cellulase production on environmental and financial metrics for lignocellulosic ethanol," *Biofuels, Bioprod. Biorefining*, vol. 7, no. 3, pp. 303–313, May 2013.

[230] O. Takimura, T. Yanagida, S. Fujimoto, and T. Minowa, "Estimation of bioethanol production cost from rice straw by on-site enzyme production," *J. JAPAN Pet. Inst.*, vol. 56, no. 3, pp. 150–155, 2013.

[231] S. Peirce *et al.*, "Development of simple protocols to solve the problems of enzyme coimmobilization. Application to coimmobilize a lipase and a β-galactosidase," *RSC Adv.*, vol. 6, no. 66, pp. 61707–61715, 2016.

[232] A. P. Borole and B. H. Davison, "Techno-economic analysis of biocatalytic processes for production of alkene epoxides," *Appl. Biochem. Biotechnol.*, vol. 137–140, no. 1–12, pp. 437–449, 2007.

[233] Q. Zhang, J. Kang, B. Yang, L. Zhao, Z. Hou, and B. Tang, "Immobilized cellulase on Fe3O4nanoparticles as a magnetically recoverable biocatalyst for the decomposition of corncob," *Cuihua Xuebao/Chinese J. Catal.*, vol. 37, no. 3, pp. 389–397, 2016.

[234] JBEI, "Cellulase Production." [Online]. Available: https://econ.jbei.org/index.php/Cellulase_Production. [Accessed: 14-Feb-2019].

[235] C. I. Soti Valentin, Godefroid Bernard, Lenaerts Silvia, "Enzyme kinetics of the detoxification reaction by laccase," 2013, p. 71.

[236] M. F. Chaplin and C. Bucke, *Enzyme technology*. Cambridge University Press, 1990.

[237] M. Langholtz, B. Stokes, and L. Eaton, “2016 Billion-Ton Report: Advancing Domestic Resources for a Thriving Bioeconomy (Executive Summary),” *Ind. Biotechnol.*, vol. 12, no. 5, pp. 282–289, Oct. 2016.

[238] A. Bhattacharya and B. I. Pletschke, “Magnetic cross-linked enzyme aggregates (CLEAs): A novel concept towards carrier free immobilization of lignocellulolytic enzymes,” *Enzyme Microb. Technol.*, vol. 61–62, pp. 17–27, 2014.

[239] Z. J. Wang, J. Y. Zhu, R. S. Zalesny, and K. F. Chen, “Ethanol production from poplar wood through enzymatic saccharification and fermentation by dilute acid and SPORL pretreatments,” *Fuel*, vol. 95, pp. 606–614, May 2012.

[240] B. Application, “Novozymes Cellic ® CTec3 HS - secure your plant ’ s lowest cost,” pp. 1–5.

APPENDIX

A.1. Arduino

Arduinos are an open-source electronics platform or board and the software used to program it. It is designed to make electronics more accessible to artists, designers, hobbyists and anyone interested in creating interactive objects or environments. The way they work and their capabilities are similar for that of Texas Instruments or other microcontrollers (40 € Mega with complete pack, 10 € for Uno with cable and adapter for standalone units).

The language is a simplified C++, but is completely capable to function with Labview (as an external add-on) and with Matlab (Simulink) as an external add-on and it is even possible to transfer the code the board and it will act as a standalone unit without connection to the PC (autosampler, PH control).

A.2. Setup for inoculum adaptation

Previous research shoved adaptation increases the viability of the inoculums greatly. Although the process is much slower (24 h to 72 h), the fact that the inoculum volume is at least 10 times lower than the fermentation broth, makes the process economical. The addition of XRF hydrolyzate (XRF + solid, hydrolyzed together to about 20 g/l glucose content) or glucose supplemented XRF (30 g/l) starts when the culture has grown already for a certain time (5.25 or 12 h). The addition is done so the percentage XRF is linearly rising up to 50 % in 24 or 36 h, equilibrated in every half hour, then it is left to grow for 24 h. The fluid transport speed of the pump is fixed to 7.74 ml/min (this is a stable setting at one of the end-point of the control potentiometer, anytime the button is moved it can be reset precisely and easily, it will remain unchanged until the pumping tube is not changed). Figure XX shows the evolution of XRF percentage in the inoculum, sum XRF volume added to the inoculum and the added XRF volume in the current half hour, in function of the number of half hour cycles. Figure YY shows the number of seconds that the pump is active to add the defined XRF volume to the inoculum in that half hour (Derivative added volume on Figure A-1), in the rest of the cycle the pump is not working. The curve is described with a third order polynomial with a good fit (R^2=9998).

This equation will be used to code the pumps control algorithm. The code is written in Arduino language, a simplified version of C. Important parts highlighted. The first line defines pin 10 as the control of the pump; high value will start, low value will stop the pump. The second line defines this pin as output. Third line waits for 12 h (43.2M ms) for the inoculum to grow. Next line starts a cycle from 1 to 80 (in theory 72 would be enough, but to make sure all 50 ml XRF is added a higher value was set). In each cycle, the pump is started (next line) for the time defined by the third order polynomial (Figure A-2), then switched off for the remaining time in the half hour (next line). The next line waits for a day, so the pump does not work until the inoculums will be used, and leaves enough time to dismantle and switch off the setup.

The program was started when the growth medium was inoculated and stopped after 72 h. The setup is shown on Figure A-3.

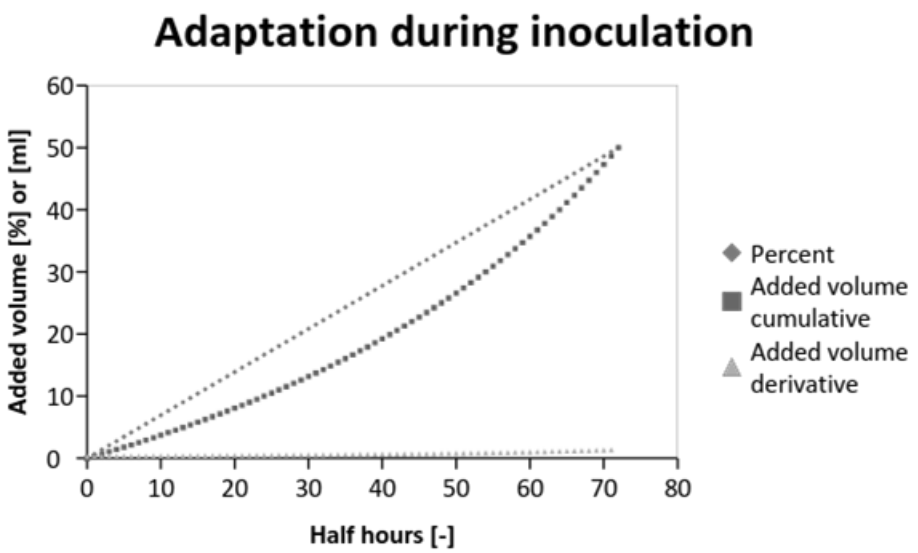

Figure A-1: The increase of XRF percent, added cumulative/derivative volume during the 72 half hour cycles during inoculum adaptation.

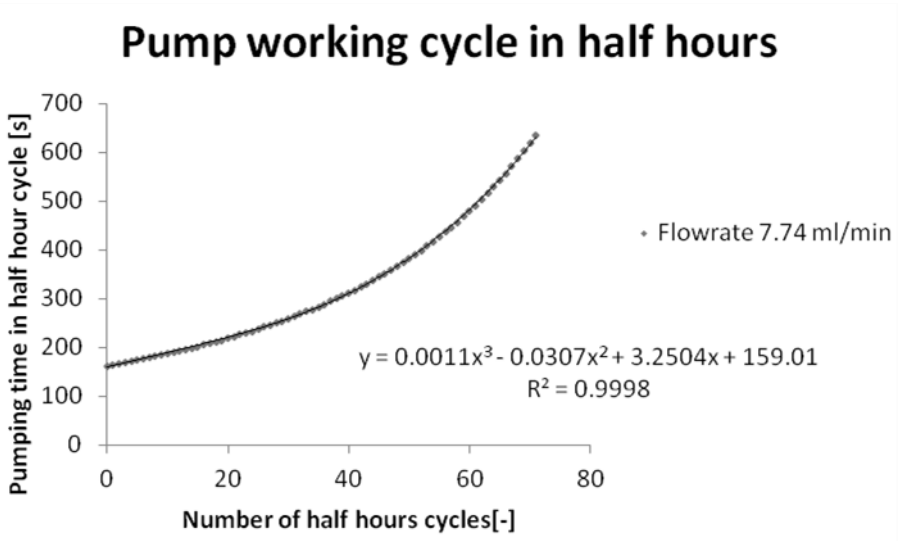

Figure A-2: The change of pumping time in the 72 cycles during adaptation.

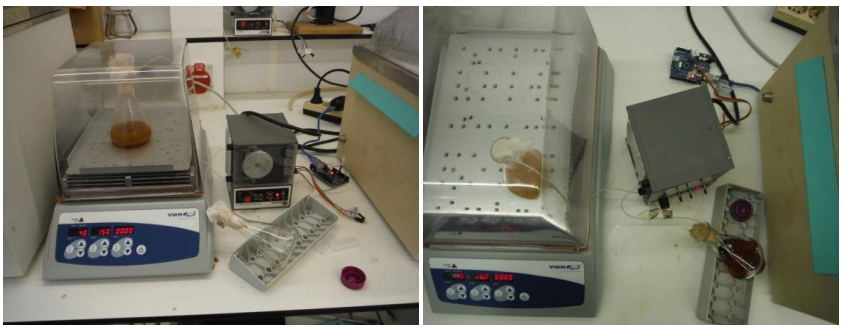

Figure A-3: Inoculation preparation with adaptation from front- (left) and top-view (right). Inoculum in the incubator, the pump controlled by the Arduino board and the XRF waiting for addition.

Arduino code

```
//pumpA define controlling pin

#define PUMP1 10


void setup() { pinMode(PUMP1, OUTPUT); }


//pump 50 ml after 12 h in 36 h, stops for days

//pumpA has 7.74246 ml/h

void loop(){

 //wait 12h before start

delay(43200000);




for (int i=0; i <= 80; i++){

 //start pump

 digitalWrite(PUMP1, HIGH);


delay((0.0011*i*i*i+0.0307*i*i+3.2504*i+159.01)*10
00);

 //stop

 digitalWrite(PUMP1, LOW);

 delay(1800000-
((0.0011*i*i*i+0.0307*i*i+3.2504*i+159.01)*1000));

 }

 //stops for days

delay(90200000)
```

A.3. pH control with lime

As it was shown in Section 0, calcium carbonate can only elevate the pH of SSF medium until 5.5 under the specific parameters, further increase has to be achieved by addition of a base. Lime is used almost exclusively in industrial processes, but its addition is more difficult than that of NaOH or KOH as it is not soluble in water but forms a sedimenting emulsion. A possible setup was made and documented, but was not thoroughly tested or applied. In the specific application (lactate fermentation), base addition is sufficient for pH control as the process itself produces acid, so the pH goes towards acidification constantly.

There are four things that need to be solved for an application: sedimentation in the base container, sedimentation in the tubes of the pump, pH measurement in the reactor and the addition settings (see later). Sedimentation problems are somewhat easy to solve, as if the container is stirred all the time and the mixture spends minimal time in the tubing, sedimentation will be minimal. The first is achieved by constant magnetic stirring, while the second is done by purging the tubes after base addition. The pH measurement is only difficult because of the stirring rods that span from one side of the glass container to the other; therefore, the probe has to be above them. This means sufficient broth has to be in the reactor to have enough material above the upper rotor, or alternatively the upper rod has to be removed and only the lower used for stirring. Simple pH probes could be bought for 10-40 €, with probe, cable and a sensor module (± 0.1 pH, 0-60 °C) that can be directly connected to the Arduino board. The active part of the probe is a few mm diameter glass bulb, which means a few cm of liquid is enough to keep the sensitive part stabile under liquid. The sides of the bulb are protected with plastic protective extensions, so a possible contact will not ruin the probe immediately.

The Arduino connection is visible on Figure A-4, the pH meter needs a GND and 5 V output, the values are read through the analog input pin. The pump control is done via DB15 plug, one output for start/stop, one to set direction, one to switch max speed (prime) on, one output in PWM (pulse width modulation) to set the speed of the pump (details available in the user's manual freely available on the internet). Both stirrer plate and pump is connected to a 5/220 V relay, so they are only powered on if they need to function, each socket needs one Arduino pin to control it.

The settings for the lime addition are somewhat more complex, so it will be discussed here. The first is the problem of the transformation of the measured potential to pH value, as the correlation is known to be non-linear and temperature dependent.

Therefore, the calibration curve has to be recorded at the given temperature (50 °C for SSD and 40 °C for SSFD) and coded in the control circuit. Strictly saying if feedback control is used a single value (V corresponding to pH 6) is sufficient for control, however it is better to know the close range better (4-7 pH for example). The second challenge in the pH control comes from non-ideal mixing. In real life applications mixing is never ideal (after addition the concentration should become homogeneous immediately), however high viscosity heterogeneous mixtures are much further from ideality than aqueous media. If the control point is set to pH 6 exactly at the time when the base addition is stopped (measurement reached pH 6), there is significant amount of non-homogenized base in the system, which will elevate the pH further in the upcoming minutes. Therefore, the set-point should be lower than pH 6. In addition, a lower limit should be set under the set-point, when the addition will start, because the control circuit can be rigid (switching on/off constantly). These two values (set-point, threshold), together with addition speed and the purge time has to be set empirically. The purge time depends on the tube properties (length and diameter) and the viscosity of the mixture (lime concentration), therefore for a fixed setup it has to be set once. The set-point and threshold depend on more parameters: added base concentration and volume (or addition speed), buffer capacity of the broth (constant if fixed composition is used: solid ratio, XRF or water), volume of the broth (linear), homogenization speed (non-linear). Once set it should be acceptable for the interesting range: 0.5-1.5 l, set-point can be lowered a bit if lower volume is used.

The steps taken should contain the following: mapping the potential-pH calibration curve: between 4-7 generally 0.5 steps, 0.1 between 5.5, and 6.5 at the corresponding temperature. Choosing lime concentration (10 % for example), measuring purging time: time needed to fill and empty the tube (the two are not strictly the same). For choice of these time values for emptying 10 % more and for filling 10 % less should be used. Next an addition speed should be chosen, two experiments with 0.5 and 1.5 l of exact mixture made to investigate how much does the pH elevate after the addition is stopped when the sensor reaches 6 pH. This value is not strictly linear, but the mistake is small if you deduce 50 % of this pH value from the set-point and convert it to volts. If the value at 0.5 and 1.5 l is significant the center should choose, and most probably, it could be used generally. The lower threshold should be between 5 and 5.5, and a “cool down time” set after the addition, to enable thorough homogenization. The final setup looks like the following: container mixed constantly, probe submerged in the top of the liquid, after

threshold reached, tubes filled, base added until set-point, tubes emptied, cool down time waited and system set to active again.

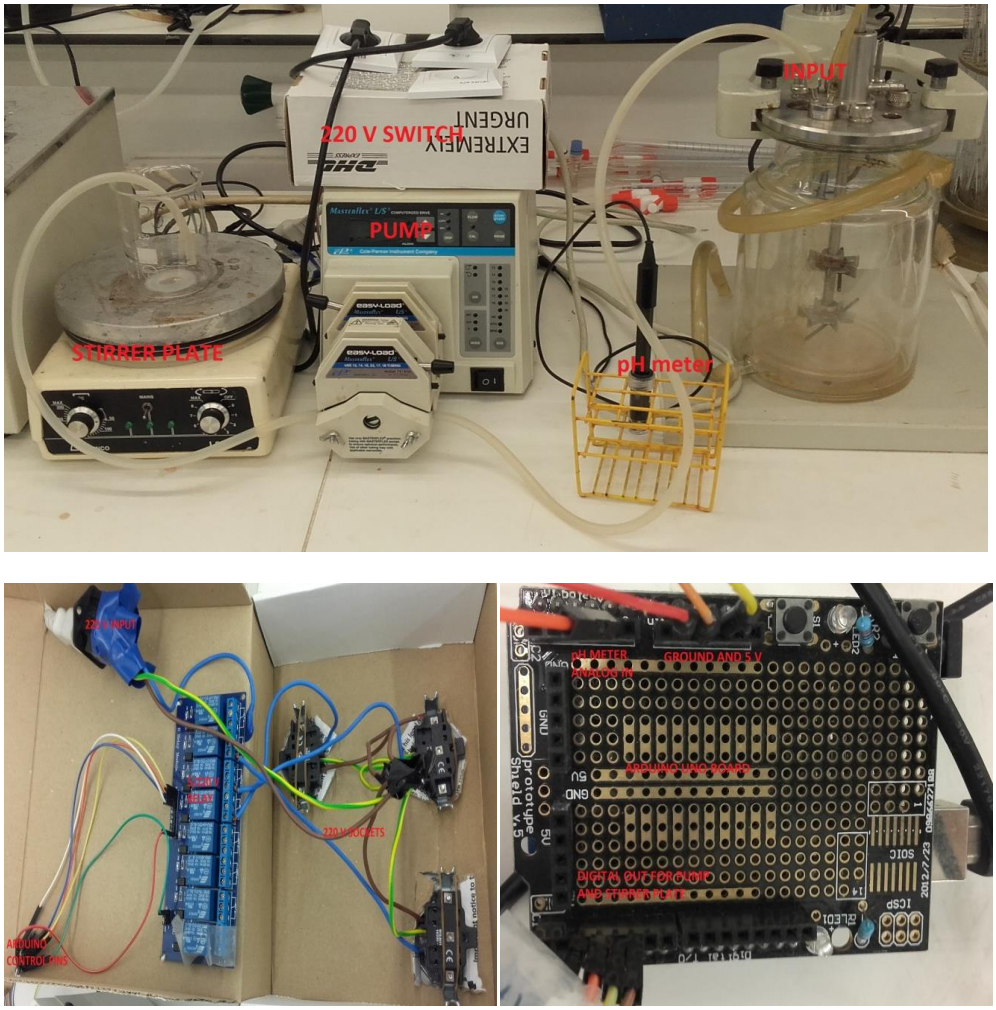

Figure A-4: The setup used for pH control with lime (top), the relay box (left) and the Arduino connections (right).

Arduino code

```
// lower pH higher value

// pump starts on low values

// the setup routine runs once when you press reset:


void setup() {

 // couple instruments to pins

int stirrer=2;

int pumpstart=3;

int pumpdirection=4;

int pumpspeed=5;

int setpoint=659; //659 pH 6; 678 ph 5.5; lower pH higher value

int tolerance=20;

int pHvalue=0;

pinMode(A1, INPUT); //pH meter

pinMode(stirrer, OUTPUT);

pinMode(pumpstart, OUTPUT);

pinMode(pumpdirection, OUTPUT);

pinMode(pumpspeed, OUTPUT);

digitalWrite(stirrer,LOW); //stir constantly

}


void loop(){

digitalWrite(pumpstart,HIGH); //return flow

pHvalue=analogRead(A1);

if (pHvalue>setpoint+tolerance) // if it is lower than setpoint+tolerance


 digitalWrite(pumpdirection,HIGH);

 analogWrite(pumpspeed,133);

 digitalWrite(pumpstart,LOW);

 delay(6000); //until tubing is full

 digitalWrite(pumpstart,HIGH);

 delay(6000);

 while (pHvalue>setpoint) // until ph is lower than setpoint

  {digitalWrite(pumpstart,LOW);

   delay(6000); //until pump adds

  digitalWrite(pumpstart,HIGH);

  delay(60000); //wait for mixing in the reactor

  pHvalue=analogRead(A1);

  }


 digitalWrite(pumpdirection,LOW); //return flow

 digitalWrite(pumpstart,LOW); //return flow

 delay(6000); //empty tube

 digitalWrite(pumpstart,HIGH); //return flow
```

A.4. Equipment for laccase screening

It was discussed in Section 3.8 that a fast-screening method is needed to select the right laccase. The setup proposed in Section 3.7.2.1 has proven to be unsuccessful in doing so, as SSFD experiments (Section 0) showed phenolic concentration evolution completely different from results recorded during screening (Section 3.7.2.2). Running a SSFD according to the method written in Section 5.7.2.1is not an option, as it requires a lot of material (laccase, SF and XRF), it is tedious and, in addition, a lot of reactors in parallel would be needed to obtain results in a reasonable time frame.

While comparing the before mentioned screening and the SSFD process and keeping in mind that the phenolic decrease should have happened during the initial time when the inoculum was not yet added, the main difference is the presence of the solid phase in SSFD. It is indeed logical that the solid matrix can also take part in the radical reaction, hence altering the results. However, once the solid phase is present, the stirring becomes more difficult and the magnetic stirrer could not be used, simply because it does not have enough power to move in the mixture. Two possibilities present themselves: the mixture is placed in a shaking water bath, accepting that the stirring will be limited in the initial phase, until the mixture is not liquefied via hydrolysis, so it is expected that the measured changes will be slower that those measured with active stirring, or an overhead stirrer, which is perfectly suited for the purpose.

An overhead stirrer can be built (see Figure A-5) using a stepper motor, which is the best suited for mixing, as it is typically a low speed (rpm) high torque process. Commercial small size stepper motors are available from around 10 €, the corresponding driver is a few €, and a single Arduino Uno board can drive multiple of them. The rotor can be attached to the stepper axis with a flexible connection. The stepper has to be fastened to the glassware so it will not rotate away. A rubber plug would be enough to seal the glassware, with a hole screwed in the center, and a bearing inserted to stabilize the rotor against movement perpendicular to the axis, or alternatively a metal cylinder with an inner thread with a diameter close to that of the rotor metal. The stirring rod has to fit through the mouth of the glassware, so either that specific size has to be used, or there is a method (see Figure A-5) to elongate it up to 3 times this size. In this case, the rotor will consist of three parts, each the size of the inlet of the glassware, attached with two wrists. The central rod has two L shaped small metal plates wielded to it, in a center point symmetric way. The side rods have also a plate wielded to them at the side, three corners rounded, so they can rotate

freely. The center rod's and the side rod's metal plate are fastened together with a screw through a hole in the plates. During operation, the fluid resistance will keep them open, and the L shaped plate assures that they are all parallel. Once the experiment is over, they are rotated in counter direction to fold, and kept rotated during removal, so they unfold completely when they arrive to the mouth of the glassware. The complete bill of materials can be seen in Table A-1.

Table A-1: List of equipment and materials needed for the test setup for SSD/SSFD.

Equipment	Material	Electronics
Wielding equipment	Erlenmeyer lombic	Arduino board
3D printer	Rubber plug	Stepper motor
Drill	3D printer polymer	Stepper driver
	Fastener	
	Screws	
	Elastic joint	
	Metal cylinder	
	Metal rods	
	Metal plates	

Aeration is difficult to solve, so it will be left out, the remaining furfural will alter the results. Lime addition is also very difficult in this specific setup. This does not count during hydrolysis, as the initial pH of the XRF is ideal for it. During fermentation, it might cause problem as calcium carbonate can only elevate pH until 5.5.

Both SSD and SSFD can be measured with this setup, although SSD easier. SSD measurement are also very describing, they provide information about the laccase cellulase interactions that were proven to be strong (Section 5.6.2) and cost determining towards utilization (Section 2.5.6). However, SSFD is also needed, as the effect of laccase treatment is the inhibition decrease, rather than just the phenolic concentration decrease. In terms of SSFD, the presents of furfural and the non-ideal pH can be problematic. In addition, only non-volatile product fermenting microorganisms can be reliably measured (lactic acid), as volatile compounds might evaporate, as it is the case of water bath fermentations with ethanol.

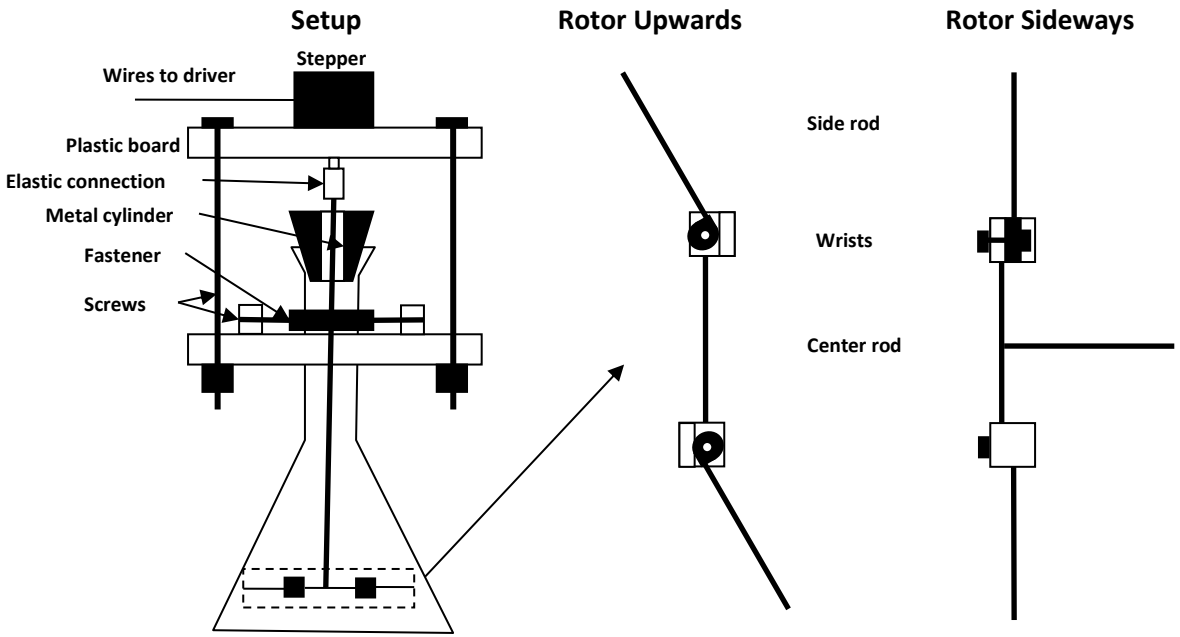

Figure A-5: Equipment sketches for low-cost, small volume, high solid SSD and SSFD.